

The Synthesis and *in vivo* Evaluation of Chemically Modified siRNAs that Contain Red-Shifted Internal Azobenzene Derivative Spacers for Selective and Tunable Photocontrol of Activity Without UV light

by

Matthew L. Hammill, MSc

A thesis submitted to the
School of Graduate and Postdoctoral Studies in partial
fulfillment of the requirements for the degree of

Doctor of Philosophy in Applied Bioscience

Faculty of Science

University of Ontario Institute of Technology (Ontario Tech University)

Oshawa, Ontario, Canada

August, 2021

© Matthew L. Hammill, 2021

THESIS EXAMINATION INFORMATION

Submitted by: **Matthew L. Hammill**

Doctor of Philosophy in Applied Bioscience

Thesis title: The Synthesis and in vivo Evaluation of Chemically Modified siRNAs that Contain Red-Shifted Internal Azobenzene Derivative Spacers for Selective and Tunable Photocontrol of Activity Without UV light

An oral defense of this thesis took place on July 19, 2021 in front of the following examining committee:

Examining Committee:

Chair of Examining Committee	Dr. Janice L. Strap
Research Supervisor	Dr. Jean-Paul Desaulniers
Examining Committee Member	Dr. Olena Zenkina
Examining Committee Member	Dr. Marc Adler, Ryerson University
University Examiner	Dr. Brad Easton
External Examiner	Dr. Andrew Wooley, University of Toronto

The above committee determined that the thesis is acceptable in form and content and that a satisfactory knowledge of the field covered by the thesis was demonstrated by the candidate during an oral examination. A signed copy of the Certificate of Approval is available from the School of Graduate and Postdoctoral Studies.

ABSTRACT

Short interfering RNAs (siRNAs) are biopolymers that are used for post-transcriptional gene regulation and act as endogenous defenses against attack from viruses and dsRNA parasites. The siRNA field is making advances for use as pharmaceuticals and biomolecular research tools for the study of gene silencing in uncontrollably upregulated genes. Through chemical modification of the RNA structure, inherent limitations found in nature can be eliminated to make better pharmaceuticals and research tools. This dissertation investigated the incorporation of azobenzene derivative spacers into RNA backbones by replacing two base pairs. Several siRNAs were synthesized, and then characterized bio-physically through several means. After bio-physical characterization, these siRNAs were tested *in vitro* against *firefly* luciferase and endogenous *BCL-2* to determine gene silencing efficacy, as well as nuclease resistance when azobenzenes were at the 3' end of the passenger strand. The ability of these azobenzene siRNAs to be reversibly controlled with UV (ultraviolet) light after transfection into the cells was investigated. Next, utilization of tetra-halogenation at the *ortho* position on the azobenzene to red-shift the $\pi \rightarrow \pi^*$ of the N=N double bond out of the UV portion of the electromagnetic spectrum into the visible region, allowing the siRNA to be inactivated with red light, which is less toxic and through constant exposure inactivates the siRNA for up to 24 h. Finally, we developed an *ortho* tetra-fluorinated azobenzene derivative to further improve the design of these siRNAs. This tetra-fluorinated derivative maintains the desirable red-shifting property of azobenzene, while having a greatly improved *cis* conformer half-life over the tetra-chlorinated azobenzene derivative. Furthermore, the tetra-fluorinated azobenzene containing siRNAs were able to remain inactive for up to 72 h with minimal green light exposure. These results in cell-based assays have shown that azobenzenes embedded within siRNAs are well tolerated in the RNA induced silencing complex (RISC). This introduces new functionality into the pathway through photo-switchable azobenzenes which can be controlled with light in real time. We further show that the properties of the siRNAs can be fine tuned through the use of different azobenzene derivatives, and can also show differences in nuclease resistance between the *trans* and *cis* isomers.

Keywords: Organic chemistry; azobenzene; photo-switch; chemical biology; siRNA

AUTHOR'S DECLARATION

I hereby declare that this thesis consists of original work of which I have authored. This is a true copy of the thesis, including any required final revisions, as accepted by my examiners.

I authorize the University of Ontario Institute of Technology (Ontario Tech University) to lend this thesis to other institutions or individuals for the purpose of scholarly research. I further authorize University of Ontario Institute of Technology (Ontario Tech University) to reproduce this thesis by photocopying or by other means, in total or in part, at the request of other institutions or individuals for the purpose of scholarly research. I understand that my thesis will be made electronically available to the public.

Matthew Hammill

STATEMENT OF CONTRIBUTIONS

Published Manuscript I (Chapter 2) Hammill, M. L., Patel, A., Abd Alla, M., and Desaulniers, J. P. (2018) Stability and evaluation of siRNAs labeled at the sense strand with a 3'-azobenzene unit, *Bioorganic & Medicinal Chemistry Letters* 28, 3613-3616.

My contributions to this manuscript were as follows: I synthesized all azobenzene and chemical derivatives utilized in these experiments, as well as the synthesis, characterization and deprotection of all oligonucleotides. I performed the bulk of the biological assays, and was responsible for data analysis, figure preparation and manuscript writing. Ayushi Patel and Maria Alla were responsible for some biological assay bio-reps. Prof. Jean-Paul Desaulniers was responsible for lab space, funding acquisition, project administration and manuscript revision.

Published Manuscript II (Chapter 3) Hammill, M. L., Islam, G., and Desaulniers, J. P. (2020) Reversible control of RNA interference by siRNAzOs, *Organic & Biomolecular Chemistry* 18, 41-46.

My contributions to this manuscript were as follows: I synthesized all azobenzene and chemical derivatives utilized in these experiments, as well as the synthesis, characterization and deprotection of all oligonucleotides. I designed the experimental procedures utilized for the light inactivation/reactivation, performed all of the photo-switching assays (except for RT-PCR, which I only assisted with) as well as being responsible for data analysis, figure preparation and manuscript writing. Golam Islam performed the bulk of the qRT-PCR data acquisition and analysis. Prof. Jean-Paul

Desaulniers was responsible for lab space, funding acquisition, project administration and manuscript revision

Published Manuscript III (Chapter 4) Hammill, M. L., Islam, G., and Desaulniers, J. P.
(2020) Synthesis, Derivatization and Photochemical Control of ortho-Functionalized Tetrachlorinated Azobenzene-Modified siRNAs, *ChemBioChem* 21, 2367-2372.

My contributions to this manuscript were as follows: I synthesized all chlorinated azobenzene and chemical derivatives utilized in these experiments, as well as the synthesis, characterization and deprotection of all oligonucleotides. I designed the experimental procedures utilized for the light inactivation/reactivation, with red light and performed photo-switching assays and biological assays, as well as being responsible for data analysis, figure preparation and manuscript writing. Golam Islam assisted with data acquisition and analysis for the red light switching. Prof. Jean-Paul Desaulniers was responsible for lab space, funding acquisition, project administration and manuscript revision

Preparation Manuscript IV (Chapter 5) Hammill, M. L., Tsubaki, K., Wang, E., and Desaulniers J.P.

My contributions to this manuscript were as follows: I synthesized, characterized and deprotected all of the oligonucleotides. I was responsible for the synthesis and characterization of compounds 8 and 9. I designed the experimental procedures utilized for the light inactivation/reactivation, with green light and performed photo-switching assays and biological assays, as well as being responsible for data analysis, figure preparation and manuscript writing. Kota Tsubaki, a visiting PhD student from Japan, was responsible for the chemical synthesis, characterizations and design of the fluorinated azobenzene

derivatives (compounds 1-8) which were then incorporated into oligonucleotides. Estelle Wang, an undergraduate thesis student was responsible for the reproduction and optimization of the synthesis developed by Kota. Prof. Jean-Paul Desaulniers was responsible for lab space, funding acquisition, project administration, international collaborations and manuscript revision.

ACKNOWLEDGEMENTS

I would first like to acknowledge my supervisor Dr. Jean-Paul Desaulniers for his support, patience and giving me this opportunity. In addition to providing lab space and funding, Dr. Desaulniers also provided me the chance to travel for conferences not only across Canada but to Germany and Japan as well. This was the first time I ever had an opportunity to travel anywhere, and I will always appreciate it. Dr. Desaulniers also was accepting of international students from China, England and Japan, and I will always be grateful for the chance to work with them in lab. It was an honor and pleasure to have worked with you on this project.

I would also like to extend my gratitude to my committee members Dr. Marc Adler and Dr. Olena Zenkina. Their helpful advice during my committee meetings was greatly appreciated, and I thank them for all their help.

I would also like to thank Dr. Brad Easton and Dr. Andrew Wooley for taking the time and being involved in the defense of my thesis.

I would like to thank all the groups who allowed me to do work in their labs for my research which otherwise wouldn't have been possible: Dr. Sean Forrester, Dr. Julia Green-Johnson and Dr. Janice Strap. I really appreciate your support!

I would also like to thank Lidya Salim who always had time for coffee on the bench with me and had helpful advice. I would also like to thank Dr. Golam Islam for all his hard work while working on my various projects. I would also like to thank Dr. Kota Tsubaki, whose expertise in organic synthesis was invaluable during fluorinated azobenzene research. I will also acknowledge Ifrodet Giorgees for all her support and encouragement.

Next I would like to acknowledge all the undergraduates and graduate students past and present that worked with me during my time here. It was a pleasure working with you.

A special mention goes out to Genevieve Barnes for always helping me with the NMR when I needed a hand, and to Michael Allison whose expertise on HPLC purification was invaluable.

Finally I would like to thank my parents, without whom none of this would be possible, thank you for your support and encouragement during the years.

TABLE OF CONTENTS

Thesis Examination Information	ii
Abstract	iii
Authors Declaration	iv
Statement of Contribution	v
Acknowledgements	viii
Table of Contents	x
List of Tables	xiv
List of Schemes	xiv
List of Figures	xv
List of Abbreviations and Symbols	xviii
Chapter 1 Introduction	1
1.1 The RNA Interference Pathway.....	1
1.2 Important Areas of siRNAs.....	4
1.3 Therapeutic challenges of siRNAs.....	5
1.4 Chemical modifications of siRNAs.....	8
1.5 Azobenzene and its Role in Nucleic Acid Modification.....	14
1.6 The Benefits of Using an Azobenzene Modification.....	22
1.7 Research Objectives	25
1.8 Reference- Chapter I- Introduction.....	28
Chapter 2 Manuscript I- Stability and Evaluation of siRNAs labeled at the sense strand with a 3'-Azobenzene Unit	34
2.1 Abstract.....	35
2.2 Introduction	35
2.3 Materials and methods.....	39
2.3.1 General	39
2.3.2 Procedure for Absorbance Spectra Experiments.....	39
2.3.3 Procedure for HPLC Characterization	39
2.3.4 Procedure for Nuclease Stability Assays	40
2.3.5 Procedure for Maintaining Cell Cultures of HeLa Cells.....	40
2.3.6 Procedure for siRNA Transfections.....	41
2.3.7 Procedure for <i>in vitro</i> Dual-Reporter Luciferase Assay.....	42
2.3.8 Procedure for Light Inactivation of Azobenzene Modified siRNA (<i>trans</i> to <i>cis</i>).....	42
2.4 Results.....	43
2.4.1 Gene-silencing activity with UV/visible exposures.....	44
2.4.2 Nuclease stability with UV/visible exposures.....	47
2.5 Conclusions.....	49
2.6 References - Chapter 2 - Manuscript I.....	52
2.7 Manuscript I Supplementary Figures and Tables.....	53
Chapter 3 Manuscript II-Reversible control of RNA interference by siRNAs	60
3.1 Abstract.....	61
3.2 Introduction	61

3.3 Materials and methods.....	64
3.3.1 Procedure for Oligonucleotide Synthesis and Purification.....	64
3.3.2 Procedure for Performing CD Experiments.....	66
3.3.3 Procedure for Absorbance Spectra Experiments.....	66
3.3.4 Procedure for Melting Temperature of siRNA Duplexes (<i>T_m</i>).....	66
3.3.5 Procedure for HPLC Characterization.....	67
3.3.6 Procedure for Reduced Glutathione (GSH) Degradation Assay	67
3.3.7 Procedure for Maintaining Cell Cultures of HeLa Cells.....	67
3.3.8 Procedure for siRNA Transfections	68
3.3.9 Procedure for in vitro Dual-Reporter Luciferase Assay.....	69
3.3.10 Procedure for Light Inactivation of Azobenzene Modified siRNA (<i>trans</i> to <i>cis</i>).....	70
3.3.11 Procedure for Light Reactivation of Azobenzene Modified siRNA (<i>cis</i> to <i>trans</i>)	70
3.3.12 Procedure for consecutive UV/Vis Light Cycling (1.5x and 2x light cycling).....	70
3.3.13 Transfection of HeLa cells with Lipofectamine 2000.....	71
3.3.14 HeLa Cell Reverse Transcription (RT) Preparation.....	71
3.3.15 RT-PCR with the Invitrogen cells to cDNA kit II.....	71
3.3.16 RNA extraction, cDNA synthesis and RT-qPCR.....	72
3.3.17 Quantitative RT-PCR.....	73
3.3.18 Procedure for XTT Assays.....	74
3.4 Results.....	74
3.5 Conclusions.....	84
3.6 References - Chapter 3 - Manuscript II.....	85
3.7 Manuscript II Supplementary Figures and Tables.....	87

Chapter 4 Manuscript III- Synthesis, Derivatization and Photochemical Control of *ortho*-Functionalized Tetrachlorinated Azobenzene-Modified siRNAs 110

4.1 Abstract.....	111
4.2 Introduction	111
4.3 Materials and methods.....	116
4.3.1 General Methods.....	116
4.3.2 Synthesis of 4,4'-bis(hydroxyethyl)-azobenzene – Compound (1).....	117
4.3.3 Synthesis of (E)-(diazene-1,2-diylbis(3,5-dichloro-4,1-phenylene)) bis(ethane-2,1-diyl) diacetate Compound (2).	117
4.3.4 Synthesis of (E)-2,2'-(diazene-1,2-diylbis(3,5-dichloro-4,1-phenylene)) bis(ethan-1-ol) – Compound (3).....	118
4.3.5 Synthesis of (E)-2-(4-((4-(2-(bis(4-methoxyphenyl)(phenyl)methoxy)ethyl - 2,6-dichlorophenyl) diazenyl) -3,5-dichlorophenyl)ethan-1-ol– Compound (4).....	118
4.3.6 Synthesis of (E)-4-((4-(2-(bis(4-methoxyphenyl)(phenyl)methoxy)ethyl)- 2,6-dichlorophenyl)diazenyl)-3,5-dichlorophenethyl (2-cyanoethyl) diisopropylphosphoramidite - Compound (5).....	119
4.3.7 Procedure for Oligonucleotide Synthesis and Purification.....	120

4.3.8 Procedure for ESI Q-TOF Measurements.	121
4.3.9 Procedure for Performing CD Experiments.....	122
4.3.10 Procedure for Melting Temperature of siRNA Duplexes (<i>T_m</i>).....	122
4.3.11 Procedure for Absorbance Spectra Experiments.....	122
4.3.12 Procedure for HPLC Characterization.....	123
4.3.13 Procedure for Reduced Glutathione (GSH) Degradation Assay.....	123
4.3.14 Procedure for Maintaining Cell Cultures of HeLa Cells.....	123
4.3.15 Procedure for siRNA Transfections.....	124
4.3.16 Procedure for in vitro Dual-Reporter Luciferase Assay.....	125
4.3.17 Procedure for Light Inactivation of Azobenzene Modified siRNA (<i>trans</i> to <i>cis</i>).....	126
4.3.18 Procedure for Thermal Relaxation and Reactivation of Azobenzene Modified siRNA (<i>cis</i> to <i>trans</i>).....	126
4.4 Results.....	126
4.5 Conclusions.....	133
4.6 References - Chapter 4- Manuscript III.....	135
4.7 Manuscript III Supplementary Figures and Tables.....	137

Chapter 5 Preparation Manuscript IV- Synthesis, Derivatization and Photochemical Control of *ortho*-Functionalized Tetra-fluorinated Azobenzene-Modified siRNAs.....143

5.1 Introduction	144
5.2 Materials and methods.....	153
5.2.1 General Methods.....	153
5.2.2 Synthesis of 4-bromo-2,6-difluoroaniline- Compound (2).....	153
5.2.3 Synthesis of 4-amino-3,5-difluorobenzonitrile-Compound (3).....	154
5.2.4 Synthesis of 4-amino-3,5-difluorobenzoic acid -Compound (4).....	154
5.2.5 Synthesis of 4-amino-N-(2-((tert-butyl)dimethylsilyloxy)ethyl)-3,5-difluorobenzamide -Compound (5).....	155
5.2.6 Synthesis of (E)-4,4'-(diazene-1,2-diyl)bis(N-(2-((tert-butyl)dimethylsilyloxy)ethyl)-3,5-difluorobenzamide -Compound (6).....	156
5.2.7 Synthesis of (E)-4,4'-(diazene-1,2-diyl)bis(3,5-difluoro-N-(2-hydroxyethyl)benzamide) Compound (7).....	156
5.2.8 Synthesis of (E)-N-(2-(bis(4-methoxyphenyl)(phenyl)methoxy)ethyl)-4-((2,6-difluoro-4-((2-hydroxyethyl)carbamoyl)phenyl)diazanyl)-3,5-difluorobenzamide – Compound (8).	157
5.2.9 Synthesis of (E)-2-(4-((4-((2-(bis(4-methoxyphenyl)(phenyl)methoxy)ethyl)carbamoyl)-2,6-difluorophenyl)diazanyl)-3,5-difluorobenzamido)ethyl (2-cyanoethyl) diisopropylphosphoramidite-Compound (9).....	158
5.2.10 Procedure for Oligonucleotide Synthesis and Purification.....	158
5.2.11 Procedure for LC/MS.....	160
5.2.12 Procedure for Performing CD Experiments.....	160
5.2.13 Procedure for Thermal Relaxation Measurements	161
5.2.14 Procedure for Melting Temperature of siRNA Duplexes (<i>T_m</i>)	161
5.2.15 Procedure for Absorbance Spectra Experiments.....	161

5.2.16 Procedure for HPLC Characterization.....	162
5.2.17 Procedure for Maintaining Cell Cultures of HeLa Cells.....	162
5.2.18 Procedure for siRNA Transfections.....	163
5.2.19 Procedure for in vitro Dual-Reporter Luciferase Assay.....	163
5.2.20 Procedure for Light Inactivation of Azobenzene Modified siRNA (<i>trans</i> to <i>cis</i>).....	164
5.2.21 Procedure for Thermal Relaxation and Reactivation of Azobenzene Modified siRNA (<i>cis</i> to <i>trans</i>).....	164
5.2.22 Procedure for consecutive Green/Blue Light Cycling (1.5x and 2x light cycling).....	165
5.3 Results.....	166
5.4 Conclusions.....	180
5.5 References - Chapter 5- Preparation Manuscript IV.....	182
5.6 Manuscript III Supplementary Figures and Tables.....	184
Chapter 6 General Conclusions.....	190
6.1 References - Chapter 6 – General Conclusions.....	196
Appendices	197
Appendix I. Manuscript I and Supplementary Data	197
Appendix II. Manuscript II and Supplementary Data	213
Appendix III. Manuscript III and Supplementary Data	250
Appendix IV. Preparation Manuscript IV and Supplementary Data	276
Appendix V. Copyright Permission Letters.....	294

LIST OF TABLES

CHAPTER 2

Table 2.1. Sequences of siRNAs.....	43
--	----

CHAPTER 3

Table 3.1. IC ₅₀ values for siRNAs 7-13 and wild type.....	75
--	----

CHAPTER 4

Table 4.1 Table of RNAs used and its target.....	129
---	-----

CHAPTER 5

Table 5.1 Table of RNAs used and its target.....	168
---	-----

List of Schemes

CHAPTER 4

Scheme 4.1. Synthesis of an <i>ortho</i> -functionalized tetrachlorinated azobenzene DMT-phosphoramidite	128
---	-----

CHAPTER 5

Scheme 5.1. Synthesis of an <i>ortho</i> -functionalized tetrafluorinated azobenzene DMT-phosphoramidite.....	165
--	-----

LIST OF FIGURES

CHAPTER 1

Figure 1.1. Dicer mediated RNA interference pathway in mammalian cells which targets mRNA for cleavage.....2

Figure 1.2. Diagram of human Ago2, including primary sequence with amino acid residue number and proposed mechanism of strand selection and mRNA targeting.3

Figure 1.3. siRNA regions of importance. Left is canonical cleavage and strand selection, right is alternate dissociation pathway due to non-cleavable central region spacers.....5

Figure 1.4. Degradation of native RNA with cleavage sites highlighted in red.6

Figure 1.5. DMT-Phosphoramidite oligonucleotide solid-phase RNA synthesis.....10

Figure 1.6. Various chemically-modified RNA bases12

Figure 1.7. Conformation change of azobenzene when exposed to light, *trans* (left) and *cis* (right)14

Figure 1.8. Conformation change of azobenzene when exposed to light, *trans* (left) and *cis* (right).....15

Figure 1.9. *o*-nitrobenzyl derivative for use as a photocage.18

Figure 1.10 Various central region modifications used within siRNAs from Dr. Jean-Paul Desaulniers' research group21

Figure 1.11 Photoinduced inactivation and reactivation of siRNAzOs..23

CHAPTER 2

Figure 2.1. Structural differences between native RNA, and siRNAs containing azobenzene derivatives.....38

Figure 2.2. Reduction in normalized firefly luciferase expression for **wt** siRNA at 8, 20, 40, 80, 160, 400 and 800 pM concentrations in HeLa.....44

Figure 2.3. Reduction in normalized firefly luciferase expression for siRNA **1** at 8, 20, 40, 80, 160, 400 and 800 pM concentrations in HeLa.....46

Figure 2.4. Reduction in normalized firefly luciferase expression for siRNA **2** at 8, 20, 40, 80, 160, 400 and 800 pM concentrations in HeLa cells.....46

Figure 2.5. Nuclease stability assay. 20% Non-denaturing polyacrylamide gel with degradation products of siRNAs **1** and **2** after incubation with 13.5% fetal bovine serum at 37 °C from 0 hours to 4 hours.....48

Figure 2.6. Quantification of remaining intact siRNA using ImageJ software.....49

CHAPTER 3

Figure 3.1. Structural differences between native RNA, and azobenzene-containing RNAs. Az2 corresponds to the azobenzene unit used in this study.....63

Figure 3.2. Photoinduced inactivation and reactivation of siRNAzOs.....64

Figure 3.3. Normalized firefly luciferase activity for siRNAzOs **1-4** and **wt** at 160, 400 and 800 pM in HeLa cells monitored 8- and 24- hours post-transfection.....77

Figure 3.4. Normalized firefly luciferase expression for siRNAzOs 1-4 and wt at 160, 400, and 800 pM in HeLa cells monitored 8- and 24-hours post-transfection.....79

Figure 3.5. Normalized firefly luciferase expression for siRNAzo 4 at 160, 400 and 800 pM in HeLa cells monitored 24 hours post-transfection.....80

Figure 3.6. *BCL2* expression normalized to 18S for siRNAzOs **5-7** at 1, 10 and 20 nM in HeLa cells monitored 8 (left) and 24 (right) hours post-transfection.....82

CHAPTER 4

Figure 4.1. Structural differences between native RNA, and azobenzene-containing RNAs (siRNAzOs).....114

Figure 4.2. Photoinduced inactivation and reactivation of siRNAzOs.....127

Figure 4.3. Absorbance profile of Cl-Az2 (compound 3) moiety when exposed to various wavelengths of visible light (red (660 nm) and violet (410 nm)) in methanol.....130

Figure 4.4. Normalized firefly luciferase expression for Cl-siRNAzOs 1-3 at 1, 2 and 4 nM in HeLa cells monitored 8- and 24-hours post-transfection.....133

CHAPTER 5

Figure 5.1. Structural differences between native RNA, and azobenzene-containing RNAs (siRNAzOs).....147

Figure 5.2. Visible wavelengths of the electromagnetic spectrum.....149

Figure 5.3. Structural and physical property differences between native RNA, and azobenzene-containing RNAs (siRNAzOs).....152

Figure 5.4. Photoinduced inactivation and reactivation of siRNAzOs.....	168
Figure 5.5. Thermal stability of diol 7 at 20 °C.....	170
Figure 5.6. Thermal stability of diol 7 at 95 °C.....	171
Figure 5.7. HPLC chromatogram of anti-sense strand of F-siRNAzo-1.....	172
Figure 5.8. Normalized firefly luciferase expression for F-siRNAzo-1 at 5, 10 and 20 nM in HeLa cells monitored 24-hours post-transfection.....	173
Figure 5.9. Normalized firefly luciferase expression for F-siRNAzo-1 at 5, 10 and 20 nM in HeLa cells monitored 48-hours post-transfection.....	175
Figure 5.10. Normalized firefly luciferase expression for F-siRNAzo-1 at 5, 10 and 20 nM in HeLa cells monitored 72-hours post-transfection.....	176
Figure 5.11. Normalized firefly luciferase expression for F-siRNAzo-1 at 5, 10 and 20 nM in HeLa cells monitored 48-hours post-transfection (2x light cycling).....	177
Figure 5.12. Normalized firefly luciferase expression for F-siRNAzo-1 at 5, 10 and 20 nM in HeLa cells monitored 72-hours post-transfection(2x light cycling).....	179

CHAPTER 6

Figure 6.1. A potential future system with multiple siRNAzOs, individually controlled by independent wavelengths of light.....	194
---	-----

LIST OF ABBREVIATIONS AND SYMBOLS

A: Adenosine

ACN: Acetonitrile

Ago: Argonaute protein

APS: Ammonium persulfate

AS: Antisense

Az1: One carbon azobenzene derivative

Az2: Two carbon azobenzene derivative

Az2-4Cl: Chlorinated azobenzene derivative

Az2-4F: Fluorinated azobenzene derivative

BCL-2: B-cell lymphoma protein 2

BCL-3: B-cell lymphoma protein 3

bp: Base pair

C: Cytosine

CD: Circular dichroism

CDCl_3 : Deuterated Chloroform

CH_2Cl_2 : Dichloromethane

CPG: Controlled pore glass

dFT: Difluorotoluene

DMEM: Dulbeccos modified eagle medium

DMSO: Dimethylsulfoxide

DMT: 4,4'-Dimethoxytrityl

DNA: Deoxyribonucleic acid

ds: Double stranded

DsRNA: Dicer siRNA

dd: Doublet of doublets

dt: Doublet of triplets

dT: Deoxythymidine

EDTA: Ethylenediaminetetraacetic acid

EMAM: Methylamine 40% wt. in H₂O and Methylamine 33% wt. in EtOH 1:1

EtOAc: Ethyl acetate

EtOH: Ethanol

FBS: Fetal Bovine Serum

G: Guanine

J: Coupling constant (Hz)

HPLC: High pressure liquid chromatography

IC₅₀: Half Maximal inhibitory concentration

IDT: Integrate DNA technologies

LCD: Liquid crystal display

m/z: mass to charge ratio

Me: Methyl

MeOH: Methanol

mRNA: Messenger RNA

NaOH: Sodium hydroxide

NaOAc: Sodium Acetate

NMR: Nuclear magnetic resonance

nt: nucleotide

OH: Hydroxyl

O-Me: *O*-Methyl

PAGE: Polyacrylamide gel electrophoresis

PBS: Phosphate buffered saline

p/s: Penicillin-Streptomycin

PS: Phosphorothioate

RET: Rearranged during transfection

RISC: RNA induced silencing complex

RNA: Ribonucleic acid

RNAi: RNA interference

RNase III: Ribonuclease III

RNase H: Ribonuclease H

rt: Room temperature

siRNA: small interfering RNA

ss: Single stranded

t: Triplet

T: Thymine

TBE: Tris-boric acid EDTA

TBDMS: *tert*-Butyldimethylsilyl

TCA: Trichloroacetic acid

TEA: Triethylamine

TEAA: Triethylamine-acetic acid

TEMED: Tetramethylethylenediamine

THF: Tetrahydrofuran

TLC: Thin layer chromatography

T_m : Melting temperature

U: Uracil

UV: Ultraviolet

vis: Visible

wt; Wild-type

Chapter 1. Introduction

1.1 The RNA Interference Pathway

The RNA interference pathway was first discovered by plant biologists who tried to design petunias with higher pigmentation and brighter more robust colours by adding extra copies of the chalcone synthase gene, an important enzyme in flower colouration. Instead of the expected darker phenotypes, many plants instead had flowers with very few pigments expressed, producing mostly uncoloured flowers. They found both the endogenous and transgenic genes were being suppressed.¹ Further research a few years later found this lack of expression was due an increase in post-transcriptional mRNA degradation through a previously undiscovered mechanism, and they called it “co-suppression of gene expression”.² Seeing this anomaly in plants prompted the study of higher clades animals to find out if the same results could be observed. Conservation of this mRNA degradation pathway indicates how critical it is to the survival of both plants and animals. The study of mRNA silencing continued in model organisms such as *Drosophila* where “co-suppression” of mRNA was first observed in insects.³ In 1998 Fire and Mello’s research team found that the pathway by which the mRNA was being degraded was through the addition of double stranded RNA (dsRNA) which was the complement of the mRNA target. This was the start of the modern utilization of RNA interference and the study of its pathways and mechanisms, and they were awarded the 2006 Nobel prize in physiology and medicine for this work.⁴

The RNA-induced-silencing-complex (RISC) can be activated through the use of synthetically produced siRNAs transfected into cells via carrier molecules or transfection

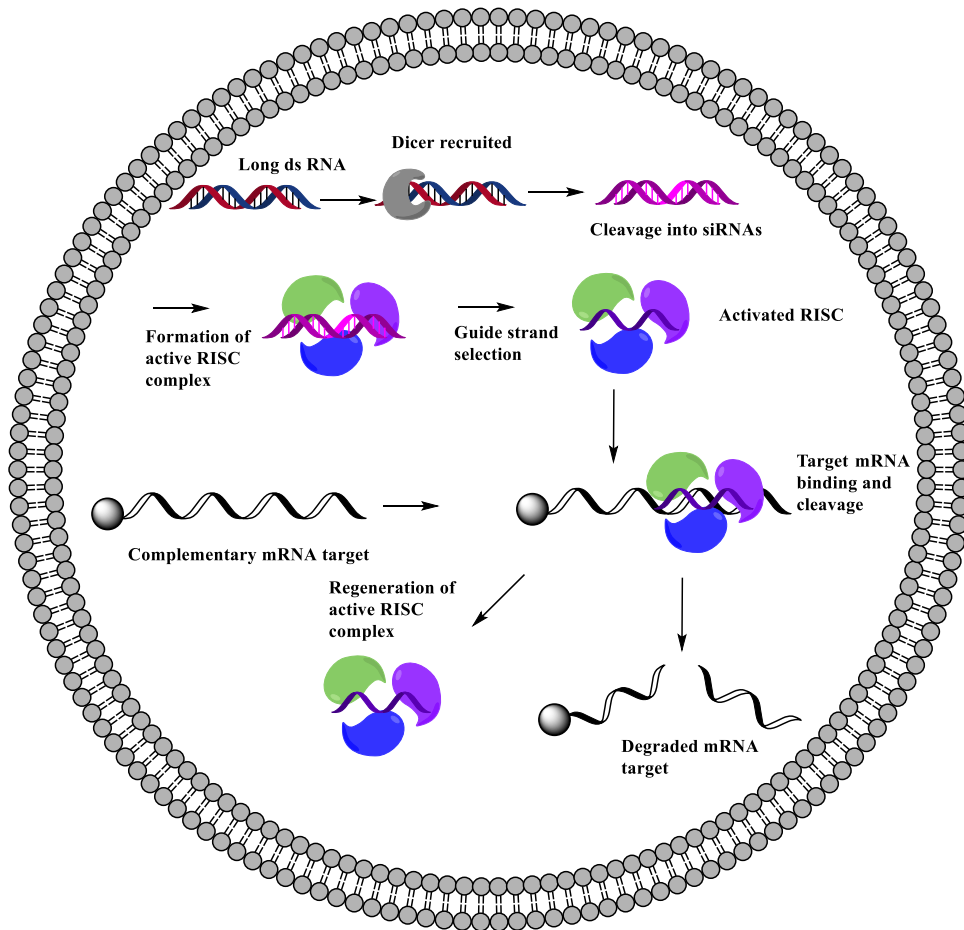


Figure 1.1. Dicer mediated RNA interference pathway in mammalian cells which targets mRNA for cleavage.

agents like viruses,^{8,9} and native long endogenous dsRNAs can be cleaved by the enzyme Dicer to form the active RISC complex through cleavage at the active site. These synthetic siRNAs are often 19-22 nucleotides long in order to bypass Dicer entirely through a secondary mechanism, although recruitment of Dicer into the pathway utilizing 27 bp long siRNAs does improve the efficacy of the gene silencing up to ten fold.¹⁰ Dicer itself is comprised of two RNase III motifs, a dsRNA binding domain and a RNA helicase domain which catalyzes the cleavage of the long dsRNA. One example of Dicer's significance is in the RISC cascade, Dicer knockdown studies in human HeLa cells showed an accumulation of dsRNAs in the cytoplasm which showed that without Dicer, these long

dsRNAs are not degraded, thus disabling the pathway for these longer duplexes. (See Figure 1.1).¹¹

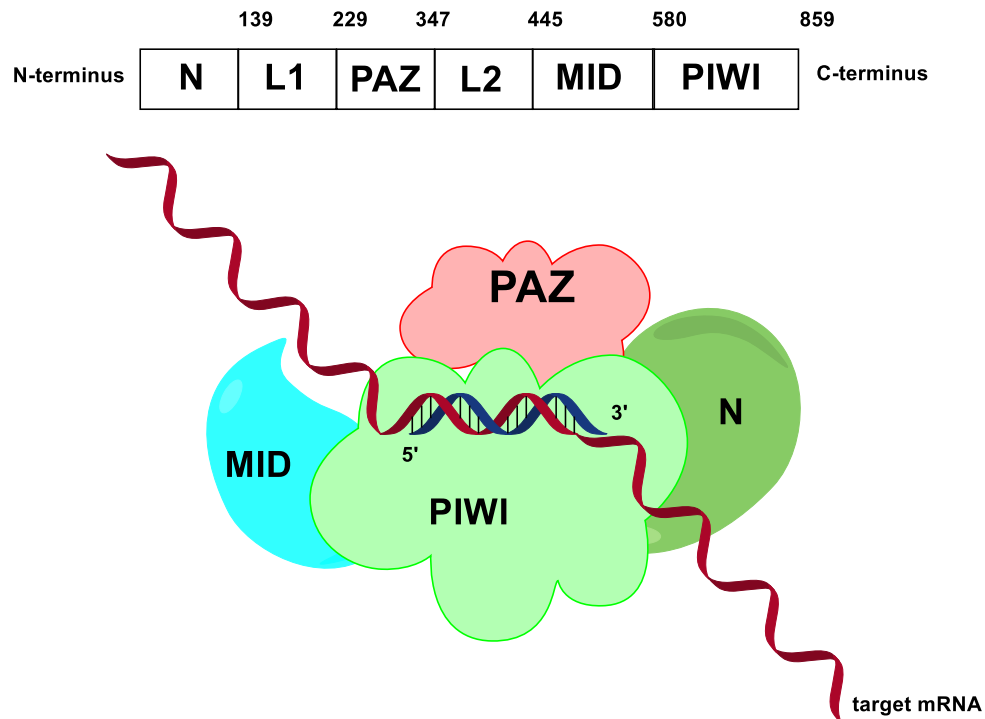


Figure 1.2. Diagram of human Ago2, including primary sequence with amino acid residue numbers (top) and proposed mechanism of strand selection and mRNA targeting.

The second component of the RISC pathway utilizes the endonuclease Argonaute 2 (Ago2) which catalyzes the cleavage of mRNAs by unwinding the passenger strand out of the duplex and retaining the guide strand as the target's complement (See Figure 1.2). Ago2 is composed of three domains; PAZ on the carboxyl terminus, a PIWI domain at the amino terminus and a central MID section.¹² The cleavage and destruction of the mRNAs is controlled by the PIWI domain, and binds to the 5' region of the passenger strand as well.¹³ The MID domain stabilizes the 5' phosphorylated end of the guide strand, while the PAZ domain binds to the 3' overhang of the passenger strand.¹⁴ Determination of these regions' interactions with each other and their mRNA targets are very important for the design, characterization and testing of chemically-altered siRNA therapeutics.¹⁵

1.2 Important areas of siRNAs

An siRNA duplex has several areas that are critical to form an active RISC complex. Since it is a duplex, it is formed of two complementary RNA strands. These strands are comprised of a sense and an antisense strand. In the field of RNAi, the sense strand is sometimes referred to as the passenger strand, and the antisense strand is sometimes named the guide strand. In this thesis, both sense (or passenger) and antisense (or guide) terms will be used interchangeably. The guide strand is the complement to the target mRNA, and the passenger strand is cleaved and discarded after the active RISC complex forms.

The guide and passenger strands are further sub-divided into regions which are important for RISC to find and cleave its target mRNA, as discussed in the previous section. They consist of a 5' end, central region, and 3' end. The 5' end is important for recognition of the correct guide strand, whereas the 3' end is often modified for nuclease resistance. The central region of the passenger strand is where Ago2 cleaves between base pairs 9 and 10 from the 5' end, although there is evidence this cleavage is not strictly required for unwinding the duplex (See Figure 1.3).^{54,77,78}

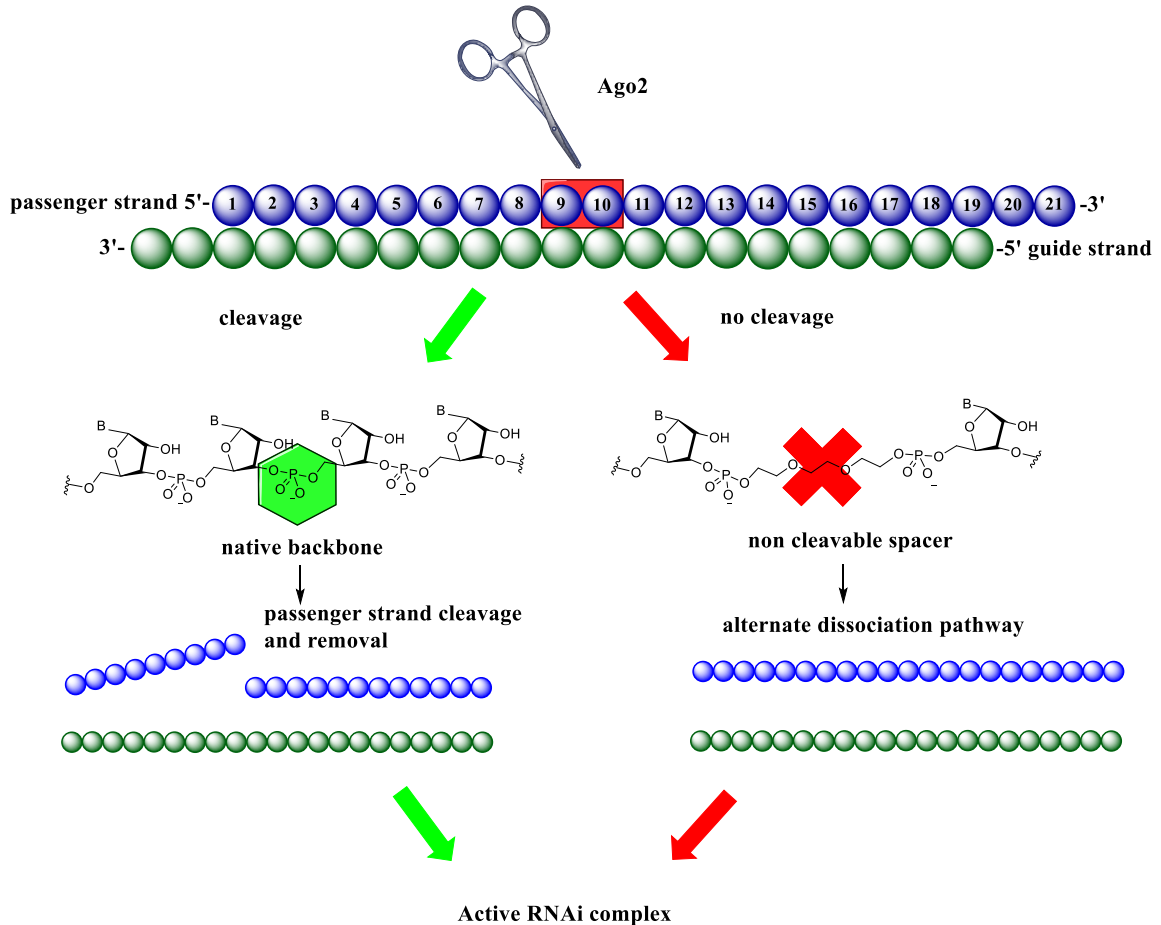


Figure 1.3. siRNA regions of importance. Left is canonical cleavage and strand selection, right is alternate dissociation pathway due to non-cleavable central region spacers.

1.3 Therapeutic challenges of siRNAs

Research into siRNA therapeutics is an expanding field with a lot of promise, focused on difficult to treat diseases such as cancer, Ebola viral infections, correction of auto immune disorders and to assist in the mitigation of symptoms from genetic defects through gene therapy.¹⁶ Several challenges need to be overcome with respect to siRNAs, such as stability, as they are targeted and degraded by exonucleases. In addition, appropriate delivery systems need to be developed in order to guarantee that the siRNA penetrates its cellular target, since they often have poor cell membrane permeability.¹⁷ One final challenge is undesired off-target effects on partially homologous targets, which can occur

with mismatch base pairing of the guide strand to non-target mRNAs, and siRNAs often accumulate or diffuse into non-target tissue types. One last challenge is the control of the siRNA in biological systems. Like most therapeutics, siRNAs once they are deployed are uncontrollable in the host. This means the therapeutic is always active, retaining activity in the host system until it is degraded, metabolized or eliminated by the body. These outcomes are based on the pharmacological profile of the specific therapeutics being utilized, which can be complex for different classes of therapeutics.

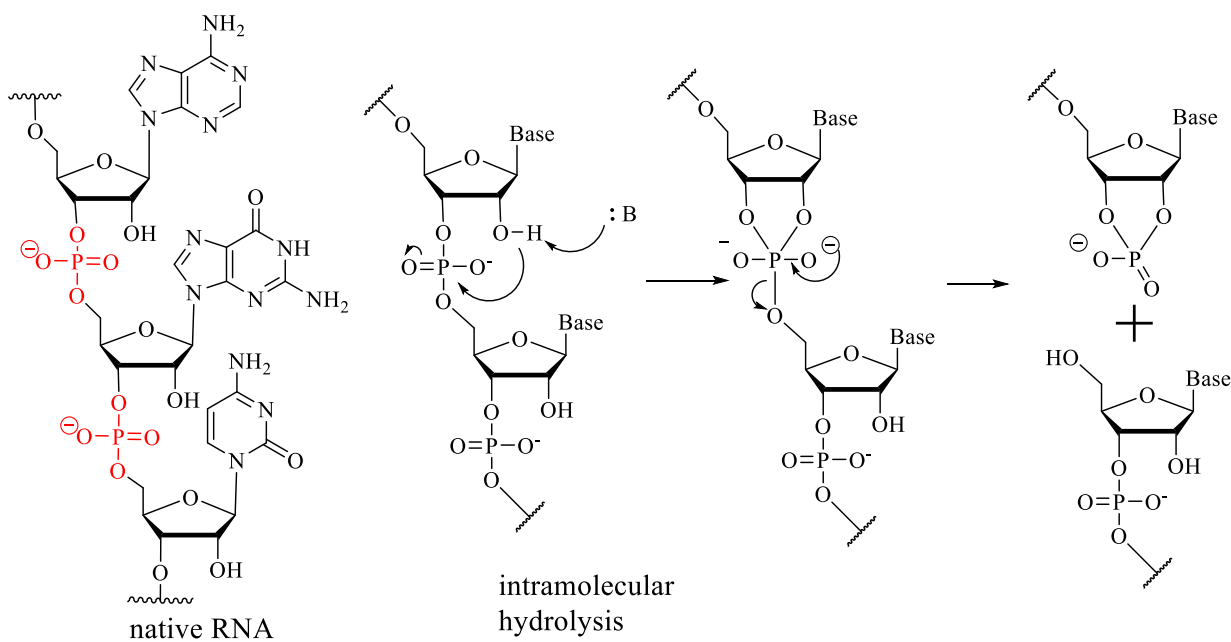


Figure 1.4. Degradation of native RNA with cleavage sites highlighted in red.

Every tissue type contains enzymes that exist for the degradation of nucleic acids, particularly exogenous DNA/RNA which provides a unique challenge by causing a reduction in the effectiveness of oligonucleotide-based therapies. These are called exo/endonucleases and are ubiquitous in the blood serum cell cytoplasm of mammals and even plants, which attacks the phosphodiester backbone of the RNA.¹⁸ The phosphodiester

bond can be hydrolyzed at physiological pH (~ 7.4) since phosphorous is oxophilic and water attacks at the electrophilic site on the phosphorus, making a thermodynamically favoured covalent bond.¹⁹ This oxophilic property of the phosphorous presents a new challenge to overcome, since it favours nucleophilic attack from the 2' hydroxyl on the ribose to the phosphorous in an intramolecular hydrolysis reaction, cleaving the oligonucleotide through self attack (Figure 1.4).²⁰ These prevalent stability challenges must be overcome or mitigated to design a more effective therapeutic.

Phosphodiester backbones are deprotonated at physiological pH because the hydroxyl group on the phosphorous has a pKa of around zero.²¹ This polyanionic RNA backbone reduces cell membrane permeability due to repulsion from the natural phospholipid bilayer.²² This does reduce cell uptake of the siRNA, which will impact the efficacy of the therapeutic.

SiRNA off-target effects are another challenge. Non-complementary base pairing occurs on mRNAs with near homologous structures and can result in RISC uptake and activation, mistakenly allowing Ago2 to cleave the wrong target mRNA.²³ Several other off-target effects exist, namely improper selection of the guide strand for cleavage, instead of the passenger strand. This results in an entirely novel mRNA target which could result in a negative outcome.²⁴ Diffusion into non target tissues from the active site, and accumulation of siRNAs into the liver and kidney are also off-target challenges that require solutions.

Controlling the timing of siRNA activity would be beneficial in several ways for therapeutics. One benefit is that the dose of the therapeutic can be high initially, and then inactivated when the desired outcome is reached. Moreover, this can be done multiple times

in a period of time to reduce drug resistance such as in the case of an antibiotic which becomes less effective overtime. In this way, resistance would be less likely to form and the therapeutic would be effective for longer periods. Another benefit is that accumulation of the siRNA in tissues like the liver and kidney, or other non-target tissues would be less of a concern since the siRNA could be inactivated where silencing activity is undesirable.

To overcome these challenges we can improve siRNAs as therapeutics through creative design of delivery systems and utilization of chemical modifications that could be used to improve the various flaws in the oligonucleotides.

1.4 Chemical modifications of siRNAs

Organic chemists utilize their unique skill sets to overcome the structural disadvantages on the siRNA. Care must be taken to generate modifications that increase the stability, but do not eliminate the gene silencing ability of the siRNA. For example, a structurally neutral, and uncleavable siRNA with no silencing activity is ineffective as a therapeutic.

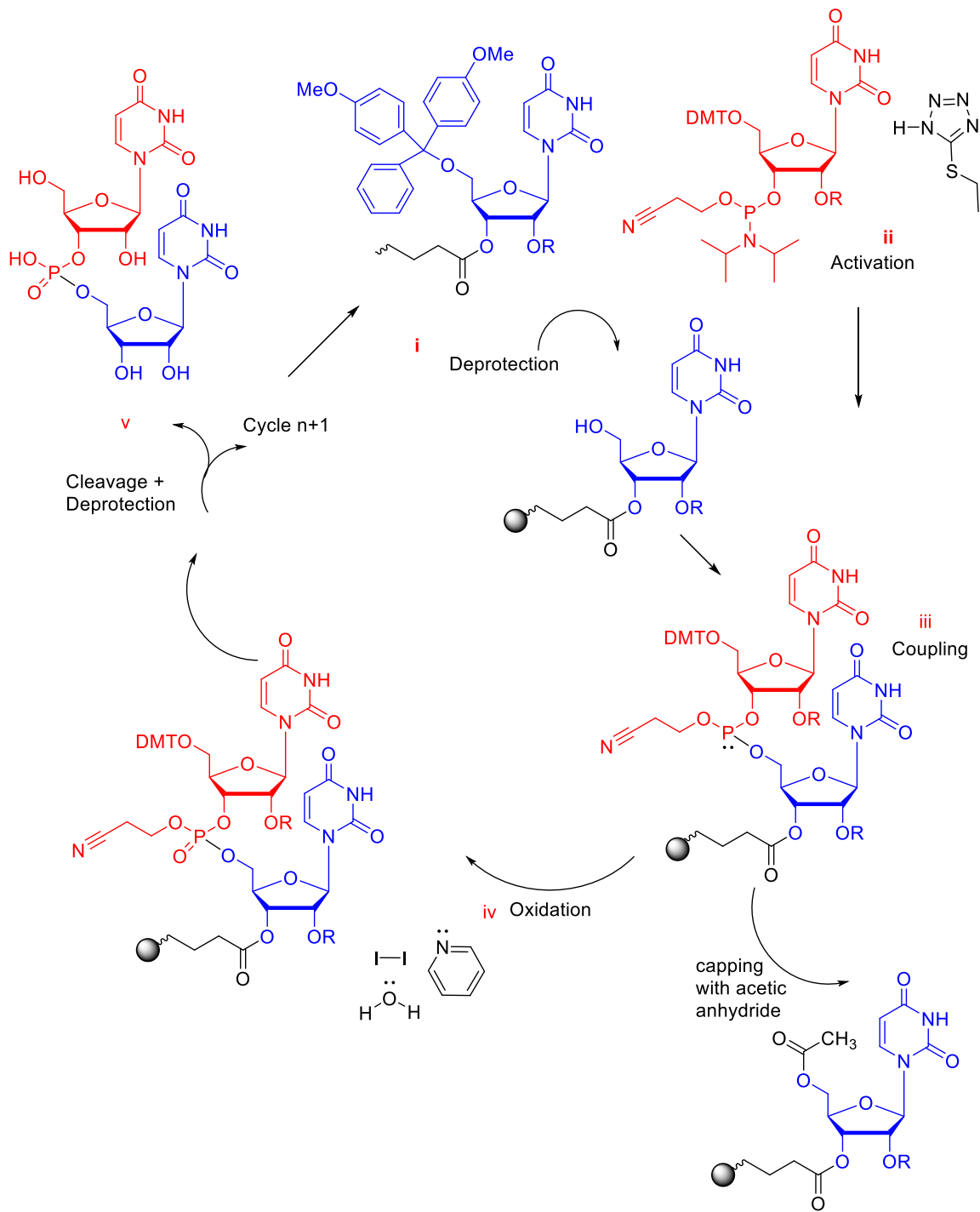


Figure 1.5. DMT-Phosphoramidite oligonucleotide solid-phase RNA synthesis.

Chemical modifications can have their own challenges, such as being expensive, easily degraded, toxic and volatile. Moreover, these modifications can disrupt secondary structure

and the hydrogen bonding with the complement strand. There are many chemical modifications which improve stability while retaining silencing ability. None of them however, will improve every aspect of siRNAs that need to be enhanced. Therefore, multiple types of modifications are required to be used simultaneously in the same oligonucleotide to effectively overcome the limitations of the wildtype siRNAs.

Since chemical modification of oligonucleotides is the goal, and wildtype biological structures are not suitable for use in adding diverse modifications to oligonucleotides, the use of commercial DMT (dimethoxytrityl)-phosphoramidites with solid phase synthesis, turns an incredibly challenging task into a reliable and secure way of adding virtually any chemical modification into the oligonucleotide.³⁶ Synthesizing oligos a single base pair at a time, solid phase synthesis using controlled pore glass (CPG) supports is one of the best and robust methods of not only chemical synthesis of DNA or RNA, but adding in unique bases that do not exist in nature (Figure 1.5).³⁷ Using these methods, novel chemical modifications can be incorporated into DNA or RNA molecules, where one end of the building block is protected with a DMT group, and a phosphoramidite electrophile is appended on the other end of the building block.³⁸

The CPG support can be purchased with a variety of bases attached to the solid support. The initial deprotection is acid catalyzed removal of the DMT using trichloroacetic acid which affords a primary alcohol that can react with the 2' phosphoramidite of the next base in the sequence (Fig 1.5, step i). Activation of the phosphoramidite base via ethylthiotetrazole displaces the diisopropylamine group from the phosphoramidite (Fig 1.5, step ii). Because of the oxophilic nature of the phosphorus as previously discussed, the now exposed primary alcohol can attack the phosphorus center, thus coupling the bases together

(Fig 1.5, step iii).³⁹ Oxidation of the phosphite to phosphate occurs in the presence of iodine, water and pyridine (Fig 1.5, step iv). At this stage the cycle can continue to the next nucleotide to be added, or if the desired length has been reached the oligos can be cleaved from the solid support, deprotected and then used in whichever experiment was planned (v).⁴⁰

Given the highly optimized DNA and RNA synthesis available to nucleic acid chemists, there are several chemical modifications that can be done to an oligonucleotide: 1) backbone substitution or addition; 2) modification of the sugar and; 3) nucleobase modifications. This dissertation will be focused on modifying the backbone, while simultaneously replacing nucleobases with neutral, non-cleavable azobenzene spacers.

Backbone modifications can replace one or several base pairs with non-cleavable, neutral spacers that prevent cleavage by endonucleases *in vivo*. Endonucleases target phosphodiester linkages between nucleobases, and with those replaced they are now unsuitable substrates for cleavage. A simple replacement modification is altering one of the non-bonding oxygen atoms with a sulfur.⁴¹ This phosphorothioate (PS) provides extra stability by imparting nuclease resistance.⁴² This modification can be disruptive when placed in or adjacent to the Ago2 cleavage site, since the PS substitution results in a chiral center and different stereoisomers are often poor substrates for enzymes like Ago2.⁴³ Sugar modifications may be simple changes such as adding a methyl group to the 2' hydroxyl to prevent self hydrolysis. This type of modification is called a 2'-O-methyl

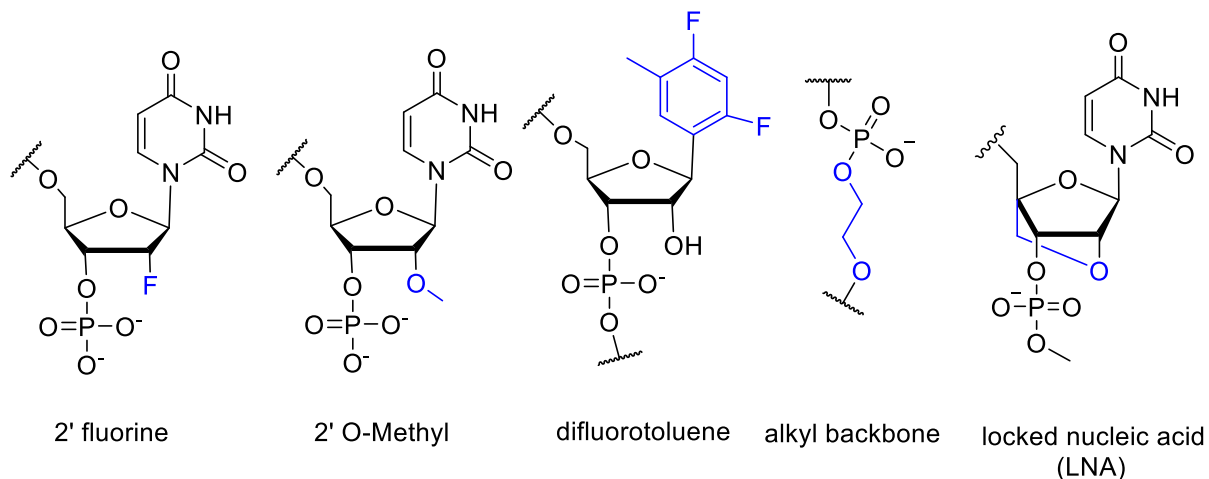


Figure 1.6. Various chemically-modified RNA bases

modification.⁴⁴ More complex sugar modifications can also be made as well. Another common sugar replacement is 2'-fluorine, which preserves the C_3' -endo conformation similarly to the 2'-OMe modification. They both increase nuclease stability and are less likely to illicit an immune response.⁸² Locked nucleic acids (LNAs) use a methylene bridge connecting the C_4' of the ribose to the 2'-OH which forces the sugar into the C_3' -endo pucker.³⁴ An individual LNA sugar replacement is able to increase melting temperature of a duplex between 5-10 °C.⁸³ It will also impart exonuclease resistance when placed at the 3' end.⁸⁴ Nucleobases can be modified as well. For example, 2,4-difluorotoluene is a nucleotide modification that has been shown to be useful in destabilizing duplexes to provide enhanced gene-silencing profiles.^{45,46} (Figure 1.6).

Despite these ground-breaking modifications, some issues persist and new ones can arise. To ensure efficient RNAi activity, the siRNA must be in a A-form helix.⁴⁷ Ensuring a sufficient amount of flexibility in the duplex to maintain A-form helix formation is essential in chemically-modified oligonucleotide design. The ribose sugar conformation

can be adjusted as well through utilizing gauche and anomeric effects. The favourable conformation of wildtype dsRNA is the C_3' -endo/ C_2' -exo conformation, and modifications such as the 2'-fluoro stabilize the C_3' -endo conformation,⁴⁸ thus providing excellent RNAi activity *in vivo* when used within siRNAs.⁴⁹

The final way to modify RNA is to alter the nitrogenous bases to create a more robust and effective siRNA. Some modifications are known to disrupt Watson-Crick base pairing, and care should be taken to minimize hydrogen bond impairment through good siRNA design. The 2,4-difluorotoluene (dFT) is a thymine (DNA) and uracil (RNA) derivative with fluorine replacing oxygens on the nitrogenous base (Figure 1.6).⁵⁰ This causes only small levels of disruption to the duplex when placed at the 5' end of the guide strand. Thusly affinity to the target is increased making it more effective. The dFT in other locations in the guide strand disrupt hydrogen bonding, making the siRNA less effective.⁵¹

The addition of novel chemical modifications to siRNAs will often alter the biophysical profile of duplexes. Two critical properties that must be maintained within critical parameters are melting temperature (T_m) which rates thermal stability based on the inflection point of duplex destabilization and the helix conformation which must be in the A-form to be recognized by RISC.⁵² Thermal stability is important since siRNAs that dissociate at low temperatures, such as physiological body temperatures (37 °C), will be inactive *in vivo* because single stranded RNA cannot act as a substrate for the active RISC complex.⁵³ A moderate reduction in T_m is well tolerated however, and that is fortuitous as most substitutions either mismatch or delete hydrogen bonding from the base pairs.⁵⁴

1.5 Azobenzene and its Role in Nucleic Acid Modification

The direction of this dissertation is to overcome some of these limitations through the development of a fine-tunable, light controllable photo-switch. This is done through the addition of an azobenzene into the guide or passenger strand of the siRNA, to develop a photo-switchable siRNA can be controlled in real time, with light. Depending on the specific azobenzene derivative, they are inactivated with either UV (chapters II and III), red light (chapter IV), or green light (chapter V) and reactivated with broadband visible light, violet light, or blue light respectively.

Azobenzene is a molecule composed of two phenyl rings linked together by a nitrogen-nitrogen double bond (Figure 1.7).⁵⁵

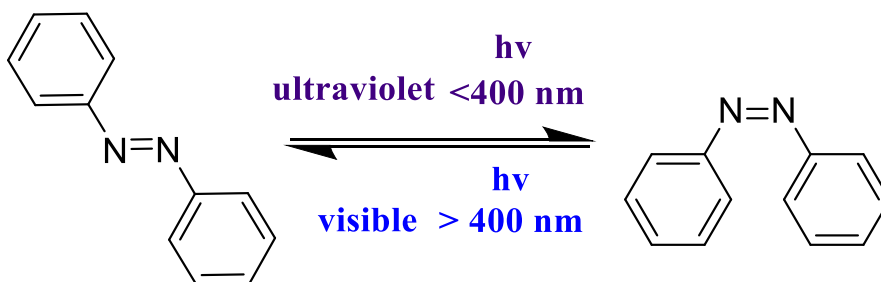


Figure 1.7. Conformation change of azobenzene when exposed to light, *trans* (left) and *cis* (right)

This molecule was chosen because when exposed to various wavelengths of light, there is a large shift in the structures' three-dimensional profile. The molecule can isomerize at the N=N bond between the *trans* and *cis* stereoisomers (Figure 1.8).⁵⁶ This photo-isomerization is labile and robust, and maintains high photodynamic conversion after several isomerizations without exhaustion.⁵⁷ The photo-switching occurs from *trans* to *cis* when the molecule is exposed to UV light in the 360 nm range, and the reverse *cis* to *trans* isomerization occurs when exposed to blue light around 430 nm.

The wavelengths at which these isomerizations occur can be altered by substitutions at the *ortho* position of the phenyl rings adjacent to the N=N bond.⁵⁸ Thermal stability of the *cis* conformer is extremely critical. Azobenzene will thermally relax back from *cis* to the *trans* form due to the ambient thermal energy, and natural instability of the adjacent phenyl rings in the *cis* conformer which are twisted out of plane towards each other.⁵⁹ Higher temperatures cause thermal relaxations to occur faster, since the molecule has more energy than at lower temperatures. Exposure over long periods of time makes this apparent when the experiment temperature exceeds the functional half-life of the molecule. For example, the half-life of *cis* azobenzene is about 4 hours at 37 °C.⁶⁰

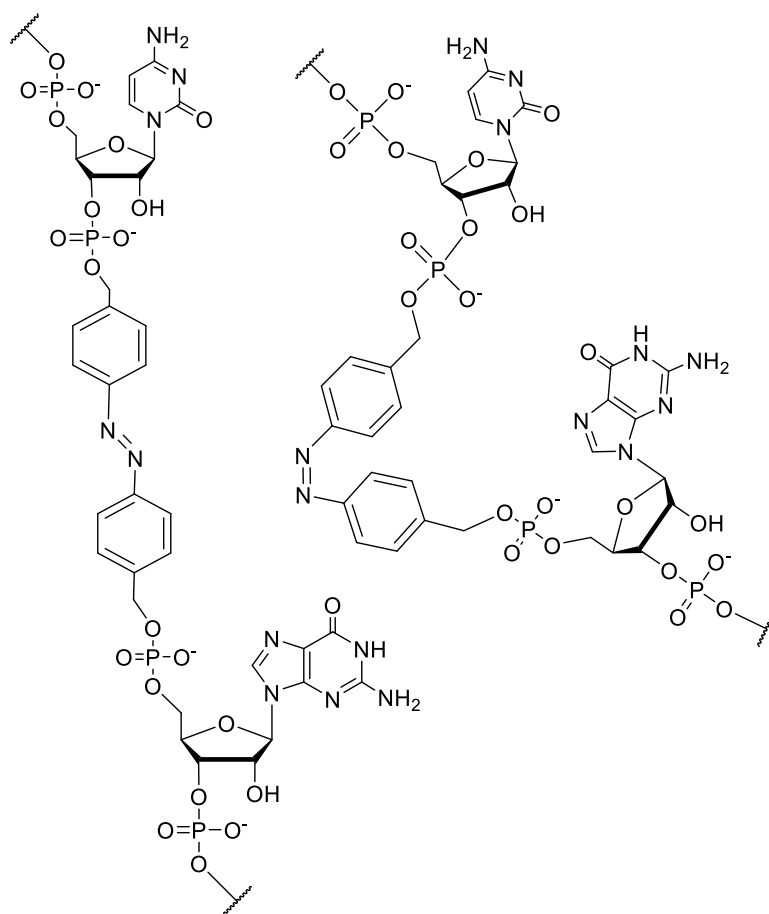


Figure 1.8. Conformational change of azobenzene *trans* (left ~9Å) and *cis* (right ~5.5Å) when inserted into RNA

These unique properties of azobenzene make it ideal for utilization in several fields for optical control. One example is liquid crystals for image storage, using azobenzenes as a liquid crystal display (LCD) in order to improve response times for computer and television screens.⁶¹ They have been used to control the rigidity of polymers with light.⁶² There has been much research in using azobenzene as a photo-switch for biopolymers *in vitro* and *in vivo* control various biological functions with light in real time. This photo-switching aspect has been discovered to be effective in proteins, DNA and RNA as well as DNA/RNA hybrids and as a method for delivery via irreversible photocaging.

Proteins utilize azobenzene by having one end of the azobenzene tethered to the protein's active site, but also attached to the ligand for the protein. Light exposure converts the conformer to *cis* from *trans* which then positions the ligand into the active site turns it on.⁶³ The protein in the more stable *trans* position then keeps the ligand in the active site until light exposure with visible wavelengths flips the ligand back out of the pocket. Azobenzene can be used to control the secondary structure of proteins, such as allowing the isomerization to disrupt an alpha helix, or make kinks in a beta sheet, actively controlling whether the protein is in an active or inactive form in real time.⁶⁴ Through its many uses azobenzene has become synonymous with photo-switch, and protein utilizations will continue well into the foreseeable future such as with RET (rearranged during transfection) kinase inhibitors. Located on chromosome ten, the RET gene has many natural alternative splices (single gene coding for many proteins). They are transmembrane receptors (proteins which span the entire membrane to which they are permanently attached), exist in many tissue types, and are necessary for healthy cell function, but can become malignant in several different cancers (notably thyroid) which make them a good

therapeutic targets with which to functionalize with azobenzene.⁶⁵ Being neurotrophic receptors, the inhibition of cancer growth by stopping the neurotransmitters from binding by plugging the active site with azobenzene or preventing the receptor protein from being expressed through the RNA interference pathway.

Nucleic acids have been shown to be promiscuous with respect to azobenzene modification. Controlling translation in real time would be advantageous for researchers. Advances in this field include controlling DNA/RNA hybridization by utilizing the azobenzene as a substitution of the nitrogenous base so when exposed to UV light the *cis* conformer breaks hydrogen bonds and the duplex turns unstable and separates into single strands of biopolymer.⁶⁶ Asunama *et al.*'s group used a threonine scaffold in the backbone with an azobenzene acting as a nitrogenous base replacement.⁶⁷ Placement of an azobenzene in the loop position of a hairpin oligo, offers control over whether the hairpin is self-annealed, or separated.⁶⁸ Short hairpin RNAs can activate RISC,⁶⁹ and could be utilized for translational control. An intriguing study in 2015 by Wu *et al.* and their group revealed that they could control RNase H activity (exclusively targets DNA/RNA hybrids) by using a deoxynucleotide complement to an RNA strand, with dumbbell shaped azobenzene overhangs adjacent to the complementary region. Exposure to light allows annealing of the RNA or DNA strands, and its subsequent digestion of the hybrid by RNase H.⁷⁰ This is the kind of temporal control that could be utilized in siRNAs to make effective therapeutics.

Work with non-reversible photo cages has been advancing as well. A photocage is a molecule or several molecules that when exposed to light either change shape or are cleaved entirely from the molecule.⁷¹ One example of a non-reversible photocage are *o*-

nitrobenzyl derivatives, that when exposed to UV light goes through an intramolecular hydrogen abstraction via the nitro group which forms the aci-nitro and goes through a rearrangement to nitroso derivatives (Figure 1.9).⁷²

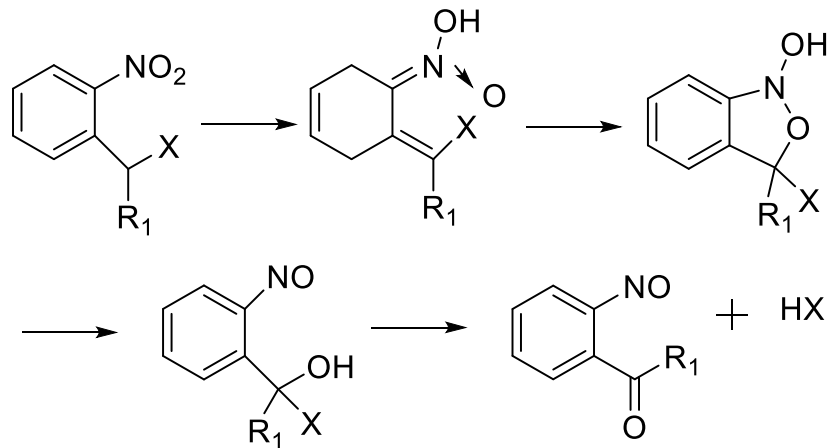


Figure 1.9. *o*-nitrobenzyl derivative for use as a photocage. Addition of UV light breaks the N=O pi bond, allowing intramolecular attack of the oxygen, forming a five member ring. Intramolecular proton transfer causes the ring to break. There is then a decarboxylation and the photocage is released from the payload, activating it.

Using photoactive compounds they can be attached to small molecules such as drugs,⁷³ or enzyme substrates⁷⁴ (as done by Hiraoka and Hamachi 2003) and have them released upon exposure to light, keeping them inactive until needed. With respect to enzymes, they are used to increase the size of the substrate so the molecule cannot go inside the active site of the enzyme. The steric bulk is removed by light, and activity will then continue as the substrate can now enter the enzyme active site.⁷⁵ Mikat and Heckel in 2007 also showed that it is possible to control RNAi with photocage materials by surrounding the mRNA cleavage site between base pairs 10 and 11 in order to disable RNAi. Irradiation of UV light at 366 nm was shown to reactivate the pathway and had similar activity to the unmodified siRNAs.⁷⁶

Work from Dr. Jean-Paul Desaulniers' research group has shown that aromatic spacer linkages⁷⁷ and non-aromatic alkyl spacer linkages⁵⁴ are substrates for the RNAi pathway when these modifications are placed within the central region of the sense strand. This suggests that a large aromatic group may also function at the central region and would make an appropriate bioactive siRNA bearing unique functionality. Desaulniers *et al.* (2017) has shown siRNAs with biphenyl aromatic linkers did in fact have excellent knockdown ability targeting the endogenous *BCL-2* gene.⁷⁸ Additional recent work from his group has also revealed that large hydrophobic groups such as cholesterol, and large polar groups such as folic acid, can cross the cell membrane and inhibit gene expression without a transfection carrier^{79,85,86} (Figure 1.10 shows the progression of some of these modifications).

With all of this evidence taken together, azobenzene has many unique properties that could be utilized within an siRNA. It has an electron dense core, is neutral in charge (that can offset the polyanionic backbone of an siRNA), is highly modifiable for fine tuning wavelengths for *cis/trans* isomerization, and is relatively non-toxic. Despite these qualities, siRNAs bearing azobenzenes in the central region have not been explored until recently. We are hopeful that this fine tuning could prevent localized off-target effects to surrounding healthy tissue, by only having the siRNA active in the specific target tissues that are problematic, through the application of light to selected areas. Many cancer treatments employ systems that harm healthy tissue, such as pharmaceuticals and excision, but some healthy tissue is always destroyed in the process. An azobenzene-modified siRNA may be able to mitigate some of these disadvantages. Homologous mRNA off-target effects may still occur, causing undesirable phenotypes or unexpected toxicity but

these are usually concentration dependant and less likely to occur at the concentrations with which we tested these siRNAs.⁸⁰

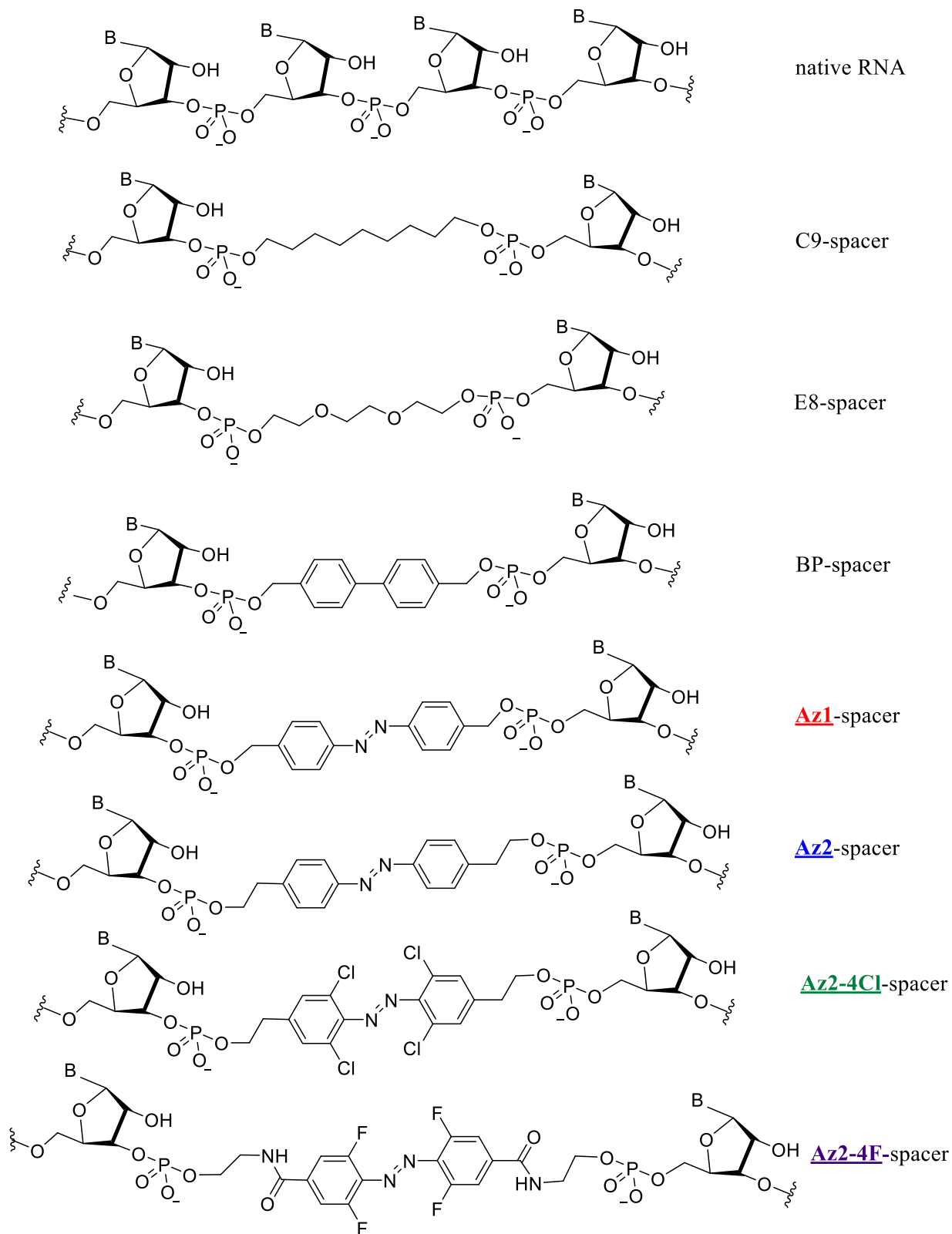


Figure 1.10 Various central region modifications used within siRNAs from Dr. Jean-Paul Desautniers' research group^{54, 77, 78, 79,87-90}

1.6 The Benefits of Using an Azobenzene Modification

Incorporating this modification into a biopolymer like siRNA, this conformational change potentially allows us to control the activation and inactivation of the siRNA through the application of the correct wavelength of light. Azobenzene as a replacement for phosphodiester bonds in the backbone is more stable, since endo- and exonucleases cannot use it as a substrate. However, azobenzene can be metabolized through the GSH (reduced glutathione) pathway, a tripeptide that is prevalent in the cytoplasm and has antioxidant properties. An additional beneficial property of azobenzene is that it has no anionic regions, thus potentially increasing cell membrane permeability due to less interactions between the negatively charged siRNA and the cell membrane, which is also composed of negatively charged phospholipids.³⁴

Utilization of a photo-switch into the siRNA would allow genes to be targeted and controlled without the addition of a second small molecule inhibitor as is often the case with drugs such as aptamers. Eliminating this extra step could make drugs easier to be controlled inside the nucleus, since the nuclear membrane can be difficult to cross with conventional pharmaceuticals. It also allows for good spatial and temporal control over translation, by targeting the mRNA preventing protein formation. Four azobenzene derivatives, Az1, Az2, Az2-4Cl, and Az2-4F (Figure 1.10) were synthesized and their stability and activity were tested biologically against both endogenous and exogenous gene targets. Further potential targets for these siRNAs could be the *BCL-2* or *BCL-3* genes involved in non-Hodgkins lymphoma⁸¹ or any other cancer oncogenes. The genes that encode *BCL-2* and *BCL-3* are anti-apoptotic proteins that control the timing of cell death. Interference in this pathway prevents apoptosis by the overexpression of the proteins and

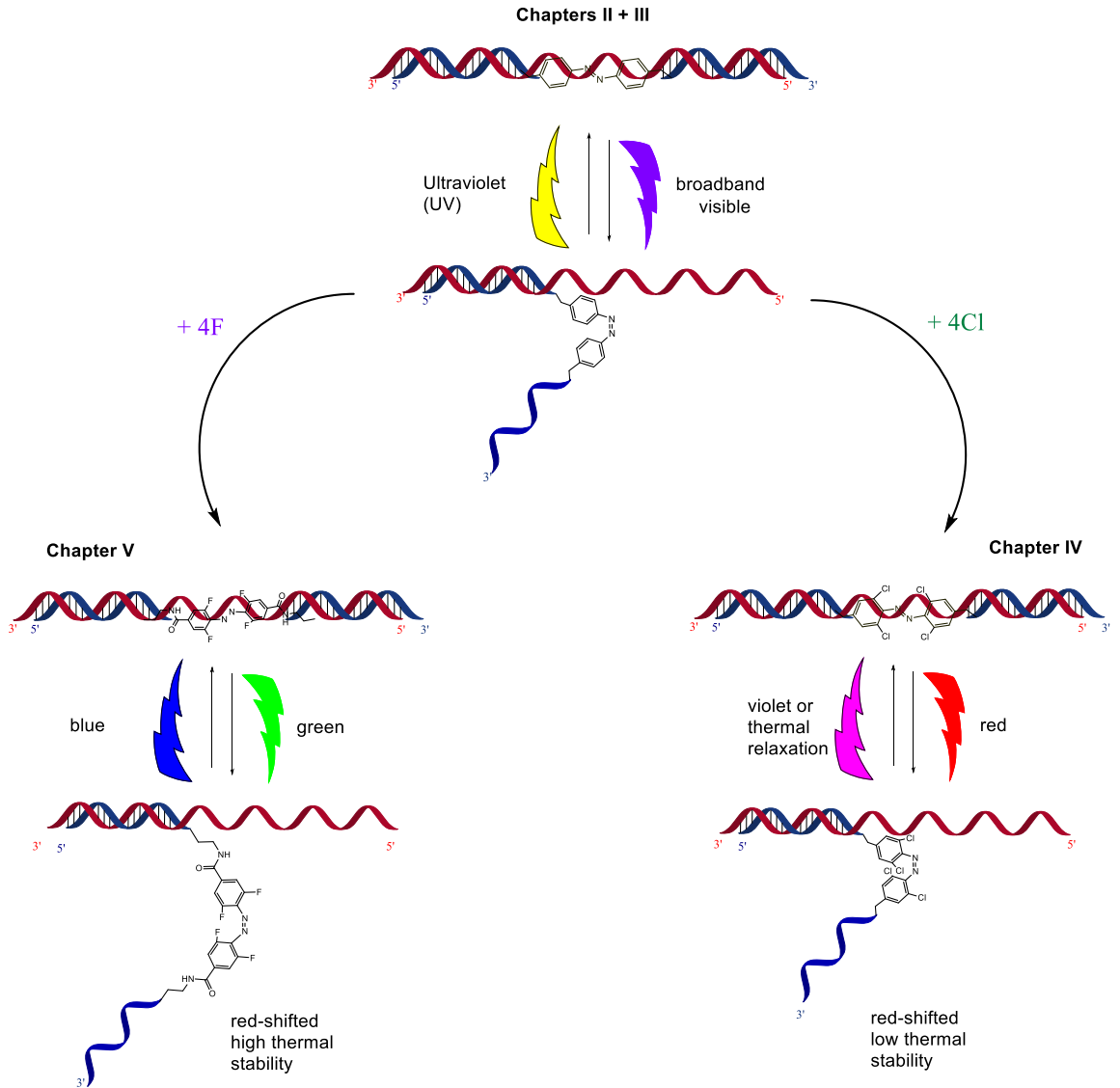


Figure 1.11 Photoinduced inactivation and reactivation of siRNAzOs. The blue strand corresponds to the sense strand and contains the azobenzene moiety. The red strand corresponds to the antisense strand. Several azobenzene derivatives are embedded within siRNA duplexes showcasing how chemical modifications affect physical properties.⁸⁷⁻⁹⁰

can allow cancer cells to persist indefinitely. Targeting the mRNA we prevent protein formation by controlling translation through degradation of the mRNA. This would allow therapeutic targets to be reached more easily, since only one membrane would have to be crossed in order to silence the gene of interest which would increase the effectiveness of the treatment. Figure 1.11 shows the predicted structures of the siRNA duplexes when exposed to various wavelengths of light. Utilizing different chemical modifications in the

ortho position of the azobenzene changes the photo-physical properties of the N=N bond energy levels.

The azobenzene N=N bond is composed of two λ_{\max} maxima, named for the energy levels of the orbitals the electrons jump from and to. The first maxima is in the UV portion of the spectra, with a large extinction coefficient called the $\pi \rightarrow \pi^*$ transition. The second maxima has a notably weaker extinction coefficient and is labelled the $n \rightarrow \pi^*$ transition.⁵⁸ An unmodified azobenzene has a very strong $\pi \rightarrow \pi^*$ and requires high energy UV light to convert from *trans* to *cis* isomerization. Conversely, the $n \rightarrow \pi^*$ transition is so weak that lower energy broadband visible light will promote *cis* to *trans* conversion, which is directly related to the *trans* conformer being the more stable isomer. Alteration of the “push and pull” electronics of the conjugated system through chemical modification influences the wavelengths necessary for photo-isomerization in both directions. This is done to overcome the azobenzene’s natural limitations.⁵⁸ As discussed in Chapter IV, the tetrachlorination of the azobenzene resulted in significant changes to the N=N bond transitions.⁹⁰⁻⁹² We show through our bio-physical data, that the synthesized tetrachloroazobenzene uses red light to induce *cis* conformer formation ($\lambda_{\max} = 456$ nm), while blue-violet region light reverses this isomerization to the *trans* isomer ($\lambda_{\max} = 438$ nm). This difference in the two $n \rightarrow \pi^*$ is almost 20 nm. This is in line with previous work by Hecht and co-workers where they show that tetra-fluorinated azobenzene groups can get separation of the $n \rightarrow \pi^*$ of 22-50 nm, depending on the specific para substitutions to the N=N bond.⁹³ Interestingly, as discussed in Chapter V, tetra-fluorinated azobenzene derivatives caused a difference of 53 nm in the $n \rightarrow \pi^*$ transitions, where ($\lambda_{\max} = 468$ nm)

uses green wavelength light to convert into the *cis* conformer, and blue wavelength will reverse it back to the *trans* conformer ($\lambda_{\text{max}} = 415 \text{ nm}$).

1.7 Research Objectives

Gene silencing at the translational level has proven to be an effective pathway for studying gene function, and in the future its development into bio-molecular tools for research and its utility as a therapeutic should not be overlooked. In this regard, the improvement of siRNAs into better therapeutics and tools through chemical modifications is a continuing area of study. The RNAi route is promiscuous to synthetic siRNAs which down regulates gene expression with high accuracy and excellent knockdown at low to moderate concentrations. Chemical modifications of siRNAs in various areas can improve cellular uptake, membrane permeability, nuclease resistance and toxicity reduction. These are limitations that exist in both DNA/RNA and can be overcome through synthetic chemical alterations which improve one or more of these properties.

The main focus of this study is to replace a two nucleobase section of the passenger strand of the siRNA with various azobenzene derivatives in order to control its activity in biological cell culture.

Our hypothesis is that by inserting an azobenzene derivative into the siRNA backbone, we will allow tunable photochemical control of the siRNA's activity through the use of light. This can be achieved by activating the complex with specific wavelength of light to ensure the azobenzene is in the *trans* conformation, and adheres to A-form RNA helical formation. Furthermore, inactivation of the RNA duplex can be achieved with a light of specific

wavelength to render the azobenzene in the *cis* conformation. This will be outlined in the next five objectives of this thesis.

1.7.1 Objective 1:

Objective 1 of this project will involve the development of a small library of central region and 3' end azobenzene containing siRNA oligonucleotides. This step adds the functionality of N=N bond, through the azobenzene moiety, and with it the photo-switch. The modification will be synthesized using organic chemistry and synthetically incorporated into RNA oligonucleotides.

1.7.2 Objective 2:

Objective 2 will investigate azobenzene containing sense strands and anneal them to their complement sequence to form active siRNA duplexes. These annealed siRNAs will undergo hybridization testing via melting temperature assays as well testing of the A-form helix with circular dichroism to confirm the secondary structure. These bio-physical characterizations will be tested under both visible and ultraviolet conditions in order to determine the activity of the photo-switch. Further bio-physical characterization of the siRNAs will be through absorbance spectra and how it changes, as well as HPLC characterizations in order to quantify the *trans* to *cis* conversions immediately and quantitatively.

1.7.3 Objective 3:

Objective 3 will test the siRNAs ability to silence gene expression using the dual luciferase reporter system from Promega. This will allow for easy quantification of the siRNAs knockdown ability. After gene silencing is confirmed the siRNAs will be treated with UV

light in order to inactivate them *in vivo* and if successful they will then be treated with visible light to see if they can be reactivated after a period of inactivity. Their reversibility will also be tested, through application of multiple rounds of UV/visible light treatments in order to keep the siRNA inactive for up to 24 h. SiRNAs with modifications at the 3' end will also be tested for nuclease resistance.

1.7.4 Objective 4:

Objective 4 will utilize organic chemistry to tetra-chlorinate the *ortho* position of the azobenzene (Az2-4Cl) in order to move the $\pi \rightarrow \pi^*$ transition out of the UV portion of the spectrum by red-shifting it and allowing inactivation with red wavelength light, instead of high energy harmful UV light. Biophysical characterizations will follow to determine the photo-switch's efficiency and determine the amount of red-shift and test gene silencing ability.

1.7.5 Objective 5:

Objective 5 will involve the use of synthetic chemistry techniques to generate a tetra-fluorinated azobenzene derivative (Az2-4F) to further improve on the photo-chemical properties of the siRNAs. After synthesis, the Az2-4F derivative will be incorporated into the antisense strand of the oligonucleotide, where it will then be tested for duplex formation, thermal stability of the duplex, photo-switching ability, amount of red-shift and *cis* conformer thermal stability. Gene silencing profiles will be measured, and the length of time that the *cis* conformer will persist in cell culture also determined.

1.8 REFERENCES- Chapter I- Introduction

1. Alberts B. (2008) *Molecular biology of the cell*. New York: Garland Science. ISBN 0-8153-4105-9
2. Li, S. Mason, C. E., Chakravarti, A.; Green, E., Eds. *Annu Rev Genomics Hum Genet* **2014**; Vol. 15, pp 127-150.
3. Egli, M. Minasov, G. Tereshko, V. Pallan, P. S. Teplova, M. Inamati, G. B. Lesnik, E. A. Owens, S. R. Ross, B. S. Prakash, T. P. Manoharan, M. *Biochemistry* **2005**, *44* (25), 9045-9057.
4. Mack, G. S. *Nat. Biotechnol.* **2007**, *25* (6), 631-638.
5. Higgs, P. G., *Q. Rev. Biophys.* **2000**, *33* (3), 199-253.
6. Parkinson, G. N. Lee, M. P. H. Neidle, S. *Nature* **2002**, *417* (6891), 876-880.
7. Burge, S. Parkinson, G. N. Hazel, P. Todd, A. K. Neidle, S. *Nucleic Acids Res.* **2006**, *34* (19), 5402-5415.
8. Frank, T. D. *J. Theor. Biol.* **2016**, *392*, 62-68.
9. Allison, L. (2007). *Fundamental Molecular Biology*. London: Blackwell Publishing. ISBN 978-1-4051-0379-4.
10. Griffiths, A. (2008). *Introduction to Genetic Analysis* (9th ed.). New York: W.H. Freeman and Company. ISBN 978-0-7167-6887-6.
11. Wei, X. P. Ghosh, S. K. Taylor, M. E. Johnson, V. A. Emini, E. A. Deutsch, P. Lifson, J. D. Bonhoeffer, S. Nowak, M. A. Hahn, B. H. Saag, M. S. Shaw, G. M., *Nature* **1995**, *373* (6510), 117-122.
12. Mattaj, I. W. Englmeier, L., *Annu. Rev. Biochem.* **1998**, *67*, 265-306.
13. Napoli, C. Lemieux, C. Jorgensen, R. *Plant Cell* **1990**, *2* (4), 279-289.
14. Vanbloklant, R. Vandergeest, N. Mol, J. N. M. Kooter, J. M., *Plant J.* **1994**, *6* (6), 861-877.
15. PalBhadra, M. Bhadra, U. Birchler, J. A. *Cell* **1997**, *90* (3), 479-490.

16. Fire, A. Xu, S. Q. Montgomery, M. K. Kostas, S. A. Driver, S. E. Mello, C. C., *Nature* **1998**, *391* (6669), 806-811.
17. Elbashir, S. M. Harborth, J. Lendeckel, W. Yalcin, A. Weber, K. Tuschl, T. *Nature* **2001**, *411* (6836), 494-498.
18. Daniels, S. M. Gatignol, A. *Microbiol. Mol. Biol. Rev.* **2012**, *76* (3), 652.
19. Schirle, N. T. MacRae, I. J. *Science* **2012**, *336* (6084), 1037-1040.
20. Zhuang, X. W. *Abstr. Pap. Am. Chem. Soc.* **2003**, 226, U299-U299.
21. Joo, K. I. Wang, P. *Gene Ther.* **2008**, *15* (20), 1384-1396.
22. Amarzguioui, M. Lundberg, P. Cantin, E. Hagstrom, J. Behlke, M. A. Rossi, J. J., *Nat. Protoc.* **2006**, *1* (2), 508-517.
23. Hutvagner, G. McLachlan, J. Pasquinelli, A. E. Balint, E. Tuschl, T. Zamore, P. D. *Science* **2001**, *293* (5531), 834-838.
24. Liu, J. D. Carmell, M. A. Rivas, F. V. Marsden, C. G. Thomson, J. M. Song, J. J. Hammond, S. M. Joshua-Tor, L. Hannon, G. J. *Science* **2004**, *305* (5689), 1437-1441.
25. Wang, Y. L. Juranek, S. Li, H. T. Sheng, G. Wardle, G. S. Tuschl, T. Patel, D. J., *Nature* **2009**, *461* (7265), 754-U3
26. Prakash, T. P. Allerson, C. R. Dande, P. Vickers, T. A. Sioufi, N. Jarres, R. Baker, B. F. Swayze, E. E. Griffey, R. H. Bhat, B. *J. Med. Chem.* **2005**, *48* (13), 4247-4253.
27. Aagaard, L. Rossi, J. J., RNAi therapeutics: Principles, prospects and challenges. *Adv. Drug Deliv. Rev.* **2007**, *59* (2-3), 75-86.
28. Wilner, S. E. Levy, M. *Methods Mol. Biol. (Clifton, N.J.)* **2016**, *1380*, 211-24.
29. Collingwood, M. A. Rose, S. D. Huang, L. Y. Hillier, C. Amarzguioui, M. Wiiger, M. T. Soifer, H. S. Rossi, J. J. Behlke, M. A. *Oligonucleotides* **2008**, *18* (2), 187-199.
30. Oivanen, M. Kuusela, S. Lonnberg, H. *Chem. Rev.* **1998**, *98* (3), 961-990.
31. Bibillo, A. Figlerowicz, M. Kierzek, R., *Nucleic Acids Res.* **1999**, *27* (19), 3931-3937.

32. Kaukinen, U. Lyytikainen, S. Mikkola, S. Lonnberg, H. *Nucleic Acids Res.* **2002**, *30* (2), 468-474.
33. Singer, S. J. Nicolson, G. L. *Science* **1972**, *175* (4023), 720-&.
34. Deleavey, G. F. Damha, M. J. *Chem. Biol.* **2012**, *19* (8), 937-954.
35. Jackson, A. L. Burchard, J. Schelter, J. Chau, B. N. Cleary, M. Lim, L. Linsley, P. S. *RNA* **2006**, *12* (7), 1179-1187.
36. Vanboom, J. H. Dahl, O. Marugg, J. E. Nielsen, J. *Phosphorus Sulfur and Silicon Relat. Elem.* **1987**, *30* (3-4), 819-819.
37. Ohtsuka, E. Ikehara, M. Soll, D. *Nucleic Acids Res.* **1982**, *10* (21), 6553-6570.
38. Sinha, N. D. Biernat, J. McManus, J. Koster, H. *Nucleic Acids Res.* **1984**, *12* (11), 4539-4557.
39. Iyer, R. P. Kuchimanchi, S. N. Pandey, R. K. *Drug Future* **2003**, *28* (1), 51-59.
40. Beaucage, S. L. *Curr. Opin. Drug Discov. Devel.* **2008**, *11* (2), 203-216.
41. Stein, C. A. Cheng, Y. C. *Science* **1993**, *261* (5124), 1004-1012.
42. Eckstein, F. *Antisense Nucleic Acid Drug Dev.* **2000**, *10* (2), 117-121.
43. Bennett, C. F. Swayze, E. E. *Annu. Rev. Pharmacol. Toxicol.* Annual Reviews: Palo Alto, **2010**, 259-293.
44. Inoue, H. Hayase, Y. Imura, A. Iwai, S. Miura, K. Ohtsuka, E. *Nucleic Acids Res.* **1987**, *15* (15), 6131-6148.
45. Guckian, K. M. Krugh, T. R. Kool, E. T. *Nat. Struct. Mol.* **1998**, *5* (11), 954-959.
46. Moran, S. Ren, R. X. F. Rumney, S. Kool, E. T. *J. Am. Chem. Soc.* **1997**, *119* (8), 2056-2057.
47. Fire, A. Xu, S. Q. Montgomery, M. K. Kostas, S. A. Driver, S. E. Mello, C. C. *Nature* **1998**, *391* (6669), 806-811.
48. Siddiqi, S. M. Jacobson, K. A. Esker, J. L. Olah, M. E. Ji, X. D. Melman, N. Tiwari, K. N. Secrist, J. A. Schneller, S. W. Cristalli, G. Stiles, G. L. Johnson, C. R. Ijzerman, A. P. *J. Med. Chem.* **1995**, *38* (7), 1174-1188.

49. Pallan, P. S. Greene, E. M. Jicman, P. A. Pandey, R. K. Manoharan, M. Rozners, E. Egli, M. *Nucleic Acids Res.* **2011**, *39* (8), 3482-3495.
50. Xia, J. Noronha, A. Toudjarska, I. Li, F. Akinc, A. Braich, R. Frank-Kamenetsky, M. Rajeev, K. G. Egli, M. Manoharan, M. *Acs Chem. Bio.* **2006**, *1* (3), 176-183.
51. Efthymiou, T. Gong, W. Desaulniers, J. P. *Molecules* **2012**, *17* (11), 12665-12703.
52. Singh, S. K. Nielsen, P. Koshkin, A. A. Wengel, J. *Chem. Comm.* **1998**, (4), 455-456.
53. Filipowicz, W. *Cell* **2005**, *122* (1), 17-20.
54. Efthymiou, T. C. Peel, B. Huynh, V. Desaulniers, J. P. *Bioorg. Med. Chem. Lett.* **2012**, *22* (17), 5590-5594.
55. Zimmerman, G. Chow, L. Y. Paik, U. J. *J. Am. Chem. Soc.* **1958**, *80* (14), 3528-3531.
56. Tait, K. M. Parkinson, J. A. Bates, S. P. Ebenezer, W. J. Jones, A. C. *J. Photochem. Photobiol.* **2003**, *154* (2-3), 179-188.
57. Bandara, H. M. D. Burdette, S. C. *Chem. Soc. Rev.* **2012**, *41* (5), 1809-1825.
58. Beharry, A. A. Woolley, G. A. *Chem. Soc. Rev.* **2011**, *40* (8), 4422-4437.
59. Hartley, G. S., 113. *J. Am. Chem. Soc.* **1938**, 633-642.
60. Yamana, K. Kan, K. Nakano, H. *Bioorg. Med. Chem.* **1999**, *7* (12), 2977-2983.
61. Ikeda, T. Tsutsumi, O. *Science* **1995**, *268* (5219), 1873-1875.
62. Natansohn, A. Rochon, P. *Chem. Rev.* **2002**, *102* (11), 4139-4175.
63. Bartels, E. Wasserma.Nh Erlanger, B. F. *Abstr. Pap. Am. Chem. Soc.* **1971**, (NSEP), 303-&.
64. Woolley, G. A. *Acc. Chem. Res.* **2005**, *38* (6), 486-493.
65. Ferreira, R. Nilsson, J. R. Solano, C. Andreasson, J. Grotli, M. *Sci. Rep.* **2015**, *5*, 8.
66. Goldau, T. Murayama, K. Brieke, C. Asanuma, H. Heckel, A. *Chem. Eur. J.* **2015**, *21* (49), 17870-17876.

67. Asanuma, H. Liang, X. G. Yoshida, T. Komiyama, M. *ChemBioChem* **2001**, 2 (1), 39-44.
68. Wu, L. Wu, Y. Jin, H. W. Zhang, L. R. He, Y. J. Tang, X. J. *Medchemcomm* **2015**, 6 (3), 461-468.
69. Paddison, P. J. Caudy, A. A. Bernstein, E. Hannon, G. J. Conklin, D. S. *Genes. Dev.* **2002**, 16 (8), 948-958.
70. Wu, L. He, Y. J. Tang, X. J. *Bioconj. Chem.* **2015**, 26 (6), 1070-1079.
71. Yu, H. T. Li, J. B. Wu, D. D. Qiu, Z. J. Zhang, Y. *Chem. Soc. Rev.* **2010**, 39 (2), 464-473.
72. Pelliccioli, A. P. Wirz, J. *Photochem. Photobiol. Sci.* **2002**, 1 (7), 441-458.
73. Zhang, Q. Ko, N. R. Oh, J. K. *Chem. Commun.* **2012**, 48 (61), 7542-7552.
74. Hiraoka, T. Hamachi, I. *Bioorg. Med. Chem. Lett.* **2003**, 13 (1), 13-15.
75. Anstaett, P. Pierroz, V. Ferrari, S. Gasser, G. *Photochem. Photobiol. Sci.* **2015**, 14 (10), 1821-1825.
76. Mikat, V. Heckel, A. *RNA* **2007**, 13 (12), 2341-2347.
77. McKim, Chris. 2014 Msc thesis, University of Ontario Institute of Technology.
78. Desaulniers, J. P. Hagen, G. Anderson, J. McKim, C. Roberts, B., *Rsc Adv.* **2017**, 7 (6), 3450-3454.
79. Peel, B. J. Hagen, G. Krishnamurthy, K. Desaulniers, J. P. *Acs Med. Chem. Lett.* **2015**, 6 (2), 117-122.
80. Jackson, A. L.; Linsley, P. S. *Nat. Rev. Drug Discov.* **2010**, 9 (1), 57-67.
81. Vogler, M. Dinsdale, D. Dyer, M. J. S. Cohen, G. M. *Cell Death Differ.* **2009**, 16 (3), 360-367.
82. Kenski, D.M. Butora, A.T., Willingham, A.J., Cooper, W. Fu, N. Qi, F. Soriano, I.W. Davies and Flanagan, W.M. *Mol. Ther. Nucleic Acids* 1, **2012**.
83. Braasch D.A, Jensen, S., Liu, Y., Kaur, K., Arar, K. White, M.A. and Corey, D.R. *Biochemistry* **2003**, 42:7967-7975.

84. Elmén J., Thonberg, H., Ljungberg, K., Frieden, M., Westergaard, M., Xu, Y., Wahren, B., Liang, Z., Ørum, H., Koch T. *Nucleic Acids Res.* **2005**, *33*:439-447.
85. Salim, L. and Desaulniers J.P. *Nucleic Acid Ther.* **2020**, *31*:21-38.
86. Salim L, C McKim and J-P Desaulniers. *RSC Adv.* **2018**, *8*:22963-22966.
87. Hammill, M. L., Isaacs-Trepanier, C., and Desaulniers, J. P. *ChemistrySelect* **2017**, *2*:9810-9814.
88. Hammill, M. L., Patel, A., Abd Alla, M., and Desaulniers, J. P. *Bioorg. Med. Chem. Lett.* **2018**, *28*:3613-3616.
89. Hammill, M. L., Islam, G., and Desaulniers, J. P. *Org. Biomol. Chem.* **2020**, *18*:41-46.
90. Hammill, M. L., Islam, G., and Desaulniers, J. P. *ChemBioChem* **2020**, *21*:2367-2372.
91. Konrad, D. B., Frank, J. A., and Trauner, D. *Chem.-Eur. J.* **2016**, *22*, 4364-4368.
92. Kalyani, D., Dick, A. R., Anani, W. Q., and Sanford, M. S. *Org. Lett.* **2006**, *8*, 2523-2526.
93. Bleger, D., Schwarz, J., Brouwer, A. M., and Hecht, S. *J. Am. Chem. Soc.* **2012**, *134*, 20597-20600.

Chapter 2: Manuscript I- Stability and Evaluation of siRNAs labeled at the sense strand with a 3'- Azobenzene Unit

Matthew L. Hammill, Ayushi Patel, Maria Abd Alla, and Jean-Paul Desaulniers*

Published in

Bioorganic and Medicinal Chemistry Letters **2018**, 28, 3613-3616

DOI: 10.1016/j.bmcl.2018.10.044

2.1 Abstract

siRNAs bearing a 3'-azobenzene derivative on the sense strand were evaluated for their gene silencing ability in mammalian cell culture and nuclease stability in nuclease-rich media. Azobenzene can be isomerized between cis and trans isomers through the incubation of UV (cis isomer) and visible light (trans isomer). It was demonstrated that subtle differences in nuclease stability and activity were observed. These small changes can be used to photochemically fine-tune the activity of an siRNA for gene-silencing applications.

2.2 Introduction

The endogenous RNA interference (RNAi) pathway regulates gene expression in eukaryotic organisms.¹ In 1998, Fire and Mello described the use of the RNAi pathway in which double-stranded RNAs (dsRNAs) were able to silence gene expression in a nematode, *Caenorhabditis elegans*.² Since then, synthetic siRNAs have been used to silence genes for potential therapeutic and biotechnological applications.³⁻⁵

Stabilization of synthetic siRNA against nuclease degradation is important for *in vivo* and therapeutic applications.⁶ Several studies have demonstrated that siRNA resistance to nucleases can be improved by introducing chemically-modified nucleotide analogs into the siRNA structure.^{7,8} siRNAs containing 2'-*O*-methyl group and 2'-fluoro substitutions in the ribose sugar backbone have shown promising results with enhanced siRNA stability in the serum.^{6,7,9,10} Moreover, other modifications such as locked nucleic acid (LNA) can be used to both increase the thermal stability and nuclease stability of siRNA molecules without affecting their function.¹¹ Such modifications offer the means to enhance the

stability of the siRNA structure without affecting its gene-silencing activity. Other studies have shown that large bulky substituents such as phenyl, naphthyl, and other large aromatic groups on the 3'-end of the siRNA duplex can also confer stability to nucleases.¹²

Azobenzene is an aromatic compound that can undergo photo-isomerization. In the presence of UV light, azobenzene exists predominantly in the *cis* conformation and in the presence of visible light, azobenzene rests in the *trans* conformation.¹³ The isomerization from *trans* to *cis* is accomplished with UV light between 330 to 365 nm. Azobenzene can be returned to its *trans* conformation with broad spectrum visible light of 450 nm or greater.¹⁴ The *trans* state of the azobenzene molecule is planar and has a dipole moment near zero. The *trans* conformation of the azobenzene molecule is more stable; hence is the dominant isomer.¹⁵ In the *cis* isomer, the two phenyl rings of azobenzene molecule are twisted approximately 55 degrees out of the plane and the *cis* isomer has a dipole moment of three Debye units.¹³⁻¹⁵ Due to these properties, azobenzene has been used in oligonucleotide modifications and biological applications because of their ease in synthesis, high efficiency, and facile controlled isomerization.^{13,16-19}

There are several approaches for modifying oligonucleotides in order to utilize azobenzene's photo-isomerization properties. For example, modifications can be placed on the sugar or nitrogenous base, or serve as the backbone core of an oligonucleotide.^{13,20} The attachment of a photo-switch as a nucleoside surrogate has been a widely used approach. Moreover, inserting azobenzene into a sequence as an additional nucleoside has been widely applied as azobenzene intercalates between the neighbouring pairing bases in the *trans* conformation. Following UV irradiation, the *cis* conformation of the azo molecule reduces its ability to intercalate in duplex oligodeoxynucleotides, and as a result, the duplex

destabilizes.²¹ Most recently, our group synthesized a class of siRNAs bearing azobenzene (siRNAzo) within the central region of siRNAs, and we were able to control the gene-silencing activity of these complexes with UV and visible light.¹⁸ Having an ability to control when the molecule is active or inactive would have an enormous benefit as potential therapeutics and/or biotechnological tools.

In this study, we investigated the effects of an azobenzene moiety on the 3'-end of the sense strand of siRNAs, and whether there was a change in stability and gene-silencing efficacy in the presence of UV light. Figure 1 illustrates the siRNAs used with the azobenzene. SiRNA **1** contains an azobenzene that contains a single carbon between the phenyl group and oxygen group, whereas siRNA **2** contains two carbons on the azobenzene atom between the phenyl group and the oxygen atom (Figure 2.1).

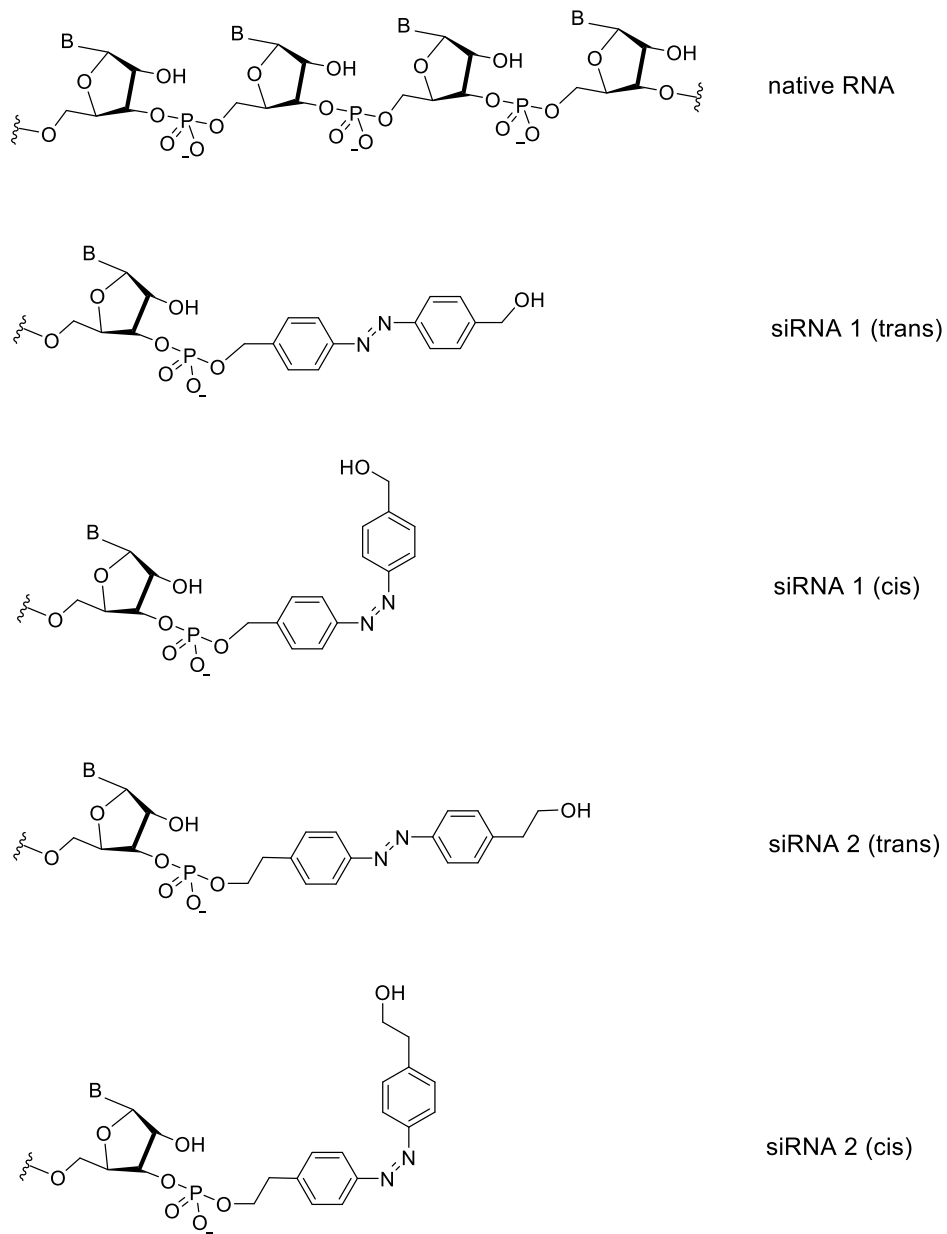


Figure 2.1. Structural differences between native RNA, and siRNAs containing azobenzene derivatives. The differences between the *trans* and *cis* forms are identified.

2.3 Materials and Methods

2.3.1 General

Unless otherwise indicated all starting reagents used were obtained from commercial sources without additional purification. Oligonucleotides were synthesized according to our groups previously published protocol, using standard solid phase synthesis and materials.¹ Antisense luciferase siRNA from Integrated DNA Technologies (IDT) was used for this study.

2.3.2 Procedure for Absorbance Spectra Experiments

All absorbance spectra measurements were done on a Jasco J-815 CD with temperature controller. Measurement was recorded from 200 -500 nm at 10 °C at least 3 times. UV treated samples were placed under a UVP UVL-23RW Compact UV lamp 4.00 W 365 nm for the indicated time at 25 °C . Visible light treated samples were placed under a 60.0 W daylight bulb from NOMA in standard desk lamp.

2.3.3 Procedure for HPLC Characterization

HPLC chromatograms were obtained on a Waters 1525 binary HPLC pump with a Waters 2489 UV/Vis detector using the Empower 3 software. A C18 4.6 mm x 150 mm reverse phase column was used. Conditions were 5% acetonitrile in 95% 0.1 M TEAA (Triethylamine-Acetic Acid) buffer up to 100% acetonitrile over 40 min.

2.3.4 Procedure for Nuclease Stability Assays

SiRNAs 1, 2 and wt were tested for nuclease stability at a concentration of 12 μM . The time points tested for the stability were 0, 0.5, 1, 2, 3 and 4 hours for each siRNA. In microcentrifuge tubes 1 μL of 12 μM siRNA stock solution was added to 9 μL distilled water (10 μL total volume, 0 h time point) or 7.65 μL distilled water along with 1.35 μL fetal bovine serum (FBS) (10 μL total volume, all other time points) mixed and then incubated at 37°C for each time point. At each hour, the sample was prepared and placed in the incubator in a sequential order, starting with the 4-hour sample first. After the incubation, samples were run on a 20% non-denaturing polyacrylamide gel. Samples were mixed with 10 μL of non-denaturing loading dye and loaded onto the gel. The gel was run using a stacking method, in which the gel was first run at 30V for approximately 2 hours until the siRNA was evenly loaded. The gel was then run for an additional 20 hours at 70V. The gel was stained using 3X GelRed nucleic acid dye for 30-45 minutes and was visualized via Flurochem SP (Fisher Scientific).

2.3.5 Procedure for Maintaining Cell Cultures of HeLa Cells

For biological analysis of these siRNAs in a live environment, human epithelial cervix carcinoma cells were used (HeLa cells). They were kept in 250 mL vented culture flasks using 25.0 mL of DMEM with 10% fetal bovine serum and 1% penicillin-streptomycin (Sigma) in an incubator set for 37 °C @ 5% CO₂ humidified atmosphere.

Once cell lines became confluent (80-90%) they were passaged by washing 3 times with 10 mL of phosphate buffered saline (NaCl 137 mM, KCl 2.70 mM, PO₄³⁻ 10.0 mM, pH 7.40) and incubated with 3.00 mL of 0.25% trypsin (SAFC bioscience) for 4 min @ 37 °C

to detach the cells. The cells were transferred to a 50.0 mL centrifuge tube after the addition of 10.0 mL of DMEM solution and pelleted at 2000 rpm for 5 minutes. The supernatant was discarded and the pellet resuspended in 5.0 mL DMEM with 10% FBS.

A standard haemocytometer was used to obtain cell counts, after which the cells were diluted to a final concentration of 1.00×10^6 cells/mL for subsequent assays. To continue the cell line 1.00 mL of freshly passaged cells was added to 24.0 mL of DMEM/10% FBS and 1% penicillin-streptomycin at 37 °C in a new culture flask while the rest were used for assays.

2.3.6 Procedure for siRNA Transfections

100 μ L of cells (total 1.00×10^5) were transfected into 12 well plates (Falcon®) with 1 mL of DMEM (10% FBS, 1% penicillin-streptomycin) and incubated at 37 °C with 5% CO₂. After 24 hours the cells were transfected with various concentrations of siRNAs, along with both pGL3 (Promega) and pRLSV40 luciferase plasmids using Lipofectamine 2000 (Invitrogen) in Gibco's 1X Opti-Mem reduced serum media (Invitrogen) according to the manufacturer's instructions. 1.00 μ L of siRNA was added along with 2.00 μ L (pGL3 200 ng) and 0.50 μ L pRLSV40 (50.0 ng) to 100 μ L of 1X Opti-Mem in a microcentrifuge tube and kept on ice for 5 min. In a different microcentrifuge tube, 1.00 μ L of Lipofectamine 2000 (Invitrogen) was mixed with 100 μ L of Gibco's 1X Opti-Mem reduced serum media (Invitrogen) and incubated at room temperature for 5 min. After 5 minutes the tubes were mixed and incubated at room temperature for 20 min and then the entire contents transferred to the wells of the 12 well plate.

2.3.7 Procedure for *in vitro* Dual-Reporter Luciferase Assay

100 μ L of cells (total of 1.00×10^5 cells) were added to 12 well plates (Falcon®) with 1 mL of growth media (DMEM 10% FBS, 1% penicillin-streptomycin) and incubated at 37 °C with 5% CO₂. After 24 hours the cells were transfected with 8.00, 20.0, 40.0, 160, 400 and 800 pM concentrations of siRNAs, along with both pGL3 (Promega) and pRLSV40 luciferase plasmids using Lipofectamine 2000 (Invitrogen) in Gibco's 1X Opti-Mem reduced serum media (Invitrogen) according to the manufacturer's instructions. After a set amount of time (8, 12 or 22h) the cells were incubated at room temperature in 1X passive lysis buffer (Promega) for 20 minutes. The lysates were collected and loaded onto a 96 well, opaque plate (Costar). With a Dual-Luciferase reporter Assay kit (Promega), Lar II and Stop & Glo® luciferase substrates were sequentially added to the lysates and enzyme activity was measured through luminescence of both *firefly/Renilla* luciferase on a Synergy HT (Bio-Tek) plate luminometer. The ratio of *firefly/Renilla* luminescence is expressed as a percentage of reduction in *firefly* protein expression to siRNA efficacy when compared to untreated controls. Each value is the average of at least 3 different experiments with standard deviation indicated.

2.3.8 Procedure for Light Inactivation of Azobenzene Modified siRNA (*trans* to *cis*)

1.00 μ L of the desired siRNA was added to a microcentrifuge tube and exposed to a 4.00 W 365 nm UV lamp (UVP) and was exposed for at least 4 hours.

After UV exposure the siRNA can be used in the transfection procedure above, but the transfection must be done in the dark room, to prevent the *cis* to *trans* conversion back into the active form.

2.4 Results

Table 2.1. Sequences of siRNAs^[a]

siRNA duplex	
wt	5'- CUUACGCUGAGUACUUCGAtt -3' 3'- ttGAAUGCGACUCAUGAAGCU - 5'
1	5'- CUUACGCUGAGUACUUCGAA <u>Az1</u> -3' 3'- ttGAAUGCGACUCAUGAAGCU - 5'
2	5'- CUUACGCUGAGUACUUCGAA <u>Az2</u> -3' 3'- ttGAAUGCGACUCAUGAAGCU - 5'

[a] Az1 corresponds to the azobenzene derivative synthesized from 4-nitrobenzyl alcohol. Az2 corresponds to the azobenzene derivative synthesized from 4-nitrophenylethyl alcohol; the top strand corresponds to the sense strand; the bottom strand corresponds to the antisense strand. In all duplexes, the 5'-end of the bottom antisense strand contains a 5'-phosphate group.

2.4.1 Gene-silencing activity with UV/visible exposures

We investigated the gene-silencing effect of siRNAs **1**, **2** and **wt** (Table 2.1) in the presence and absence of UV light. SiRNAs **1** and **2** were synthesized and characterized using our previously published method.¹⁸ In the presence of UV light, the azobenzene would adopt the *cis* form as the major isomer (Table S-1, Appendix 1), whereas in the absence of UV light, the *trans* form dominates. Briefly, the siRNAs were co-transfected with plasmids pGL3 and pRenilla into the HeLa cells, followed by cell lysis following transfection. The siRNAs were either inactivated with UV light prior to transfection, or they were not exposed to UV light, and thus the active form was transfected. The **wt** siRNA does not appear to have any change in silencing activity between the UV treated and no treatment groups. As shown in Figure 2.2, UV exposure does not have an appreciable effect on silencing. This is expected as the **wt** siRNA does not have any light-inducible isomerizable moieties.

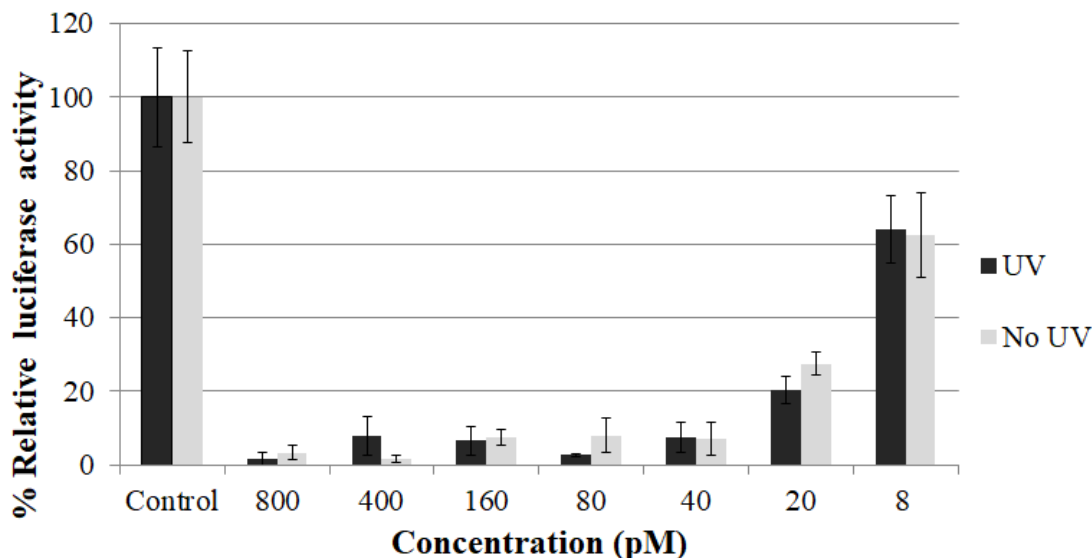


Figure 2.2. Reduction in normalized firefly luciferase expression for **wt** siRNA at 8, 20, 40, 80, 160, 400 and 800 pM concentrations in HeLa cells and lysed 22 h post transfection. ‘UV’ corresponds to the siRNA being exposed under a 365 nm UV lamp for inactivation prior to transfection. ‘No UV’ corresponds to active siRNA being transfected in HeLa cells in the absence of UV light.

siRNA **1** exhibits efficient and potent gene-silencing activity, comparable to **wt** siRNA (IC_{50} 4.69 pM), in both the presence and absence of UV light (Figure 2.3). As such, there does not appear to be a discernable difference in activity between *cis* (5.1 pM) and *trans* (5.5 pM). In contrast, siRNA **2** (*cis* 14.6 pM) against siRNA **2** (*trans* 7.4 pM) exhibits a small twofold change in gene-silencing profiles in the presence and absence of UV light (Figure 2.4) In the absence of UV light, the gene-silencing profile matches that of both siRNAs **1** and **wt** siRNA; however, in the presence of UV light, a small loss of gene-silencing ability is observed. When the azobenzene is subjected to UV light, the *cis* isomer dominates, thus rendering the siRNA slightly less effective. In these experiments, the cells are lysed 22 hours post transfection. The *cis* isomeric form of azobenzene has been shown to have a half-life at 37 °C of approximately 4 hours²² Thus the small change observed in activity with siRNA **2** is likely due to thermal relaxation of the *cis* azobenzene to its more favored *trans* form. When we perform these experiments on a shorter 8 hour time scale (Fig S-5), larger differences in IC_{50} are observed for the *cis* and *trans* azobenzene form of siRNA **2** because less time is given for the *cis* form to relax back to the *trans* form. For example, we observe a 10-fold difference in IC_{50} s for siRNA **2** (*cis*) (134.7 pM) and siRNA **2** (*trans*) (13.5 pM). This data, compared to siRNA **1** (*cis*) and siRNA **1** (*trans*), showed almost no difference in activity (5.2 pM and 3.2 pM, respectively)

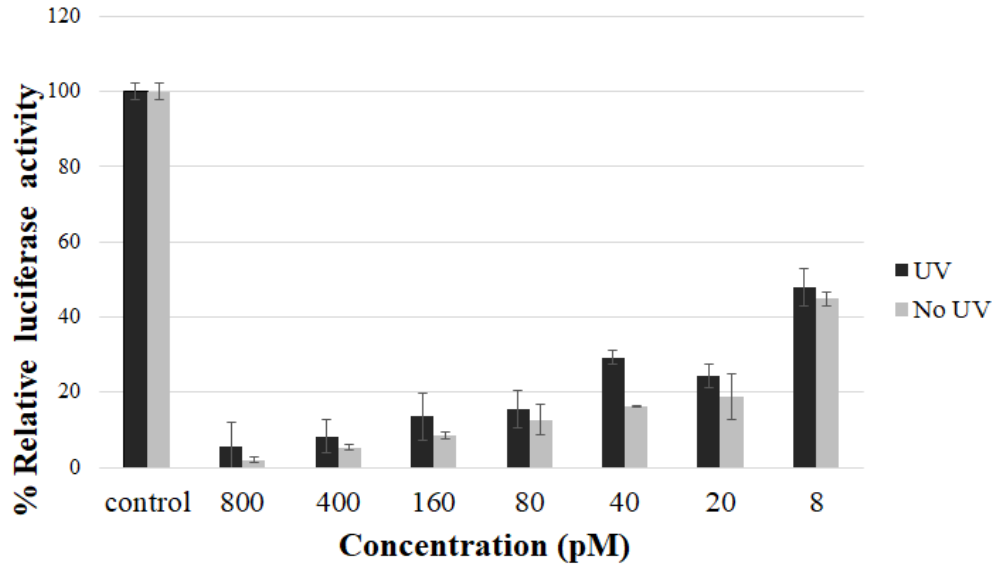


Figure 2.3. Reduction in normalized firefly luciferase expression for siRNA 1 at 8, 20, 40, 80, 160, 400 and 800 pM concentrations in HeLa cells and lysed 22 h post transfection. ‘UV’ corresponds to the siRNA being exposed under a 365 nm UV lamp for inactivation prior to transfection. ‘No UV’ corresponds to active siRNA being transfected in HeLa cells in the absence of UV light.

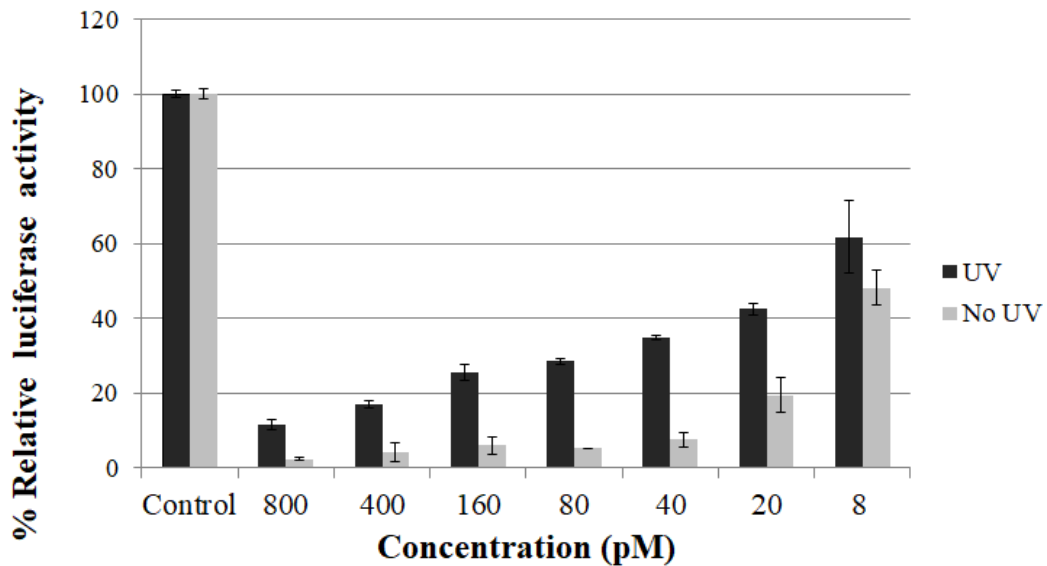


Figure 2.4. Reduction in normalized firefly luciferase expression for siRNA 2 at 8, 20, 40, 80, 160, 400 and 800 pM concentrations in HeLa cells and lysed 22 h post transfection. ‘UV’ corresponds to the siRNA being exposed under a 365 nm UV lamp for inactivation prior to transfection. ‘No light’ corresponds to active siRNA being transfected in HeLa cells in the absence of UV light.

2.4.2 Nuclease stability with UV/visible exposures

To investigate whether the effect of nuclease stability correlated to gene-silencing, we evaluated the siRNAs in the presence of nuclease-rich media, as shown in Figure 2.5. SiRNA **1** in the absence of UV light remains predominantly in the *trans* form, and as can be observed, cleavage starts around 30 minutes. Most of the siRNA **1** is cleaved after four hours. In contrast, siRNA **1** in its predominantly UV *cis* activated form, appears to be degraded at a slower rate compared to *trans*. Very little degradation occurs after 30 minutes, and a dominant band corresponding to the starting duplex remains at 4 hours. Thus, for siRNA **1**, it appears that some increase in nuclease resistance is observed when the siRNA is subjected to UV light.

For siRNA **2**, both gels show cleavage starting at 30 minutes, in addition to some fraction remaining of the intact siRNA at 4 hours. There does not appear to be a large difference in cleavage activity between them.

Figure 2.6 plots the intact remaining duplex siRNA as a function of time. When siRNA **1** was subjected to UV light, the duplex strand remained more stable compared to the siRNA that was not subjected to UV light at shorter time-points. For the siRNA **1** that was not subjected to UV light, degradation commenced immediately, and it can be seen that roughly 50% of the native structure is degraded over 30 minutes. In contrast, with siRNA

2, some increase in stability exists with the UV-treated siRNA at 1 and 2 hours, but no large difference in degradation patterns as visualized on the gel.

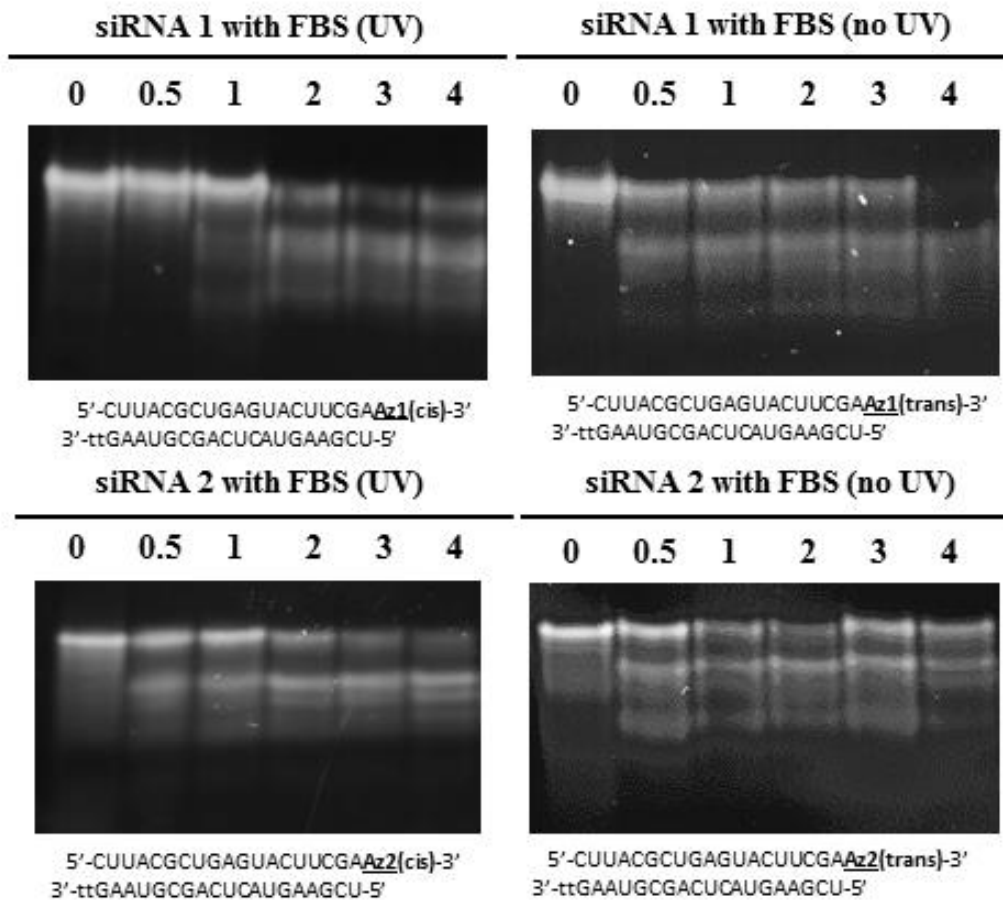


Figure 2.5. Nuclease stability assay. 20% Non-denaturing polyacrylamide gel with degradation products of siRNAs 1 and 2 after incubation with 13.5% fetal bovine serum at 37 °C from 0 hours to 4 hours.

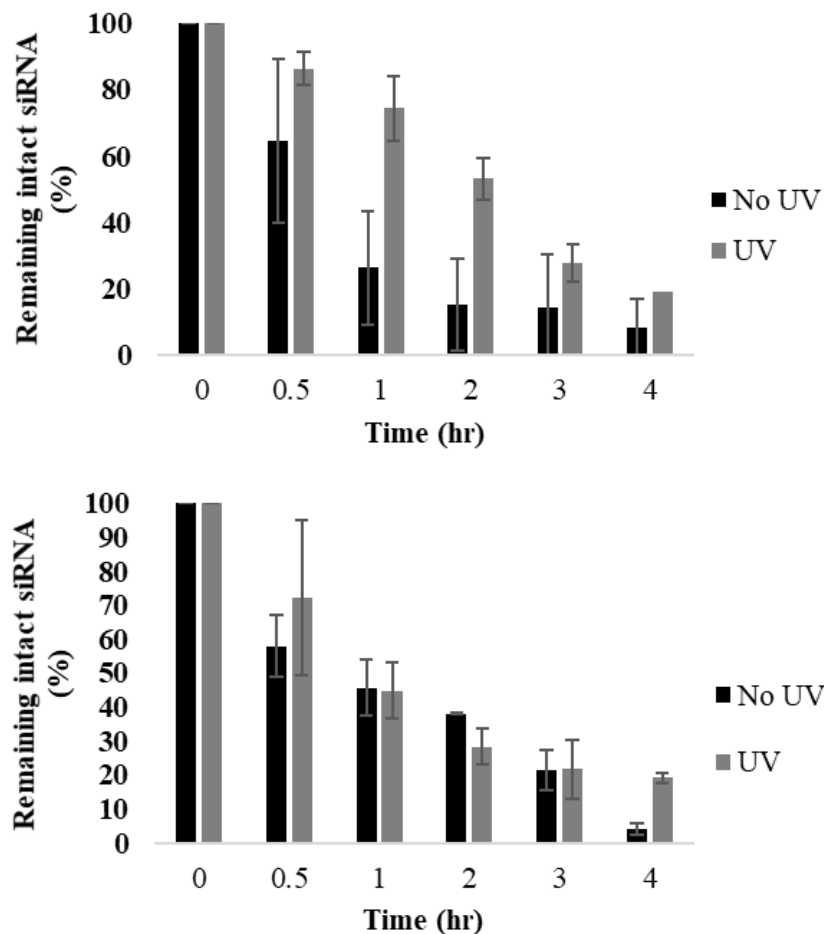


Figure 2.6. Quantification of remaining intact siRNA using ImageJ software. The 0 min time point was used as 100% intact siRNA (Top siRNA 2 and bottom siRNA 1). Graphical representation of intact siRNA derived from Figure 2.5.

2.5 Conclusions

In conclusion, we are reporting the stability and gene-silencing efficiency of siRNAs containing azobenzene at the 3'-end of the sense strand. The siRNAs differ by the number of carbons between the aromatic group and the oxygen atom. In siRNA 1, one carbon is placed between the aromatic group and the oxygen; whereas in siRNA 2, two carbons are present. In both cases, isomerization of the 3'-azobenzene to its *cis* form by UV light

appears to modestly enhance nuclease stability in the presence of fetal bovine serum at some time points. There appears to be a difference between the two azobenzene derivatives, and while they differ only in a single methylene linker on each side of the functional moiety, it could be that the components of the RISC complex and exonucleases do not distinguish siRNAs in both isomeric *cis*- and *trans*-azobenzene forms. However, we observed a larger difference in both the RNAi activity and stability assays with the larger azobenzene species, perhaps due to its slightly larger isomeric structures that can better differentiate between nucleases and components of the RISC complex. This could explain why the *cis* form of siRNA **2** shows a larger difference in stability and activity compared to the *trans* form, whereas the siRNA **1** linker showed almost the same activity. As noted, this difference is time dependent and gene-silencing data measured 8 hours post-transfection for siRNA **2** shows a large difference in IC₅₀, whereas this difference diminishes for longer experiments (22 hours). Nevertheless, both isomeric forms appear to be compatible with the siRNA pathway. Wildtype luciferase siRNAs have been shown to be effective up to one week after transfection in HeLa cells,²³ and this modification could allow for a longer effective experimental window when in the *cis* isomer, for better temporal control of nuclease stability. Interestingly, since the *cis* form of these siRNAs exhibit increased nuclease resistance they can be used to increase the duration of the gene silencing efficacy window. Most wildtype siRNAs begin degrading within 30 min to 1 hour, but our modification prevents this from occurring so rapidly, and as a result would allow the gene silencing to persist. As another application, the *cis* siRNAs could be transfected into the cells and after a certain period of time activated with visible light (or allowed to reactivate naturally). As a potential future work, we could also inactivate the

siRNAs *in vivo* after transfection to change from a time period of high gene silencing, and then through inactivation a period of moderate silencing. This could be useful in a study where moderate silencing of one gene leads to activation or inactivation of an agonist or antagonist and these effects could be studied in more detail, where complete inactivation through silencing would cause deleterious effects such as cell death if the target was an mRNA for essential proteins. In addition, the 3'-azobenzene could be used as a minimal chemical modification for other siRNA targets, also giving enhanced nuclease stability.²⁴ Furthermore, the 3'-end modification could allow for subtle fine-tuning of gene-silencing activity when small changes in inhibition over short time frames are desired. Future work involves designing photo-responsive 3'-azobenzene groups that can further improve the activity and properties of the siRNAs, as well as testing inactivation *in vivo* after transfection.

Acknowledgments

We acknowledge the Natural Sciences and Engineering Research Council (NSERC) for funding.

Supplementary Data

Refer to Appendix I for additional figures and characterization data.

2.6 REFERENCES – Chapter 2 – Manuscript I

1. Reischl, D.; Zimmer, A. *Nanomedicine* **2009**, *5*, 8-20.
2. Fire, A.; Xu, S. Q.; Montgomery, M. K.; Kostas, S. A.; Driver, S. E.; Mello, C. C. *Nature*, **1998**, *391*, 806-811.
3. Prakash, T. P.; Allerson, C. R.; Dande, P.; Vickers, T. A.; Sioufi, N.; Jarres, R.; Baker, B. F.; Swayze, E. E.; Griffey, R. H.; Bhat, B. *J. Med. Chem.* **2005**, *48*, 4247-4253.
4. Aagaard, L.; Rossi, J. J. *Adv. Drug Deliv. Rev.* **2007**, *59*, 75-86.
5. Deleavey, G. F.; Damha, M. J. *Chem. Biol.* **2012**, *19*, 937-954.
6. Robbins, M.; Judge, A.; MacLachlan, I. *Oligonucleotides* **2009**, *19*, 89-102.
7. Chernolovskaya, E. L.; Zenkova, M. A. *Curr. Opin. Mol. Ther.* **2010**, *12*, 158-167.
8. Wan, W. B.; Seth, P. P. *J. Med. Chem.* **2016**, *59*, 9645–9667.
9. Chiu, Y. L.; Rana, T. M. *RNA*, **2003**, *9*, 1034-1048.
10. Elmén, J.; Thonberg, H.; Ljungberg, K.; Frieden, M.; Westergaard, M.; Xu, Y.; Wahren, B.; Liang, Z.; Ørum, H.; Koch, T.; Wahlestedt, C. *Nucleic Acids Res.* **2005**, *33*, 439-447.
11. Braasch, D. A.; Jensen, S.; Liu, Y.; Kaur, K.; Arar, K.; White, M. A.; Corey, D. R. *Biochemistry*, **2003**, *42*, 7967-7975.
12. Terrazas, M.; Kool, E. T. *Nucleic Acids Res.* **2008**, *37*, 346-353.
13. Lubbe, A. S.; Szymanski, W.; Feringa, B. L. *Chem. Soc. Rev.* **2017**, *46*, 1052-1079.
14. Brieke, C.; Rohrbach, F.; Gottschalk, A.; Mayer, G.; Heckel, A. *Angew. Chem. Int. Ed.* **2012**, *51*, 8446-8476.
15. Beharry, A. A.; Woolley, G. A. *Chem. Soc. Rev.* **2011**, *40*, 4422-4437.
16. Asanuma, H.; Liang, X. G.; Yoshida, T.; Komiyama, M. *ChemBioChem*, **2001**, *2*, 39-44.
17. Wu, L.; Wu, Y.; Jin, H. W.; Zhang, L. R.; He, Y. J.; Tang, X. J. *MedChemComm*, **2015**, *6*, 461-468.
18. Hammill, M. L.; Isaacs-Trépanier, C.; Desaulniers, J.-P. *ChemistrySelect*, **2017**, *2*, 9810-9814.
19. Liu, Y.; Sen, D. *J. Mol. Biol.* **2004**, *341*, 887-892.
20. Yamana, K.; Kan, K.; Nakano, H. *Bioorg. Med. Chem.* **1999**, *7*, 2977-2983.
21. Li, J.; Wang, X.; Liang, X. *Chem. Asian J.* **2014**, *9*, 3344-3358.
22. Hartley, G. S. *J. Chem. Soc.* **1938**, 633-642.
23. Bartlett, D.W.; Davis, M. E. *Biotechnol. Bioeng.* **2007**, *97*, 909-921.
24. Efthymiou, T. C.; Peel, B.; Huynh, V.; Desaulniers, J.-P. *Bioorganic Med. Chem. Lett.* **2012**, *22*, 5590-5594.

2.7 Manuscript I Supplementary Figures and Tables

Full Supplementary data can be found in Appendix I

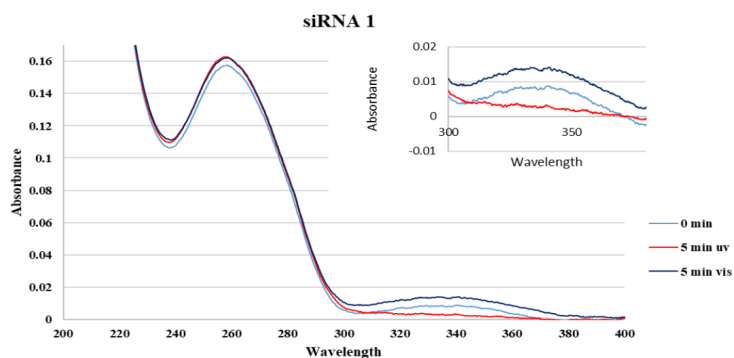


Figure S-1. Absorbance Profile of siRNAzo 1 when exposed to UV and Visible light in 500 μ L of a sodium phosphate buffer (90.0 mM NaCl, 10.0 mM Na_2HPO_4 , 1.00 mM EDTA, pH 7.00) and scanned from 200-400 nm at 10 $^\circ\text{C}$ with a screening rate of 20.0 nm/min and a 0.20 nm data pitch.

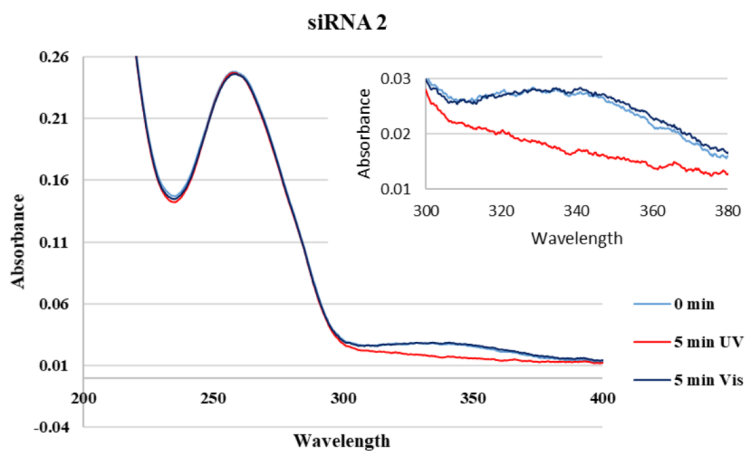
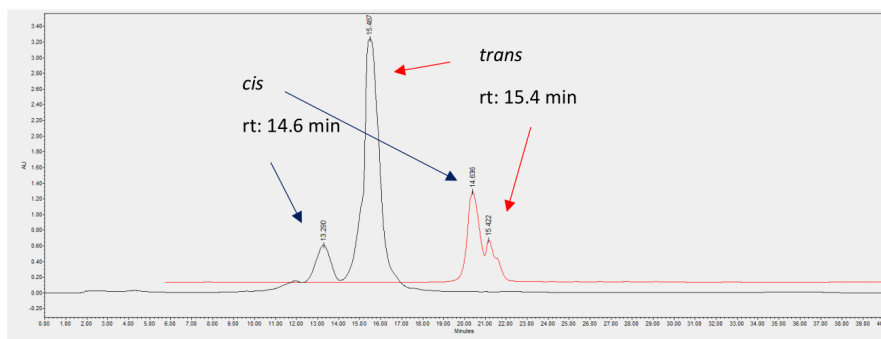
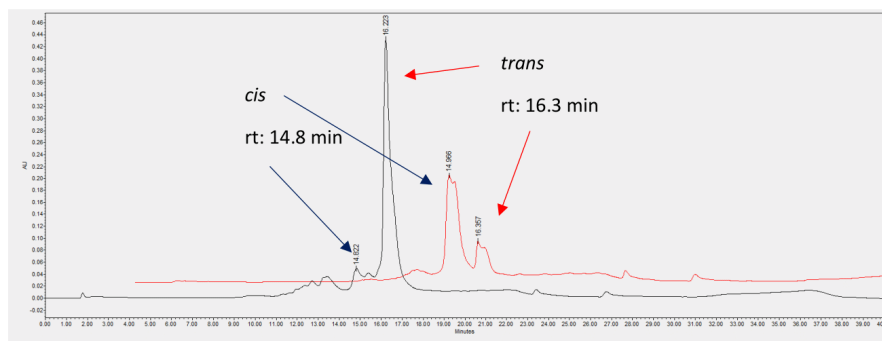


Figure S-2. Absorbance Profile of siRNAzo 2 when exposed to UV and Visible light in 500 μ L of a sodium phosphate buffer (90.0 mM NaCl, 10.0 mM Na_2HPO_4 , 1.00 mM EDTA, pH 7.00) and scanned from 200-400 nm at 10 $^\circ\text{C}$ with a screening rate of 20.0 nm/min and a 0.20 nm data pitch.



S-3. HPLC chromatogram for siRNA 1. Blue indicates no treatment, red corresponds to UV exposure. Arrows indicate *trans* and *cis* peaks and retention times. Conditions were 5% acetonitrile in 95% 0.1 M TEAA (Triethylamine-Acetic Acid) buffer up to 100% acetonitrile over 40 min.



S-4. HPLC chromatogram for siRNA 2. Blue indicates no treatment, red corresponds to 10 min UV exposure. Arrows indicate *trans* and *cis* peaks and retention times. Conditions were 5% acetonitrile in 95% 0.1 M TEAA (Triethylamine-Acetic Acid) buffer up to 100% acetonitrile over 40 min.

Table S-1. Measurement of conformer abundance in siRNAs 1 and 2, with both no UV and UV treated samples.

siRNA	Treatment	<i>trans</i>	% <i>cis</i>
1	No UV	83.9	16.1
	UV	23.5	76.5
2	No UV	90.4	9.6
	UV	77.1	22.9

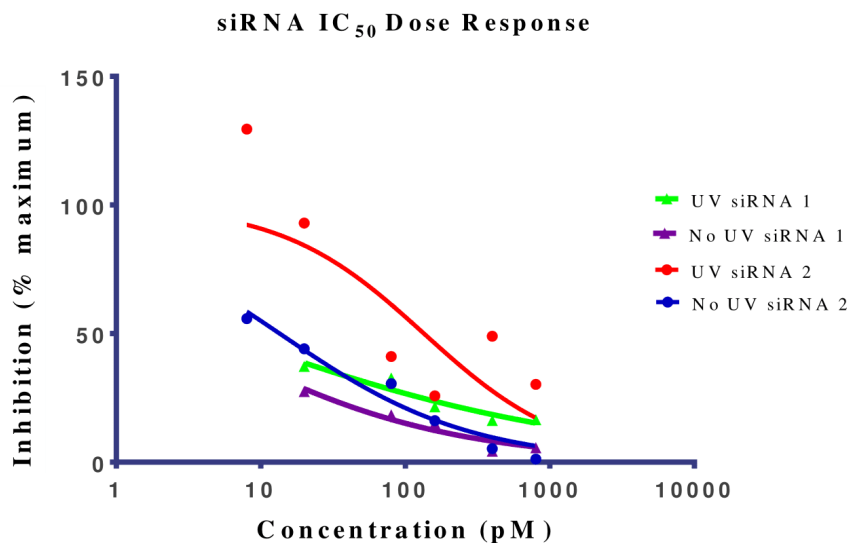


Figure S-5. Dose-responsive curves of siRNAzOs 1 and 2 with a 3' end azobenzene modification using the Dual Reporter Luciferase Assay at 8 h timepoint. The siRNAzOs were tested at 6 concentrations from 8.00-800 pM with *firefly* luciferase expression normalized to *Renilla* luciferase. All IC₅₀ values were calculated with Prism using the variable slope model. The IC₅₀ values were as follows: siRNA 1 UV (5.2 pM), No UV (3.2 pM); siRNA 2 UV (134.7 pM), No UV (13.5 pM), where UV describes exposure of the siRNA before transfection to the UV light source for 4 hours, and No UV corresponds to the active siRNA not exposed to the UV lamp.

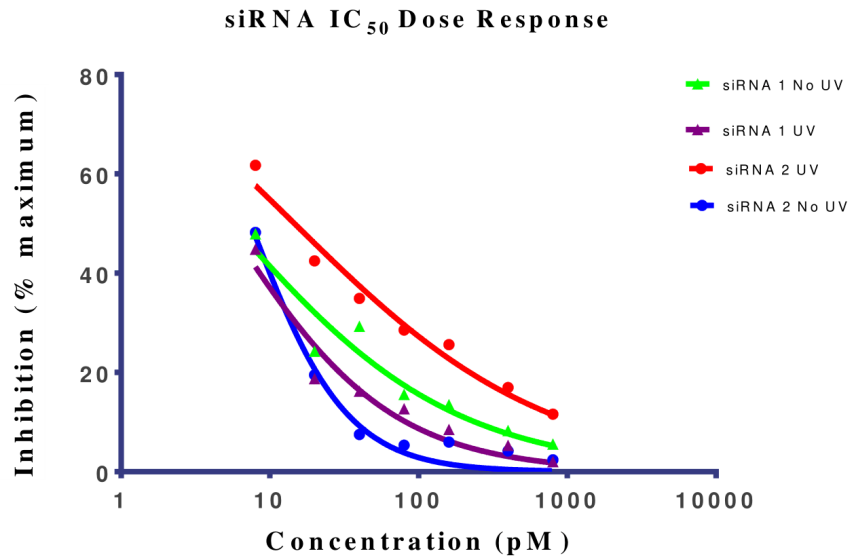


Figure S-6. Dose-responsive curves of siRNAzOs 1 and 2 with a 3' end azobenzene modification using the Dual Reporter Luciferase Assay at 22 h timepoint. The siRNAzOs were tested at 6 concentrations from 8.00-800 pM with *firefly* luciferase expression normalized to *Renilla* luciferase. All IC₅₀ values were calculated with Prism using the variable slope model. The IC₅₀ values were as follows: siRNA 1 UV (5.5 pM), No UV (5.1 pM); siRNA 2 UV (14.6 pM), No UV (7.4 pM), where UV describes exposure of the siRNA before transfection to the UV light source for 4 hours, and No UV corresponds to the active siRNA not exposed to the UV lamp.

	RNA 1		RNA 3	
UV	-	+	-	+



Figure S-7. Nuclease stability assay. 20% Non-denaturing polyacrylamide gel with no degradation products for RNAs **1** and **3** after incubation with no UV light (-) or UV light (+) for 4 hours at room temperature. RNA **1** corresponds to 5'-CUUACGCUGAGUACUUCGAAz1-3', and RNA **3** corresponds to 5'-CUUACGCUAz1GUACUUCGAdTdT-3'.¹ Az1 corresponds to the azobenzene derivative synthesized from 4-nitrobenzyl alcohol.

Connecting Statement I

During the Chapter II study we determined that azobenzene is a suitable RISC substrate when placed into the 3' end of the sense strand of the siRNA. Having shown that the azobenzene at the 3' end imparts good nuclease resistance, as well as having a small but notable difference in gene silencing profiles when exposed to UV light, we wanted to expand the utility of the system beyond just the 24 h tested previously, and against multiple targets. In the following study, we develop a system to inactivate the siRNA, and then maintain its *cis* conformer state for up to 24 h using carefully controlled doses of UV light. Using this new improved system we overcome the limitations of the *cis* conformer instability by preventing reactivation as it relaxes back to the *trans* conformer. We additionally test the robustness of the azobenzene photo-switch through exposure to multiple rounds of alternating UV and visible light. Finally, the last part of the next study was to determine whether we could target an endogenous gene, namely *BCL-2*, and utilize our system to reversibly control the endogenous target in the same way we controlled the exogenous *firefly* luciferase gene. We measured this gene silencing on endogenous targets using RT-qPCR.

Chapter 3: Manuscript II- Reversible control of RNA interference by siRNAs

Matthew L. Hammill, Golam Islam and Jean-Paul Desaulniers*

Published in

Organic & Biomolecular Chemistry **2020**, *18*, 41-46

DOI: 10.1039/C9OB02509J

3.1 Abstract

In this study, we report the reversible control of RNA interference using siRNAzOs, a class of siRNAs that contain azobenzene. Herein, we demonstrate that it is possible to take an active siRNAzo, and inactivate it for up to 24 hours. We also demonstrate reversibility of these siRNAzOs within cell culture. For example, active siRNAzOs can be inactivated in cell culture with ultraviolet light, and then reactivated with visible light. In addition, we also show that siRNAzOs can be activated and inactivated towards the endogenous target gene, *BCL2*.

3.2 Introduction

The RNA interference (RNAi) pathway is an endogenous defense mechanism that targets viral and parasitic double-stranded RNA (dsRNA), and regulates gene expression in eukaryotes. Fire and Mello published a paper in 1998, identifying double-stranded RNAs as gene-silencing agents in the nematode *Caenorhabditis elegans*.¹ Ever since this discovery, there has been interest in utilizing this pathway for therapeutics and biomolecular tools.²⁻⁴ The most recent FDA-approved siRNA is Onpattro, which is used for the treatment of hereditary transthyretin amyloidosis (hATTR).⁵ Despite this success, siRNAs as therapeutics often come with several known problems, such as poor stability, toxicity, off-target and tissue specific targeting. However, one issue in the field that has largely been overlooked in the field is reversing RNAi activity in the event of adverse siRNA off-target effects. Some recent research shows that short locked nucleic acid-modified oligonucleotides complementary to the seed region of the guide strands can reverse siRNA activity.⁶ However, despite this study, more research and methods to

inactivate siRNA function is needed. In this paper, we describe the utility of photoreversibly controlling RNAi using an siRNAzo (azobenzene-containing siRNA).

Several advances over the last decade have led the development of photoresponsive siRNAs, which generally are dsRNAs that are inactive when entered inside of the cell, and then are activated with light. The first example was developed by Friedman and coworkers, in which they used a backbone-modified siRNA labeled with 1-(1-diazoethyl)-4,5-dimethoxy-2-nitrobenzene (DMNPE-N₂). Upon exposure with UV light ($\lambda > 320$ nm), the groups are removed to yield an active siRNA.⁷ Heckel and coworkers have used photoresponsive protecting groups on guanine and thymidine nucleotides of the guide strand of siRNAs, which becomes uncaged to UV light.⁸ Most recently, Mokhir and Meyer developed a 5'-labelled alkoxyanthracenyl siRNA, which becomes uncaged via a singlet oxygen (¹O₂) photoregenerated photosensitizer on the 3'-end of the guide strand. Uncaging occurs with green or red light to yield an active siRNA.⁹ Despite these innovative advances, an inactive siRNA complex is *irreversibly* photoactivated to yield an active siRNA. The process cannot be reversed, and it is not entirely clear what effect the by-products of the caged functional groups when released may have on the cell. Having the ability to reversibly control the activity of an siRNA within the cell would offer greater spatial control of the siRNA. This reversibility could bypass and eliminate the undesired off-target side effects.

Azobenzene is an attractive photoresponsive molecule because of its ability to photoisomerize in the presence of UV and visible light. This causes a large conformational change in the molecule, which can be used to disrupt biomolecular structures.¹⁰ The more stable isomer, *trans* is the normal resting state of the molecule, but through the addition of

energy in the form of UV light between 330-365 nm, photo-isomerization occurs and the molecule adopts a *cis* isomeric form. The *cis* form of azobenzene is less stable due to steric hindrance and strain on the N=N bond and thus can be converted back to *trans* with visible light above 450 nm.¹¹ Because of these unique and useful properties, azobenzene has been used in many applications, including its incorporation into oligonucleotides (see Figure 3.1) since it is relatively easy to synthesize and has a high quantum yield when photo-switching.¹²

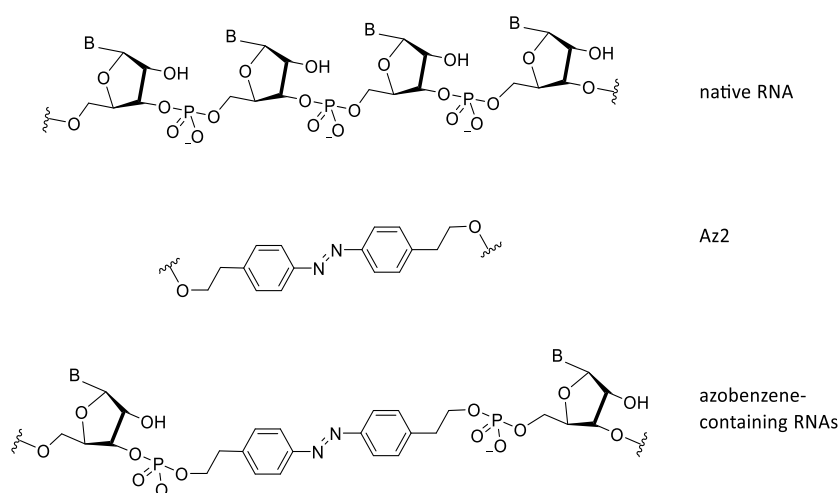


Figure 3.1. Structural differences between native RNA, and azobenzene-containing RNAs. Az2 corresponds to the azobenzene unit used in this study.

Previous work in our group utilized azobenzene's photo properties in order to make siRNAzos, which are siRNA molecules that contain azobenzene.^{13,14} Figure 3.2 highlights the photoswitching properties of the siRNAzo. In the native *trans* form, the siRNAzo is active. When the siRNAzo is treated with UV light, the azobenzene unit adopts a *cis* conformation, and thus inactivates the siRNAzo. Restoration of activity can proceed by thermal relaxation and/or visible light.

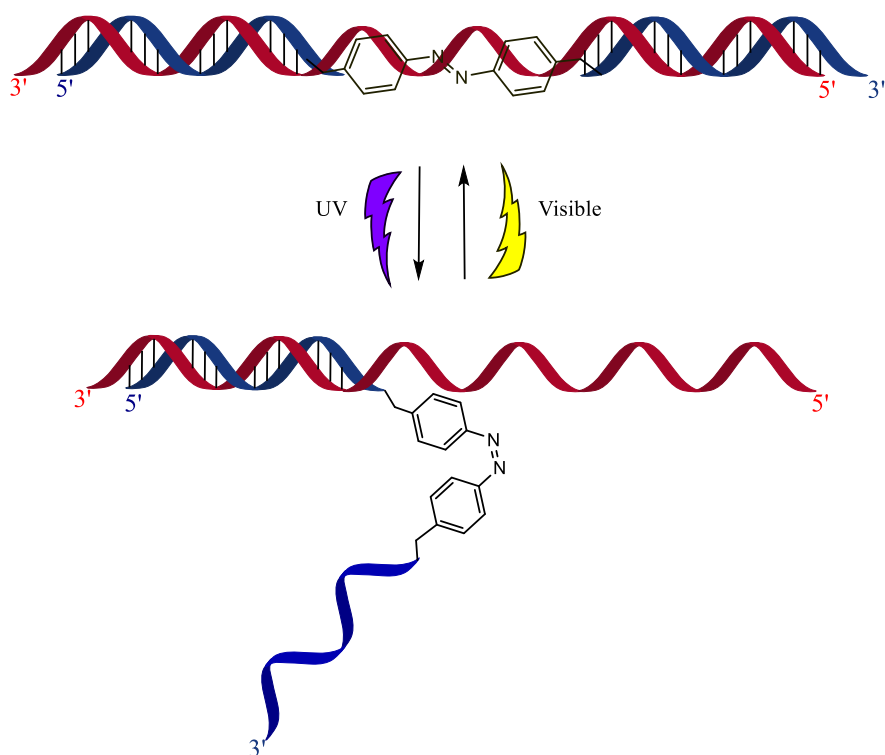


Figure 3.2. Photoinduced inactivation and reactivation of siRNAs. The blue strand corresponds to the sense strand, and contains the azobenzene moiety. The red strand corresponds to the antisense strand.

3.3 Materials and Methods

3.3.1 Procedure for Oligonucleotide Synthesis and Purification

All standard β -cyanoethyl 2'-*O*-TBDMS protected phosphoramidites, reagents and solid supports were purchased from Chemgenes Corporation and Glen Research. Wild-type luciferase strands including the sense and 5'-phosphorylated antisense strand were synthesized. All commercial phosphoramidites were dissolved in anhydrous acetonitrile to a concentration of 0.10 M. The chemically synthesized (azobenzene derivative) phosphoramidites were dissolved in 3:1 (v/v) acetonitrile:THF (anhydrous) to a concentration of 0.10 M. The reagents that were used for the phosphoramidite coupling cycle were: acetic anhydride/pyridine/THF (Cap A), 16% *N*-methylimidazole in THF (Cap

B), 0.25 M 5-ethylthio tetrazole in ACN (activator), 0.02 M iodine/pyridine/H₂O/THF (oxidation solution), and 3% trichloroacetic acid/dichloromethane. All sequences were synthesized on 0.20 μM or 1.00 μM dT solid supports except for sequences that were 3'-modified, which were synthesized on 1.00 μM Universal III solid supports. The entire synthesis ran on an Applied Biosystems 394 DNA/RNA synthesizer using 0.20 μM or 1.00 μM cycles kept under argon at 55 psi. Standard and synthetic phosphoramidites ran with coupling times of 999 seconds.

Antisense sequences were chemically phosphorylated at the 5'-end by using 2-[2-(4,4'-dimethoxytrityloxy)ethylsulfonyl]ethyl-(2-cyanoethyl)-(N,N-diisopropyl)-phosphoramidite. At the end of every cycle, the columns were removed from the synthesizer, dried with a stream of argon gas, sealed and stored at 4 °C. Cleavage of oligonucleotides from their solid supports was performed through on-column exposure to 1.50 mL of EMAM (methylamine 40% wt. in H₂O and methylamine 33% wt. in ethanol, 1:1 (Sigma-Aldrich)) for 1 hour at room temperature with the solution in full contact with the controlled pore glass. The oligonucleotides were then incubated overnight at room temperature in EMAM to deprotect the bases. On the following day, the samples were concentrated on a Speedvac evaporator overnight, resuspended in a solution of DMSO:3HF/TEA (100 μL:125 μL) and incubated at 65 °C for 3 hours in order to remove the 2'-O-TDBMS protecting groups. Crude oligonucleotides were precipitated in EtOH and desalted through Millipore Amicon Ultra 3000 MW cellulose. Oligonucleotides were separated on a 20% acrylamide gel and were used without further purification for annealing and transfection. Equimolar amounts of complimentary RNAs were annealed at 95 °C for 2 min in a binding buffer (75.0 mM KCl, 50.0 mM Tris-HCl, 3.00 mM MgCl₂, pH 8.30)

and this solution was cooled slowly to room temperature to generate siRNAs used for biological assays. A sodium phosphate buffer (90.0 mM NaCl, 10.0 mM Na₂HPO₄, 1.00 mM EDTA, pH 7.00) was used to anneal strands for biophysical measurements.

3.3.2 Procedure for Performing CD Experiments

Circular Dichroism (CD) spectroscopy was performed on a Jasco J-815 CD equipped with temperature controller. Equimolar amounts of each siRNA (10 μM) were annealed to their complement in 500 μL of a sodium phosphate buffer by incubating at 95 °C for two minutes and allowing to cool to room temperature. CD measurement of each duplex were recorded in triplicate from 200-500 nm at 25 °C with a screening rate of 20.0 nm/min and a 0.20 nm data pitch. The average of the three replicates was calculated using Jasco's Spectra Manager version 2 software and adjusted against the baseline measurement of the sodium phosphate buffer.

3.3.3 Procedure for Absorbance Spectra Experiments

All absorbance spectra measurements were done on a Jasco J-815 CD with temperature controller. Measurement was recorded from 200-500 nm at 10 °C at least 3 times. UV treated samples were placed under a UVP UVL-23RW Compact UV lamp 4.00 W 365nm for the indicated time. Visible light treated samples were placed under a 60.0 W daylight bulb from NOMA in standard desk lamp.

3.3.4 Procedure for Melting Temperature of siRNA Duplexes (T_m)

The siRNA duplexes annealed as above were placed in the Jasco J-815 CD spectropolarimeter and then UV absorbance was measured at 260 nm against a temperature gradient of 10 °C to 95 °C at a rate of 0.5 °C per minute with absorbance being measured

at each 0.5 °C increment. Absorbance was adjusted to baseline by subtracting absorbance of the buffer. The T_m values were calculated using Meltwin v3.5 software. Each siRNA result was the average of 3 independent experiments and the reported values were calculated using Meltwin v3.5 assuming the two-state model.²

3.3.5 Procedure for HPLC Characterization

HPLC chromatograms were obtained on a Waters 1525 binary HPLC pump with a Waters 2489 UV/Vis detector using the Empower 3 software. A C18 4.6 mm x 150 mm reverse phase column was used. Conditions were 5% acetonitrile in 95% 0.1 M TEAA (Triethylamine-Acetic Acid) buffer up to 100% acetonitrile over 40 min.

3.3.6 Procedure for Reduced Glutathione (GSH) Degradation Assay

The GSH assay was performed on siRNA 6 in a 96 well plate at 37 °C. A concentration of 2.7 μM of siRNA was added to 10 mM glutathione and 5 mM TCEP in PBS to a final volume of 100 μL. Dark experiments were performed with no additional treatment at 0, 4, 8, and 24 h time points after which the entire 100 μL was sample was injected into the HPLC and characterized (same conditions as above) to afford the HPLC traces at the different time points. UV treated siRNA was exposed to 5 min of UV light before incubation at 37 °C, and kept in the dark until injection for 0, 4, 8, 24 h time points. The UV 0 h time point was exposed to UV light and then injected immediately onto the HPLC.

3.3.7 Procedure for Maintaining Cell Cultures of HeLa Cells

For biological analysis of these siRNAs in a live environment, human epithelial cervix carcinoma cells were used (HeLa cells). They were kept in 250 mL vented culture

flasks using 25.0 mL of DMEM with 10% fetal bovine serum and 1% penicillin-streptomycin (Sigma) in an incubator set for 37 °C @ 5% CO₂ humidified atmosphere.

Once cell lines became confluent (80-90%) they were passaged by washing 3 times with 20 mL of phosphate buffered saline (NaCl 137 mM, KCl 2.70 mM, PO₄³⁻ 10.0 mM, pH 7.40) and incubated with 5.00 mL of 0.25% trypsin (SAFC bioscience) for 4 min @ 37 °C to detach the cells. The cells were transferred to a 50.0 mL centrifuge tube after the addition of 10.0 mL of DMEM solution and pelleted at 2000 rpm for 5 minutes. The supernatant was discarded and the pellet resuspended in 5.0 mL DMEM with 10% FBS.

A standard haemocytometer was used to obtain cell counts, after which the cells were diluted to a final concentration of 1.00 x 10⁶ cells/mL for subsequent assays. To continue the cell line 1.00 mL of freshly passaged cells was added to 24.0 mL of DMEM/10% FBS and 1% penicillin-streptomycin at 37 °C in a new culture flask while the rest were used for assays.

3.3.8 Procedure for siRNA Transfections

100 µL of cells (total 1.00 x 10⁵) were transfected into 12 well plates (Falcon®) with 1 mL of DMEM (10% FBS, 1% penicillin-streptomycin) and incubated at 37 °C with 5% CO₂. After 24 hours the cells were transfected with various concentrations of siRNAs, along with both pGL3 (Promega) and pRLSV40 luciferase plasmids using Lipofectamine 2000 (Invitrogen) in Gibco's 1X Opti-Mem reduced serum media (Invitrogen) according to the manufacturer's instructions. 1.00 µL of siRNA was added along with 2.00 µL (pGL3 200 ng) and 0.50 µL pRLSV40 (50.0 ng) to 100 µL of 1X Opti-Mem in a microcentrifuge tube and kept on ice for 5 min. In a different microcentrifuge tube 1.00 µL of Lipofectamine

2000 (Invitrogen) was mixed with 100 μ L of Gibco's 1X Opti-Mem reduced serum media (Invitrogen) and incubated at room temperature for 5 min. After 5 minutes the tubes were mixed and incubated at room temperature for 20 min and then the entire contents transferred to the wells of the 12 well plate.

3.3.9 Procedure for *in vitro* Dual-Reporter Luciferase Assay

100 μ L of cells (total of 1.00×10^5 cells) were added to 12 well plates (Falcon®) with 1 mL of growth media (DMEM 10% FBS, 1% penicillin-streptomycin) and incubated at 37 °C with 5% CO₂. After 24 hours the cells were transfected with 160, 400 and 800 pM concentrations of siRNAs, along with both pGL3 (Promega) and pRLSV40 luciferase plasmids using Lipofectamine 2000 (Invitrogen) in Gibco's 1X Opti-Mem reduced serum media (Invitrogen) according to the manufacturer's instructions. After a set amount of time (8 or 24 h) the cells were incubated at room temperature in 1X passive lysis buffer (Promega) for 20 minutes. The lysates were collected and loaded onto a 96 well, opaque plate (Costar). With a Dual-Luciferase reporter Assay kit (Promega), Lar II and Stop & Glo® luciferase substrates were sequentially added to the lysates and enzyme activity was measured through luminescence of both *firefly/Renilla* luciferase on a Synergy HT (Bio-Tek) plate luminometer. The ratio of *firefly/Renilla* luminescence is expressed as a percentage of reduction in *firefly* protein expression to siRNA efficacy when compared to untreated controls. Each value is the average of at least 3 different experiments with standard deviation indicated.

3.3.10 Procedure for Light Inactivation of Azobenzene Modified siRNA (*trans* to *cis*)

The cell culture plates were exposed to a 4.00 W 365 nm UV lamp (UVP) 2 hours after transfection for 8 h assays (1 exposure total) and every 4 h thereafter for 24 h assays (6 exposures total). Luciferase assays were then performed as indicated above at the desired time points.

3.3.11 Procedure for Light Reactivation of Azobenzene Modified siRNA (*cis* to *trans*)

4 hours after the transfection procedure, the plate was exposed to a 60.0 W daylight bulb (NOMA) and left under the visible lamp for the rest of the time before the cells were lysed and the plate read as above.

3.3.12 Procedure for consecutive UV/Vis Light Cycling (1.5x and 2x light cycling)

The first cycle was performed normally: UV inactivation after 2 hours for 45 min, and then visible light reactivation at 4 hours for 30 min. We then observed continued exposure to UV light every 4 hours for 45 min, as per the normal procedure up to 24 h (1.5x, 5 exposures total) to keep the siRNA inactive. The 2x procedure was identical except after the second UV exposure (45 min), a 1 h 15 min resting period of darkness to let the cells recover was observed after which the cells were re-exposed to visible light for 30 min which restored the siRNAzo's activity.

3.3.13 Transfection of HeLa cells with Lipofectamine 2000

Cell transfection procedure was identical to the dual assay procedure, above.

3.3.14 HeLa Cell Reverse Transcription (RT) Preparation

After the expired transfection period the growth medium was removed and the plate was washed twice with PBS. The cells were removed from the plate using 250 μ L of 0.25% trypsin to each well and incubated for 4 minutes at 37 °C with 5% CO₂. The cell suspension was then added to 1 mL of growth medium to inactivate the trypsin and centrifuged at 2000 rpm for 5 min. The supernatant was discarded and the cells were resuspended in 500 μ L of fresh media. The cells in each tube were then counted to ensure a total number of cells between 100-200k per sample. After counting the cells were repelleted as above and washed with 500 μ L of ice-cold PBS and then repelleted and the pellet was placed on ice.

3.3.15 RT-PCR with the Invitrogen cells to cDNA kit II

The following protocol uses reagents found in the Cells-to-cDNA kit purchased from Invitrogen. The pellet on ice was resuspended in 100 μ L of ice cold Cell Lysis II Buffer and each sample was mixed by vortex. The samples were then immediately transferred to a pre-heated 75 °C heat block and left to denature for 10 minutes. The samples were then removed from the water bath and placed on ice. To each centrifuge tube, 2 μ L of DNase I (2 U/ μ L stock) was added and these mixtures were gently vortexed followed by a brief centrifugation to concentrate the sample. A genomic wipeout was accomplished by incubating the DNase I reaction at 37°C for 30 minutes. The samples were then heated to 75 °C for 10 minutes to deactivate the DNase I. To new nuclease-free microfuge tubes, was added 5 μ L of cell lysate (RNA), 4 μ L of dNTP mix(2.5 mM stock

for each dNTP), 2 μ L of random decamers (50 μ M stock) and 9 μ L of nuclease-free water. The resulting mixture was then heated to 70 °C for 5 minutes to denature the RNA template, placed on ice for 1 minute, flash centrifuged, and placed on ice. The remaining RT reagents including: 2 μ L of 10X RT Buffer, 1 μ L of M-MLV Reverse Transcriptase (or 1 μ L of nuclease-free H₂O for a no reverse transcription (NRT) Control) and 1 μ L of RNase inhibitor (10 U/ μ L stock) were added, mixed and centrifuged briefly. Reverse transcription was initiated by warming the samples to 42 °C using a thermal cycler for 60 minutes. Reverse transcriptase was inactivated by incubating the samples at 95°C for 10 minutes. This lysate can be stored for up to 2 weeks at -20 °C.

3.3.16 RNA extraction, cDNA synthesis and RT-qPCR

Prior to the RNA extraction, each well of the 24-well plate washed twice with 1X PBS. Total RNA was extracted from the Hela cells using the manufacturer's instructions of the Total RNA Purification Plus Kit (Cat#: 48400. Norgen BioTek Corp, Thorold, ON, Canada). In addition, an on-column DNA digestion was performed using RNase Free DNase I Kit (Cat#:25710. Norgen BioTek Corp, Thorold, ON, Canada). Two microliter of each extracted RNA sample was used to measure the concentration and RNA integrity on the BioDrop (UK), and the presence of the RNA was confirmed by gel electrophoresis on a 1% (w vol-1) agarose. Three biological replicates were completed for each Azo-Modified SiRNA. The SiRNAs were inactivated and reactivated using the exact same procedures as listed above for the firefly/ *Renilla Luciferase* assays.

The cDNA was produced using IScript cDNA synthesis kit (Cat #: 1708891. Bio-Rad, Hercules, California) using 1 μ g of total RNA, M-MLV reverse transcriptase, oligo (DT) and random primers. Two negative controls were performed with all reactions. The

first control contained the RNA template and all DNase/RT reagents, except for the final addition of the RT enzyme. A second control contained no template (water only) to ensure that all reagents were free from possible contaminants. Once cDNA was produced, the products could be amplified (RT-qPCR).

3.3.17 Quantitative RT-PCR

To each reaction tube within the 96-well PCR plate (BIO-RAD) was added: 2 μ L of cDNA template, 2 μ L of NRT (No Reverse Transcriptase) control samples and nuclease-free water for a no template control (NTC), 10 μ L of SsoFast EvaGreen Supermix (BIO-RAD) containing SYBRgreen dye as a source of fluorescent nucleic acid dye and Sso7d-fusion polymerase to amplify DNA, 1 μ L of a 10 μ M stock of forward and reverse BCL-2 primers (final 50 nM) or 1 μ L of a 10 μ M stock of forward and reverse 18S rRNA primers (final 50 nM) and 6 μ L of nuclease-free water to give a total volume of 20 μ L.

The q-PCR reaction was performed and recorded by a CFX96 Real-Time reactor (BIO-RAD). NRT controls were performed during standard curve analysis to confirm that amplification of the PCR product was cDNA and not genomic DNA. NTC controls were also performed to ensure that amplification of the PCR product was not a result of primer-dimers. The BCL-2 forward and reverse primers were 5'-CTG GTG GGA GCT TGC ATC AC-3' and 5'-ACA GCC TGC AGC TTT GTT TC-3', respectively, yielding a 150-bp amplicon. The 18S rRNA forward and reverse primers were 5'-CGG CTA CCA CAT CCA AGG AAG-3' and 5'-CGC TCC CAA GAT CCA ACT AC-3', respectively, yielding a 247-bp amplicon. The protocol that was utilized to amplify the BCL-2 and 18S rRNA PCR products consisted of the following steps: pre-heat to 95°C for 2 minutes, 40 cycles of denaturing at 95 °C for 10 seconds, annealing at 52 °C for 30 seconds, and extension at 72

°C for 30 seconds. A melting curve analysis was performed on each amplicon by raising the temperature from 65 °C to 95 °C at 0.5 °C/min increments and measuring the absorbance at 260 nm. BCL-2 gene expression was normalized to 18S rRNA in triplicate by performing a gene study analysis using Bio-Rad CFX Manager (Version 3.1) software with 18S rRNA selected as a reference.

3.3.18 Procedure for XTT Assays

XTT reagents were allowed to thaw in the incubator at 37 °C. Once a consistent liquid with no particles was obtained after thawing, 2.5 mL of XTT Reagent was combined with 0.05 mL of Activation Reagent. 200 µL of this mixture was added to each well and the plates were placed back in the incubator for at least one hour. Plates were read using a BioTek plate reader (Fischer Scientific). All blanks and samples were averaged at both wavelengths. Specific absorbance for UV and non-UV samples were calculated using the following equation:

$$\text{Specific Absorbance at 475 nm} = \text{Test Avg}_{475\text{nm}} - \text{Blank Avg}_{475\text{nm}} - \text{Test Avg}_{660\text{nm}}$$

Cell viability was then assessed and error bars were placed based on standard deviation.

3.4 Results

The siRNAzOs that we generated contained the azobenzene within the central region of the sense strand (see Table 3.1). siRNAzo **1** replaces positions 8 and 9 from the 5'-end of the sense strand. Moving this azobenzene unit (Az2) one nucleobase at a time, siRNAzOs **2**, **3**, and **4** replace positions 9 and 10, 10 and 11, and 11 and 12 from the 5'-end of the sense strand, respectively. The siRNAzOs 5-7 designed to target the endogenous *BCL2* gene also

contain the azobenzene unit within the central region of the sense strand. Our previous work showed that not only did the siRNAzOs **1-4** have excellent knockdown at picomolar concentrations, but we could also control the siRNAzo's activity through UV inactivation prior to the transfection of the siRNAs.¹³ We also demonstrated the ability to restore siRNA activity through the application of the broadband visible light greater than 450 nm.

Table 3.1. Table of RNAs used and its target.^[a]

siRNAzo	siRNAzo duplex	target
wt	5'-CUUACGCUGAGUACUUCGAtt-3' 3'-ttGAAUGCGACUCAUGAAGCU-5'	luciferase
1	5'-CUUACGC <u>Az2</u> AGUACUUCGAtt-3' 3'-ttGAAUGCGACUCAUGAAGCU-5'	luciferase
2	5'-CUUACGCU <u>Az2</u> GUACUUCGAtt-3' 3'-ttGAAUGCGACUCAUGAAGCU-5'	luciferase
3	5'-CUUACGCUG <u>Az2</u> UACUUCGAtt-3' 3'-ttGAAUGCGACUCAUGAAGCU-5'	luciferase
4	5'-CUUACGCUGA <u>Az2</u> ACUUCGAtt-3' 3'-ttGAAUGCGACUCAUGAAGCU-5'	luciferase
5	5'-GCCUUCU <u>Az2</u> GAGUUCGGUGtt-3' 3'-ttCGGAAGAAACUCAAGCCAC-5'	<i>BCL2</i>
6	5'-GCCUUCUU <u>Az2</u> AGUUCGGUGtt-3' 3'-ttCGGAAGAAACUCAAGCCAC-5'	<i>BCL2</i>
7	5'-GCCUUCUUUG <u>Az2</u> UUCGGUGtt-3' 3'-ttCGGAAGAAACUCAAGCCAC-5'	<i>BCL2</i>

[a] Az2 corresponds to the azobenzene derivative synthesized from 4-nitrophenylethyl alcohol; the top strand corresponds to the sense strand; the bottom strand corresponds to the antisense strand. In all duplexes, the 5'-end of the bottom antisense strand contains a 5'-phosphate group.

While this work was incredibly promising and useful, we were limited by the azobenzenes propensity to thermally relax back to *trans* when in the *cis* conformation. Azobenzene's half life at 37 °C is approximately 4 hours,¹⁵ and this limited the durations we could do these experiments at, and consequently limiting their usefulness for longer term experiments.

In this current manuscript, and building from our previous work, we demonstrate that our siRNAzOs can be inactivated after transfection, inside the cells through the controlled application of UV light to the cell culture without damaging the cells. We are also able to reactivate the siRNAzOs with visible light. Furthermore, we are able to complete this deactivation/activation cycle up to two times for an siRNAzo. To the best of our knowledge, this marks the first report of using an active siRNA, and inactivating it within cell culture, and then later reversibly activating it. In order to understand the reversible gene-silencing effect observed in our study, we first must understand the RNAi gene-silencing mechanism.

When a siRNA is incorporated into an active antisense-RISC complex, the sense strand is released. This active antisense strand complex can then target its mRNA for cleavage. However, once this active antisense-RISC complex forms, we are not able to inactivate its function reversibly because the azobenzene modification is contained within the sense strand. Thus, within the cell, there is an equilibrium that exists between unbound siRNAs and its bound active antisense-RISC complex. Yet, out of the total siRNA molecules internalized into the cell, it has been shown that only around 4% or less is actively associated with the RISC complex.¹⁶ By inactivating unbound siRNAs in the cell, we can prevent further loading to the RISC complex, and prevent the formation of more active

antisense-RISC complexes. This in turn would reduce the amount of gene-silencing over time.

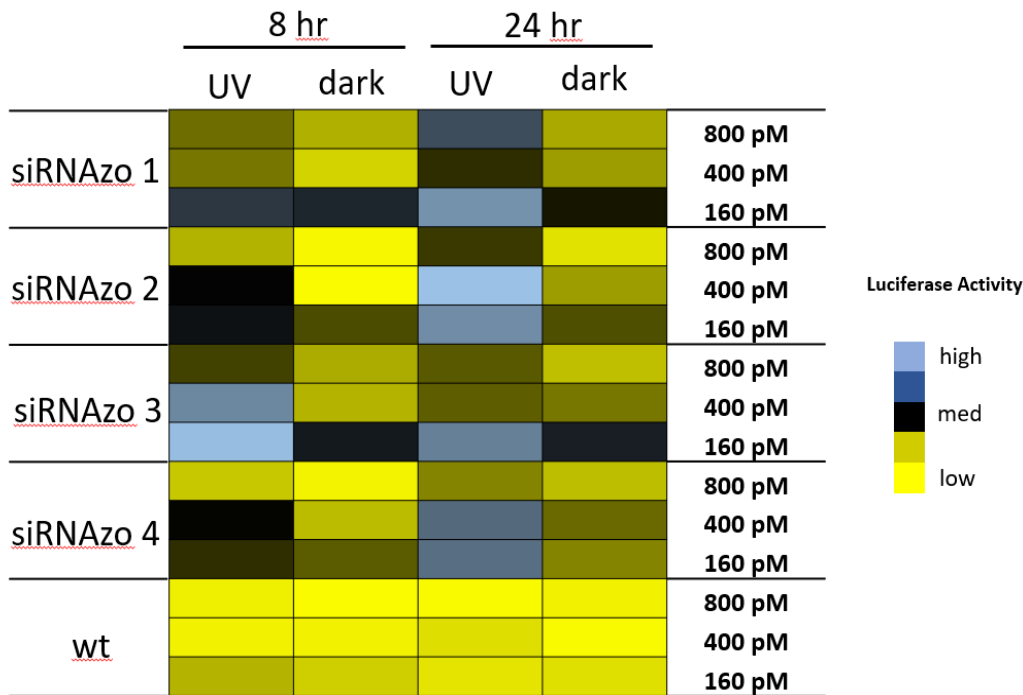


Figure 3.3. Normalized firefly luciferase activity for siRNAzOs 1-4 and wt at 160, 400 and 800 pM in HeLa cells monitored 8- and 24- hours post-transfection. UV corresponds to the siRNA being exposed under a 365nm UV lamp for inactivation 2 h post transfection for 45 min (8 hr), and for an additional 45 min of UV exposure every 4 hours (24 hr). Dark corresponds to siRNAs being transfected in HeLa cells in the absence of UV light. 8-hour fold changes differences in activity for siRNAzOs 1-4 (UV vs dark) for were between 2 – 55 fold, and 24-hour fold changes were between 1 - 7 fold. See section 3.7 for detailed silencing profiles.

In our previous study, we observed UV-mediated inactivation of the siRNAzo to be effective at 8-hour time points, but at 12 hours the siRNAzo resumed some activity.

Although the 8-hour time point is optimal for short assays, many gene expression studies go beyond 8 hours, and we wanted to develop a more robust system that was effective beyond this time window. Using the Dual-Luciferase Reporter® Assay (Promega), we modified our procedure (see Supplement for experimental procedures) to transfect active siRNAzOs, in which we could inactivate with UV exposure (45 min dose) two hours post

transfection. Within the 8-hour assay time-frame, one exposure of UV light was sufficient to keep the unbound siRNAs inactive, but in order to extend this level of inactivity to a 24 hour window, we exposed the transfected cells to low repeated doses of UV light (a 45 minute dose of low intensity 365 nm UV light, repeated every four hours, for a total of six UV exposures). Previous literature reported that this amount of UV light for up to 24 hours was not particularly harmful to the cells.¹⁷ We also conducted XTT assays on the cell cultures exposed to UV light, and no loss on cell viability was observed (See Supplement S1, Appendix II). Our gene-silencing results for these two assays are shown in Figure 3, as a color-coded chart (see Figures S12-S17 in Appendix II for the corresponding numerical bar graphs).

High luciferase activity is correlated to the intensity of the blue pixel, whereas low luciferase activity correlates to the intensity of the yellow pixel. There is a clear difference shown in luciferase activity between the UV and dark columns for both time points. Initially, at both 8- and 24-hour time points, luciferase activity is low for the dark-treated samples (dark), an indication of strong RNAi activity. Exposure to UV light causes RNAi activity to diminish and as a result luciferase activity was found to increase as shown by the black and blue pixels in the color-coded chart (UV). More importantly, we were able to keep the unbound siRNA inactive for up to 24 hours, without thermal relaxation, which is a significant improvement over our previous study where after 12 hours the

siRNAzo was active.¹³ Overall, the siRNAzos in their active form have good activity, however, we are able to inactivate their activity for up to 24 hours post transfection.

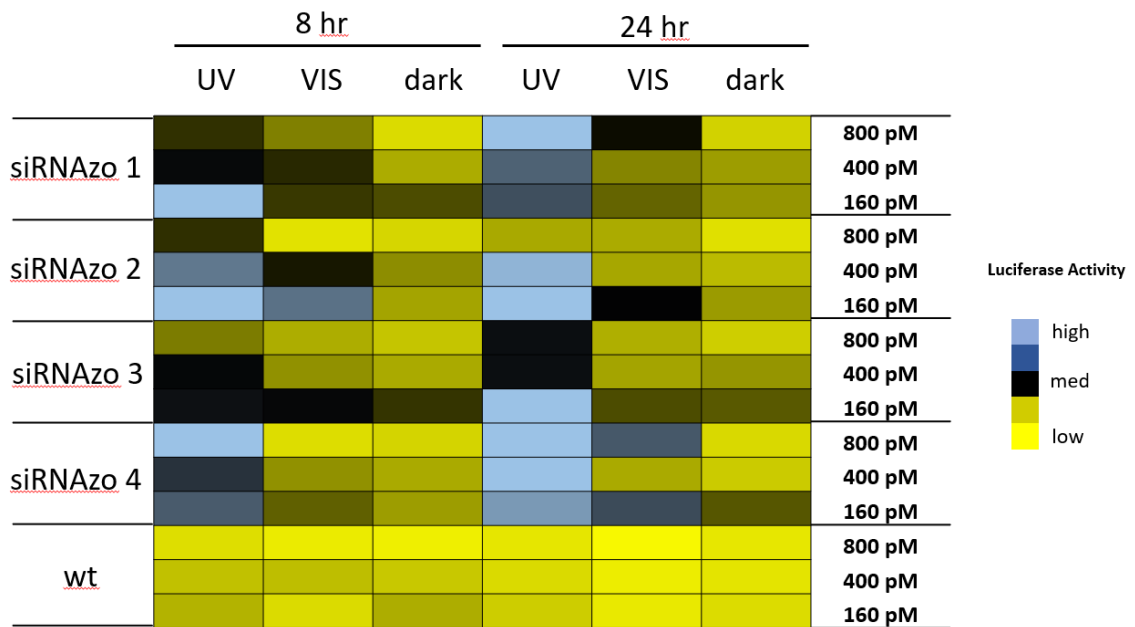


Figure 3.4. Normalized firefly luciferase expression for siRNAzos 1-4 and wt at 160, 400, and 800 pM in HeLa cells monitored 8- and 24-hours post-transfection. UV corresponds to the siRNA being exposed under a 365nm UV lamp for inactivation 2 h post transfection for 45 min (8 hr), and for an additional 45 min of UV exposure every 4 hours (24 hr). VIS corresponds to visible light exposure 4 h after transfection. Dark corresponds to siRNAs being transfected in HeLa cells in the absence of UV light. Fold changes for siRNAs 1-4 (UV vs dark) for 8 h were between 2 and 14 fold, and 24-hour fold change differences were between 3 and 21 fold. See section 3.7 for detailed silencing profiles.

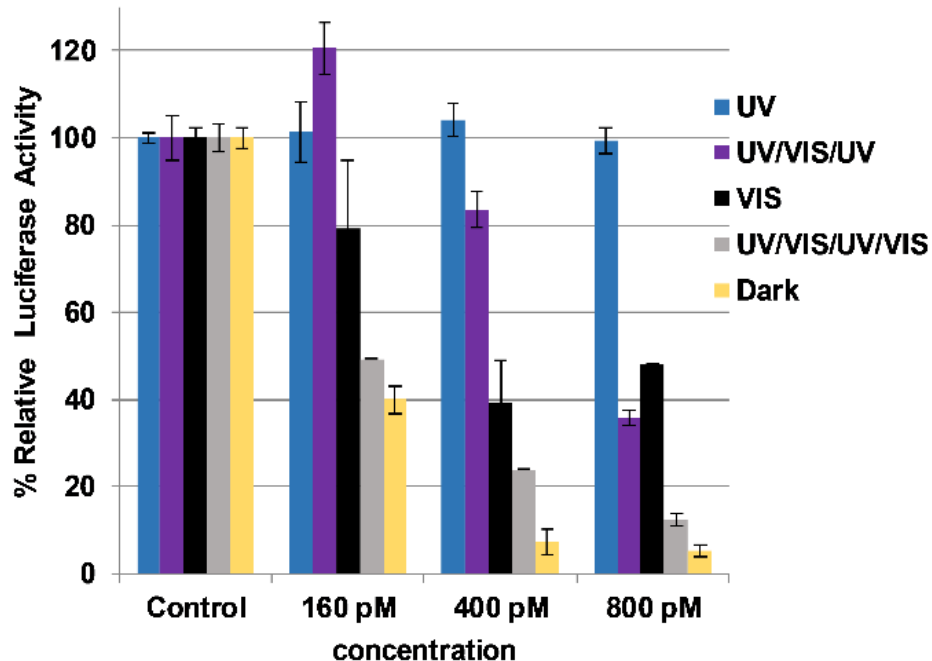


Figure 3.5. Normalized firefly luciferase expression for siRNAzo 4 at 160, 400 and 800 pM in HeLa cells monitored 24 hours post-transfection. UV corresponds to the siRNAzo being exposed under a 365nm UV lamp for inactivation 2 h post transfection for 45 min, and for an additional 45 min of UV exposure every 4 hours (six exposures total). UV/VIS/UV corresponds to one and a half consecutive UV/VIS cycles: UV inactivation, 2 hours post-transfection for 45 min, followed by visible light reactivation at 4 hours after transfection for 30 min. A 2-hour rest period of darkness followed by re-exposure to UV light for 45 min, being re-exposed every 4 hours to UV (45 min) afterwards (5 exposures total). VIS corresponds to visible light exposure 4 h after transfection. UV/VIS/UV/VIS corresponds to two consecutive UV/Vis cycles: UV inactivation, 2 hours post-transfection for 45 min, followed by visible light reactivation at 4 hours after transfection for 30 min. A 2-hour rest period of darkness followed by re-exposure to UV light for 45 min, followed by 1 h 15 min in the dark and then the visible light for 30 min (Supplement S1 in Appendix II for details). Dark corresponds to siRNAzo 4 being transfected in HeLa cells in the absence of UV light.

In the next experiment, we examined whether we could not only keep the unbound siRNAzo inactive for 24 hours, but also reactivate the unbound siRNAzos at a desired timepoint. The color-coded chart in Figure 3.4 shows this data (see Figures S18-S27 in Appendix II for the corresponding numerical bar graphs). As before, the UV-treated samples (UV) have only moderate to high luciferase activity, the visible-light treated samples (VIS) have moderate to low luciferase activity, and the no light (dark) samples

have low luciferase activity. In all cases, we were able to take an inactive siRNAzo (**1 – 4**), and restore its RNAi activity as measured by low luciferase activity after visible light exposure.

We also explored whether the siRNAzo would remain intact after multiple on/off cycles. The gene-silencing data for this experiment is shown in Figure 3.5 where the UV/VIS/UV/VIS bar (grey) shows that knockdown remains robust after two cycles. The first cycle was performed identically to the 8-hour inactivation assay highlighted in Figures 3 and 4. After 8 hours, we then observed a 2-hour resting period of darkness to let the cells recover after which the cells were re-exposed to UV light for 45 min. After this exposure, the cells were allowed to rest for 1 h 15 min in the dark and then the visible light was utilized again for 30 min to restore the siRNAzo's activity. This second cycle was an important step to show that after one cycle, siRNAzo activity was maintained. At all three concentrations (160, 400, and 800 pM), activity was restored and this is shown with the grey bar in Figure 5. There is a clear difference in gene-silencing activity between this grey bar and the blue inactivation bar, even after two doses of UV light. Additionally the UV/VIS/UV corresponds to 1.5 cycles (purple bar), and in Fig 5 the gene-silencing data illustrates that after one inactivation cycle, we can reactivate and then deactivate the siRNAzo and it remains inactive for the remaining 24 h of the assay at 160 and 400 pM. At the higher concentration 800 pM, full inactivity is not fully restored, but is less active than the two full cycles (UV/VIS/UV/VIS) and the dark control (yellow). In addition, to investigate the effect of metabolism on the siRNAzos, we performed a glutathione reduction assay on the sense strand of an siRNAzo and observed minimal degradation for up to 24 hours as monitored by HPLC (see supplement in Appendix II, S38 for details).

In addition, we also examined the inactivation and reactivation of an siRNAzo targeting the endogenous target, *BCL2* (Table 1). This anti-apoptotic endogenous target is of particular interest because it is one of the many oncogenes associated with several cancers that are upregulated.^{18,19} In a previous study of ours, we observed good knockdown of *BCL2* using siRNAs bearing a conformationally-constrained biphenyl spacer within the central region of the sense strand.²⁰ Using our photoresponsive protocol highlighted with the luciferase target, we conducted a similar experiment using real-time polymerase chain reaction (RT-PCR) to quantify the gene-silencing results.

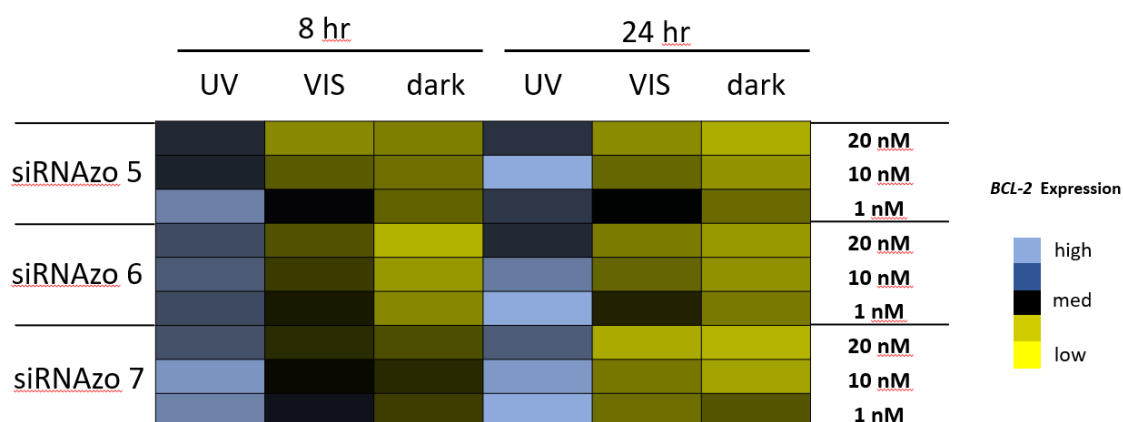


Figure 3.6. *BCL2* expression normalized to 18S for siRNAzOs **5-7** at 1, 10 and 20 nM in HeLa cells monitored 8 (left) and 24 (right) hours post-transfection. UV corresponds to the siRNA being exposed under a 365nm UV lamp for inactivation 2 h post transfection for 45 min (8 h), and for an additional 45 min of UV exposure every 4 hours (24 h). VIS corresponds to visible light exposure 4 h after transfection. Dark corresponds to siRNAzOs being transfected in HeLa cells in the absence of UV light. See section 3.7 for detailed silencing profiles.

The left half of Figure 3.6 shows the results of the *BCL2* targeting siRNAzOs **5-7** at the 8-hour time point, with the siRNAzOs being pre-inactivated prior to transfection. Four hours post-transfection, UV light was administered. As demonstrated in Figure 6, poor RNAi activity of the siRNAzo is observed as indicated by the presence of high *BCL2* expression.

In an experiment involving the same transfection setup, visible light was administered four hours post-transfection. As is indicated, excellent gene silencing was observed. The difference between the active and inactive siRNAzo complexes is between two- and five-fold which is to our knowledge the first time an endogenous gene expression silencing profile could be controlled via the RNAi pathway in this manner. A dark control experiment involved transfecting an active *BCL2* siRNAzo, and maintaining its active form in the dark. As expected, this experiment showed excellent dose-dependent gene-silencing characteristics.

The right half of Figure 3.6 shows the results for the longer 24 hour time point assay, in which we could maintain inactivation of the unbound siRNAzos over the duration of the assay. As done similarly to the luciferase assays, transfections were carried out with the active form of siRNAzos **5-7** and 2 hours later was exposed to repeated doses of 365 nm UV light to inactivate it. The changes in gene silencing activity are between three- and five-fold for the different concentrations. This is consistent with the 8-hour assay. These two experiments show that our siRNAzos are not only effective against endogenous targets, but we can inactivate their activity with UV light.

To account for the reversible gene-silencing observed by the siRNAzos, we must consider both the populations of unbound siRNAzos and siRNAzos bound to RISC in the cell. The azobenzene modification is located on the sense strand of the siRNAzo. When the RISC-antisense strand is activated, the sense strand is no longer part of the complex. Thus, when UV light enters the cell, it is not capable of reversing the antisense strand from the RISC complex. This system differs in its reversibility mechanism compared to the reported high-affinity short oligonucleotides that reversibly target the siRNA guide strand.⁶ In our system,

a population of siRNAzOs will be loaded by the RISC complex to form an active RISC-antisense complex, and another population of siRNAzOs will remain unbound. Thus, by subjecting the cells to UV light, we hypothesize that this would inhibit the loading of remaining free siRNAzOs to the RISC complex. Reactivation of this complex with visible light, would then restore siRNAzo to its active form, which can then be loaded with more RISC complexes to further gene silence. We believe that this mechanism accounts for the reversible gene-silencing observed.

3.5 Conclusions

In conclusion, we are reporting here a significant improvement over prior reports of photoresponsive siRNA technology because we can reversibly control the activity of an exogenous and endogenous target with light. This newfound ability to reversibly control an endogenous target's activity after deployment into the tissue, would be useful for controlling adverse side effects in susceptible individuals. Many prior siRNAs that targeted a variety of diseases resulted in unexpected side effects.²¹ Another potential application for these siRNAzOs is their use as biomolecular tools to examine the effect of gene expression of complex and/or interrelated genes, in real time. Currently, the simultaneous deployment of multiple siRNAs (siRNA cocktails) is limited because they are concurrently deployed at once post-transfection. Using our siRNAzo technology, we could allow for several different gene-silencing siRNAs to be controlled in real time via light. Our future works include red-shifting the azobenzene's isomerization wavelengths out of the UV portion of the spectrum, thereby allowing us to have unique photochemical control of these siRNAs using specific wavelengths.

Acknowledgements

We thank the Natural Sciences and Engineering Research Council (NSERC) for funding.

Supplementary Data

Refer to Appendix II for additional figures and characterization data.

3.6 REFERENCES– Chapter 3 – Manuscript II

- (1) A. Fire, S. Q. Xu, M. K. Montgomery, S. A. Kostas, S. E. Driver and C. C. Mello, *Nature*, 1998, **391**, 806.
- (2) L. Aagaard and J. J. Rossi, *Adv. Drug Deliv. Rev.*, 2007, **59** 75.
- (3) A. L. Hopkins and C. R. Groom, *Nat. Rev. Drug Discov.*, 2002, **1** 727.
- (4) X. Shen and D. R. Corey, *Nucleic Acids Res.*, 2017, **46**, 1584.
- (5) D. Al Shaer, O. Al Musaimi, F. Albericio and B. G. de la Torre, *Pharmaceuticals* 2019, **12**, 52.
- (6) I. Zlatev, A. Castoreno, C. R. Brown, J. Qin, S. Waldron, M. K. Schlegel, R. Degaonkar, S. Shulga-Morskaya, H. Xu, S. Gupta, S. Matsuda, A. Akinc, K. G. Rajeev, M. Manoharan and V. Jadhav, *Nat. Biotechnol.* 2018, **36**, 509.
- (7) S. Shah, S. Rangarajan and S. H. Friedman, *S. H. Angew. Chem. Int. Ed.* 2005, **44**, 1328.
- (8) V. Mikat and A. Heckel, *RNA* 2007, **13**, 2341.
- (9) A. Meyer and A. Mokhir, *Angew. Chem. Int. Ed.* 2014, **53**, 12840.
- (10) A. S. Lubbe, W. Szymanski and B. L. Feringa, *Chem. Soc. Rev.* **2017**, **46**, 1052.
- (11) C. Brieke, F. Rohrbach, A. Gottschalk, G. Mayer and A. Heckel, *Angew. Chem. Int. Ed.* 2012, **51**, 8446.
- (12) A. A. Beharry and G. A. Woolley, *Chem. Soc. Rev.* 2011, **40** 4422.
- (13) M. L. Hammill, C. Isaacs-Trépanier and J.-P. Desaulniers, *ChemistrySelect* 2017, **2**, 9810.
- (14) M. L. Hammill, A. Patel, M. A. Alla and J.-P. Desaulniers, *Bioorg. Med. Chem. Lett.* 2018, **28**, 3613.
- (15) K. Yamana, K. Kan, and H. Nakano, *Bioorg. Med. Chem.* 1999, **7**, 2977.
- (16) Y.I. Pei, P.J. Hancock, H. Zhang, R. Bartz, C. Cherrin, N. Innocent, C. J. Pomerantz, J. Seitzer, M.L. Koser, M.T. Abrams, Y. Xu, N.A. Kuklin, P.A. Burke, A.B. Sachs, L. Sepp-Lorenzino, and S. T. Barnett. *RNA* 2010, **16**, 2553.
- (17) J. D. Stoen, and R. J. Wang, *Proc. Nat. Acad. Sci. USA* 1974, **71**, 3961.
- (18) M. L. Cleary, S. D. Smith and J. Sklar, *Cell* 1986, **47**, 19.
- (19) G. Kroemer, *Nat. Med.*, 1997, **3**, 614.

- (20) J.-P. Desaulniers, G. Hagen, J. Anderson, C. McKim and B. Roberts, *RSC Adv.* 2017, **7**, 3450.
- (21) M. E. Kleinman, K. Yamada, A. Takeda, V. Chandrasekaran, M. Nozaki, J. Z. Baffi, R. J. C. Albuquerque, S. Yamasaki, M. Itaya and Y. Pan, *Nature* 2008, **452**, 591.

3.7 Manuscript II Supplementary Figures and Tables

Full Supplementary data can be found in Appendix II

Figures and Tables

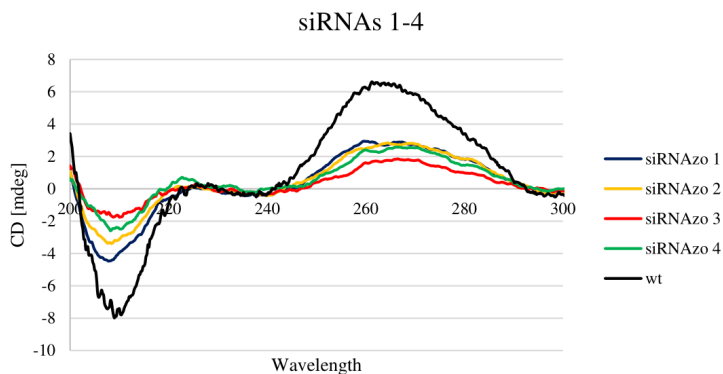


Figure S-1. CD spectra of azobenzene modified spacers replacing two nucleobases targeting firefly luciferase mRNAs. Wildtype and modified anti-*firefly* luciferase siRNAs (10 μ M/duplex) were suspended in 500 μ L of a sodium phosphate buffer (90.0 mM NaCl, 10.0 mM Na₂HPO₄, 1.00 mM EDTA, pH 7.00) and scanned from 200-300 nm at 25 °C with a screening rate of 20.0 nm/min and a 0.20 nm data pitch. All scans were performed in triplicate and averaged using Jasco's Spectra Manager version 2.

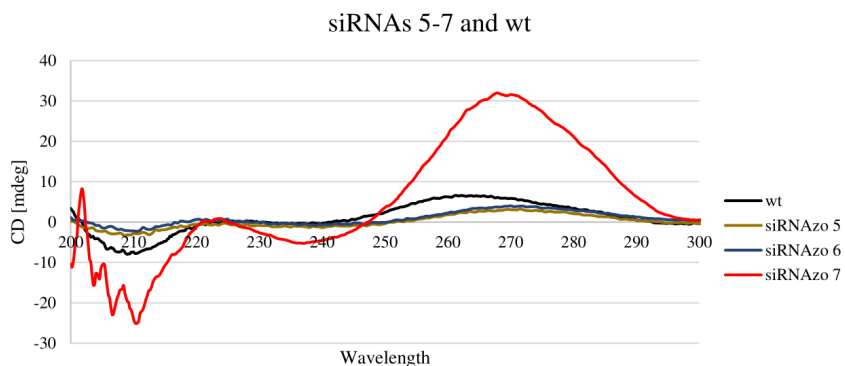


Figure S-2. CD spectra of azobenzene modified spacers replacing two nucleobases targeting *BCL2* mRNAs. Wildtype and modified anti-*BCL2* siRNAs (10 μ M/duplex) were suspended in 500 μ L of a sodium phosphate buffer (90.0 mM NaCl, 10.0 mM Na₂HPO₄, 1.00 mM EDTA, pH 7.00) and scanned from 200-300 nm at 25 °C with a screening rate of 20.0 nm/min and a 0.20 nm data pitch. All scans were performed in triplicate and averaged using Jasco's Spectra Manager version 2. Updated with siRNAs 5 and 6

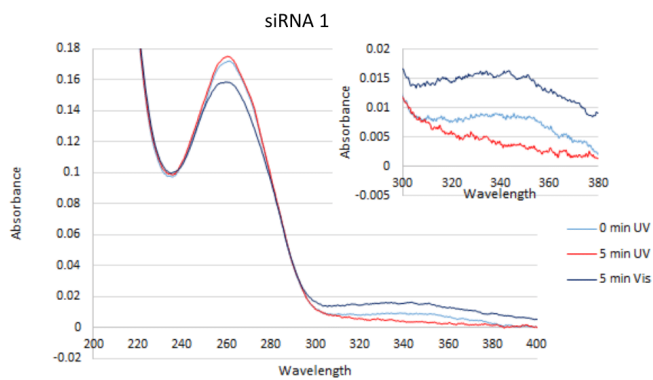


Figure S-3. Absorbance Profile of siRNA 1 when exposed to UV and Visible light in 500 μ L of a sodium phosphate buffer (90.0 mM NaCl, 10.0 mM Na_2HPO_4 , 1.00 mM EDTA, pH 7.00) and scanned from 200-400 nm at 10 $^\circ\text{C}$ with a screening rate of 20.0 nm/min and a 0.20 nm data pitch. Inset: Zoomed in portion of 320-380 nm highlighting azobenzene changes

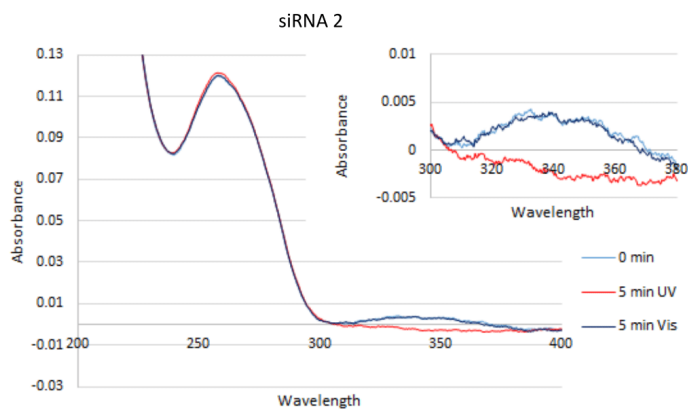


Figure S-4. Absorbance Profile of siRNA 2 when exposed to UV and Visible light in 500 μ L of a sodium phosphate buffer (90.0 mM NaCl, 10.0 mM Na_2HPO_4 , 1.00 mM EDTA, pH 7.00) and scanned from 200-400 nm at 10 $^\circ\text{C}$ with a screening rate of 20.0 nm/min and a 0.20 nm data pitch. Inset: Zoomed in portion of 320-380 nm highlighting azobenzene changes

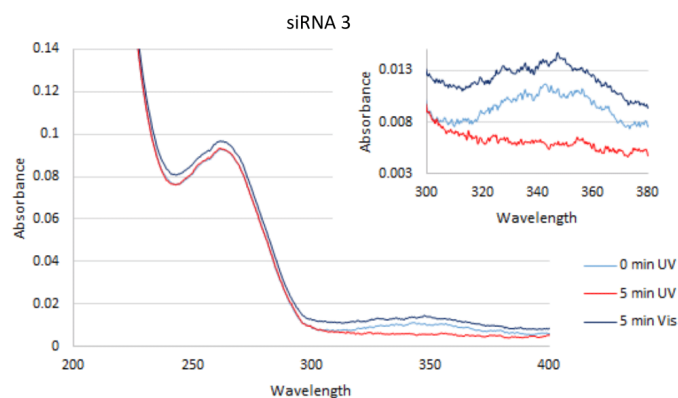


Figure S-5. Absorbance Profile of siRNA 3 when exposed to UV and Visible light in 500 μ L of a sodium phosphate buffer (90.0 mM NaCl, 10.0 mM Na_2HPO_4 , 1.00 mM EDTA, pH 7.00) and scanned from 200-400 nm at 10 $^\circ\text{C}$ with a screening rate of 20.0 nm/min and a 0.20 nm data pitch. Inset: Zoomed in portion of 320-380 nm highlighting azobenzene changes

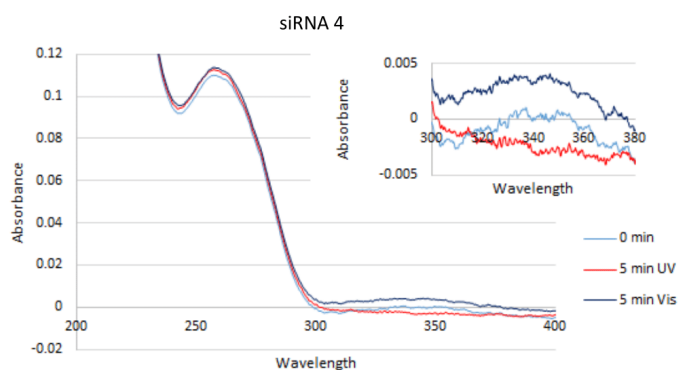


Figure S-6. Absorbance Profile of siRNA 4 when exposed to UV and Visible light in 500 μ L of a sodium phosphate buffer (90.0 mM NaCl, 10.0 mM Na_2HPO_4 , 1.00 mM EDTA, pH 7.00) and scanned from 200-400 nm at 10 $^\circ\text{C}$ with a screening rate of 20.0 nm/min and a 0.20 nm data pitch. Inset: Zoomed in portion of 320-380 nm highlighting azobenzene changes

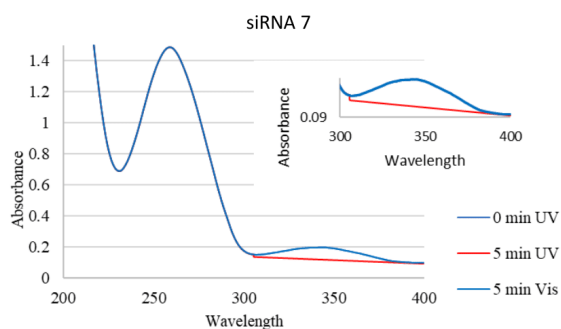


Figure S-7. Absorbance Profile of siRNA 7 when exposed to UV and Visible light in 500 μ L of a sodium phosphate buffer (90.0 mM NaCl, 10.0 mM Na_2HPO_4 , 1.00 mM EDTA, pH 7.00) and scanned from 200-400 nm at 10 $^\circ\text{C}$ with a screening rate of 20.0 nm/min and a 0.20 nm data pitch. Inset: Zoomed in portion of 320-380 nm highlighting azobenzene changes. SiRNAs 5 and 6 have similar profiles (data not shown).

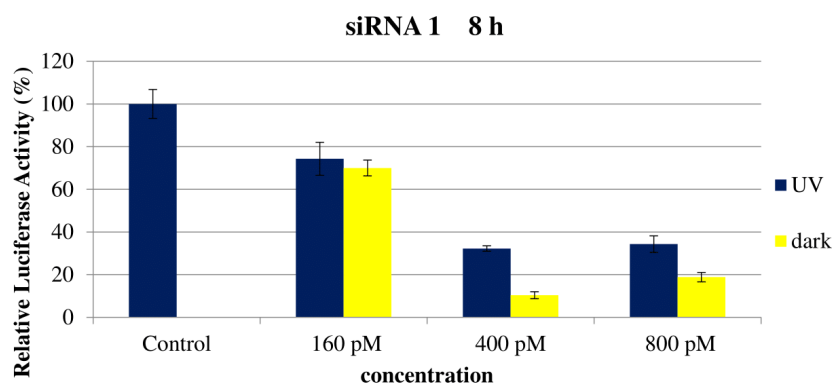


Figure S-8. Numerical bar graph showing reduction of normalized firefly luciferase expression for siRNA 1 at 160, 400 and 800 pM in HeLa cells monitored 8 hours post-transfection. 1) UV corresponds to the siRNA being exposed under a 365nm UV lamp for inactivation 2 h post transfection for 45 min (1 exposure total). 2) Dark corresponds to siRNAs being transfected in HeLa cells in the absence of UV light.

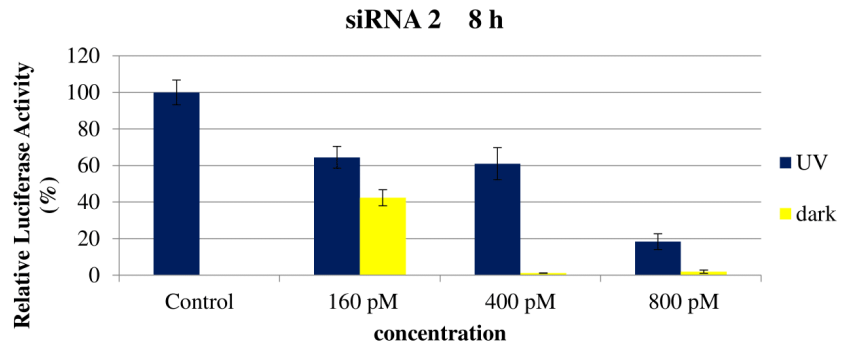


Figure S-9. Numerical bar graph showing reduction of normalized firefly luciferase expression for siRNAzo 2 at 160, 400 and 800 pM in HeLa cells monitored 8 hours post-transfection. 1) UV corresponds to the siRNA being exposed under a 365nm UV lamp for inactivation 2 h post transfection for 45 min (1 exposure total). 2) Dark corresponds to siRNAs being transfected in HeLa cells in the absence of UV light.

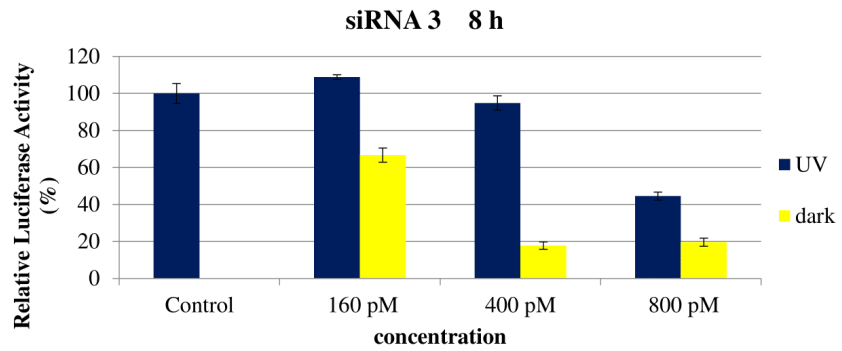


Figure S-10. Numerical bar graph showing reduction of normalized firefly luciferase expression for siRNAzo 3 at 160, 400 and 800 pM in HeLa cells monitored 8 hours post-transfection. 1) UV corresponds to the siRNA being exposed under a 365nm UV lamp for inactivation 2 h post transfection for 45 min (1 exposure total). 2) Dark corresponds to siRNAs being transfected in HeLa cells in the absence of UV light.

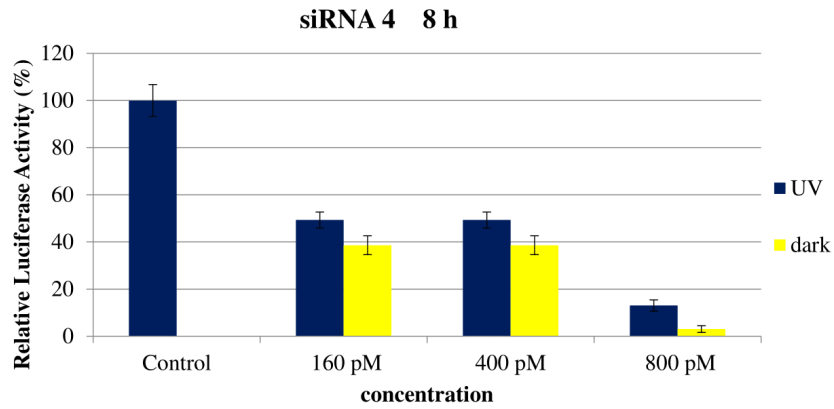


Figure S-11. Numerical bar graph showing reduction of normalized firefly luciferase expression for siRNAzo 4 at 160, 400 and 800 pM in HeLa cells monitored 8 hours post-transfection. 1) UV corresponds to the siRNA being exposed under a 365nm UV lamp for inactivation 2 h post transfection for 45 min (1 exposure total). 2) Dark corresponds to siRNAs being transfected in HeLa cells in the absence of UV light.

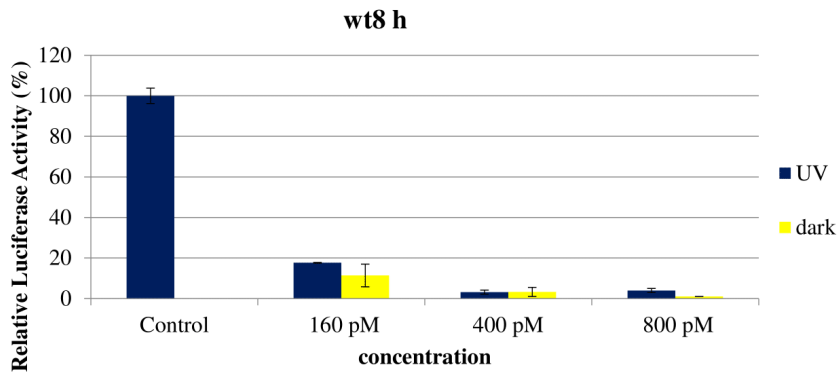


Figure S-12. Numerical bar graph showing reduction of normalized firefly luciferase expression for wt siRNA at 160, 400 and 800 pM in HeLa cells monitored 8 hours post-transfection. 1) UV corresponds to the siRNA being exposed under a 365nm UV lamp for inactivation 2 h post transfection for 45 min (1 exposure total). 2) Dark corresponds to siRNAs being transfected in HeLa cells in the absence of UV light.

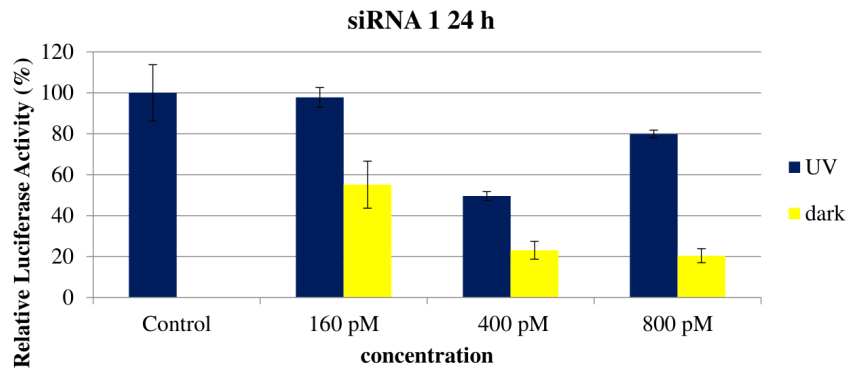


Figure S-13. Numerical bar graph showing reduction of normalized firefly luciferase expression for siRNAzo 1 at 160, 400 and 800 pM in HeLa cells monitored 24 hours post-transfection. 1) UV corresponds to the siRNA being exposed under a 365nm UV lamp for inactivation 2 h post transfection for 45 min and then for every 4 h thereafter (6 exposures total). 2) Dark corresponds to siRNAs being transfected in HeLa cells in the absence of UV light.

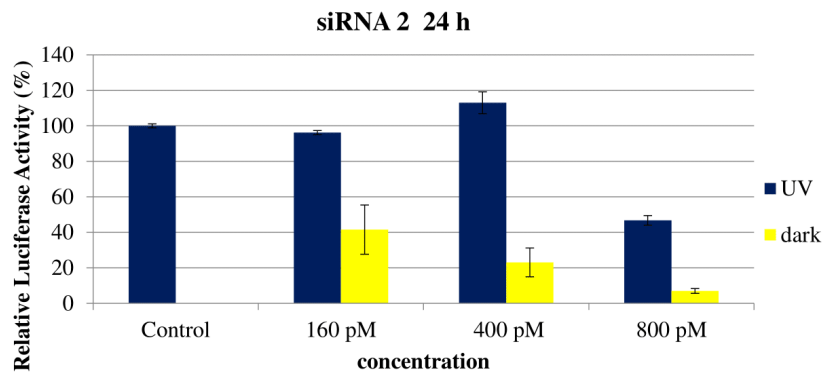


Figure S-14. Numerical bar graph showing reduction of normalized firefly luciferase expression for siRNAzo 2 at 160, 400 and 800 pM in HeLa cells monitored 24 hours post-transfection. 1) UV corresponds to the siRNA being exposed under a 365nm UV lamp for inactivation 2 h post transfection for 45 min and then for every 4 h thereafter (6 exposures total). 2) Dark corresponds to siRNAs being transfected in HeLa cells in the absence of UV light.

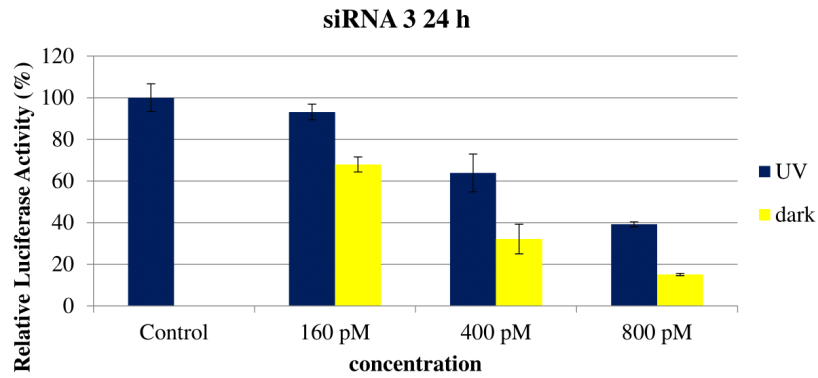


Figure S-15. Numerical bar graph showing reduction of normalized firefly luciferase expression for siRNAzo 3 at 160, 400 and 800 pM in HeLa cells monitored 24 hours post-transfection. 1) UV corresponds to the siRNA being exposed under a 365nm UV lamp for inactivation 2 h post transfection for 45 min and then for every 4 h thereafter (6 exposures total). 2) Dark corresponds to siRNAs being transfected in HeLa cells in the absence of UV light.

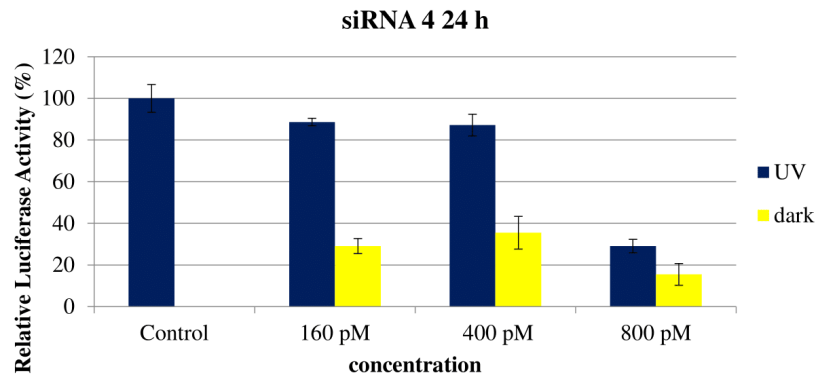


Figure S-16. Numerical bar graph showing reduction of normalized firefly luciferase expression for siRNAzo 4 at 160, 400 and 800 pM in HeLa cells monitored 24 hours post-transfection. 1) UV corresponds to the siRNA being exposed under a 365nm UV lamp for inactivation 2 h post transfection for 45 min and then for every 4 h thereafter (6 exposures total). 2) Dark corresponds to siRNAs being transfected in HeLa cells in the absence of UV light.

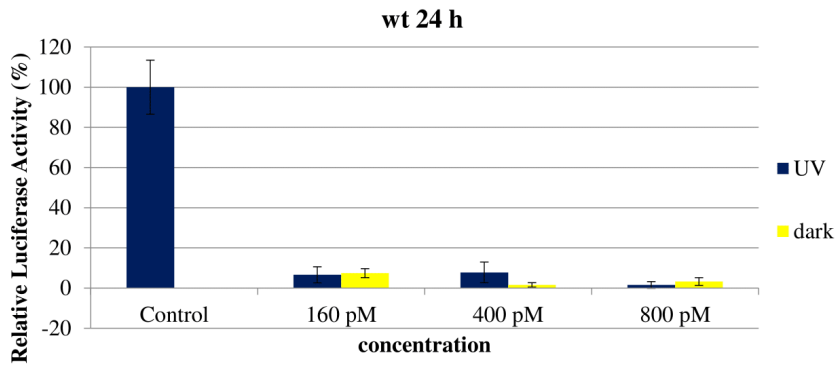


Figure S-17. Numerical bar graph showing reduction of normalized firefly luciferase expression for wt siRNA at 160, 400 and 800 pM in HeLa cells monitored 24 hours post-transfection. 1) UV corresponds to the siRNA being exposed under a 365nm UV lamp for inactivation 2 h post transfection for 45 min and then for every 4 h thereafter (6 exposures total). 2) Dark corresponds to siRNAs being transfected in HeLa cells in the absence of UV light.

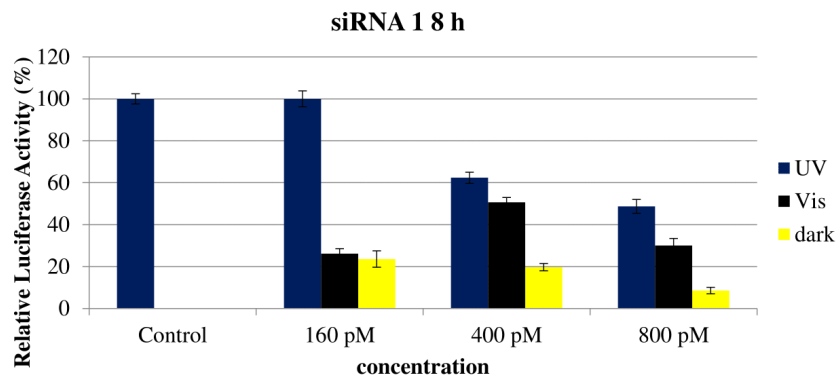


Figure S-18. Numerical bar graph showing reduction of normalized firefly luciferase expression for siRNAzo 1 at 160, 400, and 800 pM in HeLa cells monitored 8 hours post-transfection. 1) UV corresponds to the siRNA being exposed under a 365nm UV lamp for inactivation 2 h post transfection for 45 min. 2) Vis corresponds to visible light exposure 4 h after transfection. 3) Dark corresponds to siRNAs being transfected in HeLa cells in the absence of UV light.

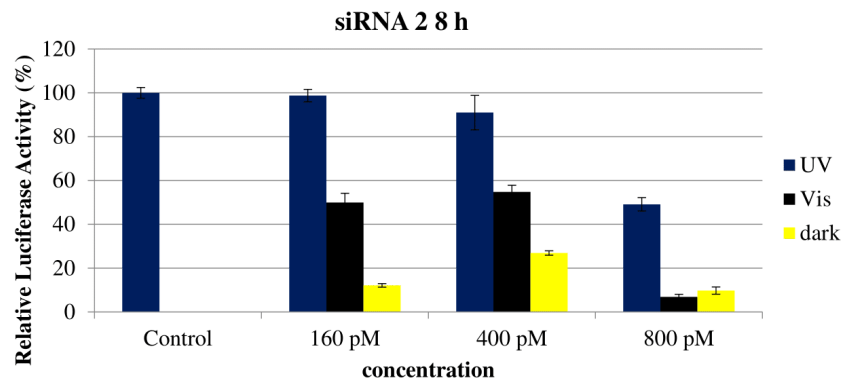


Figure S-19. Numerical bar graph showing reduction of normalized firefly luciferase expression for siRNAzo 2 at 160, 400, and 800 pM in HeLa cells monitored 8 hours post-transfection. 1) UV corresponds to the siRNA being exposed under a 365nm UV lamp for inactivation 2 h post transfection for 45 min. 2) Vis corresponds to visible light exposure 4 h after transfection. 3) Dark corresponds to siRNAs being transfected in HeLa cells in the absence of UV light.

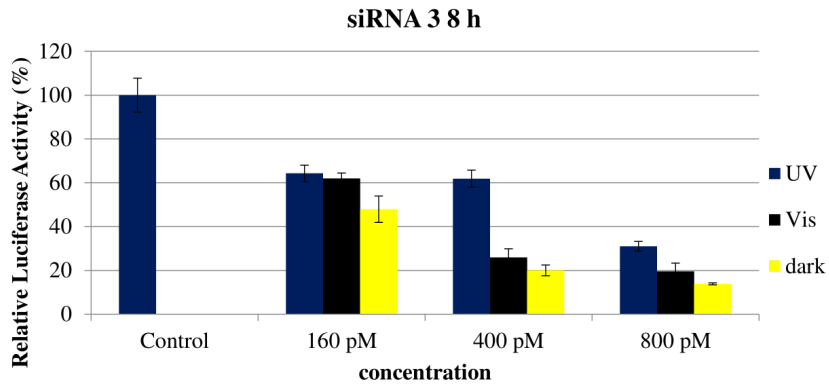


Figure S-20. Numerical bar graph showing reduction of normalized firefly luciferase expression for siRNAzo 3 at 160, 400, and 800 pM in HeLa cells monitored 8 hours post-transfection. 1) UV corresponds to the siRNA being exposed under a 365nm UV lamp for inactivation 2 h post transfection for 45 min. 2) Vis corresponds to visible light exposure 4 h after transfection. 3) Dark corresponds to siRNAs being transfected in HeLa cells in the absence of UV light.

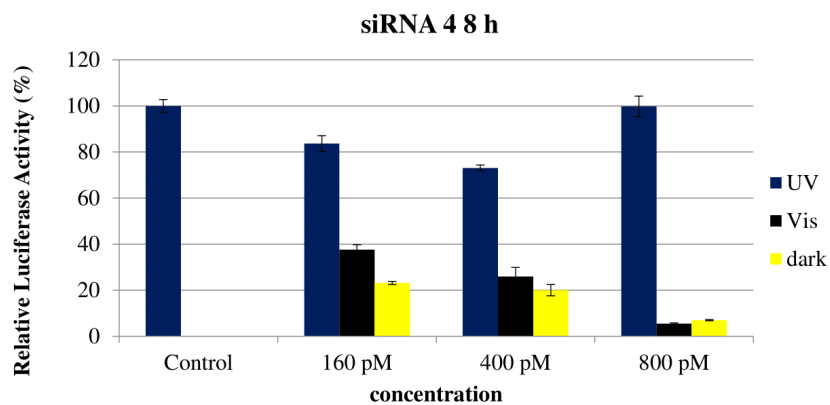


Figure S-21. Numerical bar graph showing reduction of normalized firefly luciferase expression for siRNA 4 at 160, 400, and 800 pM in HeLa cells monitored 8 hours post-transfection. 1) UV corresponds to the siRNA being exposed under a 365nm UV lamp for inactivation 2 h post transfection for 45 min. 2) Vis corresponds to visible light exposure 4 h after transfection. 3) Dark corresponds to siRNAs being transfected in HeLa cells in the absence of UV light.

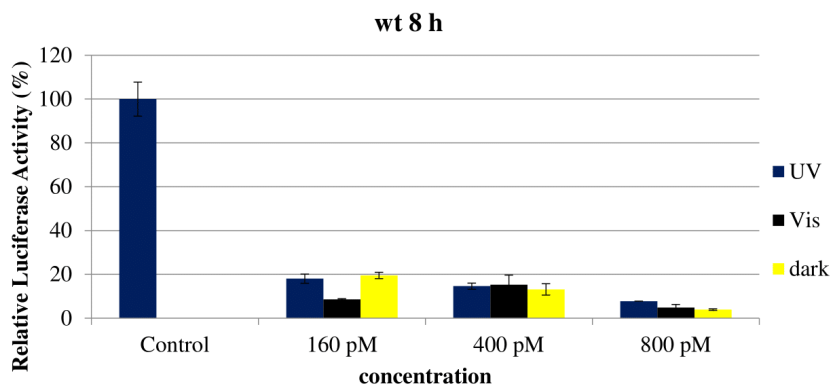


Figure S-22. Numerical bar graph showing reduction of normalized firefly luciferase expression for wt siRNA at 160, 400, and 800 pM in HeLa cells monitored 8 hours post-transfection. 1) UV corresponds to the siRNA being exposed under a 365nm UV lamp for inactivation 2 h post transfection for 45 min. 2) Vis corresponds to visible light exposure 4 h after transfection. 3) Dark corresponds to siRNAs being transfected in HeLa cells in the absence of UV light.

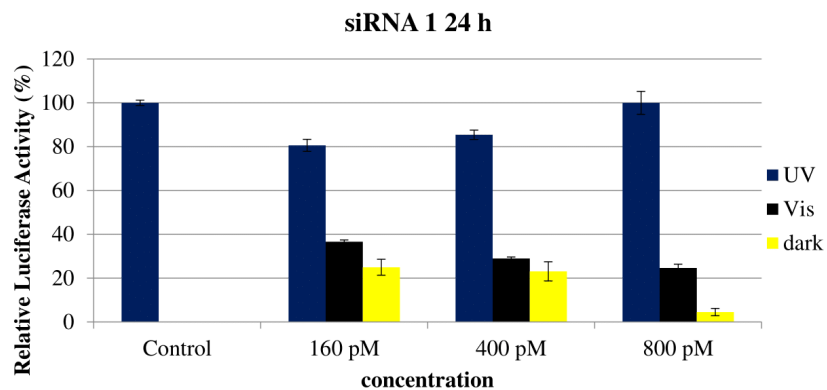


Figure S-23. Numerical bar graph showing reduction of normalized firefly luciferase expression for siRNAzo 1 at 160, 400, and 800 pM in HeLa cells monitored 24 hours post-transfection. 1) UV corresponds to the siRNA being exposed under a 365nm UV lamp for inactivation 2 h post transfection for 45 min, and for an additional 45 min of UV exposure every 4 hours (6 exposures total) 2) Vis corresponds to visible light exposure 4 h after transfection. 3) Dark corresponds to siRNAs being transfected in HeLa cells in the absence of UV light.

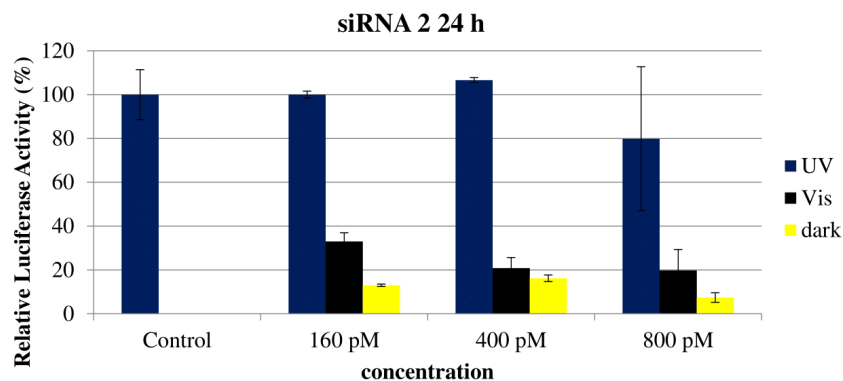


Figure S-24. Numerical bar graph showing reduction of normalized firefly luciferase expression for siRNAzo 2 at 160, 400, and 800 pM in HeLa cells monitored 24 hours post-transfection. 1) UV corresponds to the siRNA being exposed under a 365nm UV lamp for inactivation 2 h post transfection for 45 min, and for an additional 45 min of UV exposure every 4 hours (6 exposures total) 2) Vis corresponds to visible light exposure 4 h after transfection. 3) Dark corresponds to siRNAs being transfected in HeLa cells in the absence of UV light.

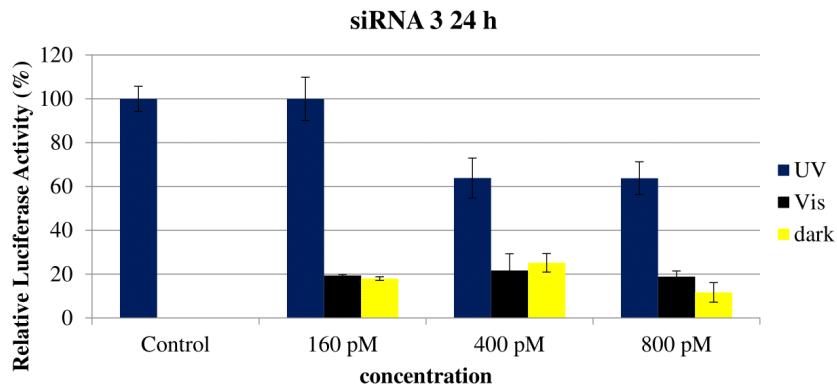


Figure S-25. Numerical bar graph showing reduction of normalized firefly luciferase expression for siRNAzo 3 at 160, 400, and 800 pM in HeLa cells monitored 24 hours post-transfection. 1) UV corresponds to the siRNA being exposed under a 365nm UV lamp for inactivation 2 h post transfection for 45 min, and for an additional 45 min of UV exposure every 4 hours (6 exposures total) 2) Vis corresponds to visible light exposure 4 h after transfection. 3) Dark corresponds to siRNAs being transfected in HeLa cells in the absence of UV light.

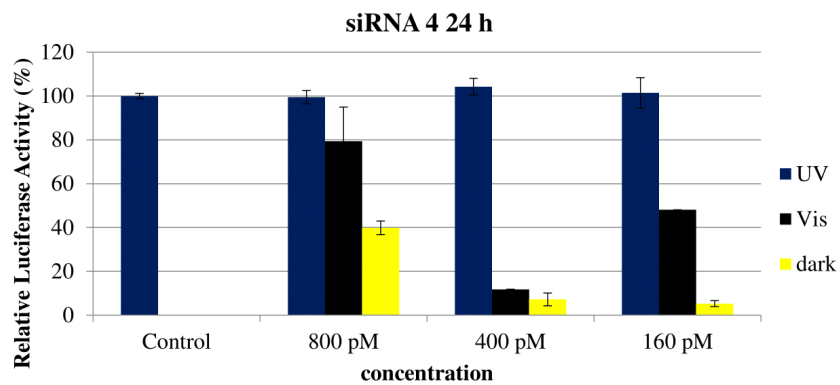


Figure S-26. Numerical bar graph showing reduction of normalized firefly luciferase expression for siRNAzo 4 at 160, 400, and 800 pM in HeLa cells monitored 24 hours post-transfection. 1) UV corresponds to the siRNA being exposed under a 365nm UV lamp for inactivation 2 h post transfection for 45 min, and for an additional 45 min of UV exposure every 4 hours (6 exposures total) 2) Vis corresponds to visible light exposure 4 h after transfection. 3) Dark corresponds to siRNAs being transfected in HeLa cells in the absence of UV light.

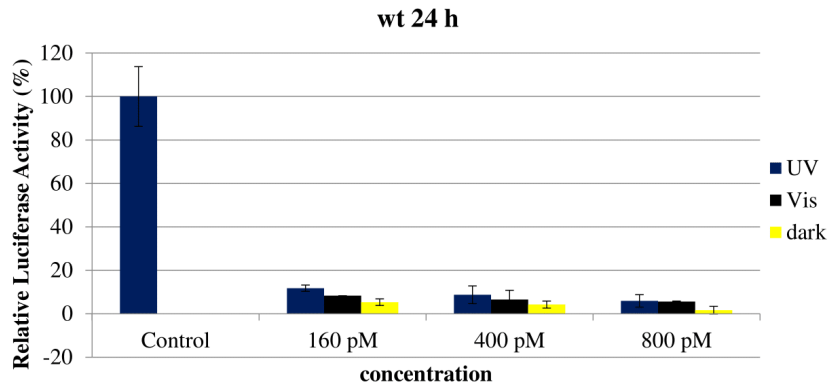


Figure S-27. Numerical bar graph showing reduction of normalized firefly luciferase expression for wt siRNA at 160, 400, and 800 pM in HeLa cells monitored 24 hours post-transfection. 1) UV corresponds to the siRNA being exposed under a 365nm UV lamp for inactivation 2 h post transfection for 45 min, and for an additional 45 min of UV exposure every 4 hours (6 exposures total) 2) Vis corresponds to visible light exposure 4 h after transfection. 3) Dark corresponds to siRNAs being transfected in HeLa cells in the absence of UV light.

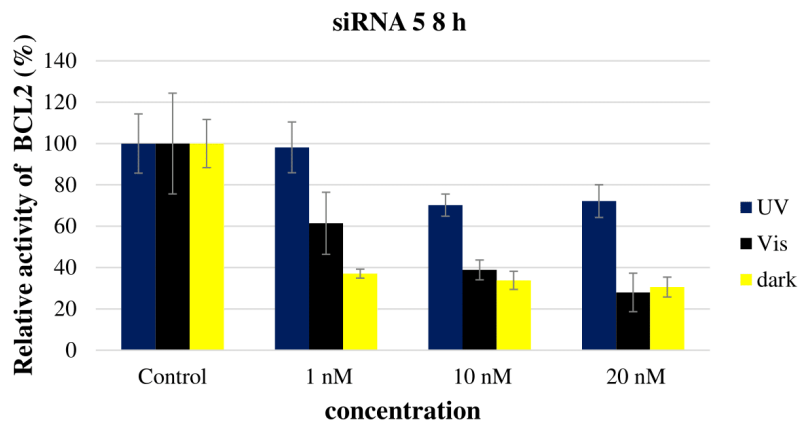


Figure S-28. Numerical bar graph showing reduction of normalized *BCL2* expression for siRNAzo 5 at 1, 10, and 20 nM in HeLa cells monitored 8 hours post-transfection. 1) UV corresponds to the siRNA being exposed under a 365nm UV lamp for inactivation 2 h post transfection for 45 min. 2) Vis corresponds to visible light exposure 4 h after transfection. 3) Dark corresponds to siRNAs being transfected in HeLa cells in the absence of UV light.

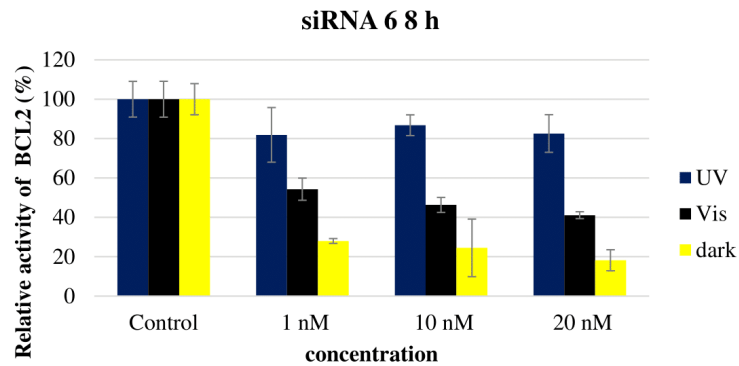


Figure S-29. Numerical bar graph showing reduction of normalized *BCL2* expression for siRNAzo 6 at 1, 10, and 20 nM in HeLa cells monitored 8 hours post-transfection. 1) UV corresponds to the siRNA being exposed under a 365nm UV lamp for inactivation 2 h post transfection for 45 min. 2) Vis corresponds to visible light exposure 4 h after transfection. 3) Dark corresponds to siRNAs being transfected in HeLa cells in the absence of UV light.

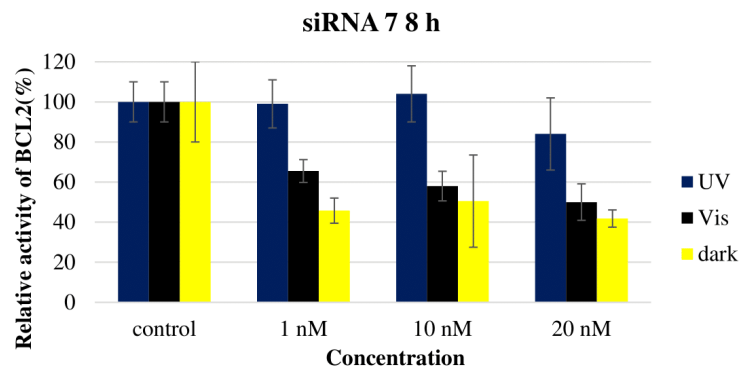


Figure S-30. Numerical bar graph showing reduction of normalized *BCL2* expression for siRNAzo 7 at 1, 10, and 20 nM in HeLa cells monitored 8 hours post-transfection. 1) UV corresponds to the siRNA being exposed under a 365nm UV lamp for inactivation 2 h post transfection for 45 min. 2) Vis corresponds to visible light exposure 4 h after transfection. 3) Dark corresponds to siRNAs being transfected in HeLa cells in the absence of UV light.

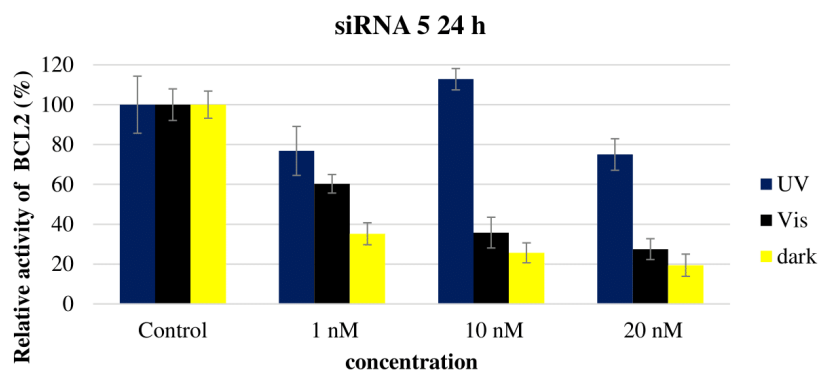


Figure S-31. Numerical bar graph showing reduction of normalized *BCL2* expression for siRNA 5 at 1, 10, and 20 nM in HeLa cells monitored 24 hours post-transfection. 1) UV corresponds to the siRNA being exposed under a 365nm UV lamp for inactivation 2 h post transfection for 45 min, and for an additional 45 min of UV exposure every 4 hours (6 exposures total) 2) Vis corresponds to visible light exposure 4 h after transfection. 3) Dark corresponds to siRNAs being transfected in HeLa cells in the absence of UV light.

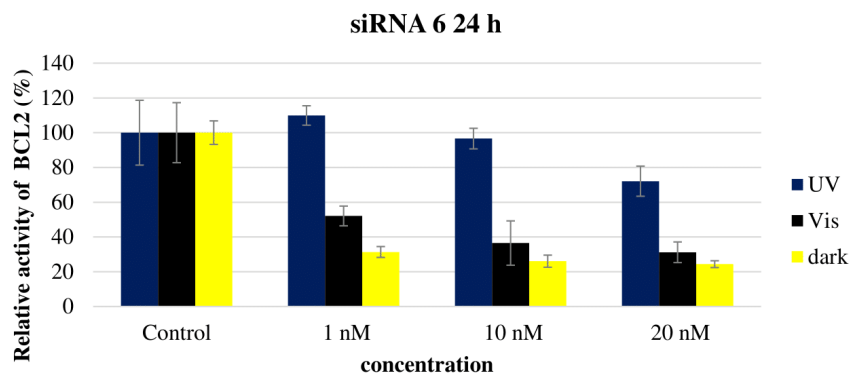


Figure S-32. Numerical bar graph showing reduction of normalized *BCL2* expression for siRNA 6 at 1, 10, and 20 nM in HeLa cells monitored 24 hours post-transfection. 1) UV corresponds to the siRNA being exposed under a 365nm UV lamp for inactivation 2 h post transfection for 45 min, and for an additional 45 min of UV exposure every 4 hours (6 exposures total) 2) Vis corresponds to visible light exposure 4 h after transfection. 3) Dark corresponds to siRNAs being transfected in HeLa cells in the absence of UV light.

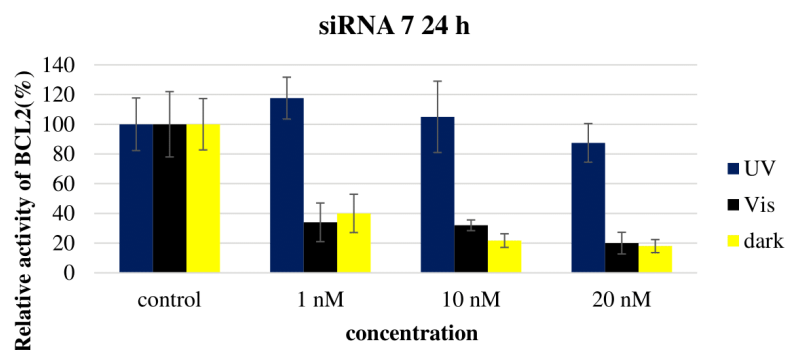


Figure S-33. Numerical bar graph showing reduction of normalized *BCL2* expression for siRNA 7 at 1, 10, and 20 nM in HeLa cells monitored 24 hours post-transfection. 1) UV corresponds to the siRNA being exposed under a 365nm UV lamp for inactivation 2 h post transfection for 45 min, and for an additional 45 min of UV exposure every 4 hours (6 exposures total) 2) Vis corresponds to visible light exposure 4 h after transfection. 3) Dark corresponds to siRNAs being transfected in HeLa cells in the absence of UV light.

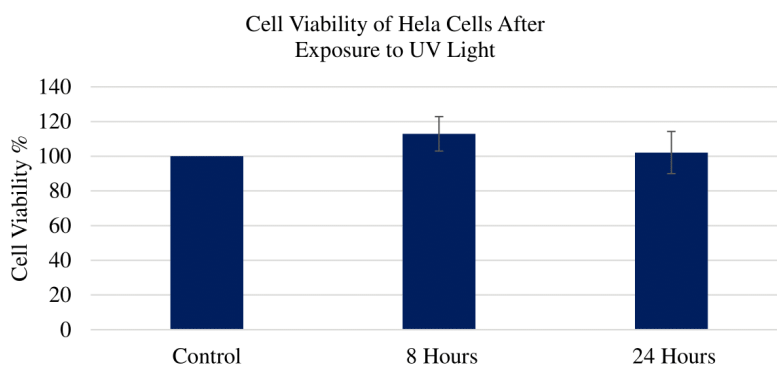


Figure S-34: HeLa cells were exposed to UV Light under a 365nm UV lamp 2 h post transfection for 45 min, (8 h assay) and for an additional 45 min of UV exposure every 4 hours (6 exposures total) (24 h assay). Data showed no significant changes in cell viability when compared to cells not exposed to UV light. The cell viability was determined using an XTT Assay (Promega).

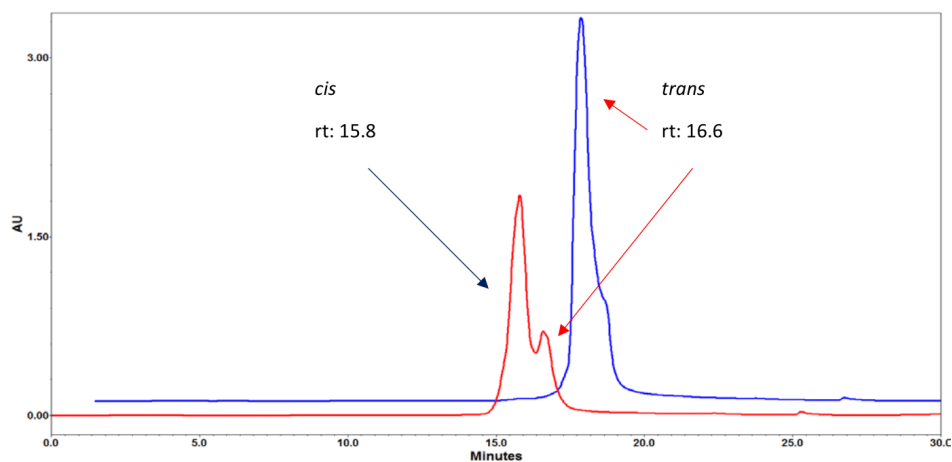


Figure S-35. HPLC chromatogram of sense strand of the sense strand of siRNA 5 showing both *cis* (left) and *trans* (right) peaks. Background (blue): The same sample of siRNA 5 collected and exposed to 60 min UV light. Foreground (red): untreated sense strand of siRNA 5 spectra. Conditions were 5% acetonitrile in 95% 0.1 M TEAA (Triethylamine-Acetic Acid) buffer up to 100% acetonitrile over 30 min. Spectra were processed using the Empower 3 software.

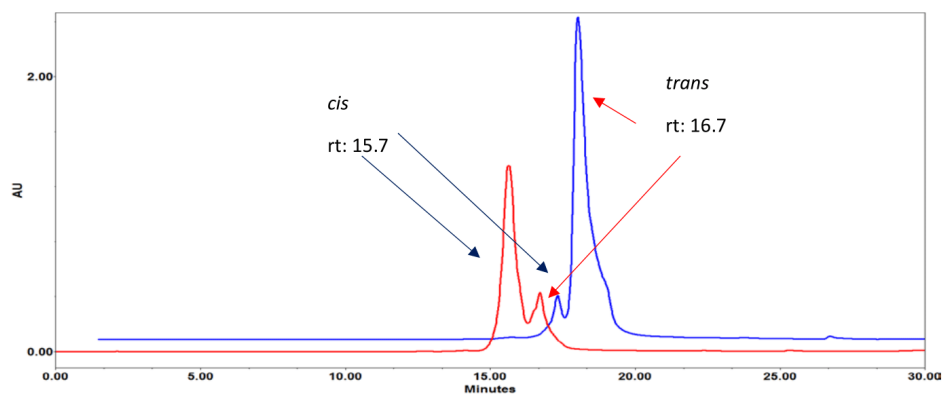


Figure S-36. HPLC chromatogram of the sense strand of siRNA 6 showing both *cis* (left) and *trans* (right) peaks. Background (blue): The same sample of siRNA 5 collected and exposed to 60 min UV light. Foreground (red): untreated sense strand of siRNA 5 spectra. Conditions were 5% acetonitrile in 95% 0.1 M TEAA (Triethylamine-Acetic Acid) buffer up to 100% acetonitrile over 30 min. Spectra were processed using the Empower 3 software.

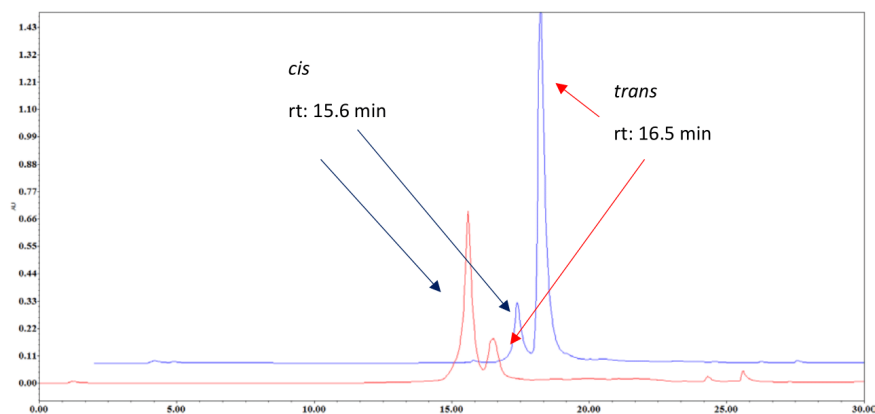


Figure S-37. HPLC chromatogram of the sense strand of siRNA 7 showing both *cis* (left) and *trans* (right) peaks. Background (blue): The same sample of siRNA 5 collected and exposed to 60 min UV light. Foreground (red): untreated sense strand of siRNA 5 spectra. Conditions were 5% acetonitrile in 95% 0.1 M TEAA (Triethylamine-Acetic Acid) buffer up to 100% acetonitrile over 30 min. Spectra were processed using the Empower 3 software.

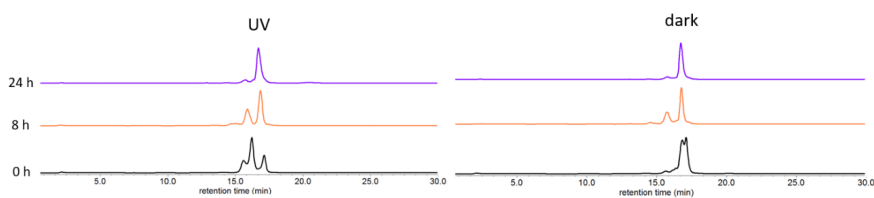


Figure S-38. GSH assay results of the sense strand of the sense strand of siRNAzo 6 showing minimal degradation due to the presence of GSH. UV treated RNA was exposed to 5 min of UV light and then kept at 37 °C until injection. Conditions were 5% acetonitrile in 95% 0.1 M TEAA (Triethylamine-Acetic Acid) buffer up to 100% acetonitrile over 30 min. Spectra were processed using the Empower 3 software.

Table S-1 Sequences of anti-luciferase and anti-*BCL2* siRNAzOs, predicted and recorded mass

siRNAzo	siRNAzo Duplex ^[a]	Predicted Mass of Sense Strand	Actual Mass of Sense Strand ^[b]	Target
1	5'- CUUACGC <u>Az2</u> AGUACUUCGAtt -3' (s) 3'- ttGAAUGCGACUCAUGAAGCU-5'(as)	6367.91	6366.89	luciferase
2	5'- CUUACGCU <u>Az2</u> GUACUUCGAtt -3' (s) 3'- ttGAAUGCGACUCAUGAAGCU-5'(as)	6344.86	6344.91	luciferase
3	5'- CUUACGCUG <u>Az2</u> UACUUCGAtt -3' (s) 3'- ttGAAUGCGACUCAUGAAGCU-5'(as)	6344.86	6344.86	luciferase
4	5'- CUUACGCUGA <u>Az2</u> ACUUCGAtt -3' (s) 3'- ttGAAUGCGACUCAUGAAGCU-5'(as)	6367.91	6366.95	luciferase
5	5'-GCCUUCU <u>Az2</u> GAGUUCGGUtt-3' (s) 3'-ttCGGAAGAAACUCAAGCCAC-5' (as)	6336.91	6336.86	<i>BCL2</i>
6	5'-GCCUUCUU <u>Az2</u> AGUUCGGUtt-3'(s) 3'-ttCGGAAGAAACUCAAGCCAC-5'(as)	6377.82	6377.81	<i>BCL2</i>
7	5'-GCCUUCUUUG <u>Az2</u> UUCGGUtt-3' (s) 3'-ttCGGAAGAAACUCAAGCCAC-5'(as)	6369.76	6369.76	<i>BCL2</i>

References

[a] **Az2** corresponds to the azobenzene derivative synthesized from 4-nitrophenylethyl alcohol; the top strand corresponds to the sense strand; the bottom strand corresponds to the antisense strand. In all duplexes, the 5'-end of the bottom antisense strand contains a 5'-phosphate group.

[b] Deconvolution results for siRNAzOs. ESI-HRMS (ES^+) m/z calculated for siRNAzOs 1-7 $[M+H]^+$

1. M. L. Hammill, C. Isaacs-Trepanier and J. P. Desaulniers, *ChemistrySelect*, **2017**, 2, 9810-9814.
2. McDowell, J.A.; Turner, D. H. *Biochemistry* **1996**, 35, 14077.

Connecting Statement II

During the Chapter III study we further enhanced the robustness of the protocols by being able to inactivate the siRNAzo, and keep it inactive for up to 24 h using carefully controlled doses of UV light. While this was a large improvement over the previous methodology, which was limited by the *cis* conformer's half life (4 h at 37°C), it still utilizes toxic UV light. We also showed that targeting endogenous *BCL-2* was viable as well, and that the same method could be used to keep the siRNAzo inactive for up to 24 h. These advancements are excellent and highlights the large potential of using azobenzene as a therapeutic or biomolecular tool. However as a next step we wanted to get away from the UV portion of the spectrum, and red shift the $\pi \rightarrow \pi^*$ transition into the red portion of the visible spectrum. We did this though a late stage tetra-chlorination of the *ortho* position on the azobenzene. This allowed us to circumvent the UV portions of the spectrum altogether and use non-toxic red light to inactivate the siRNAzos. This new compound however had its own challenges which we will discuss in the next chapter.

**Chapter 4: Manuscript III- Synthesis,
Derivatization and Photochemical Control of
ortho-Functionalized Tetrachlorinated
Azobenzene-Modified siRNAs**

Matthew L. Hammill, Golam Islam and Jean-Paul Desaulniers*

Published in

ChemBioChem **2020**, *21*, 2367-2372

DOI: 10.1002/cbic.202000188

4.1 Abstract

In this manuscript, we report the chemical synthesis and derivatization of an ortho-functionalized tetrachlorinated azobenzene diol. A 4'4-dimethoxytrityl (DMT) phosphoramidite was synthesized for its site-specific incorporation within the sense strand of an siRNA duplex to form ortho-functionalized tetrachlorinated azobenzene-containing siRNAs (Cl-siRNAzOs). Compared to a non-halogenated azobenzene, ortho-functionalized tetrachlorinated azobenzenes are capable of red-shifting the $\pi \rightarrow \pi^*$ transition from the ultraviolet (UV) portion of the electromagnetic spectrum into the visible range. Within this visible range, the azobenzene molecule can be reliably converted from trans to cis with red light (660 nm), and converted back to trans from cis with violet wavelength light (410 nm) and/or thermal relaxation. We also report the gene-silencing ability of these Cl-siRNAzOs in cell culture as well as their reversible control with visible light for up to 24 hours.

4.2 Introduction

Since the report in 1998 by Fire and Mello, the RNA interference (RNAi) pathway has been of great interest for use as an effective therapeutic pathway and as a biomolecular tool for gene silencing.¹ This endogenous pathway uses double-stranded RNA (dsRNA) as both a defence against unwanted viral infection and as an internal gene expression control. The ability to specifically silence gene targets based on the gene sequence makes this an attractive method to develop valuable therapeutics and biomolecular tools.²⁻⁴ There are currently two US FDA-approved siRNA therapeutics on the market. The first one, Onpattro, is a treatment for hereditary transthyretin amyloidosis (hATTR)⁵ and the second one, Givlaari treats acute hepatic porphyria.⁶ This recent success of siRNA therapeutics

follows a time of hardship for siRNA therapeutics due to many siRNAs failing clinical trials.⁷ Even with this renewed focus on siRNAs, siRNAs are still a challenge to use as therapeutics due to challenges that are well known to the field, such as poor stability, toxicity, off-target effects and tissue specific targeting. Another area that is of interest to siRNA design is the ability to control its activity within a cellular environment. One way to control its activity is to use a photoresponsive functional group. Advancements in the photoresponsive control of siRNAs have shown excellent results. Despite these positive experiments involving photo-switchable siRNAs, improvements are necessary. In this manuscript, we expand on the current knowledge in the field through the synthesis, characterization and biological testing of tetra *ortho*-chlorinated azobenzenes that are incorporated into the sense (passenger) strand of an siRNA duplex. These tetra *ortho*-chlorinated azobenzene-containing siRNAs are called chlorinated siRNAzOs (Cl-siRNAzOs).

The photoresponsive siRNA field has been growing rapidly over the last several years, but most of these chemical modifications involve the inactivation of the payload siRNA, which is then activated at a later time with ultraviolet (UV) light inside the cell. A great example of this technology was reported by Freidman and coworkers, in which a nitrobenzene derivative was attached to the siRNA backbone and exposure to 320 nm UV light caused the activation of the siRNA.⁸ The use of similar UV-labile protecting groups have also been used as thymidine and guanine modifications by Mikat and Heckel, which caused a bulge in the duplex, rendering the RNA-induced-silencing-complex (RISC) complex as inoperative until exposure to UV light, which cleaved the groups and activated the siRNA.⁹ Recently, Mokhir and Meyer developed a 5'-labelled alkoxyanthracenyl

siRNA, which becomes uncaged via a singlet oxygen ($^1\text{O}_2$) photo-regenerated photosensitizer on the 3'-end of the guide strand. Uncaging occurs with green or red light and yields an active siRNA.¹⁰ The limitation of these innovations is that siRNA payloads are *irreversibly* photoactivated and cannot be reversed once deployed. These photocages once released are chemical by-products which could have any number of unknown effects on the cells in the tissue. Thus, having greater spatial and temporal control of the siRNA via a *reversible* technology could have far-reaching effects on an siRNA's use as a therapeutic and as a biomolecular tool bypassing and minimizing unwanted off-target effects.

In this regard, azobenzene is a viable photo-responsive molecule because of its ability to photo-isomerize in the presence of UV and visible light. These large conformational changes in the molecule can be used to disrupt biomolecular structures such as duplexes.¹¹

The more stable *trans* isomer is the native state of the molecule, but the addition of high energy UV light in the 330-360 nm range causes the less stable *cis* isomer to become dominant. This sterically hindered *cis* conformer strains the N=N bond, allowing for the use of low energy visible light above 450 nm to be used to convert it back to the more stable *trans* isomer.¹² These unique and modular properties allow azobenzene to be used in many applications, including its incorporation into oligonucleotides (See Figure 4.1) since it is relatively easy to synthesize and contains a high quantum yield when photoswitching.¹³

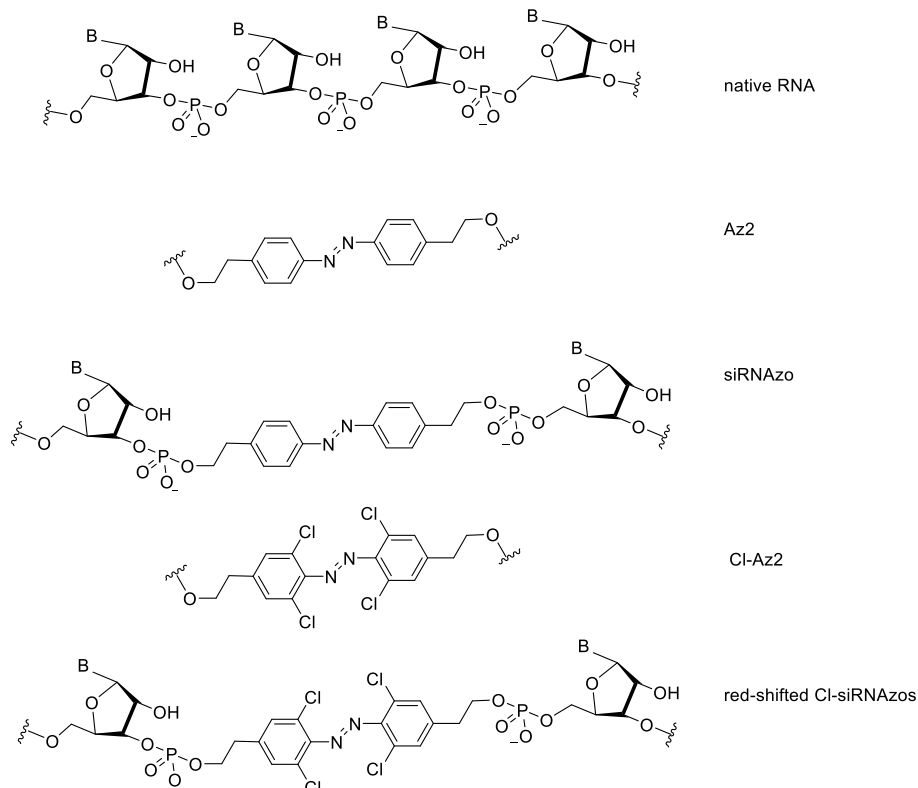


Figure 4.1. Structural differences between native RNA, and azobenzene-containing RNAs (siRNAzos). Az2 corresponds to the azobenzene unit synthesized and used by our laboratory in previous studies¹⁴⁻¹⁶, Cl-Az2 corresponds to the azobenzene unit used this study.

Previous work in our group utilized this robust ability of azobenzene to photoisomerize to make siRNAzos, which are siRNA duplexes that contain azobenzene in the sense strand.^{14,15} Even more recently, we were able to extend the utility of our photo-switchable system by keeping our siRNAs inactive for up to 24 hours.¹⁶ Our previous system¹⁴, where we inactivated the siRNA before transfection, was limited by the azobenzene's half-life of 4 hours at 37 °C.¹⁷ This caused the reactivation of the siRNA over time, however the recent advancement we made was to inactivate the siRNA *after* transfection which allowed us to push the inactivation period to 24 hours, whereas previously, after 8 h (reactivation at 12 h) the siRNA would not remain inactive.¹⁶

Despite this advancement in our technology, we are still using UV light to cause this change in activity. UV light, while useful, has several issues associated with it such as its toxicity to cells over long exposure times.¹⁷ High-energy UV light has also been known to cause pyrimidine dimers, and has poor tissue penetration in the body because human skin has evolved to scatter UV light so it could not penetrate the body to damage tissues.¹⁹ This presents a great hurdle and becomes a major limitation for photochemically-controlled siRNAs dependent on UV light for therapeutic use.

Recent research on light penetration by Basford and co-workers show that penetration into human tissue is determined not only by wavelength but also light beam intensity and width.²⁰ In their study, they reported that higher wavelength light induces deeper penetration. For example, red light penetrates to a depth of 5 mm, with maximum penetration occurring with a beam at least 10 mm wide, while UV gets less than 0.2 mm depth.²⁰ This makes red-shifting the wavelength of photo-reactive pharmaceuticals a very high priority since many active therapeutics are not necessarily on the surface of the skin, but embedded within tissues. To accomplish this goal, there has been studies aimed at modifying azobenzene at the *ortho* positions in order to strain the N=N bond so that lower energy visible light can cause the isomerization from *trans* to *cis*. Feringa and co-workers used red-shifted azobenzene derivatives as a control for microbial activity by modifying antibiotics with chlorine and fluorine at the *ortho* positions of the azobenzene moiety and they reported excellent activity and reversibility with red and green light.²¹ Other reports involving photoresponsive control of nucleoside or oligonucleotide derivatives under visible light showed effective control.²²⁻²⁵ Other modifications at the *ortho* positions include not only halogens, such as fluorine and chlorine, but thiols, methoxy substituents, and amino

containing groups like morpholino and amines.²⁶⁻²⁸ One issue with extending the isomerization point in the longer wavelength area of the spectrum is that these *cis* conformers can become increasingly unstable as they become more red-shifted.²⁹ However, this is highly dependent on the modification, as shown with *ortho*-functionalized tetra-substituted chlorines being very unstable in the *cis* conformer.³⁰ Trauner and co-workers have developed a novel synthesis system for the late stage functionalization of azobenzenes, by adding chlorinated substituents after the N=N bond has formed, as opposed to modifying the *ortho* position before the dimerization.³¹

Therefore, in this new manuscript, we report the chemical synthesis of an *ortho*-functionalized tetra-chlorinated azobenzene diol. A DMT-phosphoramidite of the chlorinated azobenzene was synthesized for its incorporation into the siRNAs using solid-phase chemistry to generate red-shifted tetra *ortho*-chlorinated azobenzene-containing siRNAs (Cl-siRNAzos). We tested these red-shifted Cl-siRNAzos in cell culture and were able to control the activity of the Cl-siRNAzo by using red light (660 nm) to convert from *trans* to *cis* and thermal relaxation to revert from *cis* to *trans*.

4.3 Materials and Methods

4.3.1 General Methods

Unless otherwise indicated all starting reagents used were obtained from commercial sources without additional purification. Anhydrous CH₂Cl₂ and THF were purchased from Sigma-Aldrich and run through a PureSolv 400 solvent purification system to maintain purity. Flash column chromatography was performed with Silicycle Siliaflash 60 (230-400 mesh), using the procedure developed by Still, Kahn and Mitra.¹ NMRs were performed on a Varian 400 MHz spectrophotometer. All ¹H NMRs were recorded for 64 transients at

400 MHz and all ^{13}C NMRs were run for 1500 transients at 101 MHz and all ^{31}P NMRs were recorded for 256 transients at 167 MHz. Spectra were processed and integrated using ACD labs NMR Processor Academic Edition.

4.3.2 Synthesis of 4,4'-bis(hydroxyethyl)-azobenzene – Compound (1)

To a solution of 90.0 mL of 5.70 M $\text{NaOH}_{(\text{aq})}$ 4.00 g of 4-nitrophenethyl alcohol (23.9 mmol, 1.00 equiv.) was added and stirred until fully dissolved. To this solution 6.00 g Zn powder (92.3 mmol, 3.85 equiv.) was slowly added to maintain stirring. After refluxing overnight for 16 h it was then filtered on a Buchner Vacuum filter, and the crystals were suspended in hot methanol. The crystals were collected and filtered again with a gravity filter to remove residual salts and then the methanol solution was removed using a rotary evaporator. Crystals were collected and purified on silica gel column using MeOH (2% to 5%) in CH_2Cl_2 to afford compound **1** as orange crystals (2.34 g, 72%). ^1H NMR (400 MHz, d_6 -DMSO) δ 7.75 - 7.81 (d, $J = 8.21$ Hz 4H) 7.41 (d, $J = 8.21$, Hz 4H) 4.71 (t, $J = 5.28$ Hz, 2H) 3.65 (td, $J = 6.84$, 5.47 Hz, 4H) 2.80 (t, $J = 6.84$ Hz, 4H). ^{13}C NMR (101 MHz, d_6 -DMSO) δ ppm 150.84, 144.02, 130.34, 122.79, 62.26, 38.87; ESI-HRMS (ES^+) m/z calculated for $\text{C}_{16}\text{H}_{18}\text{N}_2\text{O}_2$: 271.1441, found 271.1438 $[\text{M}+\text{H}]^+$

4.3.3 Synthesis of (E)-(diazene-1,2-diylbis(3,5-dichloro-4,1-phenylene))bis(ethane-2,1-diyl) diacetate Compound (2)

To a solution of 6.00 mL of glacial acetic acid 0.5 g of compound **2** (1.85 mmol, 1.00 equiv.) was added to a reactor tube. To that solution 1.9 g NCS (14 mmol, 8 equiv.) and 0.12 g of $\text{Pd}(\text{OAc})_2$ (0.5 mmol, 0.3 equiv.) and stirred at 140 °C overnight (20 h, reflux). After rotary evaporation, the compound was then purified on silica gel using a 1%:99%:

acetone/dichloromethane mobile phase. This afforded compound **4** as a dark red crystal (0.54 g, 59%). ¹H NMR (400 MHz, *d*-CDCl₃) δ ppm 7.35 (s, 4H) 4.34 (t, *J*=6.72 Hz, 4H) 4.28 (s, 1H) 2.98 (t, *J*=6.72 Hz, 4H) 2.09 (s, 6H). ¹³C NMR (101 MHz, *d*-CDCl₃) δ ppm 170.8, 170.7, 146.0, 140.6, 140.1, 129.8, 129.5, 127.4, 125.9, 63.7, 63.5, 34.2, 34.06, 20.9, 20.8; ESI-HRMS (ES⁺) *m/z* calculated for C₂₀H₁₈Cl₄N₂O₄: 492.17, found 491.0092 [M+H]⁺

4.3.4 Synthesis of (E)-2,2'-(diazene-1,2-diylbis(3,5-dichloro-4,1-phenylene))bis(ethan-1-ol) – Compound (3)

To a solution of 3.00 mL of 10 mg/mL NaOH in MeOH (0.1 equiv.) 0.2 g of compound **4** (0.4 mmol, 1.00 equiv.) was added to a 20 mL vial. That solution was stirred (1 h, rt.). After rotary evaporation, the compound was then purified on silica gel using a 5%:95%: MeOH/dichloromethane mobile phase. This afforded compound **5** as a dark red crystal (0.12 g, 60%). ¹H NMR (400 MHz, DMSO-*d*₆) δ ppm 7.57 (s, 4 H) 3.69 (t, *J*=6.36 Hz, 4 H) 2.81 (t, *J*=6.36 Hz, 4 H). ¹³C NMR (101 MHz, DMSO-*d*₆) δ ppm 144.7, 144.1 130.7, 130.4, 126.3, 124.7, 61.5, 61.2, 55.3, 40.6, 40.4, 40.2, 40.0, 39.7, 39.5, 39.3, 38.1, 37.8; ESI-HRMS (ES⁺) *m/z* calculated for C₁₆H₁₄Cl₄N₂O₄: 405.98, found 406.9882 [M+H]⁺

4.3.5 Synthesis of (E)-2-(4-((4-(2-(bis(4-methoxyphenyl)(phenyl)methoxy)ethyl)-2,6-dichlorophenyl)diazenyl) -3,5-dichlorophenyl)ethan-1-ol – Compound (4)

To a solution of anhydrous DCM 5.0 mL 0.24 g of compound **5** (0.48 mmol, 1.00 equiv.) was added and stirred until fully dissolved. To the solution 0.2 g of 4,4'-dimethoxytrityl chloride (0.59 mmol, 1.00 equiv.) was added along with 0.41 mL triethylamine (2.93 mmol, 5.00 equiv.) The reaction mixture was stirred vigorously

overnight and monitored by TLC. The crude reaction was then concentrated by rotovap and purified on silica gel column using MeOH (2% to 5%) in CH₂Cl₂ to afford compound **6** as a dark red oil (0.21 g, 50%). ¹H NMR (400 MHz, *d*-CDCl₃) δ ppm 7.17 - 7.43 (m, 14 H) 6.77 - 6.88 (m, 4 H) 3.91 (t, 2 H) 3.80 (s, 6 H) 3.37 (t, 2 H) 2.83 - 2.91 (t, 4 H). ¹³C NMR (101 MHz, *d*-CDCl₃) δ ppm 20.8, 20.9, 34.3, 54.5, 55.2, 55.2, 63.8, 76.7, 77.1, 77.4, 86.1, 113.0, 113.1, 113.6, 125.9, 126.5, 127.2, 127.4, 127.8, 127.8, 128.1, 128.3, 128.7, 129.5, 130.0, 130.2, 136.0, 136.1, 138.5, 140.1, 140.5, 142.2, 144.9, 146.9, 158.0, 158.4, 158.5, 170.7; ESI-HRMS (ES⁺) *m/z* calculated for C₃₇H₃₂Cl₄N₂O₄: 710.47, found 709.1189 [M+H]⁺

4.3.6 Synthesis of (E)-4-((4-(2-(bis(4-methoxyphenyl)(phenyl)methoxy)ethyl)-2,6-dichlorophenyl)diazanyl)-3,5-dichlorophenethyl (2-cyanoethyl) diisopropylphosphoramidite - Compound (5)

To a solution of 4.00 mL of anhydrous DCM/ACN (1:1) 0.14 g of compound **6** (0.2 mmol, 1.00 equiv.) was added to a flame dried flask. To that solution 0.28 mL of anhydrous triethylamine (2.0 mmol, 10.0 equiv.) was added along with 0.13 mL of 2-cyanoethyl *N,N*-diisopropylchlorophosphoramidite with (0.9 mmol, 3.00 equiv.) and stirred at room temperature until TLC showed starting materials were consumed (2 h). After rotary evaporation, the compound was then purified on silica gel using a 68%:30%:2% hexanes/ethyl acetate/triethylamine mobile phase. This afforded compound **7** as a dark red oil (0.1 g, 60%). ¹H NMR (400 MHz, *d*-CDCl₃) δ ppm 7.35 - 7.43 (m, 2 H) 7.16 - 7.35 (m, 12 H) 6.76 - 6.90 (m, 5 H) 3.86 (s, 1 H) 3.81 (s, 6 H) 3.74 - 3.79 (m, 1 H) 3.61 - 3.67 (m, 1 H) 3.37 (s, 1 H) 2.96 (t, *J*=6.24 Hz, 2 H) 2.88 (t, *J*=6.24 Hz, 2 H) 2.79 (t, *J*=6.24 Hz, 2 H) 2.62 - 2.67 (t, *J*=6.24 Hz, 2 H) 1.13 - 1.34 (m, 12 H). ³¹P NMR (162 MHz, *d*-CDCl₃) □

ppm 147.90. ^{13}C NMR (101 MHz, *d*- CDCl_3) δ ppm 17.0, 20.3, 20.8, 24.5, 24.6, 24.7, 42.9, 43.0, 50.6, 50.7, 53.2, 54.5, 55.2, 58.2, 58.3, 58.4, 58.5, 59.2, 76.8, 77.1, 77.4, 113.1, 113.6, 117.6, 117.7, 126.5, 127.2, 127.4, 127.8, 128.0, 128.1, 128.3, 128.7, 129.8, 129.9, 130.0, 130.2, 135.9, 136.0, 138.5, 142.6, 144.9, 146.9, 158.0, 158.5, 203.2; ESI-HRMS (ES^+) m/z calculated for $\text{C}_{46}\text{H}_{49}\text{Cl}_4\text{N}_4\text{O}_5\text{P}$: 910.69, found 910.2711 $[\text{M}+\text{H}]^+$

4.3.7 Procedure for Oligonucleotide Synthesis and Purification

All standard β -cyanoethyl 2'-*O*-TBDMS protected phosphoramidites, reagents and solid supports were purchased from Chemgenes Corporation and Glen Research. Wild-type luciferase strands including the sense and 5'-phosphorylated antisense strand were synthesized. All commercial phosphoramidites were dissolved in anhydrous acetonitrile to a concentration of 0.10 M. The chemically synthesized (azobenzene derivative) phosphoramidites were dissolved in 3:1 (v/v) acetonitrile:THF (anhydrous) to a concentration of 0.10 M. The reagents that were used for the phosphoramidite coupling cycle were: acetic anhydride/pyridine/THF (Cap A), 16% *N*-methylimidazole in THF (Cap B), 0.25 M 5-ethylthio tetrazole in ACN (activator), 0.02 M iodine/pyridine/ H_2O /THF (oxidation solution), and 3% trichloroacetic acid/dichloromethane. All sequences were synthesized on 0.20 μM or 1.00 μM dT solid supports except for sequences that were 3'-modified, which were synthesized on 1.00 μM Universal III solid supports. The entire synthesis ran on an Applied Biosystems 394 DNA/RNA synthesizer using 0.20 μM or 1.00 μM cycles kept under argon at 55 psi. Standard and synthetic phosphoramidites ran with coupling times of 999 seconds.

Antisense sequences were chemically phosphorylated at the 5'-end by using 2-[2-(4,4'-dimethoxytrityloxy)ethylsulfonyl]ethyl-(2-cyanoethyl)-(N,N-diisopropyl)-

phosphoramidite. At the end of every cycle, the columns were removed from the synthesizer, dried with a stream of argon gas, sealed and stored at 4 °C. Cleavage of oligonucleotides from their solid supports was performed through on-column exposure to 1.50 mL of EMAM (methylamine 40% wt. in H₂O and methylamine 33% wt. in ethanol, 1:1 (Sigma-Aldrich)) for 1 hour at room temperature with the solution in full contact with the controlled pore glass. The oligonucleotides were then incubated overnight at room temperature in EMAM to deprotect the bases. On the following day, the samples were concentrated on a Speedvac evaporator overnight, resuspended in a solution of DMSO:3HF/TEA (100 µL:125 µL) and incubated at 65 °C for 3 hours in order to remove the 2'-*O*-TDBMS protecting groups. Crude oligonucleotides were precipitated in EtOH and desalted through Millipore Amicon Ultra 3000 MW cellulose. Oligonucleotides were separated on a 20% acrylamide gel and were used without further purification for annealing and transfection. Equimolar amounts of complimentary RNAs were annealed at 95 °C for 2 min in a binding buffer (75.0 mM KCl, 50.0 mM Tris-HCl, 3.00 mM MgCl₂, pH 8.30) and this solution was cooled slowly to room temperature to generate siRNAs used for biological assays. A sodium phosphate buffer (90.0 mM NaCl, 10.0 mM Na₂HPO₄, 1.00 mM EDTA, pH 7.00) was used to anneal strands for biophysical measurements.

4.3.8 Procedure for ESI Q-TOF Measurements.

All single-stranded RNAs were gradient eluted through a Zorbax Extend C18 HPLC column with a MeOH/H₂O (5:95) solution containing 200 mM hexafluoroisopropyl alcohol and 8.1 mM triethylamine, and finally with 70% MeOH. The eluted RNAs were subjected to ESI-MS (ES⁻), producing raw spectra of multiply-charged anions and through resolved

isotope deconvolution, the molecular weights of the resultant neutral oligonucleotides were confirmed for all the RNAs.

4.3.9 Procedure for Performing CD Experiments

Circular Dichroism (CD) spectroscopy was performed on a Jasco J-815 CD equipped with temperature controller. Equimolar amounts of each siRNA (10 μ M) were annealed to their complement in 500 μ L of a sodium phosphate buffer by incubating at 95 $^{\circ}$ C for two minutes and allowing to cool to room temperature. CD measurement of each duplex were recorded in triplicate from 200-500 nm at 25 $^{\circ}$ C with a screening rate of 20.0 nm/min and a 0.20 nm data pitch. The average of the three replicates was calculated using Jasco's Spectra Manager version 2 software and adjusted against the baseline measurement of the sodium phosphate buffer.

4.3.10 Procedure for Melting Temperature of siRNA Duplexes (T_m)

The siRNA duplexes annealed as above were placed in the Jasco J-815 CD spectropolarimeter and then UV absorbance was measured at 260 nm against a temperature gradient of 10 $^{\circ}$ C to 95 $^{\circ}$ C at a rate of 0.5 $^{\circ}$ C per minute with absorbance being measured at each 0.5 $^{\circ}$ C increment. Absorbance was adjusted to baseline by subtracting absorbance of the buffer. The T_m values were calculated using Meltwin v3.5 software. Each siRNA result was the average of 3 independent experiments and the reported values were calculated using Meltwin v3.5 assuming the two-state model.²

4.3.11 Procedure for Absorbance Spectra Experiments

All absorbance spectra measurements were done on a Jasco J-815 CD with temperature controller. Measurement was recorded from 200 -500 nm at 10 $^{\circ}$ C at least 3 times. The

coloured visible light experiments in Figure 2 were obtained using a 15.0 Watt iLUMI multiple wavelength A19 light bulb to isolate each colour.

4.3.12 Procedure for HPLC Characterization

HPLC chromatograms were obtained on a Waters 1525 binary HPLC pump with a Waters 2489 UV/Vis detector using the Empower 3 software. A C18 4.6 mm x 150 mm reverse phase column was used. Conditions were 5% acetonitrile in 95% 0.1 M TEAA (Triethylamine-Acetic Acid) buffer up to 100% acetonitrile over 30 min.

4.3.13 Procedure for Reduced Glutathione (GSH) Degradation Assay

The GSH assay was performed on siRNA 6 in a 96 well plate at 37 °C. A concentration of 2.7 µM of siRNA was added to 10 mM glutathione and 5 mM TCEP in PBS to a final volume of 100 µL. Dark experiments were performed with no additional treatment at 0, 8, and 24 h time points after which the entire 100 µL was sample was injected into the HPLC and characterized (same conditions as above) to afford the HPLC traces at the different time points. Red treated siRNA was exposed to red light for entire duration of assay during incubation at 37 °C, and kept in the dark until injection for 0, 8, 24 h time points. The red 0 h time point was exposed to red light for 15 min and then injected immediately onto the HPLC.

4.3.14 Procedure for Maintaining Cell Cultures of HeLa Cells

For biological analysis of these siRNAs in a live environment, human epithelial cervix carcinoma cells were used (HeLa cells). They were kept in 250 mL vented culture flasks using 25.0 mL of DMEM with 10% fetal bovine serum and 1% penicillin-streptomycin (Sigma) in an incubator set for 37 °C @ 5% CO₂ humidified atmosphere.

Once cell lines became confluent (80-90%) they were passaged by washing 3 times with 10 mL of phosphate buffered saline (NaCl 137 mM, KCl 2.70 mM, PO₄³⁻ 10.0 mM, pH 7.40) and incubated with 3.00 mL of 0.25% trypsin (SAFC bioscience) for 4 min @ 37 °C to detach the cells. The cells were transferred to a 50.0 mL centrifuge tube after the addition of 10.0 mL of DMEM solution and pelleted at 2000 rpm for 5 minutes. The supernatant was discarded and the pellet resuspended in 5.0 mL DMEM with 10% FBS.

A standard haemocytometer was used to obtain cell counts, after which the cells were diluted to a final concentration of 1.00 x 10⁶ cells/mL for subsequent assays. To continue the cell line 1.00 mL of freshly passaged cells was added to 24.0 mL of DMEM/10% FBS and 1% penicillin-streptomycin at 37 °C in a new culture flask while the rest were used for assays.

4.3.15 Procedure for siRNA Transfections

100 µL of cells (total 1.00 x 10⁵) were transfected into 12 well plates (Falcon®) with 1 mL of DMEM (10% FBS, 1% penicillin-streptomycin) and incubated at 37 °C with 5% CO₂. After 24 hours the cells were transfected with various concentrations of siRNAs, along with both pGL3 (Promega) and pRLSV40 luciferase plasmids using Lipofectamine 2000 (Invitrogen) in Gibco's 1X Opti-Mem reduced serum media (Invitrogen) according to the manufacturer's instructions. 1.00 µL of siRNA was added along with 2.00 µL (pGL3 200 ng) and 0.50 µL pRLSV40 (50.0 ng) to 100 µL of 1X Opti-Mem in a microcentrifuge tube and kept on ice for 5 min. In a different microcentrifuge tube 1.00 µL of Lipofectamine 2000 (Invitrogen) was mixed with 100 µL of Gibco's 1X Opti-Mem reduced serum media (Invitrogen) and incubated at room temperature for 5 min. After 5 minutes the tubes were

mixed and incubated at room temperature for 20 min and then the entire contents transferred to the wells of the 12 well plate.

4.3.16 Procedure for *in vitro* Dual-Reporter Luciferase Assay

100 μ L of cells (total of 1.00×10^5 cells) were added to 12 well plates (Falcon®) with 1 mL of growth media (DMEM 10% FBS, 1% penicillin-streptomycin) and incubated at 37 °C with 5% CO₂. After 24 hours the cells were transfected with 8.00, 20.0, 40.0, 160, 400 and 800 pM concentrations of siRNAs, along with both pGL3 (Promega) and pRLSV40 luciferase plasmids using Lipofectamine 2000 (Invitrogen) in Gibco's 1X Opti-Mem reduced serum media (Invitrogen) according to the manufacturer's instructions. After a set amount of time (8, 12 or 22h) the cells were incubated at room temperature in 1X passive lysis buffer (Promega) for 20 minutes. The lysates were collected and loaded onto a 96 well, opaque plate (Costar). With a Dual-Luciferase reporter Assay kit (Promega), Lar II and Stop & Glo® luciferase substrates were sequentially added to the lysates and enzyme activity was measured through luminescence of both *firefly/Renilla* luciferase on a Synergy HT (Bio-Tek) plate luminometer. The ratio of *firefly/Renilla* luminescence is expressed as a percentage of reduction in *firefly* protein expression to siRNA efficacy when compared to untreated controls. Each value is the average of at least 3 different experiments with standard deviation indicated.

4.3.17 Procedure for Light Inactivation of Azobenzene Modified siRNA (*trans* to *cis*)

Cell culture was exposed to red wavelength light from time 0 h for the entire duration of the assays, either 8 or 24 hours. The lamp used was a 15.0 Watt iLUMI multiple wavelength A19 light bulb switched to red light, held directly above the cell culture plates to maximize red light exposure.

4.3.18 Procedure for Thermal Relaxation and Reactivation of Azobenzene Modified siRNA (*cis* to *trans*)

Immediately following transfection cell culture was exposed to right light as above, which was then removed 2 hours post transfection to allow the azobenzene to thermally relax back to the active form of the siRNAzo in the dark. The cells were then lysed and luminescence measured as above in the luciferase assay.

4.4 Results

Our hypothesis was that chlorinated azobenzene, in the *cis* form, would distort the siRNA helix, thus rendering it non-functional in a similar manner to our previous research, but without the use of toxic UV light (see Figure 2). Being able to control the timing of when an siRNA is active or not active would have enormous benefit for modern medicine.

To start, this involved synthesizing diol **1** from our previously reported procedure.¹⁴ This diol **1** reacted with *n*-chlorosuccinimide (NCS) and palladium acetate (Pd(OAc)₂) to the *ortho*-functionalized tetrachlorinated azobenzene diacetyl compound **2** in 59% yield.

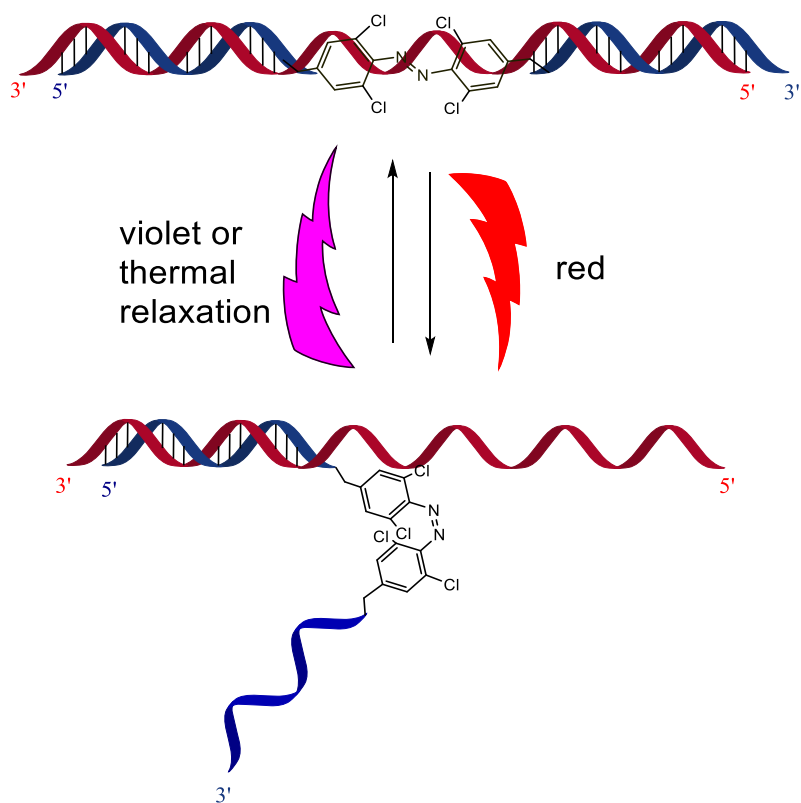
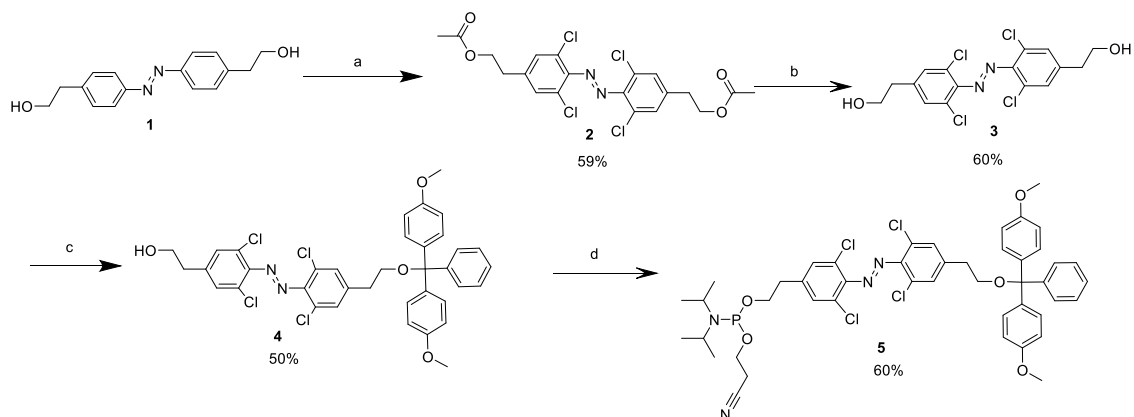


Figure 4.2. Photoinduced inactivation and reactivation of siRNAz. The blue strand corresponds to the sense strand and contains the azobenzene moiety. The red strand corresponds to the antisense strand.

This acetylated compound was deprotected in sodium hydroxide (NaOH) and methanol (MeOH) to afford the diol, compound **3**. This diol was then reacted with 4'-dimethoxytrityl (DMT) chloride to afford the monoalcohol **4**. Finally, the DMT-protected diol was phosphitylated with 2-cyanoethyl diisopropylchlorophosphoramidite in the presence of triethylamine to afford phosphoramidite **5** (Scheme 4.1). Overall, from compound **1**, phosphoramidite **4** was generated in 11% yield over four steps.



Scheme 4.1. Synthesis of an *ortho*-functionalized tetrachlorinated azobenzene DMT-phosphoramidite: (a) 0.3 equiv. of Pd(OAc)₂ and 8 equiv. of NCS AcOH, 145 °C, 59% (**2**); (b) 0.1 eq NaOH in MeOH, r.t. 0.5h, 60% (**3**); (c) 1 equiv. dimethoxytrityl chloride (DMT-Cl), 3 equiv. TEA, THF, r.t., 50% (**4**); (d) 3 equiv. 2-cyanoethyl *N,N*-diisopropylchlorophosphoramidite, 10 equiv. TEA, anhydrous DCM:ACN (1:1), r.t. 2h, 60% (**5**).

Once the phosphoramidite was synthesized, a small library of Cl-siRNAzOs were synthesized (Table 4.1). Three different Cl-siRNAzOs were synthesized that target the firefly luciferase mRNA (Table 1). In each Cl-siRNAzo, the azobenzene derivative replaces two nucleosides on the oligonucleotide sense strand. These Cl-siRNAzOs were purified and characterized by mass spectrometry (see Table S-1 in the Supporting Information, Appendix III). Cl-SiRNAzo 1 contains an azobenzene modification (Cl-Az2) that replaces positions 8 and 9, on the sense strand, counting from the 5'-end of the sense strand. This azobenzene insertion partially replaces the Argonaute 2 cleavage site.³² SiRNAzOs 2 and 3 contain the same azobenzene modification (Cl-Az2) and this modification spans two nucleosides that replace positions 9 and 10, and 10 and 11, of the sense strand, respectively.

Table 4.1. Table of RNAs used and its target.^[a]

siRNA	siRNA duplex	target
WT	5'-CUUACGCUGAGUACUUCGAtt-3' 3'-ttGAAUGCGACUCAUGAAGCU-5'	luciferase
1	5'-CUUACGCC Cl-Az2 AGUACUUCGAtt-3' 3'-ttGAAUGCGACUCAUGAAGCU-5'	luciferase
2	5'-CUUACGCU Cl-Az2 GUACUUCGAtt-3' 3'-ttGAAUGCGACUCAUGAAGCU-5'	luciferase
3	5'-CUUACGCUG Cl-Az2 UACUUCGAtt-3' 3'-ttGAAUGCGACUCAUGAAGCU-5'	luciferase

[a] **Cl-Az2** corresponds to the azobenzene derivative synthesized from Az2; the top strand corresponds to the sense strand; the bottom strand corresponds to the antisense strand. In all duplexes, the 5'-end of the bottom antisense strand contains a 5'-phosphate group.

These siRNAs were then tested for *cis-trans* isomerization, but due to the short half-life of the *cis* isomer, it was difficult to characterize via HPLC (Figures S2 to S4 in supplement S1, Appendix III) in any significant amount after exposure to red light. We performed some time-dependent absorbance studies after exposure to red light, and estimate the half-life at 37 °C to be approximately 2 minutes (data not shown). Previous studies of various azobenzene structures (with and without *ortho*-chlorination) show a half-life from tens of milliseconds³³ up to 3.5 hours.¹³ Our specific modification turned out to have a very unstable half-life of less than one minute, and so we chose thermal relaxation as the reactivation protocol. Also due to the smaller absorbance profile of the chlorinated azobenzene compared to the original non-chlorinated one, there was no discernible peak representing the Cl-Az2 moiety in the absorbance spectra (data not shown). Despite these

challenges, we were still able to characterize the Cl-siRNAzOs via mass spectrophotometry (Table S1 Supplement S1, Appendix III). The *ortho*-functionalized tetrachlorinated azobenzene diol 3 itself was characterized via an absorbance graph, and both the *trans* and *cis* isomers and their change in absorbance are visible, with red wavelength light causing the change to *cis*, while violet light or thermal relaxation will restore the *trans* isomer (Figure 4.3). This finding is in agreement with the literature.³³

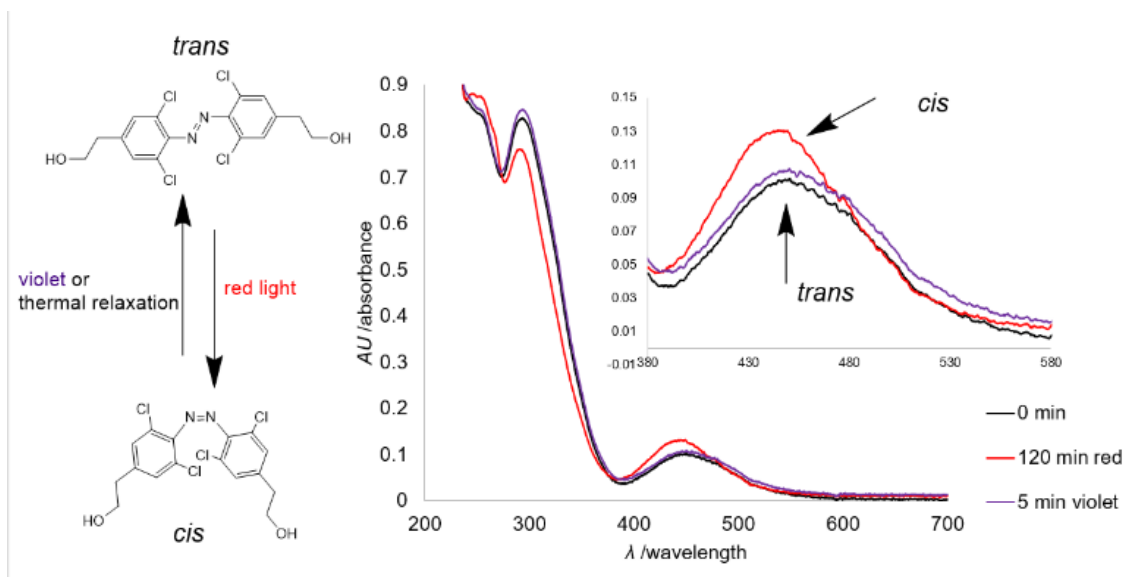


Figure 4.3. Absorbance profile of Cl-Az2 (compound 3) moiety when exposed to various wavelengths of visible light (red (660 nm) and violet (410 nm)) in methanol. Inset: Zoomed in portion of 400-580 nm highlighting azobenzene changes.

In addition, these Cl-siRNAzOs also exhibited thermal destabilization because the chlorinated azobenzene moiety replaces two nucleotides within the central region, as measured by UV absorption profiles in melting experiments (Table S-1 in Supporting Information, Appendix III). This is consistent with other studies that place thermally destabilizing units into the central region of the sense strand.³⁴⁻³⁶ Lastly, these siRNAzOs all retained classic A-type helix conformation which is required for the RNAi pathway to function, characterized by circular dichroism (Figure S1 in the Supporting Information, Appendix III).

Once the biophysical characterizations were completed, gene silencing was evaluated in the dark with no exposure to light. Since the more thermally stable *trans* isomer is dominant at 37 °C, we expected the siRNA to be in the active *trans* form and achieve efficient gene silencing. As expected, and observed in Fig. 4.4, all the Cl-siRNAzOs demonstrated good dose-dependent silencing of the firefly luciferase gene at concentrations between 1 and 4 nM (blue bars). This was observed for both time points, 8 and 24 hours. All three Cl-siRNAzOs show around 90% knockdown at 4 nM, with a decrease to approximately 70-80% knockdown at 1 nM for the various time points and Cl-siRNAzOs. Next, we screened these Cl-siRNAzOs with exposure to red light in order to test for the inactivation, preventing their uptake into the RNAi pathway, and thus preventing gene silencing with the less toxic, low energy and high wavelength light. Previously, it was shown that exposure to higher energy low wavelength UV light could accomplish this effectively, and it could successfully be reversed with broadband visible light.¹⁶ We hypothesized that instead of disrupting the RISC complex after it had bound the siRNAzo, that we were preventing the uptake of remaining unbound siRNAs in the RNAi pathway with our system. At any one time, it has been reported that only about 4% of the active siRNAs are taken up into the RISC complex immediately upon transfection.³⁷ Thus, within our system, the remaining unbound population of siRNAzOs can be inactivated and their uptake into the RNAi pathway prevented.¹⁷ Our finding demonstrated, that with the new chlorinated azobenzene moiety, we could inactivate the unbound Cl-siRNAzOs with red light and keep them inactive for up to 24 hours as long as the cells were exposed to the red light. In every case, all concentrations and both time points, luciferase activity increased to levels similar to untreated cells, thus indicating poor gene silencing when the cells were exposed to red

light (grey bars, Figure 4.4). There is also a very large difference in gene silencing as compared to the dark exposed Cl-siRNAzOs, demonstrating the functionality of active vs inactive Cl-siRNAzOs. As mentioned previously, due to the poor half-life of the Cl-Az2 moiety, the cell culture had to be exposed to the red light for the entire duration of the assay. The next phase of our experiment involved testing the gene silencing by initially inactivating the siRNA with red light, then allowing the ambient thermal energy to convert our inactive *cis* form back to its active *trans* isomer. To achieve this, cells were exposed to red light for only the first 2 hours of the assay and the resulting luminescence of the luciferase was determined after 8 or 24 hours. We found that at both the 8- and 24-hour time points, excellent gene silencing was achieved to comparable levels to the control dark treatment (yellow bars). Additionally, we found no degradation of the siRNAzOs via glutathione for up to 24 hours, whether exposed to red light, or kept in the dark (See Figure S5 in Supplement, Appendix III). This study demonstrated that we can actively control siRNA activity using chlorinated siRNAzOs (Cl-siRNAzOs) by using only visible wavelength light, which represents a significant advancement over the UV light utilized in our previous system and other reported technologies.^{8-10,14-16} This is an enhancement over our previous generation of siRNAzOs, where higher energy UV light, which is toxic, was required to control the activity of gene-silencing within mammalian cells

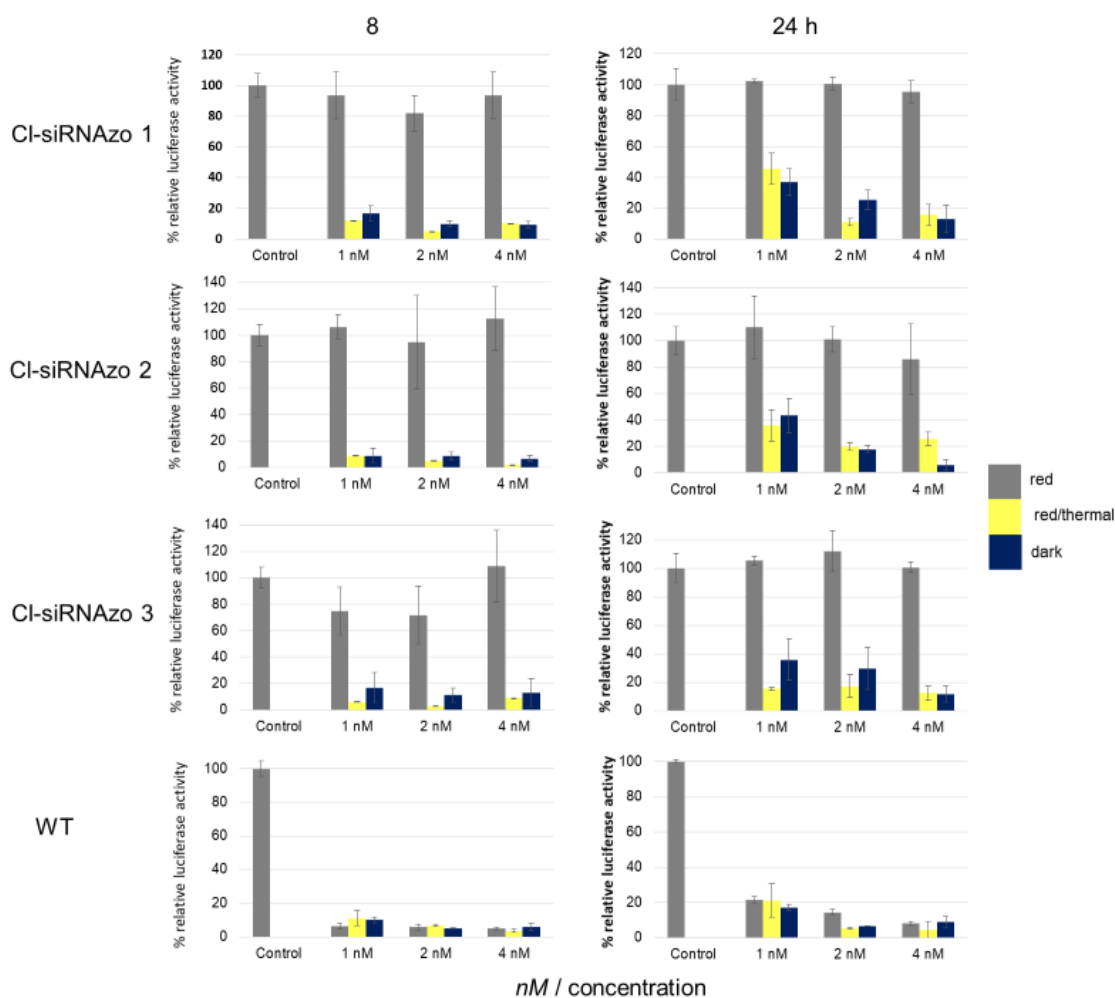


Figure 4.4. Normalized firefly luciferase expression for CI-siRNAs 1-3 at 1, 2 and 4 nM in HeLa cells monitored 8- and 24-hours post-transfection. Red corresponds to the siRNA being exposed under a multi-wavelength lamp tuned to red light for inactivation immediately after transfection for the entire length of the assay (8 or 24 hr). Red/thermal corresponds to red light exposure for the first 2 h after transfection, after which the light was removed and the siRNA allowed to thermally relax back to the active state for the remaining of the assay (8 or 24 hr). Dark corresponds to siRNAs being transfected in HeLa cells in the absence of red light. WT corresponds to wild-type anti-firefly luciferase siRNA.

4.5 Conclusions

We have synthesized and evaluated red-shifted CI-siRNAs that can be photo-chemically controlled using visible wavelength light. To our knowledge this is the first time, a system utilizing siRNAs with an azobenzene moiety could be photo-controlled using only visible light, using wavelengths of 660 nm for red, and 410 nm for violet light. We believe this to

be an improvement over the previous system, which until now required the use of toxic UV light to induce photo-chemical control of the siRNA.¹⁶ Using visible light should not only prove to be less toxic, but there are also no photo-chemical by-products released, such as in the case of photocages. In addition, this system is also reversible, another improvement over the caging systems available. The short half-life of the *cis* conformer however remains problematic, since constant exposure to red light is inconvenient for use as a bio-molecular tool or a therapeutic. One way to overcome this challenge, is to continue exploring different chemical modifications which not only allow the photo-control with visible light, but also allow longer half-lives at physiological relevant temperatures, so that inactivation can occur with one short exposure of light, and then be red-activated later at a time of our choice. If overcome, a visible light controllable therapeutic with a long half-life would be very beneficial to the research sector for use as a biomolecular tool, as well as within the pharmaceutical industry where fine-tuned spatio-temporal control of a drug would be desirable. This is an important issue: a paper published from Alnylam® Pharmaceuticals in 2018 disclosed that a short oligonucleotide was capable of reversing the activity of an active siRNA.³⁸ Utilization of this system to control off-target effects in a patient undergoing treatment would also be ideal, where red light exposure on sensitive adjacent tissues or surrounding healthy tissue could prevent off-target effects and siRNA-mediated toxicity. Future directions include further exploration of chemical modifications to improve functionality, as well as development of a multi-siRNAzo system, where multiple targets could be activated/inactivated selectively with different wavelengths of light.

Acknowledgements

We thank the Natural Sciences and Engineering Research Council (NSERC) for funding.

Supplementary Data

Refer to Appendix III for additional figures and characterization data.

4.6 REFERENCES – Chapter 4 – Manuscript III

- [1] A. Fire, S. Q. Xu, M. K. Montgomery, S. A. Kostas, S. E. Driver and C. C. Mello, *Nature* **1998**, *391*, 806.
- [2] L. Aagaard and J. J. Rossi, *Adv. Drug Deliv. Rev.* **2007**, *59*, 75.
- [3] A. L. Hopkins and C. R. Groom, *Nat. Rev. Drug Discov.* **2002**, *1*, 727.
- [4] X. Shen and D. R. Corey, *Nucleic Acids Res.* **2017**, *46*, 1584.
- [5] D. Al Shaer, O. Al Musaimi, F. Albericio and B. G. de la Torre, *Pharmaceuticals* **2019**, *12*, 52.
- [6] P.R.D. Brandao, S.S. Titze-de-Almeida, and R. Titze-de-Almeida, *Mol. Diagn. Ther.* **2019**, *8*.
- [7] R.L. Setten, J.J. Rossi and S. P. Han, *Nat. Rev. Drug Discov.* **2019**, *18*, 421.
- [8] S. Shah, S. Rangarajan and S. H. Friedman, *S. H. Angew. Chem. Int. Ed.* **2005**, *44*, 1328.
- [9] V. Mikat and A. Heckel, *RNA* **2007**, *13*, 2341.
- [10] A. Meyer and A. Mokhir, *Angew. Chem. Int. Ed.* **2014**, *53*, 12840.
- [11] A. S. Lubbe, W. Szymanski and B. L. Feringa, *Chem. Soc. Rev.* **2017**, *46*, 1052.
- [12] C. Brieke, F. Rohrbach, A. Gottschalk, G. Mayer and A. Heckel, *Angew. Chem. Int. Ed.* **2012**, *51*, 8446.
- [13] A. A. Beharry and G. A. Woolley, *Chem. Soc. Rev.* **2011**, *40*, 4422.
- [14] M. L. Hammill, C. Isaacs-Trépanier and J.-P. Desaulniers, *ChemistrySelect* **2017**, *2*, 9810.
- [15] M. L. Hammill, A. Patel, M. A. Alla and J.-P. Desaulniers, *Bioorg. Med. Chem. Lett.* **2018**, *28*, 3613.
- [16] M. L. Hammill, G. Islam and J.-P. Desaulniers, *Org. Biomol. Chem.*, **2020**, *18*, 41.
- [17] K. Yamana, K. Kan, and H. Nakano, *Bioorg. Med. Chem.* **1999**, *7*, 2977.
- [18] Abrams, Y. Xu, N.A. Kuklin, P.A. Burke, A.B. Sachs, L. Sepp-Lorenzino, and S. T. Barnett. *RNA* **2010**, *16*, 2553.
- [19] J. D'Orazio, S. Jarrett, A. Amaro-Ortiz and T. Scott, *Int. J Mol. Sci.* **2013**, *14*, 12222.
- [20] C. Ash, M. Dubec, K. Donne and T. Bashford, *Lasers Med. Sci.* **2017**, *32*, 1909.
- [21] M. Wegener, M.J. Hansen, A. J. M. Driessen, W. Szymanski and B. Feringa, *J. Am. Chem. Soc.*, **2017**, *139*, 17979.
- [22] O. Shinzi, I. Syoji, M. Hiroshi and M. Mizuo *Chem. Lett.* **2010**, *39*, 956
- [23] H. Nishioka, X. Liang, T. Kato, and H. Asanuma *Angew. Chem. Int. Ed.* **2012**, *51*, 1165

- [24] Y. Kamiya, T. Takagi, H. Ooi, H. Ito, X. Liang, and H. Asanuma *ACS Synth. Biol.* **2015**, 365
- [25] D. Kolarski, W. Szymanski, and B. L. Feringa *Org. Lett.* **2017**, 19, 5090
- [26] S. Samanta, T. M. McCormick, S. K. Schmidt, D. S. Seferos and G. A. Woolley, *Chem. Commun.* **2013**, 49, 10314.
- [27] M. Dong, A. Babalhavaeji, S. Samanta, A. A. Beharry and G. A. Woolley, *Acc. Chem. Res.* **2015**, 48, 2662.
- [28] O. Sadovski, A. A. Beharry, F. Zhang and G. A. Woolley, *Angew. Chem. Int. Ed. Engl.* **2009**, 48, 1484.
- [29] J. García-Amorós and D. Velasco, *Beilstein J. Org. Chem.*, **2012**, 8, 1003.
- [30] D. Bleger, J. Schwarz, A. M. Brouwer and S. Hecht, *J. Am. Chem. Soc.*, **2012**, 134, 20597.
- [31] D. B. Konrad, J. A. Frank and D. Trauner, *Chem.: Eur. J.* **2016**, 22, 4364.
- [32] C. Matranga, Y. Tomari, C. Shin, D. P. Bartel and P. D. Zamore, *Cell* **2005**, 123, 607.
- [33] J. Broichhagen, J. A. Frank and D. Trauner *Acc. Chem. Res.* **2015**, 48, 1947.
- [34] T. C. Efthymiou, B. Peel, V. Huynh and J.-P. Desaulniers, *Bioorg. Med. Chem. Lett.* **2012**, 22, 5590.
- [35] H. Addepalli, Meena, C. G. Peng, G. Wang, Y. Fan, K. Charisse, K. N. Jayaprakash, K. G. Rajeev, R. K. Pandey, G. Lavine, L. Zhang, K. Jahn-Hofmann, P. Hadwiger, M. Manoharan and M. A. Maier, *Nucleic Acids Res.* **2010**, 38, 7320.
- [36] B. J. Peel, G. Hagen, K. Krishnamurthy and J.-P. Desaulniers, *ACS Med. Chem. Lett.* **2015**, 6, 117.
- [37] Y.I. Pei, P.J. Hancock, H. Zhang, R. Bartz, C. Cherrin, N. Innocent, C. J. Pomerantz, J. Seitzer, M.L. Koser, M.T. Abrams, Y. Xu, N.A. Kuklin, P.A. Burke, A.B. Sachs, L. Sepp-Lorenzino, and S. T. Barnett. *RNA* **2010**, 16, 2553.
- [38] I. Zlatev, A. Castoreno, C. R. Brown, J. Qin, S. Waldron, M. K. Schlegel, R. Degaonkar, S. Shulga-Morskaya, H. Xu, S. Gupta, S. Matsuda, A. Akinc, K. G. Rajeev, M. Manoharan and V. Jadhav, *Nat. Biotechnol.* **2018**, 36, 509.

4.7 Manuscript III Supplementary Tables and Figures

Full Supplementary data can be found in Appendix III

Figures and Tables

Table S-1 Sequences of anti-luciferase siRNAs, predicted and recorded mass and T_m 's of siRNAs containing the azobenzene spacers.^a

siRNAzo	siRNA Duplex	Predicted Mass	Actual Mass ^(b)	aT_m (°C)	ΔT_m (°C)
wt	5'- CUUACGCU <u>G</u> AGUACUUCGAtt -3' 3'- ttGAAUGCGACUCAUGAAGCU – 5'			74.0	--
1	5'-CUUACG <u>CCl-Az2</u> AGUACUUCGAtt-3' 3'-ttGAAUGCGACUCAUGAAGCU-5'	6482.63	6482.66	61.9	- 12.1
2	5'-CUUACGCU <u>Cl-Az2</u> GUACUUCGAtt-3' 3'-ttGAAUGCGACUCAUGAAGCU-5'	6505.67	6504.75	62.5	- 11.5
3	5'-CUUACGCU <u>GCl-Az2</u> UACUUCGAtt-3' 3'-ttGAAUGCGACUCAUGAAGCU-5'	6482.63	6482.67	58.4	- 15.6

[a] **Cl-Az2** corresponds to the azobenzene derivative synthesized from Az2; the top strand corresponds to the sense strand; the bottom strand corresponds to the antisense strand. In all duplexes, the 5'-end of the bottom antisense strand contains a 5'-phosphate group. [b] Deconvolution results for siRNAs. ESI-HRMS (ES^+) m/z calculated for siRNAzos 1-7 $[M+H]^+$

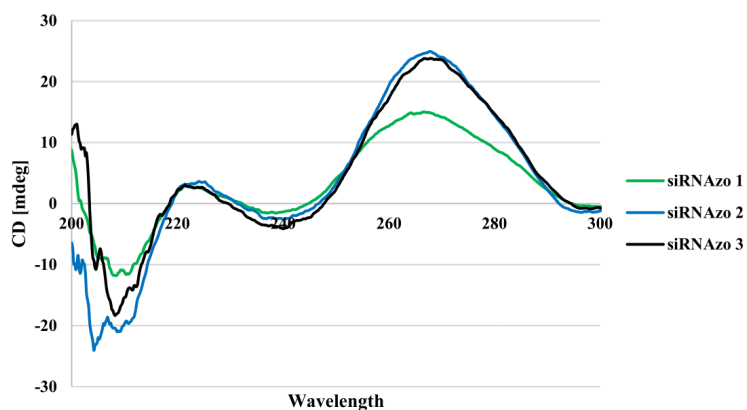


Figure S-1. CD spectra of azobenzene modified spacers replacing two nucleobases targeting firefly luciferase mRNAs. Wildtype and modified anti-*firefly* luciferase siRNAs (10 μ M/duplex) were suspended in 500 μ L of a sodium phosphate buffer (90.0 mM NaCl, 10.0 mM Na_2HPO_4 , 1.00 mM EDTA, pH 7.00) and scanned from 200-300 nm at 25 °C with a screening rate of 20.0 nm/min and a 0.20 nm data pitch. All scans were performed in triplicate and averaged using Jasco's Spectra Manager version 2.

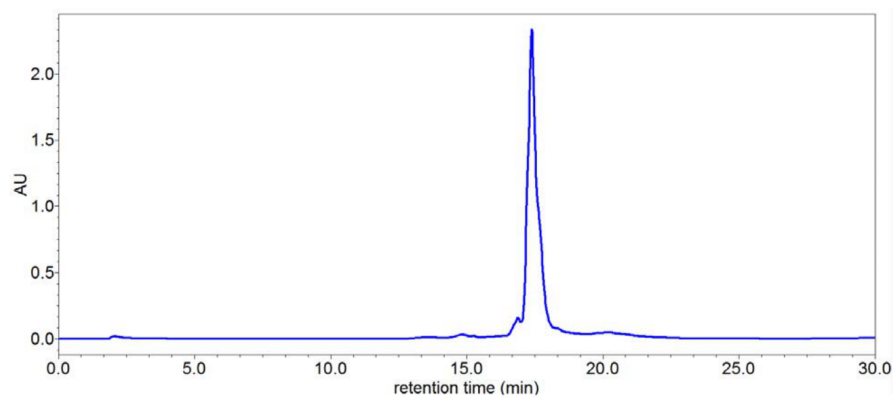


Figure S-2. HPLC chromatogram of siRNA 1. Conditions were 5% acetonitrile in 95% 0.1 M TEAA (Triethylamine-Acetic Acid) buffer up to 100% acetonitrile over 40 min. Spectra were processed using the Empower 3 software.

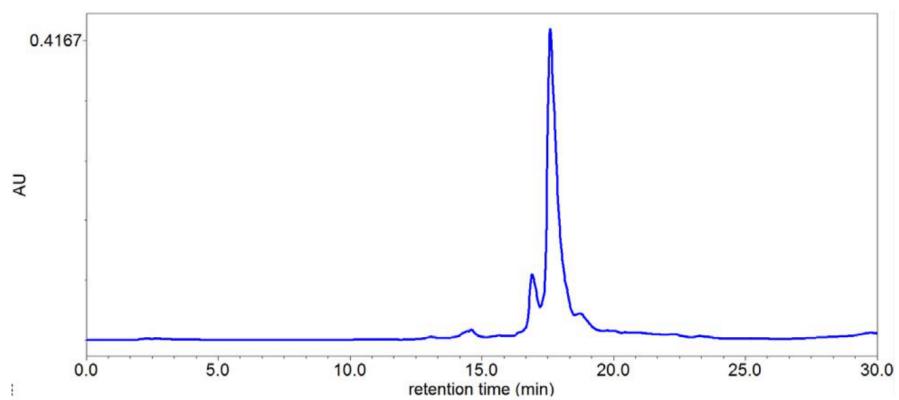


Figure S-3. HPLC chromatogram of siRNA 2. Conditions were 5% acetonitrile in 95% 0.1 M TEAA (Triethylamine-Acetic Acid) buffer up to 100% acetonitrile over 40 min. Spectra were processed using the Empower 3 software.

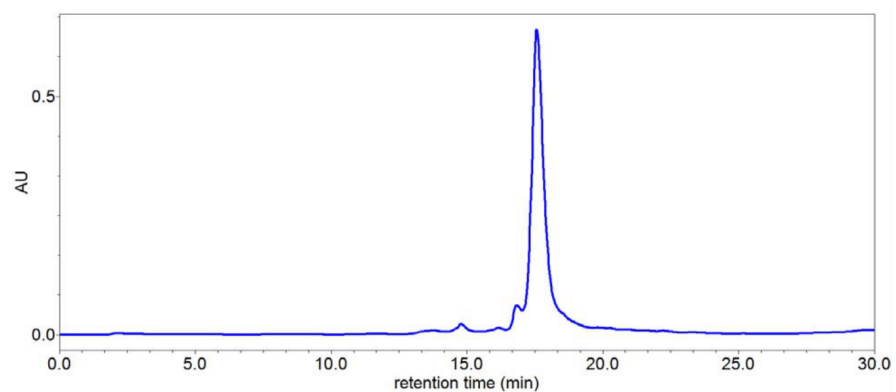


Figure S-4. HPLC chromatogram of siRNA 3. Conditions were 5% acetonitrile in 95% 0.1 M TEAA (Triethylamine-Acetic Acid) buffer up to 100% acetonitrile over 40 min. Spectra were processed using the Empower 3 software.

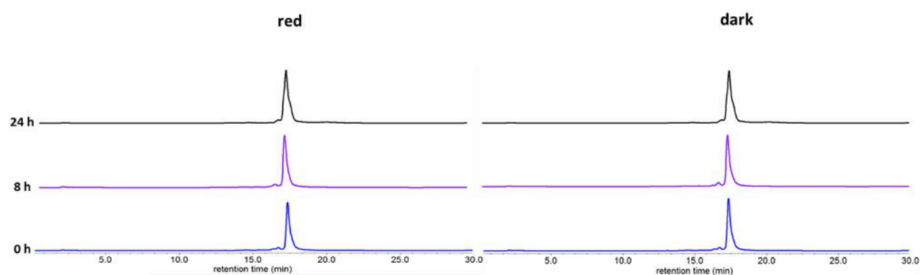


Figure S-5. GSH assay results of the sense strand of siRNA 1 showing minimal degradation due to the presence of GSH. Red treated siRNA was exposed to red light for entire duration of assay during incubation at 37 °C, and kept exposed until injection at 0, 8, 24 h time points. The red 0 h time point was exposed to red light for 15 min and then injected immediately onto the HPLC. Conditions were 5% acetonitrile in 95% 0.1 M TEAA (Triethylamine-Acetic Acid) buffer up to 100% acetonitrile over 30 min. Spectra were processed using the Empower 3 software.

Connecting Statement III

In the Chapter IV study we successfully red-shifted the $\pi \rightarrow \pi^*$ transition into the visible spectrum, in order to inactivate the siRNAs with non-toxic red light. This was an improvement over the non-halogenated azobenzene in two ways: 1) we could keep the red light on the cells in order to keep the siRNA inactive for up to 24 h; 2) red light is low energy and non-toxic. While these properties were greatly improved over the original siRNAs, we were actually limited by the incredibly short half-life of the chlorinated azobenzene, which is less than 2 min at 37 °C. While we overcame this fast reactivation by simply keeping the cell culture under the red light, having to keep it exposed to red light is limiting. The short half life is due to the size of the chlorine atoms, which forces the *cis* conformer out of plane and causes the quick relaxation back to *trans*. To overcome this flaw in the azobenzene derivative, a visiting researcher from Japan, Kota Tsubaki, designed and synthesized a tetra-fluorinated azobenzene derivative. Due to the smaller size of the fluorine atom and its high electronegativity, we hypothesized that a red-shifted tetra-fluorinated azobenzene derivative would have a much longer half-life. In the literature, fluorinated azobenzene derivatives have been shown to have a predicted *cis* half-life of up to 2 years in the dark at room temperature. Thus, we synthesized the tetra-fluorinated azobenzene (Az2-4F) derivative and then incorporated it into our siRNA system and proceeded to do the bio-physical characterizations and biological testing on the tetra-fluorinated azobenzene from the siRNA we synthesized from it. Interestingly, due to the new modifications at the *ortho* (Cl \rightarrow F) and *para* (CH₂ \rightarrow O=C-NH-) positions, red light in the 620 nm range did not have the same high efficacy that it did with the tetra-chlorinated azobenzene. Alternately, green light in the 535 nm range was the most effective at inducing

trans→*cis* isomerization, and this came with the benefit of a more stable *cis* conformer half-life. Our results are presented in the next chapter.

Chapter 5: Preparation Manuscript IV- Synthesis,
Derivatization and Photochemical Control of
ortho-Functionalized Tetra-fluorinated
Azobenzene-Modified siRNAs

Matthew L. Hammill, Kota Tsubaki, Estelle Wang and Jean-Paul Desaulniers*

Published in

In preparation

5.1 Introduction

The discovery of the RNA interference (RNAi) mechanism by Fire and Mello in 1998 has developed into several significant fields of study, mostly focused on gene-silencing, but also on the control and utilization of the pathway for therapeutic benefits.¹ The endogenous pathway they discovered utilizes double-stranded RNA (dsRNA) to control gene expression and as defenses against viruses. Through this highly robust and target specific pathway, researchers have been developing therapeutics and bio-molecular tools to take advantage of RNAi.²⁻⁴ siRNA based therapeutics are rare, and currently there are only three, with one fast tracked for approval most recently, which are US-FDA approved for use against rare, untreatable diseases. Onpatro, the originally approved therapeutic, treats hereditary transthyretin amyloidosis (hATTR)⁵. More recently, Givlaari which targets acute hepatic porphyria, was also approved for use.⁶ Both of these were landmark approvals, since prior to this, most siRNAs would fail clinical trials for a multitude of reasons.⁷ Lumasiran is the third approved siRNA from Alnylam, and it targets primary hyperoxaluria type 1 (PH1). This is a rare genetic disease caused by overproduction of oxalate in hepatic tissues and the symptoms range from kidney stones, nephrocalcinosis to kidney failure.⁸ The most recent siRNA therapeutic fast tracked for approval is Vutrisiran, targeting transthyretin (TTR)-mediated amyloidosis.⁹ Poor stability, toxicity, off-target effects and tissue specific targeting still plague siRNAs as therapeutics. A way to overcome this limitations is through chemical adaptation and modification, improving the properties of the siRNA to increase its viability leading to increased clinical trial successes. Designing the siRNA so that its activity can be controlled after deployment with small molecules such as aptamers or ideally, non-invasive light exposures are constantly being explored by researchers. Photoresponsive functional groups are one way to control activity. The

advancing field of photo-controlled siRNAs have been showing promise, but many improvements are still needed to be explored. Here, we push the boundaries of the current knowledge through the synthesis, characterization and biological testing of tetra *ortho*-fluorinated azobenzenes that are introduced into the anti-sense (guide strand) of an siRNA duplex. These tetra *ortho*-fluorinated azobenzene containing units are named fluorinated siRNAzOs (F-siRNAzOs).

In the last decade, photoresponsive siRNAs as a field has expanded rapidly, incorporating several strategies to improve siRNA's therapeutic properties. These have been mostly focused on inactivated payload siRNAs, which are inactive siRNAs which are deployed and then activated at a later time with ultraviolet (UV) light inside the target. Freidman and his team utilized a nitrobenzene derivative attached to the siRNA phosphodiester backbone directly via a phosphonate linkage. Exposure to 320 nm UV light removes this nitrobenzene through light mediated cleavage and activates the payload siRNA.¹⁰ UV-mediated cleavable groups are utilized in several different ways, such as Mikat and Heckel's modification of thymidine and guanine. Through modification, they created a bulge in the RNA induced silencing complex (RISC) active site which made the siRNA uncleavable and thus inactive. Exposure to UV light cleaves the bulge-inducing groups and allows for RISC activation.¹¹ A more recent development by Mokhir and Meyer utilized a 5'-labelled alkoxyanthracenyl siRNA, which becomes uncaged through singlet oxygen (¹O₂) generation by a photo-regenerated photosensitizer on the 3'-end of the guide (anti-sense) strand. The cage is removed with red or green light, and yields the active siRNA.¹² These leading edge modifications are innovative, however, they are limited in a single regard, in that they are *irreversibly* uncaged through photo-activation and they cannot be returned the

previously inactive state. In addition, photocages may also release chemical cleavage products which have unknown effects on the targeted tissues and surrounding area. There is therefore a need for a *reversible*, non-cleavable siRNA that can be photocontrolled. Such a molecule would advance the photo-switchable siRNA field even further towards the ideal therapeutic which minimizes off target effects through non-invasive light control.

All of the properties we are looking for, to move ever closer to the ideal therapeutic can be achieved with azobenzenes, due to its large conformational changes when exposed to differing wavelengths of light. These large changes have been shown to disrupt biomolecular secondary structures like duplexes.¹³

The azobenzene molecule itself has a dual nature, consisting of a more stable *trans* conformer, and when exposed to high energy UV light (330-360 nm) goes through an intramolecular conformational change to the *cis* conformer. Because of sterics, the *cis* conformer is strained out of plane with the N=N bond, allowing for the use of lower energy broad band visible light (<450 nm) to convert it back to the more stable *trans* isomer.¹⁴ Another unique property of azobenzene is its modularity. It can be chemically modified to change its properties to suit the application, such as its incorporation into oligonucleotides (See Figure 5.1), is relatively easy to synthesize and has a high quantum yield for photoswitching.¹⁵

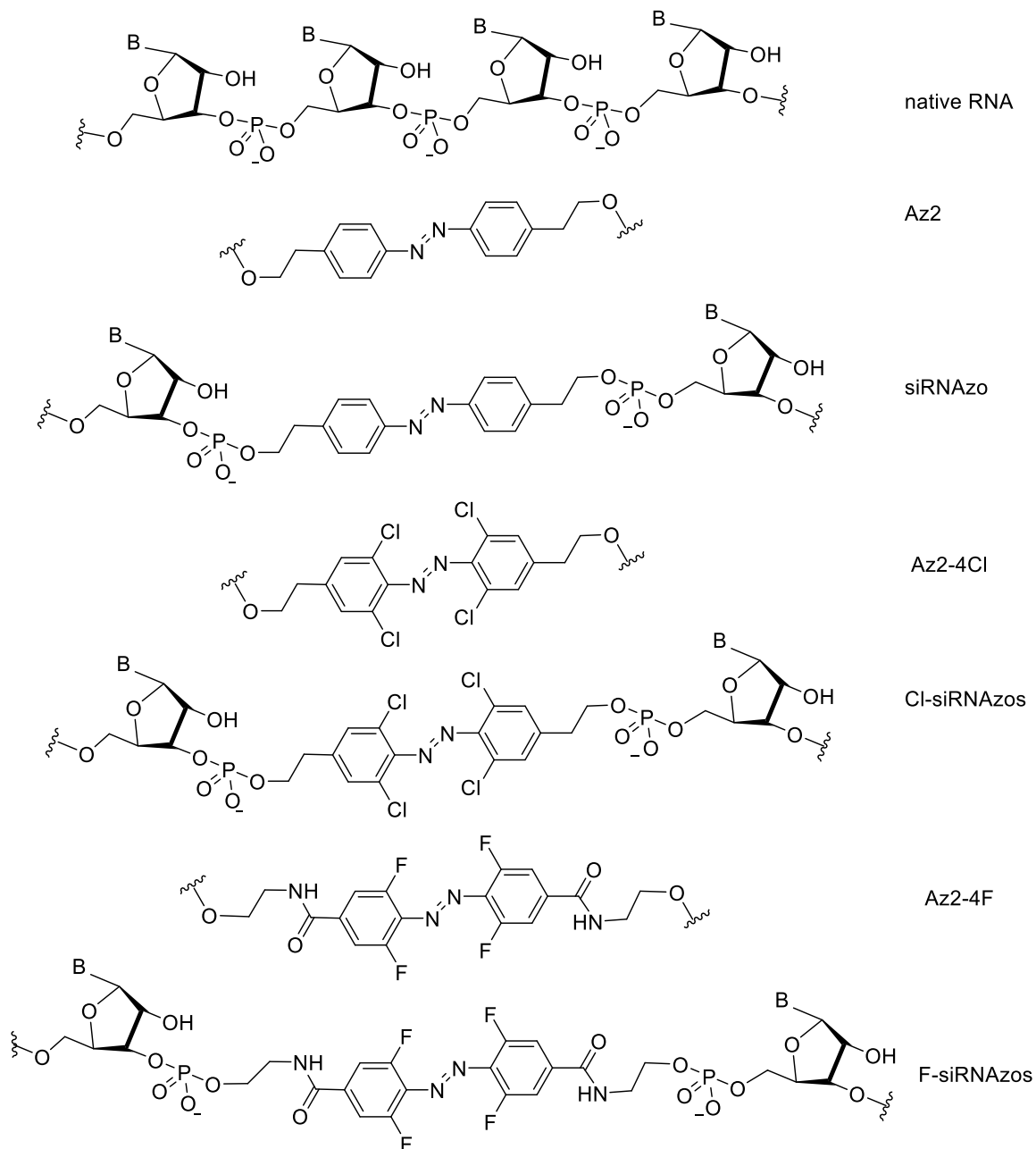


Figure 5.1. Structural differences between native RNA, and azobenzene-containing RNAs (siRNAzos). Az2 and Cl-Az2 corresponds to the azobenzene units synthesized and used by our laboratory in previous studies¹⁶⁻¹⁹, F-Az2 corresponds to the azobenzene unit used this study.

Our prior studies focused on the photo-isomerization of azobenzene to control the gene silencing ability of siRNAs, which we named siRNAzOs.^{16,17} Additionally, we have made advances in our ability to keep the siRNA inactive for up to 24 h¹⁸, increasing the utility of our system by 4- fold, whereas before reactivation would begin to occur after 8 h, due to the half-life (4 h @ 37 °C) of the *cis* conformer of the azobenzene.²¹ The first iteration of the system,¹⁶ where the siRNA was transfected in the *cis* conformer, inactive form, lacked utility since reactivation would occur over time. Our next advancement allowed us to keep the siRNA inactive for up to 24 h by using carefully controlled doses of UV light *after* transfection, thus preventing reactivation after 12 h due to the short half-life.¹⁸

These advancements were significant towards our goals, but using UV light limits its usefulness due to the photochemical and physical properties of the UV light itself. The main issues of UV light are toxicity from long term exposure, and its high energy which has the potential to cause pyrimidine dimers.²¹ It also has poor penetration into human tissues since skin has evolved to reflect UV light away from deeper more sensitive tissues.²² These become limitations for our photo-controllable system, and our reliance on UV light, while effective, is not ideal for therapeutic use.

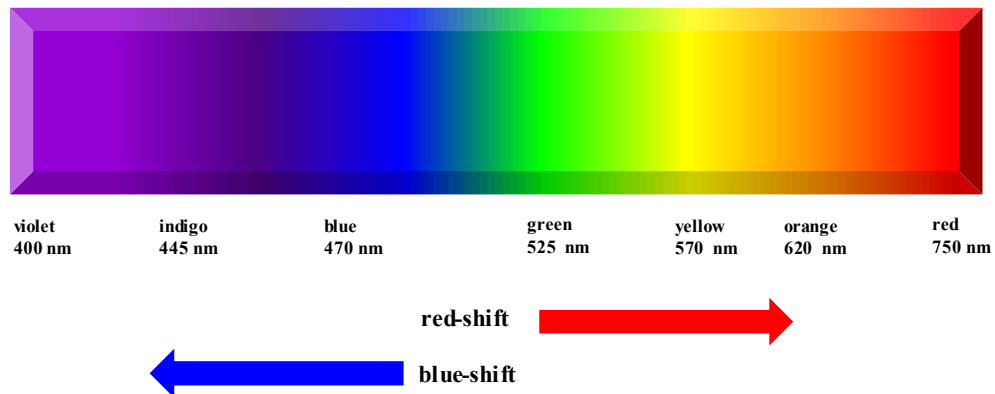


Figure 5.2. Visible wavelengths of the electromagnetic spectrum. Movement towards the right indicates a red-shift, while the opposite direction results in a blue-shift of the wavelengths.

Red-shifting the wavelength means moving it from its current position λ_X , towards the right (increasing wavelength) into the lower frequency and energy portion of the spectrum resulting in $\lambda_{X+\text{shift}}$. In a similar fashion, moving left (decreasing wavelength) into the higher energy and frequency portion of the spectrum results in a blue-shift, or $\lambda_{X-\text{shift}}$ (See Figure 5.2). These terms are not related to the actual colour of the final wavelength. For example, a change from blue to green wavelengths is a red-shift, while a change from orange to green wavelength is a blue-shift.

Research into light penetration by Bashford and co-workers show that the depth of ingress into human tissues is determined by wavelength but significantly, also light beam intensity and width.²³ In their study, they reported that higher wavelength light gets deeper penetration through tissues. Red light penetrates to a depth of 5 mm, with maximum penetration occurring with a beam at least 10 mm wide, while UV gets less than 0.2 mm

depth.²³ Because of these properties, visible light is a better choice than UV, and where possible its utilization should be made a priority in order to access deeper embedded tissues, since most therapeutics do not target the surface of the skin. One way to red-shift the $\pi \rightarrow \pi^*$ transition of the N=N bond is through chemical modification of the *ortho* positions, which strains the π bond and allows low energy red light to cause the *trans* to *cis* isomerization.

Feringa and his research group developed red-shifted azobenzene derivatives by chlorinating or fluorinating the *ortho* positions. These were modified antibiotics that were able to control microbial activity using red or green light, with high activity and reversibility.²⁴ There exist multiple other instances of photo-responsive control of nucleoside or oligonucleotide derivatives under visible light which showed effective switching ability.²⁵⁻²⁸ Other modifications at the *ortho* positions include not only halogens, such as fluorine and chlorine, but thiols, methoxy substituents, and amino containing groups like morpholino and amines.²⁹⁻³¹ An issue that develops as these azobenzenes become more red-shifted is that the *cis* half-life becomes more unstable the more red-shifted it becomes.³² This unintentional consequence of moving into longer wavelengths however is highly dependent on the specific functional groups in the *ortho* positions of the azobenzene. This is prevalent with chlorine atoms in the *ortho* position, which due to their size causes large strain on the *cis* conformer and results in a very short half-life.³³

One issue with extending the isomerization point in the longer wavelength area of the spectrum is that these *cis* conformers can become increasingly unstable as they become more red-shifted.³² However, this is highly dependent on the modification, as shown with *ortho*-functionalized tetra-substituted chlorines being very unstable in the *cis* conformer.³³

Trauner and co-workers have developed a novel synthesis system for the late stage functionalization of azobenzenes, by adding chlorinated substituents after the N=N bond has formed, as opposed to modifying the *ortho* position before the dimerization.³⁴ Utilizing the late stage chlorination procedure, we developed our own tetra-chlorinated siRNAzOs, and were able to inactivate the RISC complex with red light. We were able to keep the siRNA inactive for up to 24 h, but were plagued by the short half-life of the *cis* conformer (< 2min at 37 °C).¹⁹ This was still an overall improvement, since we were no longer subjected to the toxicity and high energy of UV light. Because of this, while the length of the half-life was not desirable, we simply kept the red light on the cell culture for the entire 24 h assay. Since it was low energy and non-toxic, we were not strictly limited by the half-life, but it having to keep the light in place for the entire assay is more limiting than we would like. Hecht and co-workers however, reported that the synthesis of tetra-fluorinated azobenzene derivatives, in the *ortho* position, was incredibly stable, and depending on the specific azobenzene molecule, had a calculated *cis* conformer half-life of up to two years, in the dark.³³

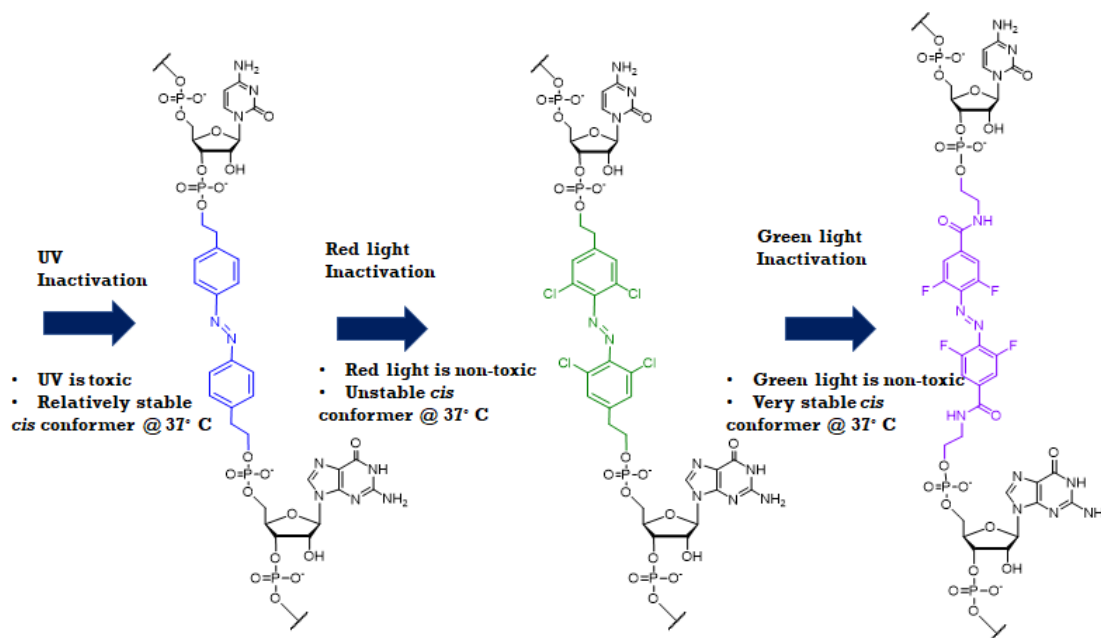


Figure 5.3. Structural and physical property differences between native RNA, and azobenzene-containing RNAs (siRNAzOs). From left to right, Az2, Az2-4Cl and Az2-4F are shown along with the improvements over each previous siRNAzo.

As a result, we report here the chemical synthesis of an *ortho*-functionalized tetra-fluorinated azobenzene diol. From the diol, a dimethoxytrityl (DMT)-phosphoramidite of the fluorinated azobenzene was synthesized for its incorporation into the siRNAs using solid-phase chemistry to generate red-shifted tetra *ortho*-fluorinated azobenzene-containing siRNAs (F-siRNAzOs). Figure 5.3 shows the progression of useful properties as we further modify the azobenzene core to get the desired tunability for our system. Each iteration improves a desired property (red-shifted, increased *cis* half life). We then tested these red-shifted F-siRNAzOs in cell culture and were able to control the activity of the F-siRNAzo by using green light (535 nm) to convert from *trans* to *cis* and used blue light (470 nm) relaxation to revert from *cis* to *trans*.

5.2 Materials and Methods

5.2.1 General Methods

Unless otherwise indicated all starting reagents used were obtained from commercial sources without additional purification. Anhydrous CH_2Cl_2 and THF were purchased from Sigma-Aldrich and run through a PureSolv 400 solvent purification system to maintain purity. Flash column chromatography was performed with Silicycle Siliaflash 60 (230-400 mesh), using the procedure developed by Still, Kahn and Mitra.⁴¹ NMRs were performed on a Varian 400 MHz spectrophotometer. All ^1H NMRs were recorded for 64 transients at 400 MHz and all ^{13}C NMRs were run for 1500 transients at 101 MHz and all ^{31}P NMRs were recorded for 256 transients at 167 MHz. Spectra were processed and integrated using ACD labs NMR Processor Academic Edition. 2,6 difluoroaniline (compound **1**) was purchased from TCI chemicals and used without further purification.

5.2.2 Synthesis of 4-bromo-2,6-difluoroaniline- Compound (**2**)

To a solution of 2,6-difluoroaniline **1** (12.9 g, 100 mmol) in acetonitrile (200 ml) was added NBS (17.8 g 100 mmol) at room temperature. The mixture was stirred for 22 h, and then diluted with water and hexanes. The organic phase was dried over Na_2SO_4 , filtered, and concentrated under reduced pressure. The crude residue was purified by column chromatography (DCM / hexanes = 1 / 1) to give 2,6-difluoro-4-bromoaniline **2** as a brown solid. (15.9 g, 76 %), ^1H NMR (400 MHz, CDCl_3) δ 6.99 (dd, $^3J_{\text{H,F}} = 6.4$ Hz, $J = 1.4$ Hz, 2H), 3.71 (br, 2H). ^{13}C NMR (100 MHz, CDCl_3) δ 151.74 (dd, $^1J_{\text{C,F}} = 243$ Hz, $J = 8.7$ Hz), 123.60 (t, $^3J_{\text{C,F}} = 16.0$ Hz), 114.73 (dd, $^2J_{\text{C,F}} = 16.8$ Hz, $^4J_{\text{C,F}} = 8.7$ Hz), 107.07 (t, $^2J_{\text{C,F}} = 11.6$ Hz). ^{19}F NMR (470 MHz, CDCl_3 , Internal standard: Hexafluorobenzene) δ 31.03 (d, $J = 6.5$ Hz). IR (ATR) 3422, 3325, 3197, 3092, 1696, 1642, 1604, 1583, 1497, 1427, 1298,

1241, 1217, 1150, 963, 869, 869, 839, 760, 717 cm^{-1} . HRMS (ESI) calcd for $\text{C}_6\text{H}_5\text{Br}_1\text{F}_2\text{N}_1$ $(\text{M}+\text{H})^+$ 207.95, found 207.95.

5.2.3 Synthesis of 4-amino-3,5-difluorobenzonitrile-Compound (3)

To a solution of 2,6-difluoroaniline **2** (1.78 g, 8.6 mmol) in DMF (15 ml) was added CuCN (2.3 g, 26 mmol). The mixture was refluxed for 18 h. A lot of solids precipitated by adding a NH_3 12 % aqueous solution. After filtering out solids, organic layer was separated by EtOAc, dried over Na_2SO_4 , filtered, and concentrated under reduced pressure. The crude product was purified by column chromatography (DCM / hexanes = 1 / 1) to give 4-amino-3,5-difluorobenzonitrile **3** as a white solid. (932 mg, 70 %). ^1H NMR (400 MHz, CDCl_3) δ 7.14 (dd, $^3J_{\text{H,F}} = 6.2$ Hz, $J = 1.5$ Hz, 2H), 4.28 (br, 2H), ^{13}C NMR (100 MHz, CDCl_3) 150.5 (dd, $J_{\text{C,F}} = 242$ Hz, $^3J_{\text{C,F}} = 8.8$ Hz), 129.6 (t, $J = 15.6$ Hz), 117.9, 115.4 (dd, $^2J_{\text{C,F}} = 16.0$ Hz, $^4J_{\text{C,F}} = 8.6$ Hz), 98.3 (t, $J = 11.0$ Hz). ^{19}F NMR (470 MHz, CDCl_3 , Internal standard: Hexafluorobenzene) δ 30.96 (d, $J = 7.6$ Hz). IR (ATR) 3481, 3362, 3229, 2228, 1637, 1576, 1428, 1444, 1349, 1277, 1144, 970, 865, 775, 725, 674 cm^{-1} . HRMS (ESI) calcd for $\text{C}_7\text{H}_4\text{F}_2\text{N}_2$ (M) 154.03, found 154.03.

5.2.4 Synthesis of 4-amino-3,5-difluorobenzoic acid -Compound (4)

4-amino-3,5-difluorobenzonitrile **3** was suspended in 1M NaOH aqueous solution () and refluxed for 16 h. After confirming disappearance of starting material by TLC (DCM / Hexanes = 1 / 1), the reaction was quenched by addition of 1M HCl until salts precipitate. The salts were then dissolved in EtOAc. The organic layer was dried over Na_2SO_4 , filtered, and concentrated under reduced pressure. the resulting orange solid was used in the next

step without further purifications. ^1H NMR (400 MHz, DMSO- d_6) δ 12.65 (br, 1H), 7.38 (dd, $^3J_{\text{H,F}} = 7.1$ Hz, $J = 2.0$ Hz, 2H), 3.34 (br, 3H).

5.2.5 Synthesis of 4-amino-N-(2-((tert-butyldimethylsilyl)oxy)ethyl)-3,5-difluorobenzamide -Compound (5)

A mixture of 4-amino-3,5-difluorobenzoic acid **4** (1.11 g, 5.3 mmol), 2-((tert-Butyldimethylsilyl)oxy) ethanolamine (1.12 g, 6.4 mmol), HOBT (81 mg, 0.6 mmol) and EDC \cdot HCl (1.22 g, 6.4 mmol) was stirred at room temperature for 21 h. The reaction mixture was dissolved in AcOEt, and then washed with water. The organic layer was dried over Na_2SO_4 , filtered, and concentrated under reduced pressure. The residue was purified by column chromatography (AcOEt / Hexanes = 1 / 2) to give the target product **5** as a white solid (1.77 g, 93 % from 6.27 mmol of 4-amino-3,5-difluorobenzonitrile **4**), ^1H NMR (400 MHz, CDCl_3) δ 7.27 (d, $^3J_{\text{H,F}} = 8.92$ Hz, 2H), 6.35 (br, 1H), 3.77 (t, $J = 5.1$ Hz, 2H), 3.54 (q, $J = 5.2$ Hz, 2H), 0.91 (s, 9H), 0.08 (s, 6H), ^{13}C NMR (100 MHz, CDCl_3) δ 165.2, 151.0 (dd, $^1J_{\text{C,F}} = 240$ Hz, $^3J_{\text{C,F}} = 7.9$ Hz), 127.2 (t, $J = 16.0$ Hz), 122.8 (t, $J = 7.3$ Hz), 110.0 (dd, $^2J_{\text{C,F}} = 15.0$ Hz, $^4J_{\text{C,F}} = 7.6$ Hz), 61.7, 42.1, 25.8, 18.2, -5.3. ^{19}F NMR (470 MHz, CDCl_3 , Internal standard: Hexafluorobenzene) δ 29.75 (d, $J = 7.4$ Hz). IR (ATR) 3480, 3359, 3282, 3200, 2951, 2928, 2857, 1645, 1618, 1578, 1511, 1462, 1338, 1298, 1254, 1988, 931, 829, 779 cm^{-1} . HRMS (ESI) calcd for $\text{C}_{15}\text{H}_{24}\text{F}_2\text{N}_2\text{Na}_1\text{O}_2\text{Si}_1$ ($\text{M}+\text{Na}$) $^+$ 353.14, found 353.14.

5.2.6 Synthesis of (E)-4,4'-(diazene-1,2-diyl)bis(N-(2-((tert-butyl)dimethylsilyloxy)ethyl)-3,5-difluorobenzamide) -Compound (6)

To a prepared dry ice bath with acetone at -78°C , 4-amino-N-(2-((tert-butyl)dimethylsilyloxy)ethyl)-3,5-difluorobenzamide (compound **5**) (0.12g, 3.6 mmol) was dissolved in 5 mL DCM. DBU (0.11g, 7.2 mmol) was added to the solution and stirred at -78°C for 20 minutes. NaHCO_3 solution (15 ml) was added to the solution, then the washed with water three times. Collected the organic layer and dried under reduced pressure. The crude product was purified with column chromatography (1:2 EtOAc : hexanes) to give a orange solid. (0.20g, 84%). ^1H NMR (400 MHz, CDCl_3) δ 7.48 (d, $^3J_{\text{H,F}} = 9.2$ Hz, 4H), 6.57 (t, $J = 5.2$ Hz, 2H), 3.83 (t, $J = 4.8$ Hz, 4H), 3.61 (q, $J = 5.2$ Hz, 4H), 0.94 (s, 18H), 0.12 (s, 12H), ^{13}C NMR (100 MHz, CDCl_3) δ 164.0, 155.6 (d, $J=203.75$ Hz), 138.0 (t, $J = 8.33$ Hz), 133.1 (s), 111.3 (dd, $^2J_{\text{C,F}} = 22.43$ Hz, $^4J_{\text{C,F}} = 2.88$ Hz), 61.4, 42.3, 25.8, 18.2, -5.3. ^{19}F NMR (470 MHz, CDCl_3 , Internal standard: Hexafluorobenzene) (E isomer) δ 43.11 (d, $J = 9.3$ Hz). IR (ATR) 3271, 3085, 2929, 2853, 1719, 1638, 1547, 1472, 1427, 1340, 1250, 1203, 1124, 1097, 934, 828, 689 cm^{-1} . HRMS (ESI) calcd for $\text{C}_{30}\text{H}_{44}\text{F}_4\text{N}_4\text{Na}_1\text{O}_4\text{Si}_2$ ($\text{M}+\text{Na}$) $^+$ 679.27, found 679.27.

5.2.7 Synthesis of (E)-4,4'-(diazene-1,2-diyl)bis(3,5-difluoro-N-(2-hydroxyethyl)benzamide) Compound (7)

To a solution of azobenzene **6** (1.21 g, 1.84 mmol) dissolved in 10 ml of EtOH was 1% of HCl in EtOH (10 ml) at room temperature. The reaction mixture was stirred under argon for 3 h and then, EtOH and HCl were removed under reduced pressure. The solid was dissolved in MeOH, washed with hexane and concentrated under reduced pressure to give target diol **13** as a brown solid. (790 mg, 100 %) ^1H NMR (400 MHz, DMSO-d_6) 8.83 (t,

$J = 5.5$ Hz, 2H), 7.84 (d, $^3J_{\text{H,F}} = 10.2$ Hz, 4H), 3.55 (t, $J = 6.0$ Hz, 3H), 3.36 (q, $J = 5.7$ Hz, 2H), 3.36 (br, 2H). ^{13}C NMR (126 MHz, CDCl_3) (E isomer) δ 162.9, 154.3 (dd, $J = 260.7$, 4.0 Hz), 138.5 (t, $J = 2.6$ Hz), 131.8 (t, $J = 2.6$ Hz), 112.1 (dd, $J = 21.8$, 2.8 Hz), 59.4. ^{19}F NMR (470 MHz, CDCl_3 , Internal standard: Hexafluorobenzene) (E isomer) δ 42.39 (d, $J = 10.7$ Hz). IR (ATR) 3326, 3075, 2938, 2882, 1639, 1546, 1432, 1364, 1336, 1275, 1210, 1132, 884, 725 cm^{-1} . HRMS (ESI) calcd for $\text{C}_{18}\text{H}_{16}\text{F}_4\text{N}_4\text{Na}_1\text{O}_4$ ($\text{M}+\text{Na}$) $^+$ 451.10, found 451.10.

5.2.8 Synthesis of (E)-N-(2-(bis(4-methoxyphenyl)(phenyl)methoxy)ethyl)-4-((2,6-difluoro-4-((2-hydroxyethyl)carbamoyl)phenyl)diazenyl)-3,5-difluorobenzamide— Compound (8)

To a solution of anhydrous pyridine 5.0 mL 0.20 g of compound **7** (0.46 mmol, 1.00 equiv.) was added and stirred until fully dissolved. To the solution 0.158 g of 4,4'-dimethoxytrityl chloride (0.47 mmol, 1.00 equiv.) The reaction mixture was stirred vigorously overnight and monitored by TLC. The crude reaction was then concentrated by rotovap and purified on silica gel column using MeOH (5% to 10%) in CH_2Cl_2 to afford compound **8** as a dark red oil (0.341 g, 58%). ^1H NMR (500 MHz, CDCl_3) (E isomer) δ 7.28-7.17 (m, 13H), 6.88 (t, $J = 5.3$ Hz, 1H), 6.84-6.81 (m, 4H), 6.47 (t, $J = 5.4$ Hz, 1H), 3.87-3.84 (m, 2H), 3.77 (s, 6H), 3.66-3.61 (m, 4H), 3.41 (t, $J = 5.0$ Hz, 2H). ^{13}C NMR (126 MHz, CDCl_3) (E isomer) δ 164.8, 164.2, 158.6, 158.5, 155.2 (dd, $J = 264.4$, 3.8 Hz), 144.5, 137.9 (t, $J = 8.6$ Hz), 137.6 (t, $J = 8.6$ Hz), 135.7, 133.0 (t, $J = 10.0$ Hz), 129.9, 127.9, 127.9, 127.0, 113.2, 111.7-111.3 (m), 86.4, 61.7, 61.7, 61.6, 55.2, 55.2. ^{19}F NMR (470 MHz, CDCl_3 , Internal standard: Hexafluorobenzene) (E isomer) δ 43.25 (d, $J = 9.3$ Hz), 43.21 (d, $J = 9.4$ Hz). IR (ATR) 3296, 3064, 2933, 1643, 1607, 1570, 1541, 1507, 1427, 1334,

1300, 1247, 1218, 1174, 1032, 876, 826, 750, 701 cm^{-1} . HRMS (ESI) calcd for $\text{C}_{39}\text{H}_{34}\text{F}_4\text{N}_4\text{Na}_1\text{O}_6$ ($\text{M}+\text{Na}$)⁺ 753.23, found 753.23.

5.2.9 Synthesis of (E)-2-(4-((4-((2-(bis(4-methoxyphenyl)(phenyl)methoxy)ethyl)carbamoyl)-2,6-difluorophenyl)diazanyl)-3,5-difluorobenzamido)ethyl (2-cyanoethyl) diisopropylphosphoramidite-Compound (9)

To a solution of 5.00 mL of anhydrous THF 0.22 g of compound **8** (0.30 mmol, 1.00 equiv.) was added to a flame dried flask. To that solution 0.419 mL of anhydrous triethylamine (5.7 mmol, 10.0 equiv.) was added along with 0.45 mL of 2-cyanoethyl *N,N*-diisopropylchlorophosphoramidite with (1.91 mmol, 3.00 equiv.) and stirred at room temperature until TLC showed starting materials were consumed (2 h). After rotary evaporation, the compound was then purified on silica gel using a 86%:10%:4% acetone/ethyl acetate/triethylamine mobile phase. This afforded compound **9** as a dark red oil (0.15 g, 58%). ¹H NMR (400 MHz, CDCl_3) δ ppm 7.44- 7.30 (m, 13H), 7.18 (d, $J=9.05$ Hz, 2H), 6.78 - 6.87 (m, 4H), 3.78 - 3.80 (m, 6H), 3.66-3.61 (m, 4H), 2.16 - 2.20 (m, 4H), 1.17 - 1.24 (m, 12H). ³¹P NMR (162 MHz, CDCl_3) δ ppm 148.45 (s, 1 P).

5.2.10 Procedure for Oligonucleotide Synthesis and Purification

All standard β -cyanoethyl 2'-*O*-TBDMS protected phosphoramidites, reagents and solid supports were purchased from Chemgenes Corporation and Glen Research. Wild-type luciferase strands including the sense and 5'-phosphorylated antisense strand were synthesized. All commercial phosphoramidites were dissolved in anhydrous acetonitrile to a concentration of 0.10 M. The chemically synthesized (azobenzene derivative)

phosphoramidites were dissolved in 3:1 (v/v) acetonitrile:THF (anhydrous) to a concentration of 0.10 M. The reagents that were used for the phosphoramidite coupling cycle were: acetic anhydride/pyridine/THF (Cap A), 16% *N*-methylimidazole in THF (Cap B), 0.25 M 5-ethylthio tetrazole in ACN (activator), 0.02 M iodine/pyridine/H₂O/THF (oxidation solution), and 3% trichloroacetic acid/dichloromethane. All sequences were synthesized on 0.20 μM or 1.00 μM dT solid supports except for sequences that were 3'-modified, which were synthesized on 1.00 μM Universal III solid supports. The entire synthesis ran on an Applied Biosystems 394 DNA/RNA synthesizer using 0.20 μM or 1.00 μM cycles kept under argon at 55 psi. Standard and synthetic phosphoramidites ran with coupling times of 999 seconds.

Antisense sequences were chemically phosphorylated at the 5'-end by using 2-[2-(4,4'-dimethoxytrityloxy)ethylsulfonyl]ethyl-(2-cyanoethyl)-(N,N-diisopropyl)-phosphoramidite. At the end of every cycle, the columns were removed from the synthesizer, dried with a stream of argon gas, sealed and stored at 4 °C. Cleavage of oligonucleotides from their solid supports was performed through on-column exposure to 1.50 mL of EMAM (methylamine 40% wt. in H₂O and methylamine 33% wt. in ethanol, 1:1 (Sigma-Aldrich)) for 1 hour at room temperature with the solution in full contact with the controlled pore glass. The oligonucleotides were then incubated overnight at room temperature in EMAM to deprotect the bases. On the following day, the samples were concentrated on a Speedvac evaporator overnight, resuspended in a solution of DMSO:3HF/TEA (100 μL:125 μL) and incubated at 65 °C for 3 hours in order to remove the 2'-*O*-TDBMS protecting groups. Crude oligonucleotides were precipitated in EtOH and desalted through Millipore Amicon Ultra 3000 MW cellulose. Oligonucleotides were

separated on a 20% acrylamide gel and were used without further purification for annealing and transfection. Equimolar amounts of complimentary RNAs were annealed at 95 °C for 2 min in a binding buffer (75.0 mM KCl, 50.0 mM Tris-HCl, 3.00 mM MgCl₂, pH 8.30) and this solution was cooled slowly to room temperature to generate siRNAs used for biological assays. A sodium phosphate buffer (90.0 mM NaCl, 10.0 mM Na₂HPO₄, 1.00 mM EDTA, pH 7.00) was used to anneal strands for biophysical measurements.

5.2.11 Procedure for LC/MS: LC/MS chromatograms were acquired on an Agilent 6545 QTOF-MS with Agilent 1260 Infinity Binary Pump HPLC using a ZORBAX Eclipse Plus C18 2.1x100mm 1.8-Micron Agilent column and a mobile phase of 5 mM ammonium acetate buffer (pH 7)/acetonitrile (95:5). Oligonucleotide samples were prepared at a concentration of 0.01 O.D/μL with an injection volume of 20 μL. Data were analysed using Agilent Technologies MassHunter Workstation Qualitative Analysis Software (Qual. 10.0).

5.2.12 Procedure for Performing CD Experiments

Circular Dichroism (CD) spectroscopy was performed on a Jasco J-815 CD equipped with temperature controller. Equimolar amounts of each siRNA (10 μM) were annealed to their compliment strand in 500 μL of a sodium phosphate buffer by incubating at 95 °C for two minutes and allowing to cool to room temperature. CD measurement of each duplex were recorded in triplicate from 200-500 nm at 25 °C with a screening rate of 20.0 nm/min and a 0.20 nm data pitch. The average of the three replicates was calculated using Jasco's Spectra Manager version 2 software and adjusted against the baseline measurement of the sodium phosphate buffer.

5.2.13 Procedure for Thermal Relaxation Measurements

The AZ2-4F azobenzene diol in DMSO was exposed to 15 min of green light (530 nm) to obtain the *cis* conformer. It was then placed in the Jasco J-815 CD spectropolarimeter and then absorbance was measured 250-500 nm at a temperature of 95 °C. Absorbance was read every 5 min for 30 min to track changes in the absorbance profile. Temperatures (20-60 °C) were left 24 h at the required temperature and then measured. Temperatures (70-90 °C) were measured at various time points to showcase the thermal relaxation. Absorbance was adjusted to baseline by subtracting absorbance of the DMSO.

5.2.14 Procedure for Melting Temperature of siRNA Duplexes (T_m)

The siRNA duplexes annealed as above were placed in the Jasco J-815 CD spectropolarimeter and then UV absorbance was measured at 260 nm against a temperature gradient of 10 °C to 95 °C at a rate of 0.5 °C per minute with absorbance being measured at each 0.5 °C increment. Absorbance was adjusted to baseline by subtracting absorbance of the buffer. The T_m values were calculated using Meltwin v3.5 software. Each siRNA result was the average of 3 independent experiments and the reported values were calculated using Meltwin v3.5 assuming the two-state model.⁴²

5.2.15 Procedure for Absorbance Spectra Experiments

All absorbance spectra measurements were done on a Jasco J-815 CD with temperature controller. Measurement was recorded from 200 -500 nm at 10 °C at least 3 times.

5.2.16 Procedure for HPLC Characterization

HPLC chromatograms were obtained on a Waters 1525 binary HPLC pump with a Waters 2489 UV/Vis detector using the Empower 3 software. A C18 4.6 mm x 150 mm reverse phase column was used. Conditions were 5% acetonitrile in 95% 0.1 M TEAA (Triethylamine-Acetic Acid) buffer up to 100% acetonitrile over 30 min. *Cis* conformers were obtained by green light exposure for at least 15 min (530 nm), and left in the dark for duration of the assay (0 or 72 h).

5.2.17 Procedure for Maintaining Cell Cultures of HeLa Cells

For biological analysis of these siRNAs in a live environment, human epithelial cervix carcinoma cells were used (HeLa cells). They were kept in 250 mL vented culture flasks using 25.0 mL of DMEM with 10% fetal bovine serum and 1% penicillin-streptomycin (Sigma) in an incubator set for 37 °C @ 5% CO₂ humidified atmosphere.

Once cell lines became confluent (80-90%) they were passaged by washing 3 times with 10 mL of phosphate buffered saline (NaCl 137 mM, KCl 2.70 mM, PO₄³⁻ 10.0 mM, pH 7.40) and incubated with 3.00 mL of 0.25% trypsin (SAFC bioscience) for 4 min @ 37 °C to detach the cells. The cells were transferred to a 50.0 mL centrifuge tube after the addition of 10.0 mL of DMEM solution and pelleted at 2000 rpm for 5 minutes. The supernatant was discarded and the pellet resuspended in 5.0 mL DMEM with 10% FBS.

A standard haemocytometer was used to obtain cell counts, after which the cells were diluted to a final concentration of 1.00 x 10⁶ cells/mL for subsequent assays. To continue the cell line 1.00 mL of freshly passaged cells was added to 24.0 mL of

DMEM/10% FBS and 1% penicillin-streptomycin at 37 °C in a new culture flask while the rest were used for assays.

5.2.18 Procedure for siRNA Transfections

100 μ L of cells (total 1.00×10^5) were transfected into 12 well plates (Falcon®) with 1 mL of DMEM (10% FBS, 1% penicillin-streptomycin) and incubated at 37 °C with 5% CO₂. After 24 hours the cells were transfected with various concentrations of siRNAs, along with both pGL3 (Promega) and pRLSV40 luciferase plasmids using Lipofectamine 2000 (Invitrogen) in Gibco's 1X Opti-Mem reduced serum media (Invitrogen) according to the manufacturer's instructions. 1.00 μ L of siRNA was added along with 2.00 μ L (pGL3 200 ng) and 0.50 μ L pRLSV40 (50.0 ng) to 100 μ L of 1X Opti-Mem in a microcentrifuge tube and kept on ice for 5 min. In a different microcentrifuge tube 1.00 μ L of Lipofectamine 2000 (Invitrogen) was mixed with 100 μ L of Gibco's 1X Opti-Mem reduced serum media (Invitrogen) and incubated at room temperature for 5 min. After 5 minutes the tubes were mixed and incubated at room temperature for 20 min and then the entire contents transferred to the wells of the 12 well plate.

5.2.19 Procedure for *in vitro* Dual-Reporter Luciferase Assay

100 μ L of cells (total of 1.00×10^5 cells) were added to 12 well plates (Falcon®) with 1 mL of growth media (DMEM 10% FBS, 1% penicillin-streptomycin) and incubated at 37 °C with 5% CO₂. After 24 hours the cells were transfected with 8.00, 20.0, 40.0, 160, 400 and 800 pM concentrations of siRNAs, along with both pGL3 (Promega) and pRLSV40 luciferase plasmids using Lipofectamine 2000 (Invitrogen) in Gibco's 1X Opti-Mem reduced serum media (Invitrogen) according to the manufacturer's instructions. After a set

amount of time (24, 48 or 72 h) the cells were incubated at room temperature in 1X passive lysis buffer (Promega) for 20 minutes. The lysates were collected and loaded onto a 96 well, opaque plate (Costar). With a Dual-Luciferase reporter Assay kit (Promega), Lar II and Stop & Glo® luciferase substrates were sequentially added to the lysates and enzyme activity was measured through luminescence of both *firefly/Renilla* luciferase on a Synergy HT (Bio-Tek) plate luminometer. The ratio of *firefly/Renilla* luminescence is expressed as a percentage of reduction in *firefly* protein expression to siRNA efficacy when compared to untreated controls. Each value is the average of at least 3 different experiments with standard deviation indicated.

5.2.20 Procedure for Light Inactivation of Azobenzene Modified siRNA (*trans* to *cis*)

Cell culture was exposed to green wavelength light (530 nm) from time 0 h for 1 h. The light was then removed and the assay left for the duration of 24, 48,72 hours. The lamp used was a 4.0 Watt discrete green LED wavelength 530 nm, held directly above the cell culture plates to maximize green light exposure.

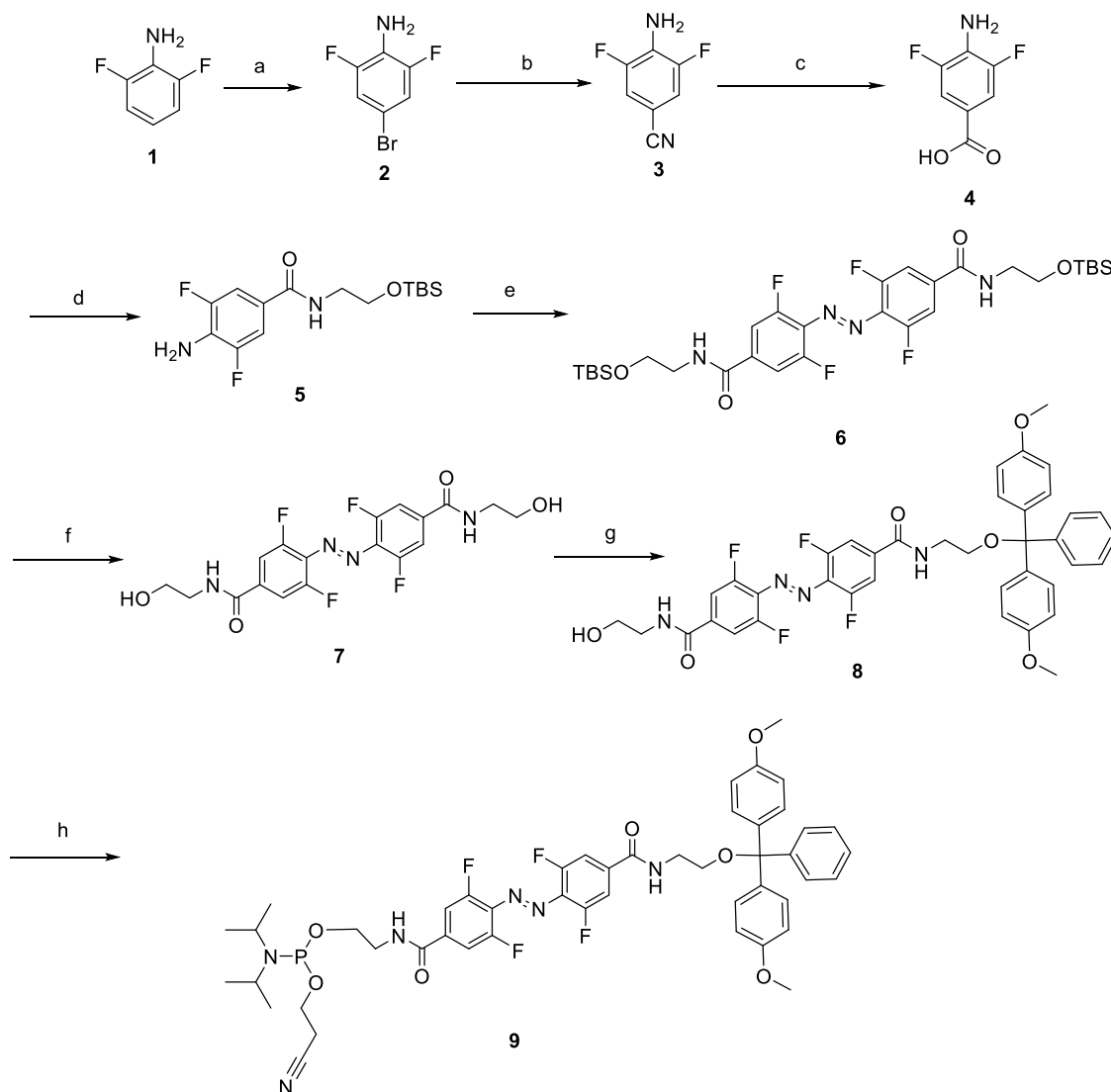
5.2.21 Procedure for Thermal Relaxation and Reactivation of Azobenzene Modified siRNA (*cis* to *trans*)

Immediately following transfection, cell culture was exposed to green wavelength light (530 nm) from time 0 h for 1 h as above, which was then removed 1 hour post transfection. Using a 4.0 Watt blue LED, 470 nm wavelength 3 hours post transfection for 1 h to reactivate the siRNA to the active form. The cells were then lysed and luminescence measured as above in the luciferase assay.

5.2.22 Procedure for consecutive Green/Blue Light Cycling (1.5x and 2x light cycling)

The first cycle was performed normally: green light inactivation at time 0 hours, for 1 hour, and then blue light reactivation at time point 2 hours for 1 hour. We then re-exposed cells to green light at time 24 hours (1.5x, 2 green and 1 blue exposures total. Both 48 and 72 h endpoints) to keep the siRNA inactive. The 2x procedure was identical except after the second green exposure, blue light was re-administered to reactivate the siRNA (2x, 2 green and 2 blue exposures total. Both 48 and 72 h endpoints).

5.3 Results



Scheme 5.1. Synthesis of an *ortho*-functionalized tetrafluorinated azobenzene DMT-phosphoramidite: (a) 1 equiv. NBS in ACN, r.t, 22 h, 95% (**2**); (b) 3 eq CuCN, reflux 18 h, in DMF, 88% (**3**); (c) 1M NaOH, reflux 16 h, add 1M HCl, 84% (**4**); (d) 1.2 eq. ethanolamine, 0.8 eq HOBt, 1 eq EDC-Cl, r.t, 21 h 93% (**5**); (e) 2eq. DBU, -78 °C, 20 min, add 15 mL NaHCO₃, 84% (**6**); (f) 1% HCl in EtOH, r.t, 3 h 100% (**7**); (g) 1 equiv. dimethoxytrityl chloride (DMT-Cl), in anh. pyridine, r.t., o/n 58% (**8**); (h) 3 equiv. 2-

cianoethyl *N,N*-diisopropylchlorophosphoramidite, 10 equiv. TEA, anhydrous THF, r.t. 2h, 58% (**9**).

Our hypothesis was that the fluorinated azobenzene, in the *cis* form, would distort the siRNA helix, thus rendering it non-functional in a similar manner to our previous research, without the use of toxic UV light, but with the added benefit of a stable *cis* conformer (see Figure 5.4). Controlling the timing of activation of an siRNA with minimal amounts of light exposure would make the system more practical in a clinical setting.

The synthesis starts with 2,6 difluoroaniline, which brominated at the para position with N-bromo-succinimide (NBS) to afford compound **2** in 95% yield. The next step replaced the bromine with cyanide group, using CuCN as the donating compound, to afford compound **3** in 88% yield. The copper cyanide is very dangerous and care must be taken to ensure that is always in a basic solution otherwise hydrogen cyanide (HCN) gas can form. After refluxing **3** in 1 M NaOH for 16 h and then precipitating it out with 1 M HCl, compound **4** was generated in 84% yield. Next, compound **4** was reacted with ethanolamine, EDC-Cl and HOBt to afford compound **5**. Using DBU as a coupling reagent, compound **5** dimerizes to form the N=N bond, providing us with the fluorinated azobenzene core of compound **6** in 84% yield. After this coupling, the TBS groups are removed with 1% HCl in EtOH, affording diol **7** in 100% yield. The next step is to react the diol with 1 eq. of DMT-Cl, in order to protect one of the diols. This resulted in a good yield of 58%,

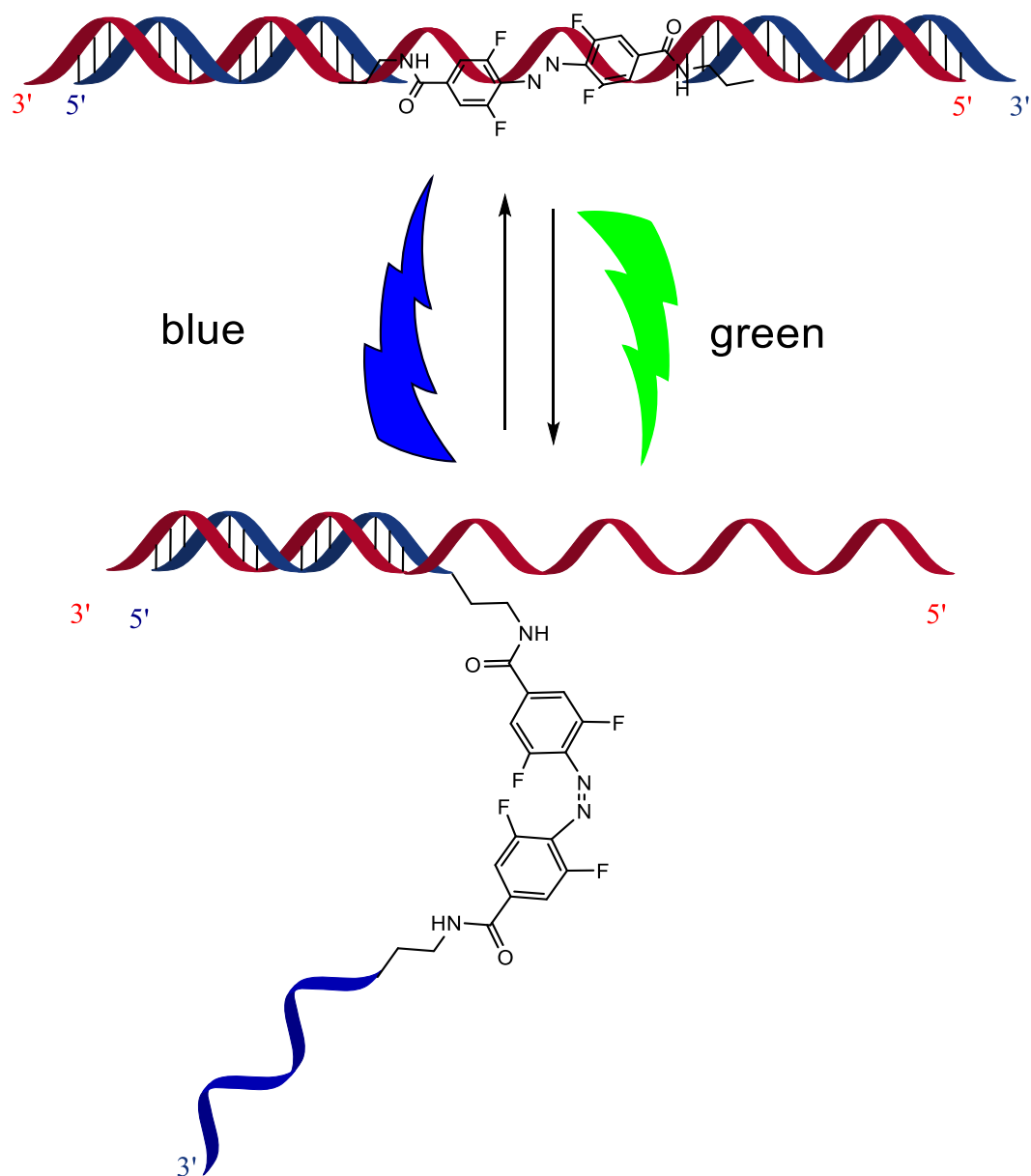


Figure 5.4. Photoinduced inactivation and reactivation of siRNAzOs. The blue strand corresponds to the anti-sense strand and contains the azobenzene moiety. The red strand corresponds to the sense strand.

affording the DMT-mono alcohol **8**. The final step was to react the mono-alcohol with 2-cyanoethyl *N,N*-diisopropylchlorophosphoramidite, which resulted in a 58% yield to afford our DMT-phosphoramidite building block, compound **9**, for solid phase synthesis. Overall, from compound **1**, phosphoramidite **9** was generated in 19.8 % total yield over eight steps.

Once the phosphoramidite was synthesized, a single F-siRNAz was synthesized (Table 5.1). In the F-siRNAz, the azobenzene derivative replaces two nucleosides on the oligonucleotide anti-sense strand. These F-siRNAz were purified and characterized by mass spectrometry (see Table S1 in the Supporting Information, Appendix IV). F-SiRNAz-1 contains an azobenzene modification (Az2-4F) that replaces positions 11 and 12, on the anti-sense strand, counting from the 5'-end of the anti-sense strand. This azobenzene insertion is opposite from the Argonaute 2 cleavage site.³⁵

Table 5.1. Table of RNAs used and its target.^[a]

siRNA	siRNA duplex	target	αT_m (°C)	ΔT_m (°C)
WT	5'-CUUACGCUGAGUACUUCGAtt-3' 3'-ttGAAUGCGACUCAUGAAGCU-5'	luciferase	74.0	--
F-SiRNAz-1	5'-CUUACGCUGAGUACUUCGAtt-3' 3'-ttGAAUGCG <u>Az2-4F</u> UCAUGAAGCU-5'	luciferase	56	- 17.1

[a] Az2-4F is the azobenzene derivative synthesized from Az2; the top strand corresponds to the sense strand; the bottom strand corresponds to the antisense strand. In all duplexes, the 5'-end of the bottom antisense strand contains a 5'-phosphate group.

Prior to biophysical characterization of the F-SiRNAz1, we first characterized the monomer diol (compound **7**). Firstly, we tested its thermal stability at 20 °C, where there was minimal thermal relaxation after 24 h in the dark (Figure 5.5). This trend continued until 60 °C, where 24 h allowed the trans isomer to relax back to unexposed levels. We tested 70,80 and 90 °C temperatures as well (See Figures S2-S8 in appendix IV), and found the cis stability was exponentially worse until lastly the half-life thermal

stability of this diol at 95°C was approximately 15 min (Figure 5.6). This was an excellent result, and was promising as a solution to our previous half-life issues.

These siRNAzOs were then tested for *cis-trans* isomerization, via HPLC, and we were excited to see that not only were the *trans* and *cis* conformers separated, they had a high quantum yield and the *cis* conformer was stable for up to 72 h (Figure 5.7). This was a massive improvement over the unstable Cl-siRNAzo's half-life of < 2 min.

Az2-4F Thermal Stability at 20 °C

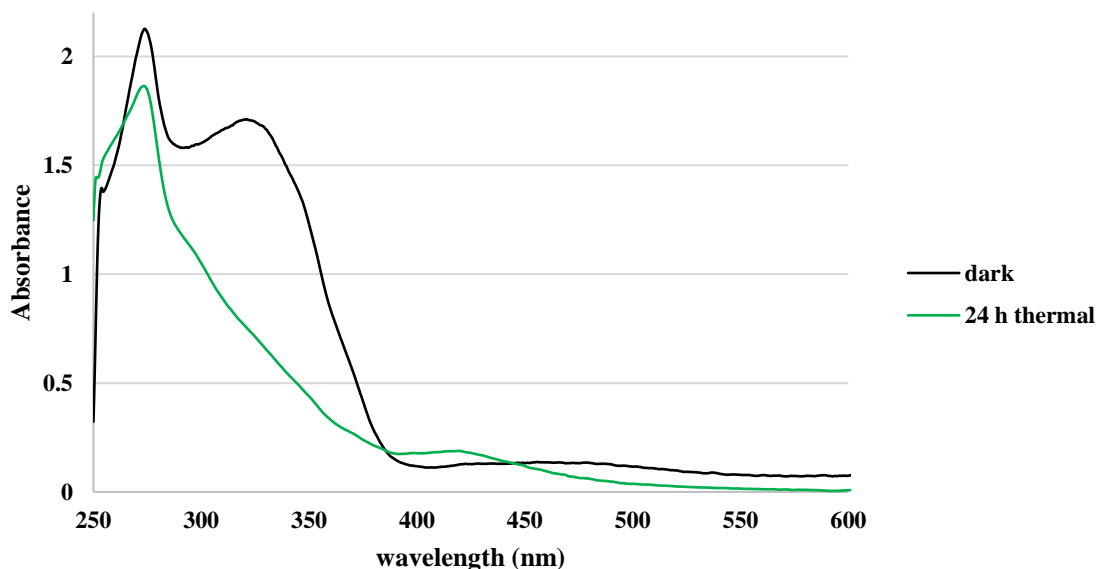


Figure 5.5. Thermal stability of diol **7** at 20 °C. 15 min of green light exposure prior to being left in the dark for 24 h showing minimal thermal relaxation.

Previously, our Az2-4Cl tetra-chlorinated derivative achieved a difference of almost 20 nm between the *trans* and *cis* isomers λ_{\max} due to the red-shifting of the N=N bond.¹⁹ Figure 5.5 clearly shows a much larger difference between the $n \rightarrow \pi^*$ λ_{\max} peaks for the Az2-4F monomer. The dark spectra, corresponding to the *trans* isomer has a $\lambda_{\max} = 468$ nm. The *cis* conformer however has a λ_{\max} 415 nm which is a difference of over 50 nm, which is a two and a half fold increase in separation over Az2-4Cl.

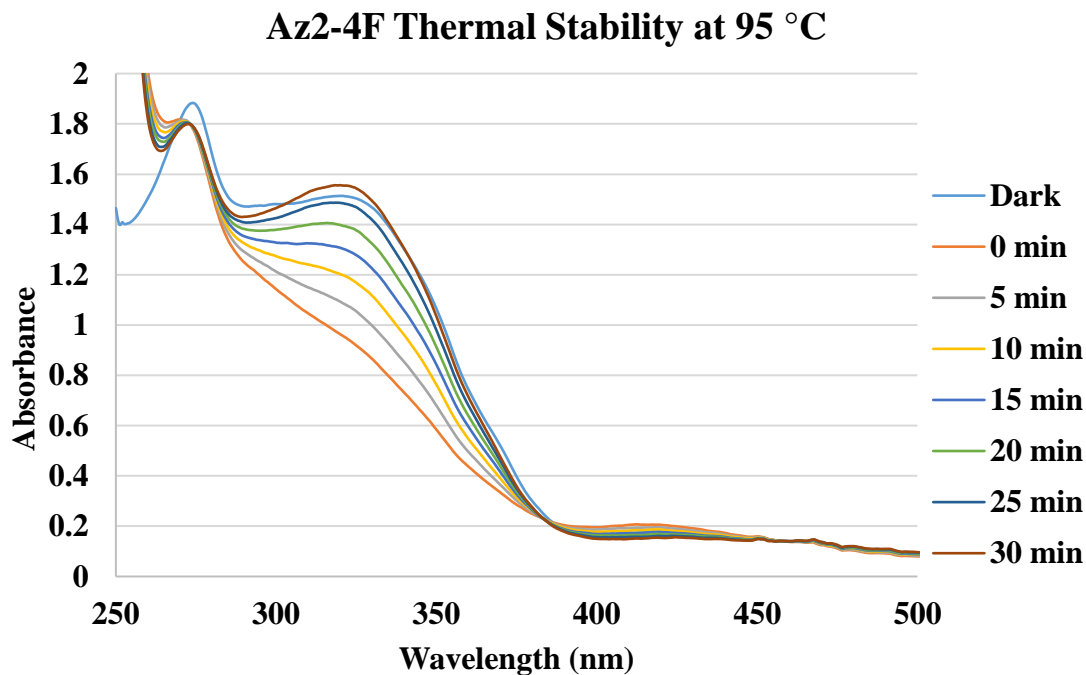


Figure 5.6. Thermal stability of diol 7 at 95 °C. 15 min of green light exposure prior to time 0 min. It was then left at 95 °C, readings taken every 5 min.

These F-siRNAzOs also exhibited thermal destabilization of the duplex since there are no bases to hydrogen bond and pi stack inside the duplex (Table 5.1). This is consistent with other studies that place thermal destabilizers into the central region of the sense strand.³⁶⁻³⁸ The results are similar even when placed in the anti-sense strand like we have done here. These siRNAs also retained the A-type duplex is required for an active RISC complex, characterized by circular dichroism (Figure S1 Appendix IV).

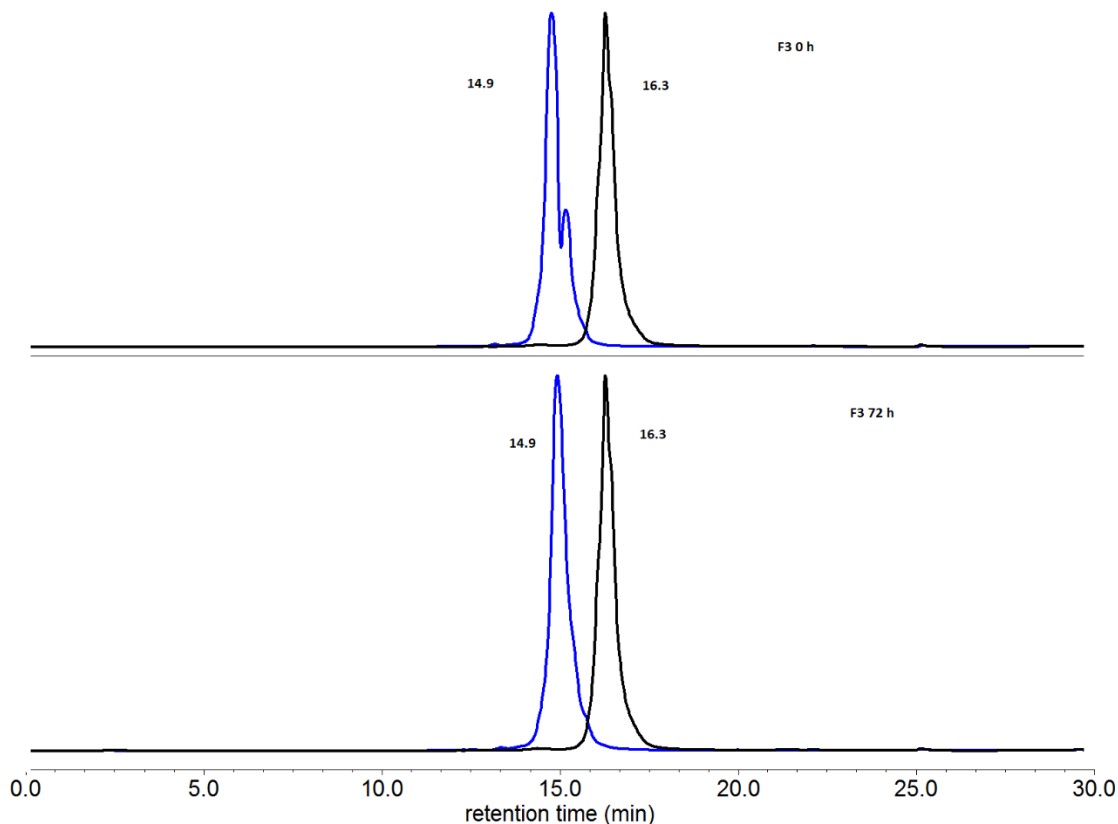


Figure 5.7. HPLC chromatogram of anti-sense strand of F-siRNAzo-1 Conditions were 5% acetonitrile in 95% 0.1 M TEAA (Triethylamine-Acetic Acid) buffer up to 100% acetonitrile over 40 min. Black traces are 0 min of green light, the *trans* conformer. Blue spectra were exposed to 20 min of green light and then injected, or left in the dark for 72 h and then injected. Top spectra is 0 h time point, bottom spectra is 72 h time point. Spectra were processed using the Empower 3 software.

After the bio-physical characterizations, our siRNA's gene silencing was tested against the endogenous firefly luciferase gene using the Promega Dual Reporter Assay. As per our prior results, we expected the *trans* isomer to be the active form of the siRNA, while isomerization to *cis* would cause it to inactivate through disruption of the duplex.

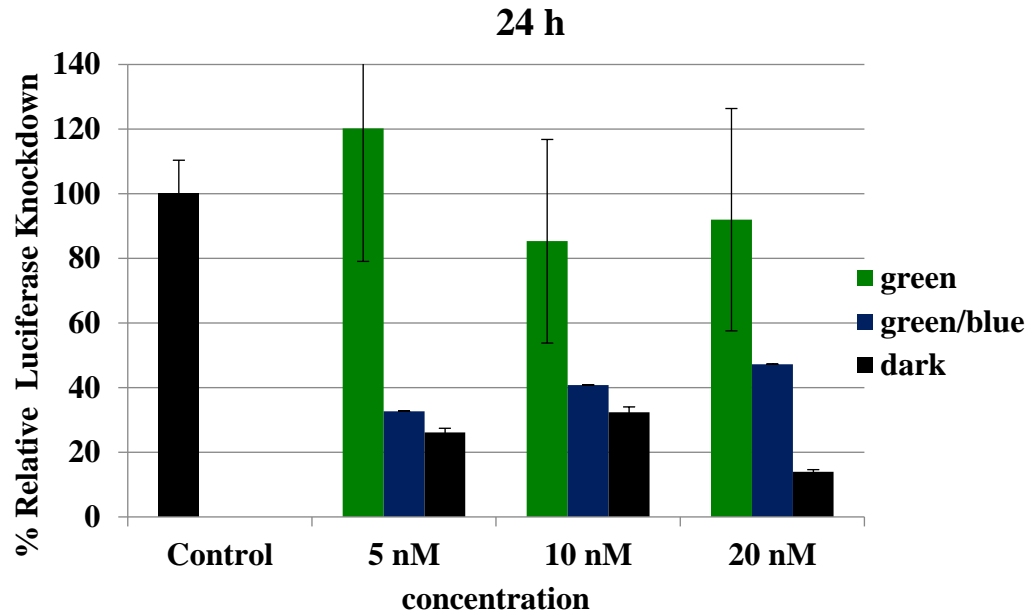


Figure 5.8. Normalized firefly luciferase expression for F-siRNAzo-1 at 5, 10 and 20 nM in HeLa cells monitored 24-hours post-transfection. Green corresponds to the siRNA being exposed under a 530 nm LED lamp immediately after transfection for 1 h, it is then removed. Green/blue corresponds to green light exposure for the first hour after transfection, after which the light was removed and the siRNA exposed to blue, 470 nm LED light for 1 h, after which it was removed for the remainder of the assay. Dark corresponds to siRNAs being transfected in HeLa cells in the absence of green light.

As expected siRNAzo F3 exhibited excellent knockdown in the active form, which corresponds to the black bars, dark treatment Figure 5.8. Exposure to one hour of green light, causes the siRNAzo to go into the *cis* conformer and inactivate the siRNA (green bars). This inactivation shows wt (control) levels of gene expression which is what is expected for a poor silencing profile. This is a great result, being able to maintain the inactive form for 24 h, with minimal light exposure because a persistent inactive *cis* conformer makes a better therapeutic and research tool, by simplifying treatments and protocols by removing steps that could introduce variability into the results. Finally, to ensure the siRNAzo can be returned to its active form, after exposure to green light, the

cells were then allowed a 2 hour rest period in the inactive form, and then exposed to blue, 470 nm light to reactivate the siRNA. This can be seen in Figure 5.5, as the blue bars. The reactivation pushes the silencing to levels similar to the siRNA exposed to no light, near dark levels of silencing, which is the expected result since the luciferase protein has been known to persist for long periods of time in cell culture.

Previously, we hypothesized that our inactivation was preventing uptake into the RISC complex, rather than being a truly reversible system. This was because our modifications were on the sense, or passenger strand, which is discarded after strand selection. We hypothesized that instead of disrupting the RISC complex after it had bound the siRNAzo, that we were preventing the uptake of remaining unbound siRNAs in the RNAi pathway with our system. At any one time, it has been reported that only about 4% of the active siRNAs are taken up into the RISC complex immediately upon transfection.³⁷ Our system would only allow the unbound population of siRNAzos to be affected by light control.¹⁷ In this case, our F3 siRNAzo has the modification in the central region of the anti-sense, or guide strand. This allows us to retain the true reversibility of being able to disrupt the active RISC complex after it has formed, since the light-switching moiety is retained in the RISC complex after strand selection. This is an improvement over our previous system, since we are no longer limited by the unbound population of siRNAs, it should afford greater tunability and control over the silencing activity.

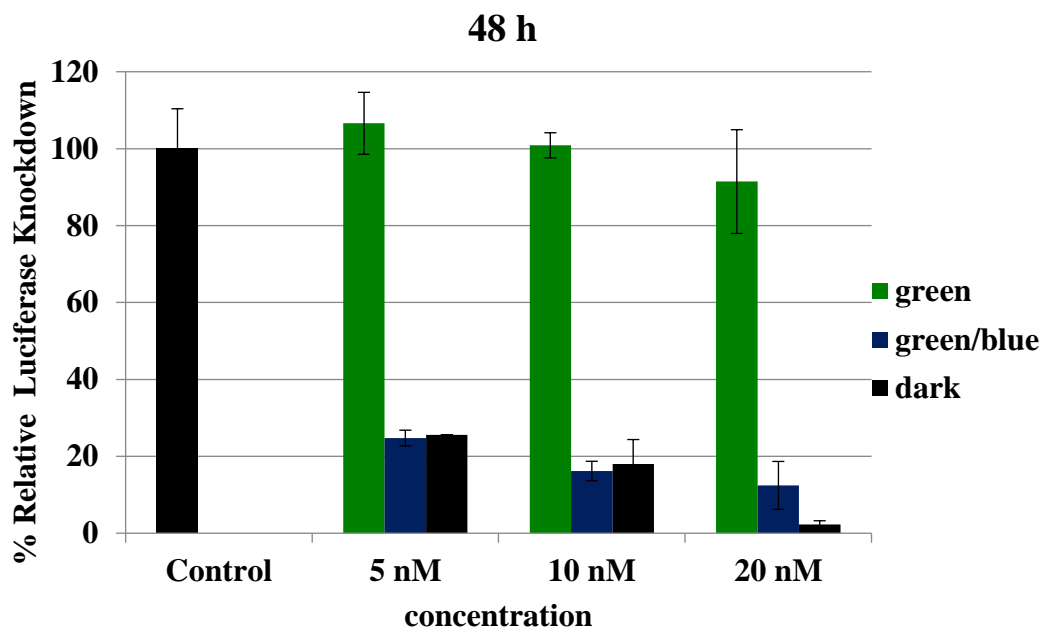


Figure 5.9. Normalized firefly luciferase expression for F-siRNAzo-1 at 5, 10 and 20 nM in HeLa cells monitored 48-hours post-transfection. Green corresponds to the siRNA being exposed under a 530 nm LED lamp immediately after transfection for 1 h, it is then removed. Green/blue corresponds to green light exposure for the first hour after transfection, after which the light was removed and the siRNA exposed to blue, 470 nm LED light for 1 h, after which it was removed for the remainder of the assay. Dark corresponds to siRNAs being transfected in HeLa cells in the absence of green light.

Next we tested the siRNAzo at a longer time point, 48 h (Figure 5.9). As shown, the active form retains its excellent gene silencing ability at 48 h, and like before, 1 h of green light at the beginning of the assay keeps the siRNA off for the entire 48 h, showing how stable the *cis* conformer is. Addition of blue light after green also reactivates the siRNA, like before with little to no loss of silencing activity.

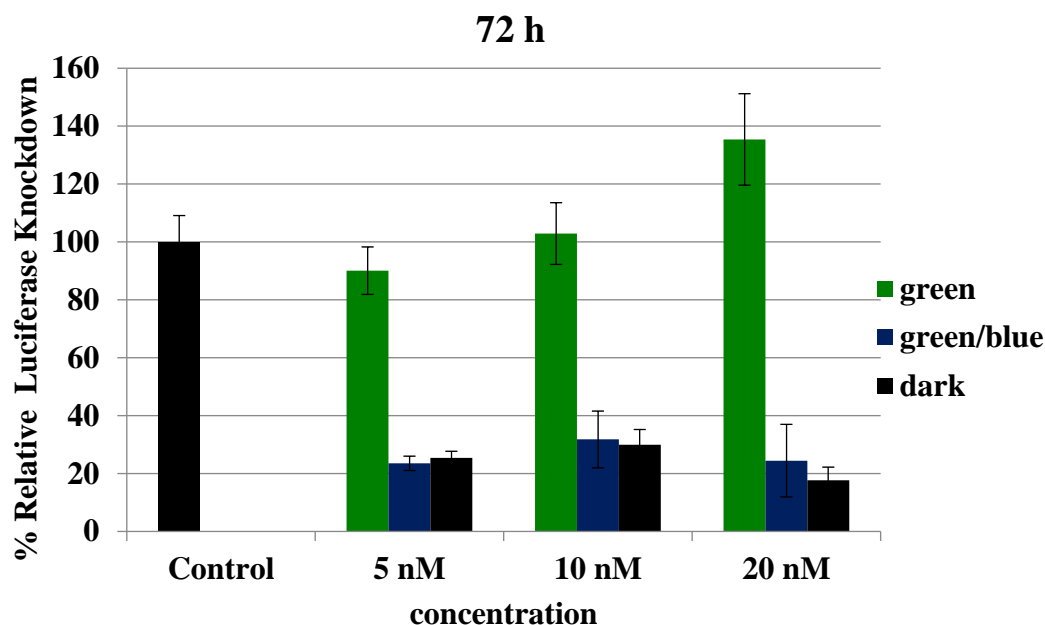


Figure 5.10. Normalized firefly luciferase expression for F-siRNAzo-1 at 5, 10 and 20 nM in HeLa cells monitored 72-hours post-transfection. Green corresponds to the siRNA being exposed under a 530 nm LED lamp immediately after transfection for 1 h, it is then removed. Green/blue corresponds to green light exposure for the first hour after transfection, after which the light was removed and the siRNA exposed to blue, 470 nm LED light for 1 h, after which it was removed for the remainder of the assay. Dark corresponds to siRNAs being transfected in HeLa cells in the absence of green light.

Figure 5.10 shows the results 72 h post-transfection. Even after 72 h, the *cis* conformer remains inactive at 37 °C, with only 1 h of green light exposure. The dark treatment retains approximately 80% silencing after 72 h, and exposure to blue light to re-activate the siRNA shows similar silencing with no loss of activity despite being turned off for the first few hours of the assay.

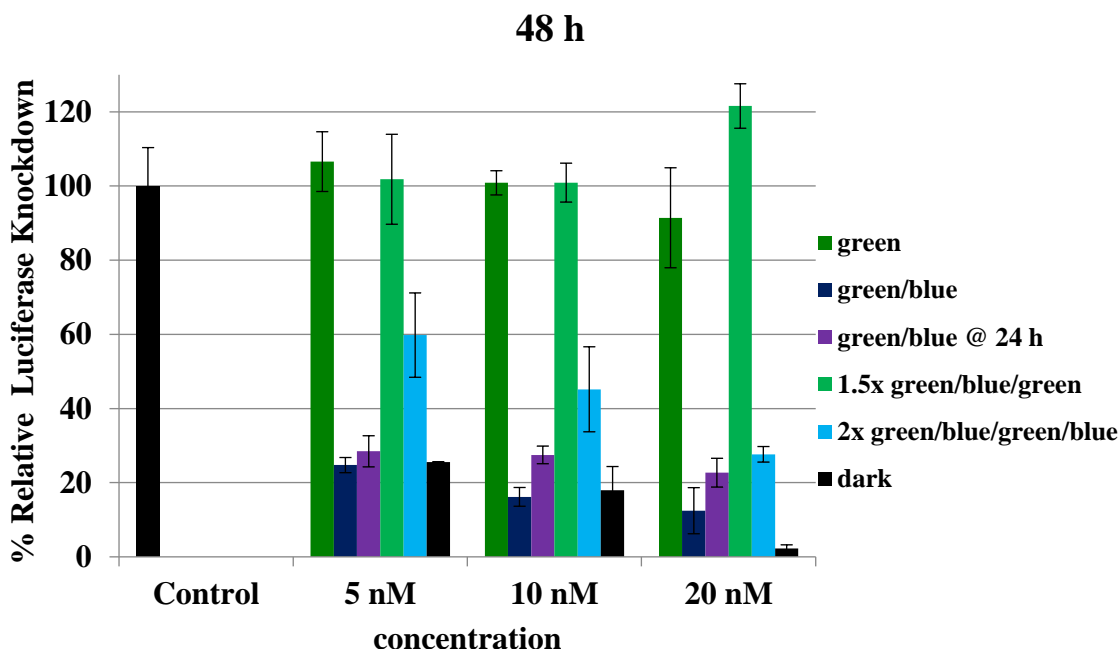


Figure 5.11. Normalized firefly luciferase expression for F-siRNAzo-1 at 5, 10 and 20 nM in HeLa cells monitored 48-hours post-transfection. Green corresponds to the siRNA being exposed under a 530 nm LED lamp immediately after transfection for 1 h, it is then removed. Green/blue corresponds to green light exposure for the first hour after transfection, after which the light was removed and the siRNA exposed to blue, 470 nm LED light for 1 h, after which it was removed for the remainder of the assay. Green/blue @24 h corresponds to green light exposure for the first hour after transfection, after which the light was removed and the siRNA exposed to blue, 470 nm LED light for 1 h at time point 24 h, after which it was removed for the remainder of the assay. 1.5x green/blue/green corresponds to green light exposure at time 0 and 24 h, with one exposure of blue light occurring at time 2 h. 2x green/blue/green/blue corresponds to green light exposure at time 0 and 24 h, with two exposures of blue light occurring in between at time 2 and 26 h. Dark corresponds to siRNAs being transfected in HeLa cells in the absence of green light.

Figure 5.11 shows the results 48 h post-transfection of OFF/ON cycling. To test the durability of the fluorinated photo-switch, we performed multiple OFF/ON cycles in the 48 h window. The green, green/blue and dark conditions were as previous studies. The purple bar, “green/blue @ 24 h” data series, was performed by turning the photo-switch off at time 0 h, like in previous studies. We then reactivated the the azobenzene with blue

at time 24 h, not time 2 h. This result shows that the siRNA does not need to be reactivated immediately, can be allowed to sit in the *cis* conformer for an extended period of time before resuming activity, whereas before the off window was only 2 h, now reactivation is shown to be effective after 24 h in the *cis* conformer as well. Having shown this retention in activity, we then went ahead with the OFF/ON cycling assays. These assays were designed to test the robustness of the azobenzene photo-switch through multiple OFF/ON cycles through various time points. The light green bar represents 1.5 cycles, where it was turned off at time 0 h with green light, turned back on at 2 h through exposure to blue light, and then returned to its inactive state through the exposure of green light at time 24 h. It then remained inactive for the remainder of the assay. This result shows after one OFF/ON cycle, the azobenzene is still available to be inactivated and kept inactive until the 48 h endpoint of the assay. Finally, the light blue bar shows 2 full cycles where it was turned off at time 0 h with green light, turned back on at 2 h through exposure to blue light, and then returned to its inactive state through the exposure of green light at time 24 , and the final exposure of bluee light occuring at 26 h to reactivate the siRNA for the final time. It then remained active for the remainder of the assay. Figure 5.12 shows the same experiments conducted at the same time points but with a 72 h endpoint. Both the 48 and 72 h endpoints show good photo-switch robustness, and show that we can are able to activate or inactivate the siRNA at any point during the assay, with no loss of photo-switch function.

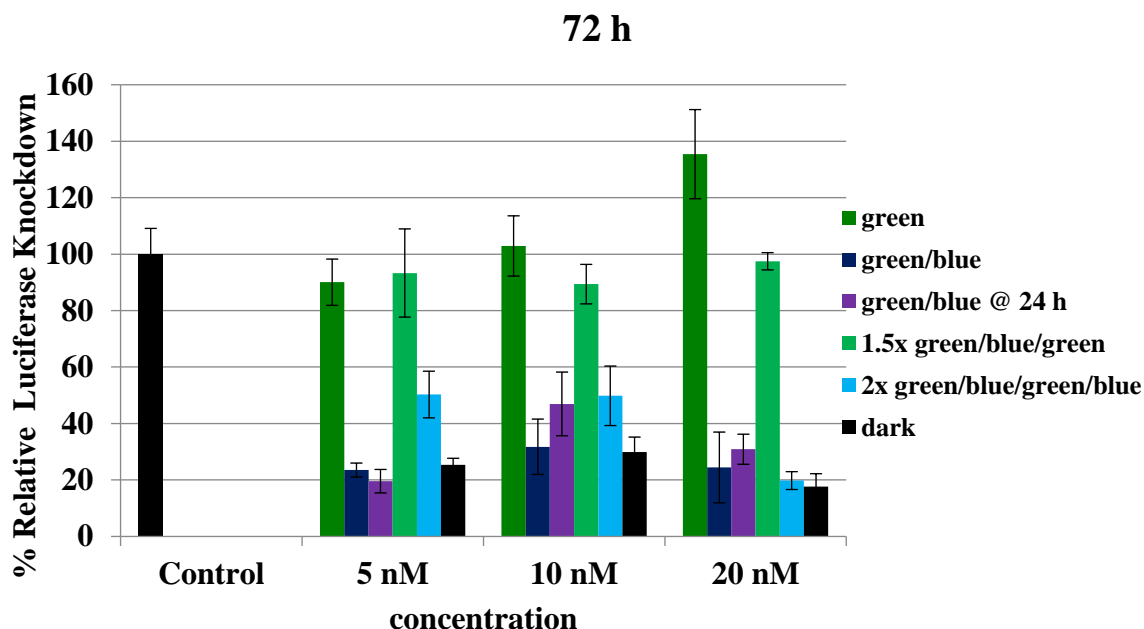


Figure 5.11. Normalized firefly luciferase expression for F-siRNAzo-1 at 5, 10 and 20 nM in HeLa cells monitored 72-hours post-transfection. Green corresponds to the siRNA being exposed under a 530 nm LED lamp immediately after transfection for 1 h, it is then removed. Green/blue corresponds to green light exposure for the first hour after transfection, after which the light was removed and the siRNA exposed to blue, 470 nm LED light for 1 h, after which it was removed for the remainder of the assay. Green/blue @24 h corresponds to green light exposure for the first hour after transfection, after which the light was removed and the siRNA exposed to blue, 470 nm LED light for 1 h at time point 24 h, after which it was removed for the remainder of the assay. 1.5x green/blue/green corresponds to green light exposure at time 0 and 24 h, with one exposure of blue light occurring at time 2 h. 2x green/blue/green/blue corresponds to green light exposure at time 0 and 24 h, with two exposures of blue light occurring in between at time 2 and 26 h. Dark corresponds to siRNAs being transfected in HeLa cells in the absence of green light.

This study demonstrated that we can actively control siRNA activity using fluorinated siRNAzOs (F-siRNAzOs) by using only visible wavelength light, which represents a significant advancement over the UV and red light utilized in our previous system and other reported technologies.^{8-10,14-17} This is an enhancement over our previous generation of siRNAzOs, where we have eliminated the need for harmful UV light, have overcome the

unstable half-life of the *cis* conformer, and can keep the siRNA inactive for up to 72 h with a minimum amount of light exposure.

5.4 Conclusions

We have synthesized and evaluated red-shifted F-siRNAzOs that can be photo-chemically controlled using visible wavelength light. To our knowledge this is the first time, a system utilizing siRNAs with an azobenzene moiety could be photo-controlled using only visible light, using wavelengths of 530 nm for green, and 470 nm for blue light. We believe this to be an improvement over the previous systems, which either required the use of toxic UV light to induce photo-chemical control of the siRNA, or utilized red light with an unstable *cis* conformer which limited its utility for long term use.^{16,17} Using this new improved system, light exposures are minimal and inactivation can last for up to 72 h with one short term exposure of green light. Additionally, we have improved the spatial control by not being limited to only the unbound siRNAs. Having the photo-switch on the anti-sense strand allows for the disruption of fully formed RISC complexes, rather than only being able to control uptake of the unbound population. It also retains all the previous advantages over photocages, by producing no toxic by-products and being reversible.

A visible light controllable therapeutic with a long half-life would be very beneficial to the research sector for use as a biomolecular tool, as well as within the pharmaceutical industry where fine-tuned spatio-temporal control of a drug would be desirable. This is an important issue: a paper published from Alnylam® Pharmaceuticals in 2018 disclosed that a short oligonucleotide was capable of reversing the activity of an active siRNA.⁴⁰ Due to these advances over the previous system, this opens the way for patients undergoing treatment

for at home care. Because it requires minimal light exposures and interactions, it is something the patient could control themselves at home with their LED light systems. It can also reduce siRNA-mediated toxicity since the inactive form is stable, and should not interfere with normal biological functions in that state. Further directions include exploration of further chemical modifications to improve desired properties in the siRNAs, and the development of a multi-siRNAzo system where multiple targets could be controlled selectively with different wavelengths of light.

Acknowledgements

We thank the Natural Sciences and Engineering Research Council (NSERC) for funding.

Supplementary Data

Refer to Appendix IV for additional figures and characterization data.

5.5 REFERENCES – Chapter 5 – Preparation Manuscript IV

- [1] A. Fire, S. Q. Xu, M. K. Montgomery, S. A. Kostas, S. E. Driver and C. C. Mello, *Nature* **1998**, *391*, 806.
- [2] L. Aagaard and J. J. Rossi, *Adv. Drug Deliv. Rev.* **2007**, *59*, 75.
- [3] A. L. Hopkins and C. R. Groom, *Nat. Rev. Drug Discov.* **2002**, *1*, 727.
- [4] X. Shen and D. R. Corey, *Nucleic Acids Res.* **2017**, *46*, 1584.
- [5] D. Al Shaer, O. Al Musaimi, F. Albericio and B. G. de la Torre, *Pharmaceuticals* **2019**, *12*, 52.
- [6] P.R.D. Brandao, S.S. Titze-de-Almeida, and R. Titze-de-Almeida, *Mol. Diagn. Ther.* **2019**, *8*.
- [7] R.L. Setten, J.J. Rossi and S. P. Han, *Nat. Rev. Drug Discov.* **2019**, *18*, 421.
- [8] B. A. Habtemariam, V. Karsten, H. Attarwala, V. Goel, M. Melch, V. A. Clausen, P. Garg, A. K. Vaishnav, M. T. Sweetser, G. J. Robbie and J. Vest, *Clin. Pharmacol. Ther.* **2021**, *109*, 372-382.
- [9] S. F. Garrelfs, Y. Frishberg, S. A. Hulton, M. J. Koren, W. D. O'Riordan, P. Cochat, G. Deschenes, H. Shasha-Lavsky, J. M. Saland, W. G. van't Hoff, D. G. Fuster, D. Magen, S. H. Mochhala, G. Schalk, E. Simkova, J. W. Grothoff, D. J. Sas, K. A. Meliambro, J. Lu, M. T. Sweetser, P. P. Garg, A. K. Vaishnav, J. M. Gansner, T. L. McGregor, J. C. Lieske and I.-A. Collaborators, *N. Engl. J. Med.* **2021**, *384*, 1216-1226.
- [10] S. Shah, S. Rangarajan and S. H. Friedman, *S. H. Angew. Chem. Int. Ed.* **2005**, *44*, 1328.
- [11] V. Mikat and A. Heckel, *RNA* **2007**, *13*, 2341.
- [12] A. Meyer and A. Mokhir, *Angew. Chem. Int. Ed.* **2014**, *53*, 12840.
- [13] A. S. Lubbe, W. Szymanski and B. L. Feringa, *Chem. Soc. Rev.* **2017**, *46*, 1052.
- [14] C. Brieke, F. Rohrbach, A. Gottschalk, G. Mayer and A. Heckel, *Angew. Chem. Int. Ed.* **2012**, *51*, 8446.
- [15] A. A. Beharry and G. A. Woolley, *Chem. Soc. Rev.* **2011**, *40*, 4422.
- [16] M. L. Hammill, C. Isaacs-Trépanier and J.-P. Desaulniers, *ChemistrySelect* **2017**, *2*, 9810.
- [17] M. L. Hammill, A. Patel, M. A. Alla and J.-P. Desaulniers, *Bioorg. Med. Chem. Lett.* **2018**, *28*, 3613.
- [18] M. L. Hammill, G. Islam and J.-P. Desaulniers, *Org. Biomol. Chem.*, **2020**, *18*, 41.
- [19] M. L. Hammill, G. Islam and J.-P. Desaulniers, *ChemBioChem*, **2020**, *21*, 2367-2372.
- [20] K. Yamana, K. Kan, and H. Nakano, *Bioorg. Med. Chem.* **1999**, *7*, 2977.
- [21] Abrams, Y. Xu, N.A. Kuklin, P.A. Burke, A.B. Sachs, L. Sepp-Lorenzino, and S. T. Barnett. *RNA* **2010**, *16*, 2553.
- [22] J. D'Orazio, S. Jarrett, A. Amaro-Ortiz and T. Scott, *Int. J Mol. Sci.* **2013**, *14*, 12222.
- [23] C. Ash, M. Dubec, K. Donne and T. Bashford, *Lasers Med. Sci.* **2017**, *32*, 1909.
- [24] M. Wegener, M.J. Hansen, A. J. M. Driessen, W. Szymanski and B. Feringa, *J. Am. Chem. Soc.*, **2017**, *139*, 17979.
- [25] O. Shinzi, I. Syoji, M. Hiroshi and M. Mizuo *Chem. Lett.* **2010**, *39*, 956

- [26] H. Nishioka, X. Liang, T. Kato, and H. Asanuma *Angew. Chem. Int. Ed.* **2012**, *51*, 1165
- [27] Y. Kamiya, T. Takagi, H. Ooi, H. Ito, X. Liang, and H. Asanuma *ACS Synth. Biol.* **2015**, 365
- [28] D. Kolarski, W. Szymanski, and B. L. Feringa *Org. Lett.* **2017**, *19*, 5090
- [29] S. Samanta, T. M. McCormick, S. K. Schmidt, D. S. Seferos and G. A. Woolley, *Chem. Commun.* **2013**, *49*, 10314.
- [30] M. Dong, A. Babalhavaeji, S. Samanta, A. A. Beharry and G. A. Woolley, *Acc. Chem. Res.* **2015**, *48*, 2662.
- [31] O. Sadvovskii, A. A. Beharry, F. Zhang and G. A. Woolley, *Angew. Chem. Int. Ed. Engl.* **2009**, *48*, 1484.
- [32] J. García-Amorós and D. Velasco, *Beilstein J. Org. Chem.*, **2012**, *8*, 1003.
- [33] D. Bleger, J. Schwarz, A. M. Brouwer and S. Hecht, *J. Am. Chem. Soc.*, **2012**, *134*, 20597.
- [34] D. B. Konrad, J. A. Frank and D. Trauner, *Chem.: Eur. J.* **2016**, *22*, 4364.
- [35] C. Matranga, Y. Tomari, C. Shin, D. P. Bartel and P. D. Zamore, *Cell* **2005**, *123*, 607.
- [36] T. C. Efthymiou, B. Peel, V. Huynh and J.-P. Desaulniers, *Bioorg. Med. Chem. Lett.* **2012**, *22*, 5590.
- [37] H. Addepalli, Meena, C. G. Peng, G. Wang, Y. Fan, K. Charisse, K. N. Jayaprakash, K. G. Rajeev, R. K. Pandey, G. Lavine, L. Zhang, K. Jahn-Hofmann, P. Hadwiger, M. Manoharan and M. A. Maier, *Nucleic Acids Res.* **2010**, *38*, 7320.
- [38] B. J. Peel, G. Hagen, K. Krishnamurthy and J.-P. Desaulniers, *ACS Med. Chem. Lett.* **2015**, *6*, 117.
- [39] Y.I. Pei, P.J. Hancock, H. Zhang, R. Bartz, C. Cherrin, N. Innocent, C. J. Pomerantz, J. Seitzer, M.L. Koser, M.T. Abrams, Y. Xu, N.A. Kuklin, P.A. Burke, A.B. Sachs, L. Sepp-Lorenzino, and S. T. Barnett. *RNA* **2010**, *16*, 2553.
- [40] I. Zlatev, A. Castoreno, C. R. Brown, J. Qin, S. Waldron, M. K. Schlegel, R. Degaonkar, S. Shulga-Morskaya, H. Xu, S. Gupta, S. Matsuda, A. Akinc, K. G. Rajeev, M. Manoharan and V. Jadhav, *Nat. Biotechnol.* **2018**, *36*, 509.
- [41] Still, W. C.; Kahn, M.; Mitra, A. *J. Org. Chem.* **1978**, *43*, 2923
- [42] McDowell, J.A.; Turner, D. H. *Biochemistry* **1996**, *35*, 14077.

5.6 Manuscript I Supplementary Figures and Tables

Full Supplementary information can be found in Appendix IV

Table 5.1. Table of RNAs used and its target.^[a]

siRNAzo	siRNA Duplex	Predicted Mass	Actual Mass ^[b]	^a T _m (°C)	ΔT _m (°C)
wt	5'- CUUACGCUGAGUACUUCGAtt -3' 3'- ttGAAUGCGACUCAUGAAGCU – 5'			74.0	--
F-SiRNAzo-1	5'-CUUACGCUGAGUACUUCGAtt-3' 3'-ttGAAUGCG <u>Az2-4F</u> FUCAUGAAGCU-5'	6625.89	6625.25	56	- 17.1

[a] **Az2-4F** corresponds to the azobenzene derivative synthesized from Az2; the top strand corresponds to the sense strand; the bottom strand corresponds to the antisense strand. In all duplexes, the 5'-end of the bottom antisense strand contains a 5'-phosphate group. [b] Deconvolution results for siRNAzos. ESI-qTOF (ES⁺) m/z calculated for F-siRNAzo-1 [M+H]⁺

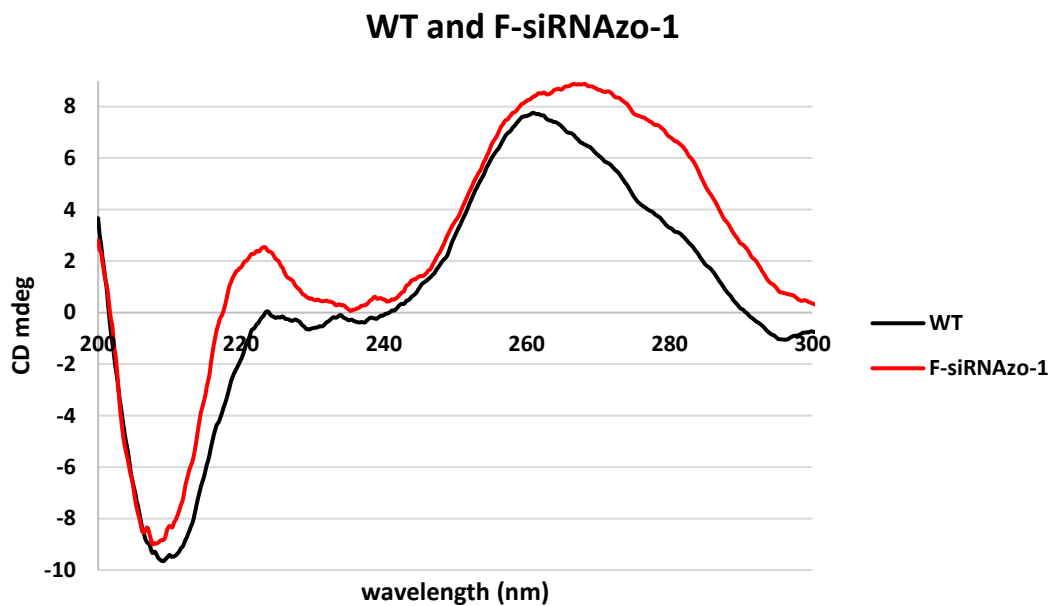


Figure S1. CD spectra of tetra-fluorinated azobenzene modified spacers replacing two nucleobases targeting firefly luciferase mRNAs. Wildtype and modified anti-*firefly* luciferase siRNAs (10 μ M/duplex) were suspended in 500 μ L of a sodium phosphate buffer (90.0 mM NaCl, 10.0 mM Na₂HPO₄, 1.00 mM EDTA, pH 7.00) and scanned from 200-300 nm at 25 °C with a screening rate of 20.0 nm/min and a 0.20 nm data pitch. All scans were performed in triplicate and averaged using Jasco's Spectra Manager version 2.

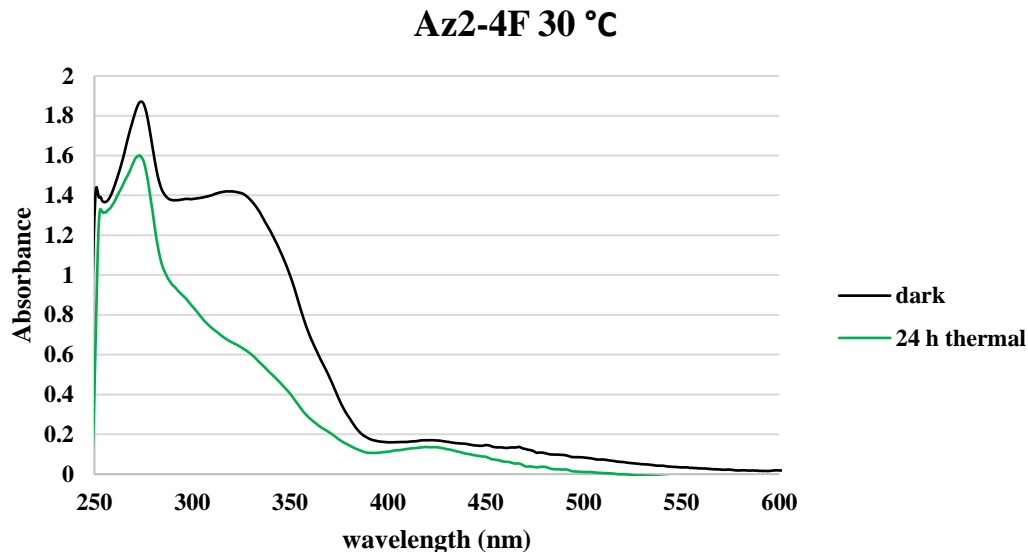


Figure S2. Absorbance Profile of Az2-4F when exposed to 15 min of green 530 nm light using a 4W LED in DMSO, scanned from 250-600 nm at 30 °C with a screening rate of 20.0 nm/min and a 0.20 nm data pitch. 24 h thermal was allowed to sit in the dark at temperature until time elapsed.

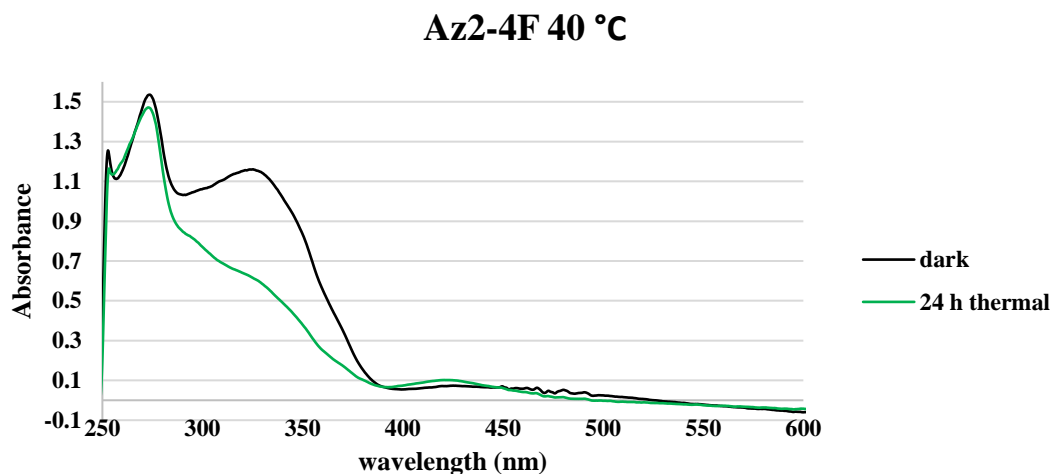


Figure S3. Absorbance Profile of Az2-4F when exposed to 15 min of green 530 nm light using a 4W LED in DMSO, scanned from 250-600 nm at 40 °C with a screening rate of 20.0 nm/min and a 0.20 nm data pitch. 24 h thermal was allowed to sit in the dark at temperature until time elapsed.

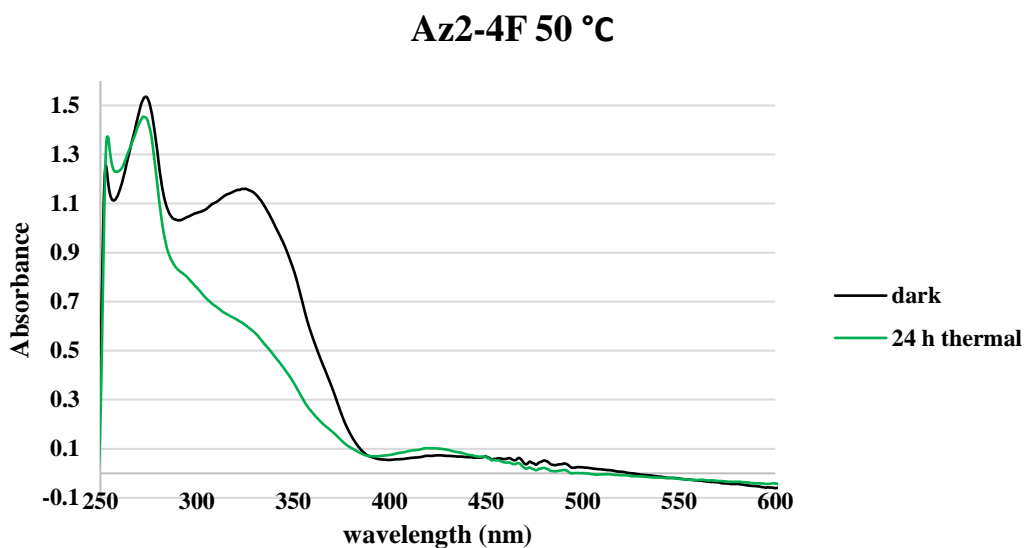


Figure S4. Absorbance Profile of Az2-4F when exposed to 15 min of green 530 nm light using a 4W LED in DMSO, scanned from 250-600 nm at 50 °C with a screening rate of 20.0 nm/min and a 0.20 nm data pitch. 24 h thermal was allowed to sit in the dark at temperature until time elapsed.

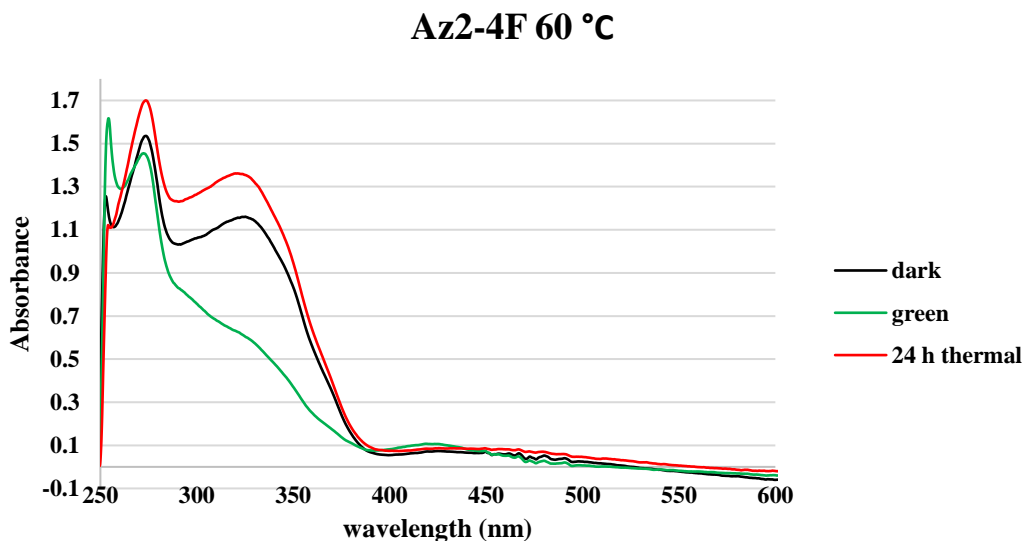


Figure S5. Absorbance Profile of Az2-4F when exposed to 15 min of green 530 nm light using a 4W LED in DMSO, scanned from 250-600 nm at 60 °C with a screening rate of 20.0 nm/min and a 0.20 nm data pitch. 24 h thermal was allowed to sit in the dark at temperature until time elapsed. *Trans* isomer restored after 24 h.

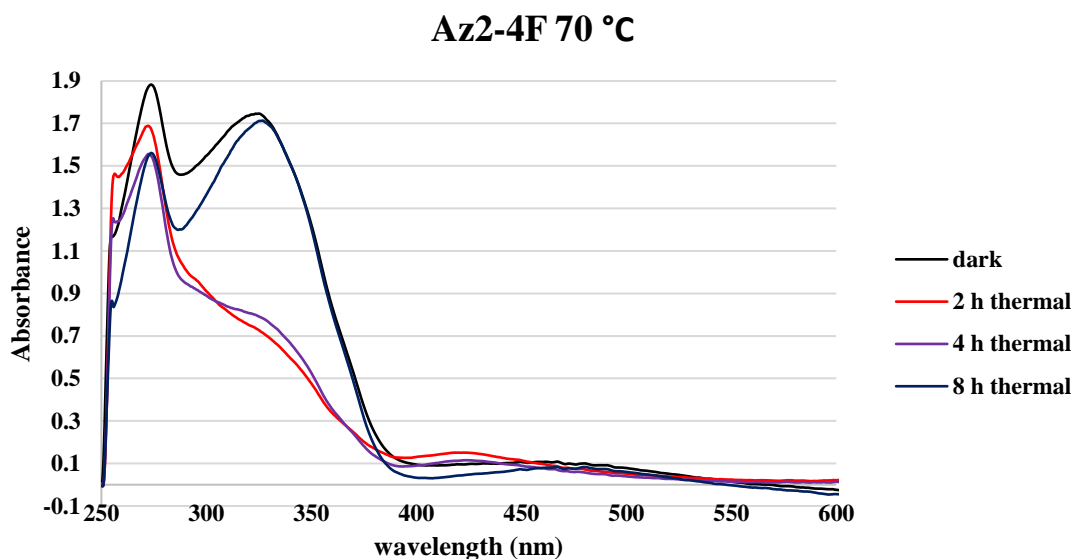


Figure S6. Absorbance Profile of Az2-4F when exposed to 15 min of green 530 nm light using a 4W LED in DMSO, scanned from 250-600 nm at 70 °C with a screening rate of 20.0 nm/min and a 0.20 nm data pitch. 2,4 and 8 h thermal was allowed to sit in the dark at temperature until time elapsed. *Trans* isomer restored after 8 h.

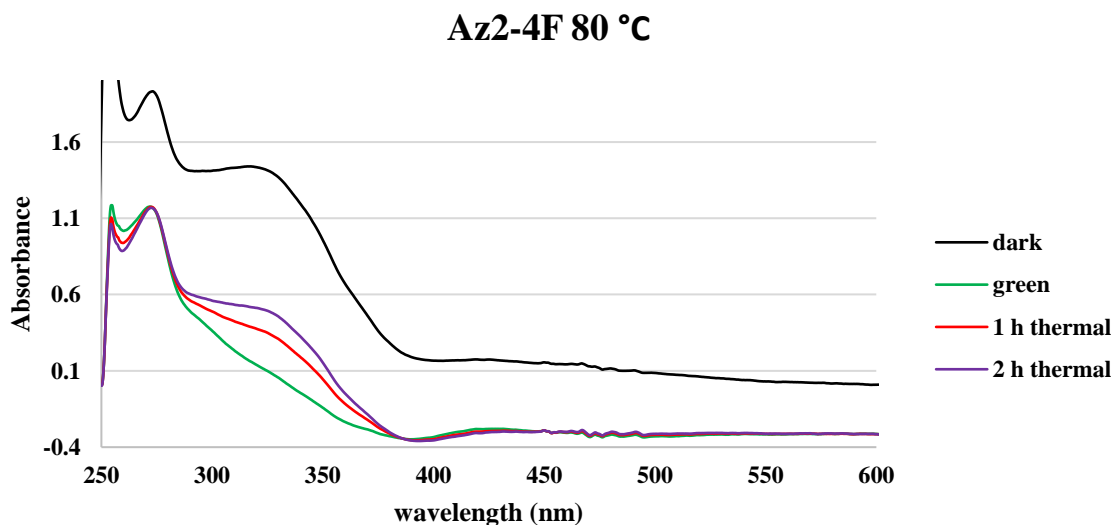


Figure S7. Absorbance Profile of Az2-4F when exposed to 15 min of green 530 nm light using a 4W LED in DMSO, scanned from 250-600 nm at 80 °C with a screening rate of 20.0 nm/min and a 0.20 nm data pitch. 1 and 2 h thermal was allowed to sit in the dark at temperature until time elapsed. *Trans* isomer restored after 2 h.

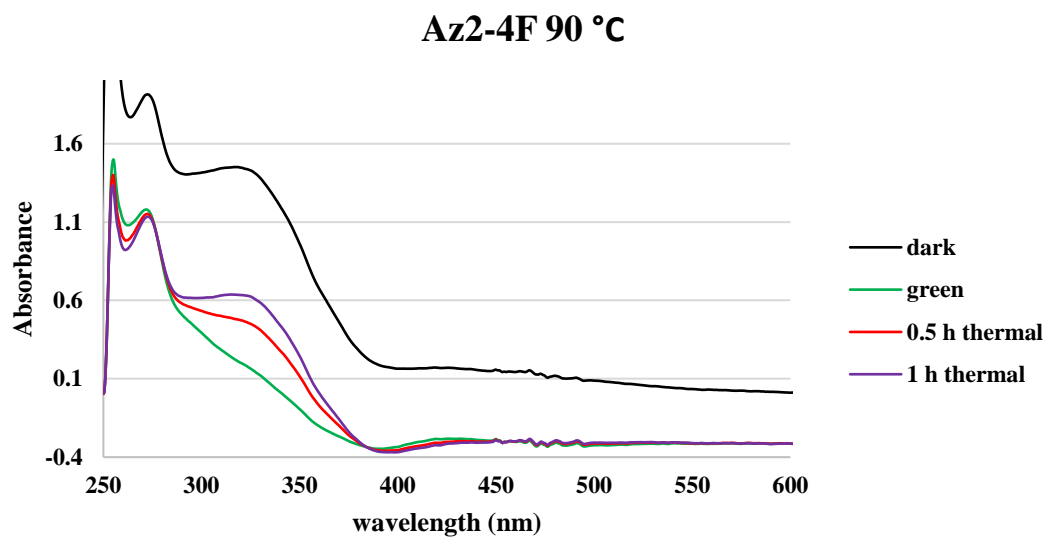


Figure S8. Absorbance Profile of Az2-4F when exposed to 15 min of green 530 nm light using a 4W LED in DMSO, scanned from 250-600 nm at 90 °C with a screening rate of 20.0 nm/min and a 0.20 nm data pitch. 0.5 and 1 h thermal was allowed to sit in the dark at temperature until time elapsed. *Trans* isomer restored after 1 h.

Chapter 6: General Conclusions

RISC-mediated gene silencing is quickly becoming a new field of research dedicated to difficult to treat genetic diseases, as evidenced by the three US FDA approved RNAi therapeutics developed by Alnylam.¹⁻³ There are still several limitations to surpass before they can be in widespread use for a variety of different applications. The work presented in this dissertation utilized three different azobenzene derivatives to overcome three of the barriers preventing siRNAs widespread use: off-target effects, toxicity and controlling the siRNA's activity *in situ* inside the host system.

The first azobenzenes we explored, Az1 and Az2, were synthesized previously in our lab and then incorporated into the sense strand of the oligonucleotides.¹ After determining the gene silencing and photo-control ability of the central region siRNAzOs, we placed the Az2 moiety at the 3'-end of the sense strand, to measure the nuclease resistance and gene silencing capability. A secondary goal was to determine the difference, if any of the *trans* and *cis* conformers for both of these applications. We hypothesized there would be only a minimal difference in gene silencing between the isomers since the 3'-end modification was suspected to be less disruptive than a central region one. In Chapter II, we report the stability and gene-silencing efficiency of two siRNAs containing azobenzene at the 3'-end of the sense strand. In siRNA **1** (Az1 moiety), one carbon is placed between the aromatic group and the oxygen; whereas in siRNA **2** (Az2 moiety), two carbons are present. We found that isomerization of the 3'-azobenzene to its *cis* form by UV light appears to modestly enhance nuclease stability in the presence of fetal bovine serum at some time points. Each siRNAzo also showed differences between each other, likely because the active RISC complex itself and exonucleases do not distinguish the isomeric

forms of the *cis* and *trans* azobenzenes. That being said, there was an observed larger difference between the isomeric forms of Az2, likely due to its slightly larger size and flexibility. Wildtype luciferase siRNAs have been shown to be effective up to one week after transfection in HeLa cells,⁵ and this modification could allow for better temporal control of nuclease stability when in the *cis* isomer. Most wildtype siRNAs are degraded within 30 min but our modification prevents this rapid degradation, allowing the gene silencing to persist. We developed two siRNAs that are useful for moderate changes in gene silencing between *trans* and *cis* conformers, but always imparts moderate nuclease resistance that can be controlled with light. In addition, the 3'-azobenzene could be used as a minimal chemical modification for other siRNA targets, also giving enhanced nuclease stability.⁶

Based on our previous results, we then wanted to expand the scope of the protocol to include longer inactivation times, as well as endogenous targets. In Chapter III, we developed the methodology to be compatible for long term inactivation with UV light, for up to 24 h using carefully controlled doses of UV light.⁷ This was a large improvement over the previous protocol, where reactivation would occur after 12 h due to the unstable half-life of the Az2 *cis* conformer. Additionally, we demonstrated the system's ability to go through multiple inactivation/activation cycles over a 24 h period. This was an important advancement, because it shows the siRNA remains available for photo-switching after multiple inactivations. We also showed its efficacy against the endogenous *BCL-2* oncogene, by keeping it inactive for up to 24 h. This system differs in its reversibility mechanism compared to the reported high-affinity short oligonucleotides that reversibly target the siRNA guide strand.⁸ In our system, a population of siRNAzOs will be loaded by

the RISC complex to form an active RISC-antisense complex, and another population of siRNAs will remain unbound. Thus, by subjecting the cells to UV light, we hypothesized that the inhibition of RISC loading and formation of active RISC complex would be inhibited. Many prior siRNAs that targeted a variety of diseases resulted in unexpected side effects.⁹ Unlike the system mentioned above, our system does not require the addition of an extra aptamer or chemical to disable the system, only the application of UV light.

Next in Chapter IV, we utilized a late stage chlorination procedure to develop a novel chlorinated azobenzene derivative, that we then used to make chlorinated siRNAs. This was an advancement over the previous technology by red-shifting the $\pi \rightarrow \pi^*$ and $n \rightarrow \pi^*$ transition of the N=N bond into the visible region of the electromagnetic spectrum.¹⁰ This enhancement over the previous molecule allowed us to use only visible wavelength light, to control the Cl-siRNA's activity, thus eliminating the need for high energy, toxic UV light. This red-shift came with an extra problem however, an incredibly short *cis* conformer half life at 37 °C (< 2min). Fortunately, this could be circumvented by simply keeping the cell culture under red light ($\lambda = 660$ nm) for the entire assay, since it is non-toxic to the cells. That allowed us to keep the siRNA inactive for up to 24 h, without toxic UV light. To reactivate the siRNA, removal of the red light source was sufficient to allow for immediate thermal relaxation back to the *trans* isomer for gene silencing to resume. This system retains all the advantages over photocages: no toxic by-products released, and is reversible. The short half-life of the *cis* conformer however remains problematic, since constant exposure to red light is inconvenient for use as a bio-molecular tool or a therapeutic.

In Chapter 5, we developed the final improvements to our system that was discussed in this thesis, the replacement of the chlorines in the *ortho* position with fluorines. We synthesized and evaluated these red-shifted F-siRNAzOs, using green light to inactivate it ($\lambda = 530$ nm) and blue light to reactivate it ($\lambda = 470$ nm). This was an upgrade over the previous systems, since we eliminated the need for toxic UV light, but also improved the half life of the *cis* conformer considerably. While the large bulky chlorines prevented a stable *cis* conformer, the smaller fluorines had the opposite effect, making it more stable than even the original Az2 which had only hydrogens in the *ortho* position. This new improved system utilizes only minimal light exposures (1 h of light exposure) with inactivation lasting for up to 72 h with only one dose of green light. Additionally, because the Az2-4F moiety is on the antisense strand, we are no longer limited to the unbound population of siRNAzOs, and may be able to disrupt active RISC formations with the green light. This is in addition to retaining all previous advantages over photocages, producing no toxic by-products and being reversible. A visible light controllable therapeutic with a long half-life would be very beneficial to the research sector for use as a biomolecular tool, as well as within the pharmaceutical industry where fine-tuned spatio-temporal control of a drug would be desirable. These advancements also open the path for patients undergoing at home care. Because it requires minimal light exposures and interactions, it is something the patient could control themselves at home with their LED systems. The next step is the development of a multi-siRNAzo system where multiple targets could be controlled selectively with different wavelengths of light. In Figure 6.1 the potential of such a finely tuned, controllable system with multiple siRNAzOs utilized at the same time is highlighted.

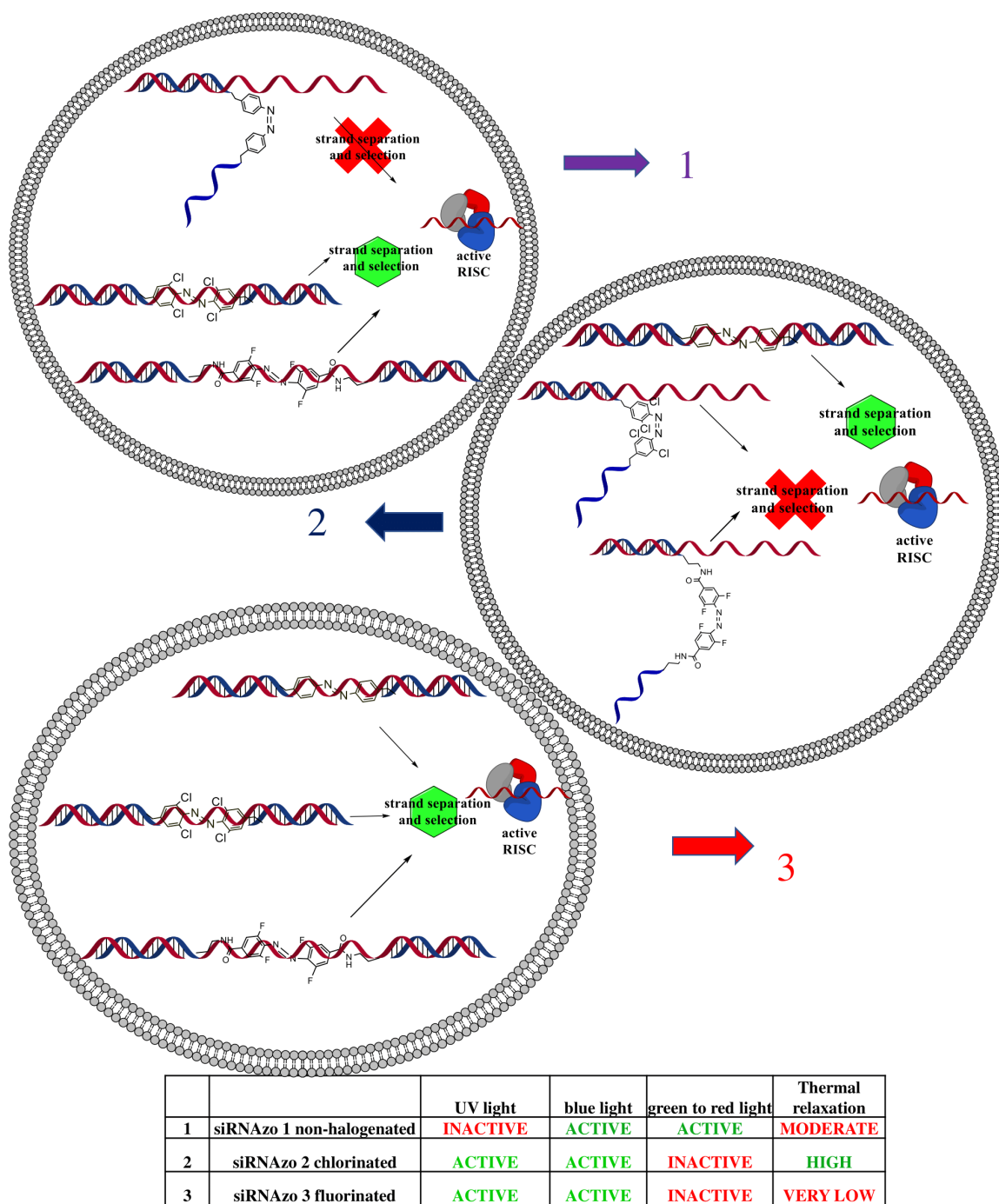


Figure 6.1. A potential future system with multiple siRNAzOs, individually controlled by independent wavelengths of light.

In this kind of scenario, there are 3 options: 1) exposure to UV light prevents silencing on target 1, but targets 2 and 3 are affected; 2) exposure to blue light causes all 3 targets to be silenced and 3) green to red light inactivates targets 2 and 3 while silencing is retained on target 1. There also the additional exploitable property of the thermal stability, which could be useful in different scenarios, such as inactivating an siRNAzo, and leaving it to turn itself back on overtime (moderate thermal relaxation) or immediately (high relaxation). Another alternative is to keep the siRNA inactive, until it is ready to be turned on with a very low thermal relaxation profile. Having shown these scenarios are possible individually, next steps would be to try combing the different systems in order to have silencing on different targets, in real time individually. A visible light controllable therapeutic with a long half-life would be very beneficial to the research sector for use as a biomolecular tool, as well as within the pharmaceutical industry where fine-tuned spatio-temporal control of a drug would be desirable. This is an important issue: a paper published from Alnylam® Pharmaceuticals in 2018 disclosed that a short oligonucleotide was capable of reversing the activity of an active siRNA.⁴ Further design and optimization is required before a multi-siRNAzo could be a reality however. If successful, it could lead to advancements in therapeutics where multiple targets could be activated or inactivated in real time, leading to more effective treatments. It could also be utilized to study complicated biological pathways in real time, such as developmental pathways for G-protein mediated cascades.^{11,12}

Combined, the research summarized in this thesis exhibits the utility of adding a photo-switch into a system that previously had no way to control its activity with light. It also demonstrates that building on the initial system, how it can be modified and fine-tuned

through chemical modification to add or remove specific properties that are desirable. In the future, the development of a multi-siRNAzo system, that utilizes multiple discrete wavelengths of light to attack multiple targets has the potential for many future breakthroughs in the pharmaceutical industry and in the research sector.

6.1 REFERENCES – Chapter 6 – General Conclusions

1. Al Shaer, D.; Al Musaimi, O.; Albericio F. and de la Torre, B.G. *Pharmaceuticals* **2019**, *12*, 52.
2. Brandao, P.R.D.; Titze-de-Almeida, S.S. and Titze-de-Almeida, R. *Mol. Diagn. Ther.* **2019**, *8*.
3. Setten, R.L.; Rossi J.J and Han, S.P. *Nat. Rev. Drug Discov.* **2019**, *18*, 421.
4. Hammill, M. L.; Isaacs-Trépanier, C.; Desaulniers, J.P. *ChemistrySelect*, **2017**, *2*, 9810-9814.
5. Bartlett, D.W.; Davis, M. E. *Biotechnol. Bioeng.* **2007**, *97*, 909-921.
6. Efthymiou, T. C.; Peel, B.; Huynh, V.; Desaulniers, J.-P. *Bioorganic Med. Chem. Lett.* **2012**, *22*, 5590-5594.
7. Hammill, M. L.; Islam, G.; and Desaulniers, J. P. *Org. Biomol. Chem.* **2020**, *18*:41-46.
8. Zlatev, I.; Castoreno, A.; Brown, C.R.; Qin, J.; Waldron, S.; Schlegel, M.K.; Degaonkar, R.; Shulga-Morskaya, S.; Xu, H.; Gupta, S.; Matsuda, S.; Akinc, A.; Rajeev, G.K.; Manoharan M. and Jadhav, V. *Nat. Biotechnol.* **2018**, *36*, 509.
9. Kleinman, M.E.; Yamada, K.; Takeda, A.; Chandrasekaran, V.; Nozaki, M.; Baffi, J.Z.; Albuquerque, R.J.C; Yamasaki, S.; Itaya M. and Pan, Y. *Nature* **2008**, *452*, 591.
10. Hammill, M. L.; Islam, G.; and Desaulniers, J. P. *Chembiochem* **2020**, *21*:2367-2372.
11. Syrovatkina, V.; Alegre, A.G; Dey R. and Huang, X.Y. *J. Mol. Biol.* **2016**, *428*, 3850-3868.
12. Khafizov, K.; Lattanzi G. and Carloni, P. *Proteins: Struct., Funct., Bioinf.* **2009**, *75*, 919-930.

Appendix I. Manuscript I and Supplementary Data



Contents lists available at ScienceDirect

Bioorganic & Medicinal Chemistry Letters

journal homepage: www.elsevier.com/locate/bmcl

Stability and evaluation of siRNAs labeled at the sense strand with a 3'-azobenzene unit



Matthew L. Hammill, Ayushi Patel, Maria Abd Alla, Jean-Paul Desaulniers*

Faculty of Science, University of Ontario Institute of Technology, 2000 Simcoe Street North, Oshawa, Ontario L1H 7K4, Canada

ARTICLE INFO

Keywords:
siRNA
Azobenzene
Photocontrol
Nucleic acid
Isomerization

ABSTRACT

siRNAs bearing a 3'-azobenzene derivative on the sense strand were evaluated for their gene silencing ability in mammalian cell culture and nuclease stability in nuclease-rich media. Azobenzene can be isomerized between *cis* and *trans* isomers through the incubation of UV (*cis* isomer) and visible light (*trans* isomer). It was demonstrated that subtle differences in nuclease stability and activity were observed. These small changes can be used to photochemically fine-tune the activity of an siRNA for gene-silencing applications.

The endogenous RNA interference (RNAi) pathway regulates gene expression in eukaryotic organisms.¹ In 1998, Fire and Mello described the use of the RNAi pathway in which double-stranded RNAs (dsRNAs) were able to silence gene expression in a nematode, *Caenorhabditis elegans*.² Since then, synthetic siRNAs have been used to silence genes for potential therapeutic and biotechnological applications.^{3–5}

Stabilization of synthetic siRNA against nuclease degradation is important for *in vivo* and therapeutic applications.⁶ Several studies have demonstrated that siRNA resistance to nucleases can be improved by introducing chemically-modified nucleotide analogs into the siRNA structure.^{7,8} siRNAs containing 2'-O-methyl group and 2'-fluoro substitutions in the ribose sugar backbone have shown promising results with enhanced siRNA stability in the serum.^{6,7,9,10} Moreover, other modifications such as locked nucleic acid (LNA) can be used to both increase the thermal stability and nuclease stability of siRNA molecules without affecting their function.¹¹ Such modifications offer the means to enhance the stability of the siRNA structure without affecting its gene-silencing activity. Other studies have shown that large bulky substituents such as phenyl, naphthyl, and other large aromatic groups on the 3'-end of the siRNA duplex can also confer stability to nucleases.¹²

Azobenzene is an aromatic compound that can undergo photo-isomerization. In the presence of UV light, azobenzene exists predominantly in the *cis* conformation and in the presence of visible light, azobenzene rests in the *trans* conformation.¹³ The isomerization from *trans* to *cis* is accomplished with UV light between 330 and 365 nm. Azobenzene can be returned to its *trans* conformation with broad spectrum visible light of 450 nm or greater.¹⁴ The *trans* state of the azobenzene molecule is planar and has a dipole moment near zero. The

trans conformation of the azobenzene molecule is more stable; hence is the dominant isomer.¹⁵ In the *cis* isomer, the two phenyl rings of azobenzene molecule are twisted approximately 55° out of the plane and the *cis* isomer has a dipole moment of three Debye units.^{13–15} Due to these properties, azobenzene has been used in oligonucleotide modifications and biological applications because of their ease in synthesis, high efficiency, and facile controlled isomerization.^{13,16–19}

There are several approaches for modifying oligonucleotides in order to utilize azobenzene's photo-isomerization properties. For example, modifications can be placed on the sugar or nitrogenous base, or serve as the backbone core of an oligonucleotide.^{13,20} The attachment of a photo-switch as a nucleoside surrogate has been a widely used approach. Moreover, inserting azobenzene into a sequence as an additional nucleoside has been widely applied as azobenzene intercalates between the neighbouring pairing bases in the *trans* conformation. Following UV irradiation, the *cis* conformation of the azo molecule reduces its ability to intercalate in duplex oligodeoxynucleotides, and as a result, the duplex destabilizes.²¹ Most recently, our group synthesized a class of siRNAs bearing azobenzene (siRNAzo) within the central region of siRNAs, and we were able to control the gene-silencing activity of these complexes with UV and visible light.¹⁸ Having an ability to control when the molecule is active or inactive would have an enormous benefit as potential therapeutics and/or biotechnological tools.

In this study, we investigated the effects of an azobenzene moiety on the 3'-end of the sense strand of siRNAs, and whether there was a change in stability and gene-silencing efficacy in the presence of UV light. Fig. 1 illustrates the siRNAs used with the azobenzene. siRNA 1 contains an azobenzene that contains a single carbon between the phenyl group and oxygen group, whereas siRNA 2 contains two carbons

* Corresponding author.

E-mail address: jean-paul.desaulniers@uoit.ca (J.-P. Desaulniers).<https://doi.org/10.1016/j.bmcl.2018.10.044>

Received 28 August 2018; Received in revised form 24 October 2018; Accepted 26 October 2018

Available online 26 October 2018

0960-894X/ Crown Copyright © 2018 Published by Elsevier Ltd. All rights reserved.

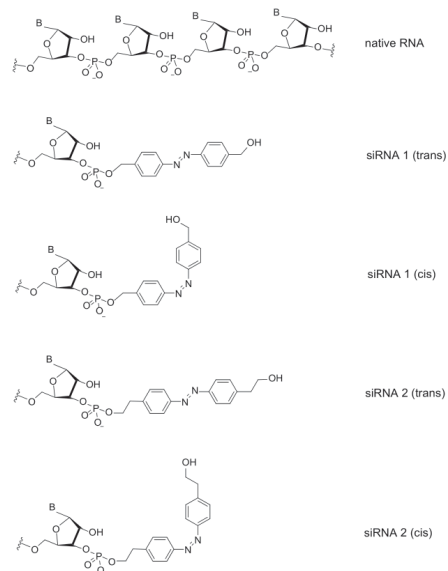


Fig. 1. Structural differences between native RNA, and siRNAs containing azobenzene derivatives. The differences between the *trans* and *cis* forms are identified.

on the azobenzene atom between the phenyl group and the oxygen atom (Fig. 1).

We investigated the gene-silencing effect of siRNAs 1, 2 and wt (Table 1) in the presence and absence of UV light. siRNAs 1 and 2 were synthesized and characterized using our previously published method.¹⁸ In the presence of UV light, the azobenzene would adopt the *cis* form as the major isomer (Table S-1), whereas in the absence of UV light, the *trans* form dominates. Briefly, the siRNAs were co-transfected with plasmids pGL3 and pRenilla into the HeLa cells, followed by cell lysis following transfection. The siRNAs were either inactivated with UV light prior to transfection, or they were not exposed to UV light, and thus the active form was transfected. The wt siRNA does not appear to have any change in silencing activity between the UV treated and no treatment groups. As shown in Fig. 2, UV exposure does not have an appreciable effect on silencing. This is expected as the wt siRNA does not have any light-inducible isomerizable moieties.

Table 1
Sequences of siRNAs.^[a]

	siRNA duplex
wt	5'- CUUACGCUGAGUACUUCGAtt -3' 3'- ttGAAUGCGACUCAUGAAGCU - 5'
1	5'- CUUACGCUGAGUACUUCGAz1 -3' 3'- ttGAAUGCGACUCAUGAAGCU - 5'
2	5'- CUUACGCUGAGUACUUCGAz2 -3' 3'- ttGAAUGCGACUCAUGAAGCU - 5'

^[a] Az1 corresponds to the azobenzene derivative synthesized from 4-nitrobenzyl alcohol. Az2 corresponds to the azobenzene derivative synthesized from 4-nitrophenylethyl alcohol; the top strand corresponds to the sense strand; the bottom strand corresponds to the antisense strand. In all duplexes, the 5'-end of the bottom antisense strand contains a 5'-phosphate group.

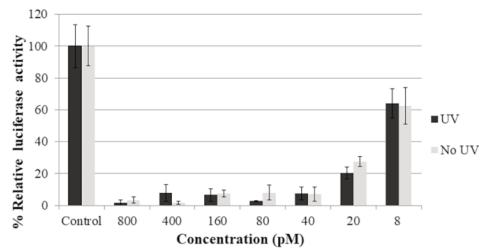


Fig. 2. Reduction in normalized firefly luciferase expression for wt siRNA 1 at 8, 20, 40, 80, 160, 400 and 800 pM concentrations in HeLa cells and lysed 22 h post transfection. 'UV' corresponds to the siRNA being exposed under a 365 nm UV lamp for inactivation prior to transfection. 'No UV' corresponds to active siRNA being transfected in HeLa cells in the absence of UV light.

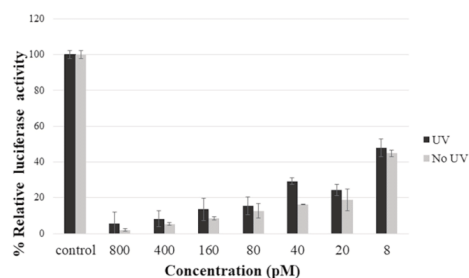


Fig. 3. Reduction in normalized firefly luciferase expression for siRNA 1 at 8, 20, 40, 80, 160, 400 and 800 pM concentrations in HeLa cells and lysed 22 h post transfection. 'UV' corresponds to the siRNA being exposed under a 365 nm UV lamp for inactivation prior to transfection. 'No UV' corresponds to active siRNA being transfected in HeLa cells in the absence of UV light.

In the first set of experiments, the cells were lysed 22 h post transfection and luciferase activity was monitored. siRNA 1 exhibits efficient and potent gene-silencing activity, comparable to wt siRNA ($IC_{50} = 4.69$ pM), in both the presence and absence of UV light (Fig. 3). As such, there does not appear to be a discernible difference in activity between the *cis* ($IC_{50} = 5.1$ pM) and *trans* ($IC_{50} = 5.5$ pM) form of siRNA 1. In contrast, a small two-fold change in gene-silencing activity between the isomeric forms of siRNA 2 (*cis*)

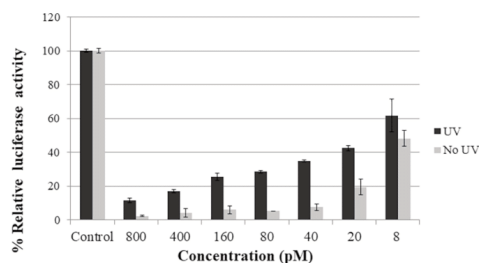


Fig. 4. Reduction in normalized firefly luciferase expression for siRNA 2 at 8, 20, 40, 80, 160, 400 and 800 pM concentrations in HeLa cells and lysed 22 h post transfection. 'UV' corresponds to the siRNA being exposed under a 365 nm UV lamp for inactivation prior to transfection. 'No light' corresponds to active siRNA being transfected in HeLa cells in the absence of UV light.

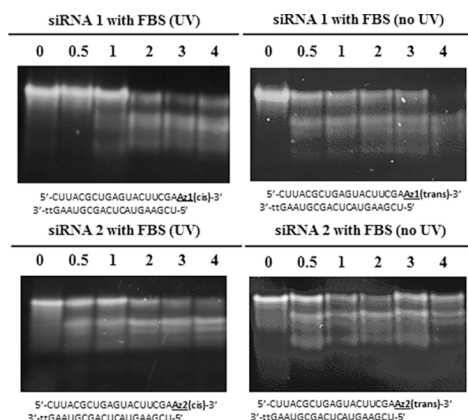


Fig. 5. Nuclease stability assay. 20% Non-denaturing polyacrylamide gel with degradation products of siRNAs 1 and 2 after incubation with 13.5% fetal bovine serum at 37 °C from 0 h to 4 h.

(IC_{50} = 14.6 pM) and siRNA 2 (*trans*) (IC_{50} = 7.4 pM) was observed (Fig. 4). Thus, in the absence of UV light, the gene-silencing profile matches that of both siRNAs 1 and wt siRNA; however, in the presence of UV light, a small loss of gene-silencing ability is observed. When the azobenzene is subjected to UV light, the *cis* isomer dominates, thus rendering the siRNA slightly less effective. In these experiments, the cells are lysed 22 h post transfection. The *cis* isomeric form of azobenzene has been shown to have a half-life at 37 °C of approximately 4 hours²². Thus, the small change observed in activity with siRNA 2 is likely due to thermal relaxation of the *cis* azobenzene to its more favored *trans* form.

When we perform these experiments on a shorter 8 h time scale (Fig. S-5), larger differences in IC_{50} are observed for the *cis* and *trans* azobenzene form of siRNA 2 because less time is given for the *cis* form to relax back to the *trans* form. For example, we observe a 10-fold difference in IC_{50} s for siRNA 2 (*cis*) (134.7 pM) and siRNA 2 (*trans*) (13.5 pM). In contrast to the 22 h post-transfection experiment, siRNA 1 (*cis*) and siRNA 1 (*trans*), showed no significant difference in activity (5.2 pM and 3.2 pM, respectively) in the 8 h post-transfection experiment.

To investigate whether the effect of nuclease stability correlated to gene-silencing, we evaluated the siRNAs in the presence of nuclease-rich media, as shown in Fig. 5. siRNA 1 in the absence of UV light remains predominantly in the *trans* form, and as can be observed, cleavage starts around 30 min. Most of the siRNA 1 is cleaved after four hours. In contrast, siRNA 1, in its predominantly UV *cis* activated form, appears to be degraded at a slower rate compared to *trans*. Very little degradation occurs after 30 min, and a dominant band corresponding to the starting duplex remains at 4 h. Thus, for siRNA 1, it appears that some increase in nuclease resistance is observed when the siRNA is subjected to UV light.

For siRNA 2, both gels show cleavage starting at 30 min, in addition to some fraction remaining of the intact siRNA at 4 h. There does not appear to be a large difference in cleavage activity between them.

Fig. 6 plots the intact remaining duplex siRNA as a function of time. When siRNA 1 was subjected to UV light, the duplex strand remained more stable compared to the siRNA that was not subjected to UV light at shorter time-points. For the siRNA 1 that was not subjected to UV light, degradation commenced immediately, and it can be seen that roughly 50% of the native structure is degraded over 30 min. In contrast, with siRNA 2, some increase in stability exists with the UV-treated

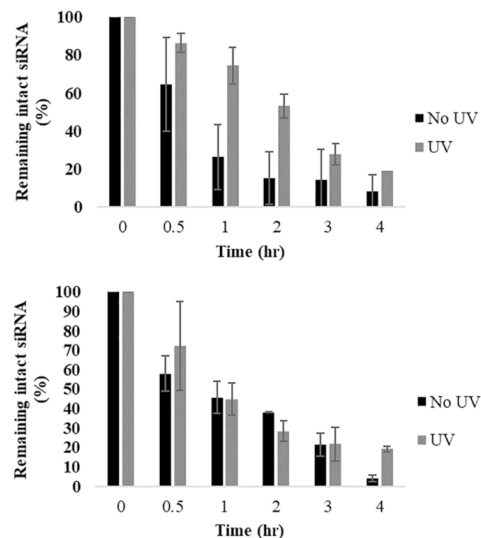


Fig. 6. Quantification of remaining intact siRNA using ImageJ software. The 0 min time point was used as 100% intact siRNA (Top siRNA 2 and bottom siRNA 1). Graphical representation of intact siRNA derived from Fig. 5.

siRNA at 1 and 2 h, but no large difference in degradation patterns as visualized on the gel.

In conclusion, we are reporting the stability and gene-silencing efficiency of siRNAs containing azobenzene at the 3'-end of the sense strand. The siRNAs differ by the number of carbons between the aromatic group and the oxygen atom. In siRNA 1, one carbon is placed between the aromatic group and the oxygen; whereas in siRNA 2, two carbons are present. In both cases, isomerization of the 3'-azobenzene to its *cis* form by UV light appears to modestly enhance nuclease stability in the presence of fetal bovine serum at some time points. There appears to be a difference between the two azobenzene derivatives, and while they differ only in a single methylene linker on each side of the functional moiety, it could be that the components of the RISC complex and exonucleases do not distinguish siRNAs in both isomeric *cis*- and *trans*-azobenzene forms. However, we observed a larger difference in both the RNAi activity and stability assays with the larger azobenzene species, perhaps due to its slightly larger isomeric structures that can better differentiate between nucleases and components of the RISC complex. This could explain why the *cis* form of siRNA 2 shows a larger difference in stability and activity compared to the *trans* form, whereas the siRNA 1 linker showed almost the same activity. As noted, this difference is time dependent and gene-silencing data measured 8 h post-transfection for siRNA 2 shows a large difference in IC_{50} , whereas this difference diminishes for longer experiments (22 h). Nevertheless, both isomeric forms appear to be compatible with the siRNA pathway. Wild-type luciferase siRNAs have been shown to be effective up to one week after transfection in HeLa cells,²³ and this modification could allow for a longer effective experimental window when in the *cis* isomer, for better temporal control of nuclease stability. Interestingly, since the *cis*-azobenzene form of these siRNAs exhibit increased nuclease resistance they can be used to increase the duration of the gene silencing efficacy window. Most wild-type siRNAs begin degrading within 30 min to 1 h, but our modification prevents this from occurring so rapidly, and as a result would allow the gene silencing to persist. As another application, the siRNA in the isomeric *cis*-azobenzene form could be transfected into

the cells and after a certain period of time activated with visible light (or allowed to reactivate naturally). As a potential future work, we could also inactivate the siRNAs *in vivo* after transfection to change from a time period of high gene silencing to a period of moderate gene silencing to examine subtle effects of gene function. In addition, the 3'-azobenzene could be used as a minimal chemical modification for other siRNA targets, also giving enhanced nuclease stability.²⁴ Furthermore, the 3'-end modification could allow for subtle fine-tuning of gene-silencing activity when small changes in inhibition over short time frames are desired. Future work involves designing photo-responsive 3'-azobenzene groups that can further improve the activity and properties of the siRNAs, as well as testing inactivation *in vivo* after transfection.

Acknowledgment

We acknowledge the Natural Sciences and Engineering Research Council (NSERC) for funding.

Appendix A. Supplementary data

Supplementary data to this article can be found online at <https://doi.org/10.1016/j.bmcl.2018.10.044>.

References

1. Reischl D, Zimmer A. *Nanomedicine*. 2009;5:8–20.
2. Fire A, Xu SQ, Montgomery MK, Kostas SA, Driver SE, Mello CC. *Nature*. 1998;391:806–811.
3. Prakash TP, Allerson CR, Dande P, et al. *J Med Chem*. 2005;48:4247–4253.
4. Aagaard L, Rossi JJ. *Adv Drug Deliv Rev*. 2007;59:75–86.
5. Deleavey GF, Damha MJ. *Chem Biol*. 2012;19:937–954.
6. Robbins M, Judge A, MacLachlan I. *Oligonucleotides*. 2009;19:89–102.
7. Chernolovskaya EL, Zenkova MA. *Curr Opin Mol Ther*. 2010;12:158–167.
8. Wan WB, Seth PP. *J Med Chem*. 2016;59:9645–9667.
9. Chiu YL, Rana TM. *RNA*. 2003;9:1034–1048.
10. Elmén J, Thonberg H, Ljungberg K, et al. *Nucl Acids Res*. 2005;33:439–447.
11. Braasch DA, Jensen S, Liu Y, et al. *Biochemistry*. 2003;42:7967–7975.
12. Terrazas M, Kool ET. *Nucl Acids Res*. 2008;37:346–353.
13. Lubbe AS, Szymanski W, Feringa BL. *Chem Soc Rev*. 2017;46:1052–1079.
14. Brieke C, Rohrbach F, Gottschalk A, Mayer G, Heckel A. *Angew Chem Int Ed*. 2012;51:8446–8476.
15. Beharry AA, Woolley GA. *Chem Soc Rev*. 2011;40:4422–4437.
16. Asanuma H, Liang XG, Yoshida T, Komiyama M. *ChemBioChem*. 2001;2:39–44.
17. Wu L, Wu Y, Jin HW, Zhang LR, He YJ, Tang XJ. *MedChemComm*. 2015;6:461–468.
18. Hammill ML, Isaacs-Trépanier C, Desaulniers J-P. *ChemistrySelect*. 2017;2:9810–9814.
19. Liu Y, Sen D. *J Mol Biol*. 2004;341:887–892.
20. Yamana K, Kan K, Nakano H. *Bioorg Med Chem*. 1999;7:2977–2983.
21. Li J, Wang X, Liang X. *Chem Asian J*. 2014;9:3344–3358.
22. Hartley GS. *J Chem Soc*. 1938:633–642.
23. Bartlett DW, Davis ME. *Biotechnol Bioeng*. 2007;97:909–921.
24. Eithymiou TC, Peel B, Huynh V, Desaulniers J-P. *Bioorg Med Chem Lett*. 2012;22:5590–5594.

Supporting Information

Stability and Evaluation of 3'-Azobenzene Modified Short Interfering RNAs

Matthew Hammill, Ayushi Patel, Maria Abd Alla and Jean-Paul Desaulniers

Faculty of Science, University of Ontario Institute of Technology, 2000 Simcoe Street North,

Oshawa, Ontario L1H 7K4 Canada

Jean-Paul.Desaulniers@uoit.ca

Table of Contents

General.....	S2
Procedure for for Absorbance Spectra Experiments.....	S2
Procedure for HPLC Characterization	S2
Procedure for Nuclease Stability Assays.....	S2
Procedure for Maintaining Cell Cultures of HeLa Cells.....	S3
Procedure for siRNA Transfections.....	S3
Procedure for <i>in vitro</i> Dual Luciferase Assay.....	S3
Procedure for light inactivation of azobenzene modified siRNA (<i>trans</i> to <i>cis</i>).....	S4
Figures and Tables	
Figure S-1: Absorbance Profile of siRNA 1 when exposed to UV and Visible light.....	S5
Figure S-2: Absorbance Profile of siRNA 2 when exposed to UV and Visible light.....	S5
Figure S-3: Comparative HPLC Chromatogram of untreated siRNA 1 and UV light exposure.....	S6
Figure S-4: Comparative HPLC Chromatogram of untreated siRNAzo 2 and UV light exposure.....	S6
Figure S-5: Dose-responsive Curves of selected siRNAs using the Dual-Reporter Luciferase Assay 8 hour timepoint.....	S7
Figure S-6: Dose-responsive Curves of selected siRNAs using the Dual-Reporter Luciferase Assay 24 h timepoint.....	S8
Figure S-7: UV Light Degradation Assay.....	S9
Figure S-8: Deconvolution Results for siRNA 1.....	S10
Figure S-9: Deconvolution Results for siRNA 2.....	S11
References.....	S11

General

Unless otherwise indicated all starting reagents used were obtained from commercial sources without additional purification. Oligonucleotides were synthesized according to our groups previously published protocol, using standard solid phase synthesis and materials.¹ Antisense luciferase siRNA from Integrated DNA Technologies (IDT) was used for this study.

Procedure for Absorbance Spectra Experiments

All absorbance spectra measurements were done on a Jasco J-815 CD with temperature controller. Measurement was recorded from 200 -500 nm at 10 °C at least 3 times. UV treated samples were placed under a UVP UVL-23RW Compact UV lamp 4.00 W 365 nm for the indicated time at 25 °C . Visible light treated samples were placed under a 60.0 W daylight bulb from NOMA in standard desk lamp.

Procedure for HPLC Characterization

HPLC chromatograms were obtained on a Waters 1525 binary HPLC pump with a Waters 2489 UV/Vis detector using the Empower 3 software. A C18 4.6 mm x 150 mm reverse phase column was used. Conditions were 5% acetonitrile in 95% 0.1 M TEAA (Triethylamine-Acetic Acid) buffer up to 100% acetonitrile over 40 min.

Procedure for Nuclease Stability Assays

SiRNAs 8, 13 and wt were tested for nuclease stability at a concentration of 12 μ M. The time points tested for the stability were 0, 0.5, 1, 2, 3 and 4 hours for each siRNA. In micro-centrifuge tubes 1 μ L of 12 μ M siRNA stock solution was added to 9 μ L distilled water (10 μ L total volume, 0 h time point) or 7.65 μ L distilled water along with 1.35 μ L fetal bovine serum (FBS) (10 μ L total volume, all other time points) mixed and then incubated at 37°C for each time point. At each hour, the sample was prepared and placed in the incubator in a sequential order, starting with the 4-hour sample first. After the incubation, samples were run on a 20% non-denaturing polyacrylamide gel. Samples were mixed with 10 μ L of non-denaturing loading dye and loaded onto the gel. The gel was run using a stacking method, in which the gel was first run at 30V for approximately 2 hours until the siRNA was evenly loaded. The gel was then run for an additional 20 hours at 70V. The gel was stained using 3X GelRed nucleic acid dye for 30-45 minutes and was visualized via Flurochem SP (Fisher Scientific).

Procedure for Maintaining Cell Cultures of HeLa Cells

For biological analysis of these siRNAs in a live environment, human epithelial cervix carcinoma cells were used (HeLa cells). They were kept in 250 mL vented culture flasks using 25.0 mL of DMEM with 10% fetal bovine serum and 1% penicillin-streptomycin (Sigma) in an incubator set for 37 °C @ 5% CO₂ humidified atmosphere.

Once cell lines became confluent (80-90%) they were passaged by washing 3 times with 10 mL of phosphate buffered saline (NaCl 137 mM, KCl 2.70 mM, PO₄³⁻ 10.0 mM, pH 7.40) and incubated with 3.00 mL of 0.25% trypsin (SAFC bioscience) for 4 min @ 37 °C to detach the cells. The cells were transferred to a 50.0 mL centrifuge tube after the addition of 10.0 mL of DMEM solution and pelleted at 2000 rpm for 5 minutes. The supernatant was discarded and the pellet resuspended in 5.0 mL DMEM with 10% FBS.

A standard haemocytometer was used to obtain cell counts, after which the cells were diluted to a final concentration of 1.00 x 10⁶ cells/mL for subsequent assays. To continue the cell line 1.00 mL of freshly passaged cells was added to 24.0 mL of DMEM/10% FBS and 1% penicillin-streptomycin at 37 °C in a new culture flask while the rest were used for assays.

Procedure for siRNA Transfections

100 µL of cells (total 1.00 x 10⁵) were transfected into 12 well plates (Falcon®) with 1 mL of DMEM (10% FBS, 1% penicillin-streptomycin) and incubated at 37 °C with 5% CO₂. After 24 hours the cells were transfected with various concentrations of siRNAs, along with both pGL3 (Promega) and pRLSV40 luciferase plasmids using Lipofectamine 2000 (Invitrogen) in Gibco's 1X Opti-Mem reduced serum media (Invitrogen) according to the manufacturer's instructions. 1.00 µL of siRNA was added along with 2.00 µL (pGL3 200 ng) and 0.50 µL pRLSV40 (50.0 ng) to 100 µL of 1X Opti-Mem in a microcentrifuge tube and kept on ice for 5 min. In a different microcentrifuge tube, 1.00 µL of Lipofectamine 2000 (Invitrogen) was mixed with 100 µL of Gibco's 1X Opti-Mem reduced serum media (Invitrogen) and incubated at room temperature for 5 min. After 5 minutes the tubes were mixed and incubated at room temperature for 20 min and then the entire contents transferred to the wells of the 12 well plate.

Procedure for *in vitro* Dual-Reporter Luciferase Assay

100 µL of cells (total of 1.00 x 10⁵ cells) were added to 12 well plates (Falcon®) with 1 mL of growth media (DMEM 10% FBS, 1% penicillin-streptomycin) and incubated at 37 °C with 5% CO₂. After 24 hours the cells were transfected with 8.00, 20.0, 40.0, 160, 400 and 800 pM concentrations of siRNAs, along with both pGL3 (Promega) and pRLSV40 luciferase plasmids using Lipofectamine 2000 (Invitrogen) in Gibco's 1X Opti-Mem reduced serum media (Invitrogen) according to the manufacturer's instructions. After a set amount of time (8, 12 or 22h) the cells were incubated at room temperature in 1X passive lysis buffer (Promega) for 20 minutes. The lysates were collected and loaded onto a 96 well, opaque plate (Costar). With a Dual-Luciferase reporter Assay kit (Promega), Lar II and Stop & Glo® luciferase substrates were sequentially added to the lysates and enzyme activity was measured through luminescence of both *firefly/Renilla* luciferase on a Synergy HT (Bio-Tek) plate luminometer. The ratio of *firefly/Renilla*

luminescence is expressed as a percentage of reduction in *firefly* protein expression to siRNA efficacy when compared to untreated controls. Each value is the average of at least 3 different experiments with standard deviation indicated.

Procedure for Light Inactivation of Azobenzene Modified siRNA (*trans* to *cis*)

1.00 μ L of the desired siRNA was added to a microcentrifuge tube and exposed to a 4.00 W 365 nm UV lamp (UVP) and was exposed for at least 4 hours.

After UV exposure the siRNA can be used in the transfection procedure above, but the transfection must be done in the dark room, to prevent the *cis* to *trans* conversion back into the active form.

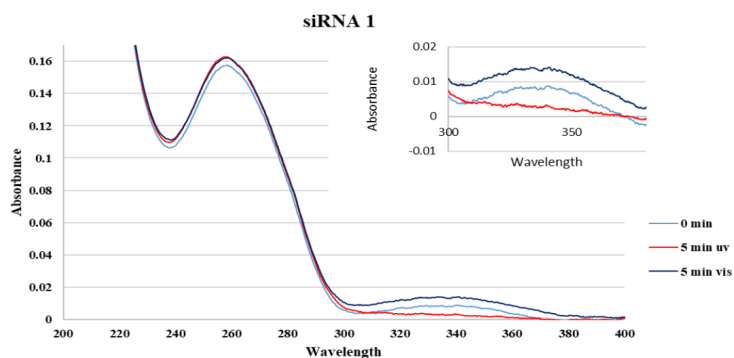


Figure S-1. Absorbance Profile of siRNAzo 1 when exposed to UV and Visible light in 500 μ L of a sodium phosphate buffer (90.0 mM NaCl, 10.0 mM Na₂HPO₄, 1.00 mM EDTA, pH 7.00) and scanned from 200-400 nm at 10 $^{\circ}$ C with a screening rate of 20.0 nm/min and a 0.20 nm data pitch.

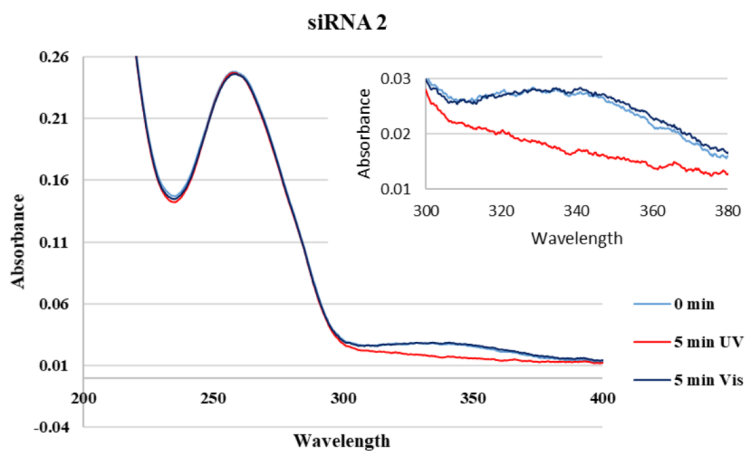
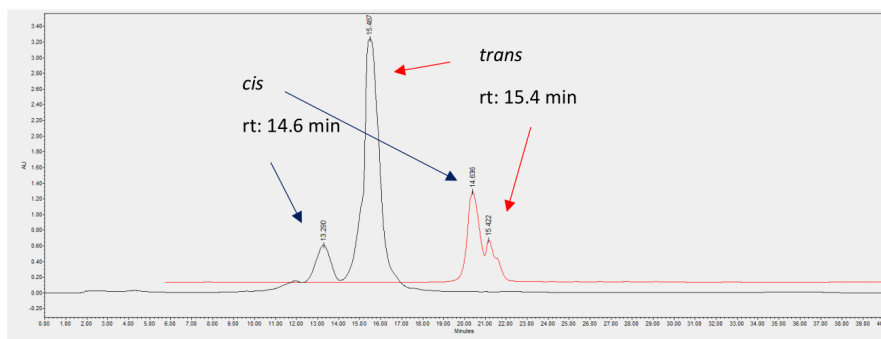
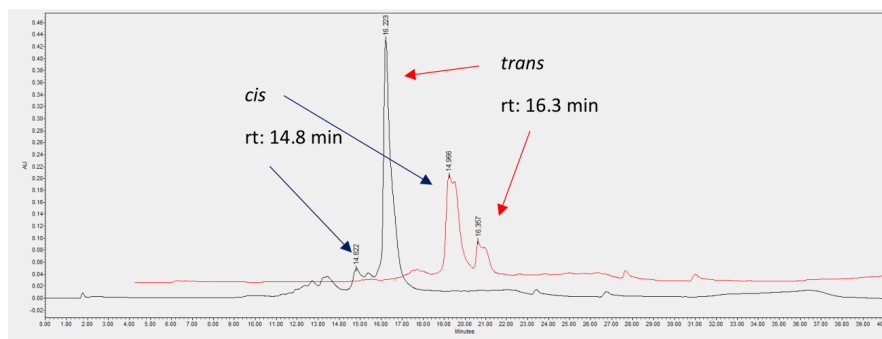


Figure S-2. Absorbance Profile of siRNAzo 2 when exposed to UV and Visible light in 500 μ L of a sodium phosphate buffer (90.0 mM NaCl, 10.0 mM Na₂HPO₄, 1.00 mM EDTA, pH 7.00) and scanned from 200-400 nm at 10 $^{\circ}$ C with a screening rate of 20.0 nm/min and a 0.20 nm data pitch.



S-3. HPLC chromatogram for siRNA 1. Blue indicates no treatment, red corresponds to UV exposure. Arrows indicate *trans* and *cis* peaks and retention times. Conditions were 5% acetonitrile in 95% 0.1 M TEAA (Triethylamine-Acetic Acid) buffer up to 100% acetonitrile over 40 min.



S-4. HPLC chromatogram for siRNA 2. Blue indicates no treatment, red corresponds to 10 min UV exposure. Arrows indicate *trans* and *cis* peaks and retention times. Conditions were 5% acetonitrile in 95% 0.1 M TEAA (Triethylamine-Acetic Acid) buffer up to 100% acetonitrile over 40 min.

Table S-1. Measurement of conformer abundance in siRNAs 1 and 2, with both no UV and UV treated samples.

siRNA	Treatment	<i>trans</i>	% <i>cis</i>
1	No UV	83.9	16.1
	UV	23.5	76.5
2	No UV	90.4	9.6
	UV	77.1	22.9

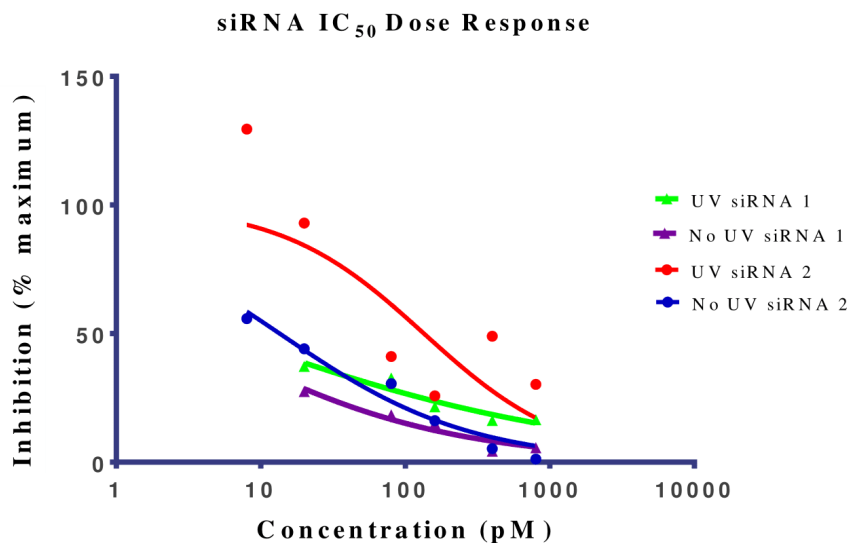


Figure S-5. Dose-responsive curves of siRNAzOs 1 and 2 with a 3' end azobenzene modification using the Dual Reporter Luciferase Assay at 8 h timepoint. The siRNAzOs were tested at 6 concentrations from 8.00-800 pM with *firefly* luciferase expression normalized to *Renilla* luciferase. All IC₅₀ values were calculated with Prism using the variable slope model. The IC₅₀ values were as follows: siRNA 1 UV (5.2 pM), No UV (3.2 pM); siRNA 2 UV (134.7 pM), No UV (13.5 pM), where UV describes exposure of the siRNA before transfection to the UV light source for 4 hours, and No UV corresponds to the active siRNA not exposed to the UV lamp.

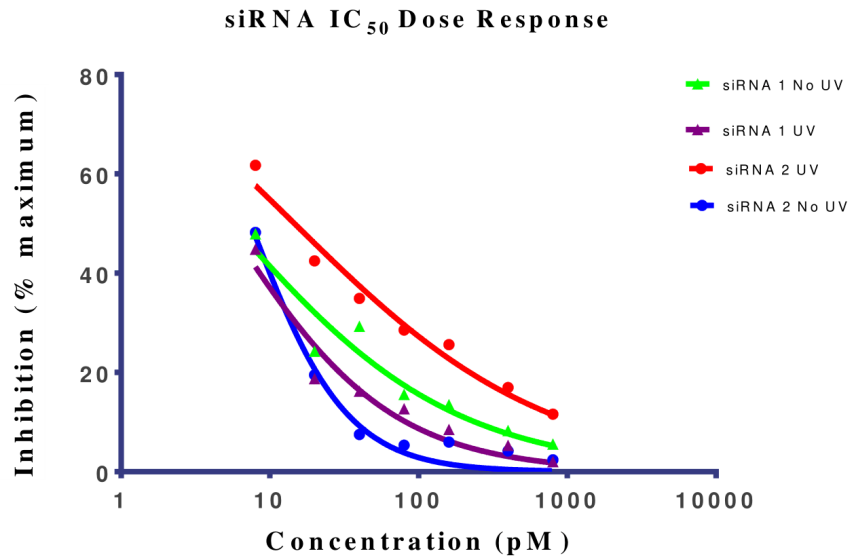


Figure S-6. Dose-responsive curves of siRNAzOs 1 and 2 with a 3' end azobenzene modification using the Dual Reporter Luciferase Assay at 22 h timepoint. The siRNAzOs were tested at 6 concentrations from 8.00-800 pM with *firefly* luciferase expression normalized to *Renilla* luciferase. All IC₅₀ values were calculated with Prism using the variable slope model. The IC₅₀ values were as follows: siRNA 1 UV (5.5 pM), No UV (5.1 pM); siRNA 2 UV (14.6 pM), No UV (7.4 pM), where UV describes exposure of the siRNA before transfection to the UV light source for 4 hours, and No UV corresponds to the active siRNA not exposed to the UV lamp.

	RNA 1		RNA 3	
UV	-	+	-	+



Figure S-7. Nuclease stability assay. 20% Non-denaturing polyacrylamide gel with no degradation products for RNAs **1** and **3** after incubation with no UV light (-) or UV light (+) for 4 hours at room temperature. RNA **1** corresponds to 5'-CUUACGCUGAGUACUUCGAAz1-3', and RNA **3** corresponds to 5'-CUUACGCUAz1GUACUUCGAdTdT-3'.¹ Az1 corresponds to the azobenzene derivative synthesized from 4-nitrobenzyl alcohol.

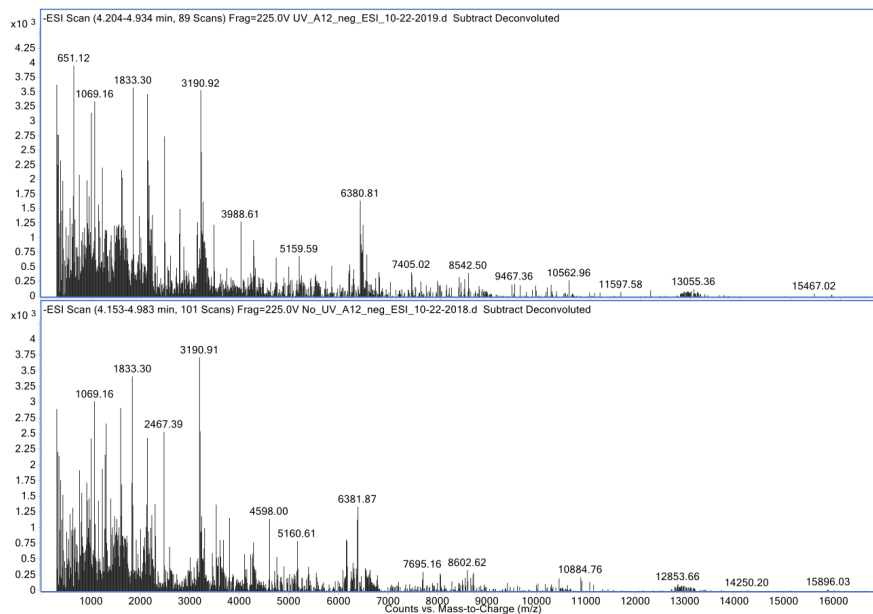


Figure S-8. Deconvolution results for the sense strand of siRNA **1**. ESI-HRMS (ES^-) m/z calculated for this strand is 6382.84, found 6381.87. Top: UV exposed siRNA (4 hours). Bottom: no UV exposure.

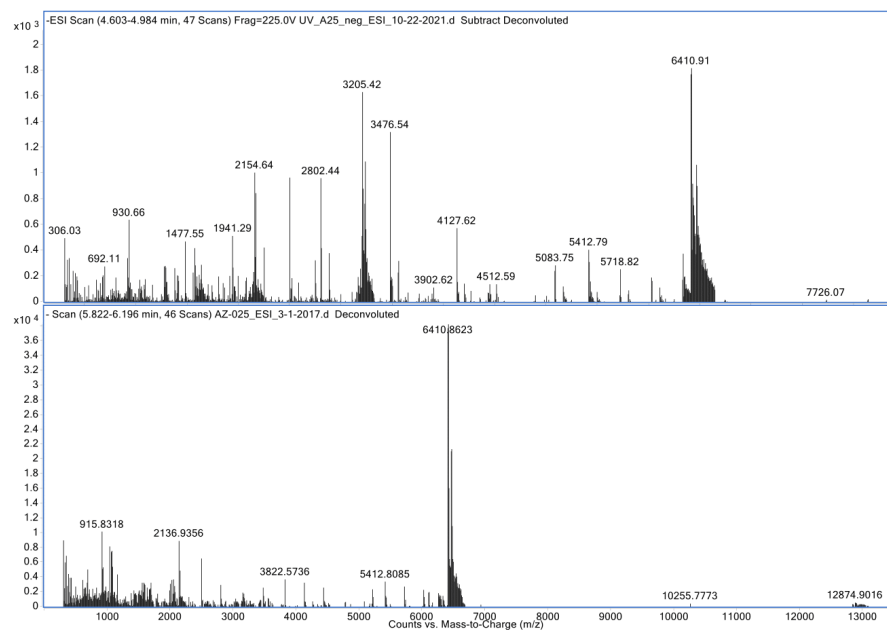


Figure S-9. Deconvolution results for siRNA 2. ESI-HRMS (ES⁻) m/z calculated for the sense strand of siRNA 2 is 6410.84, found 6410.91. Top: UV exposed siRNA (4 hours). Bottom: no UV exposure.

References

1. M. L. Hammill, C. Isaacs-Trepanier and J. P. Desaulniers, *ChemistrySelect*, **2017**, 2, 9810-9814.

Appendix II. Manuscript II and Supplementary Data



Reversible control of RNA interference by siRNAzost†

Cite this: *Org. Biomol. Chem.*, 2020, **18**, 41Received 21st November 2019,
Accepted 22nd November 2019

DOI: 10.1039/c9ob02509j

rsc.li/obc

Matthew L. Hammill, Golam Islam and Jean-Paul Desaulniers *

In this study, we report the reversible control of RNA interference using siRNAzost, a class of siRNAs that contain azobenzene. Herein, we demonstrate that it is possible to take an active siRNAzo, and inactivate it for up to 24 hours. We also demonstrate reversibility of these siRNAzost within cell culture. For example, active siRNAzost can be inactivated in cell culture with ultraviolet light, and then reactivated with visible light. In addition, we also show that siRNAzost can be activated and inactivated towards the endogenous target gene, *BCL2*.

The RNA interference (RNAi) pathway is an endogenous defense mechanism that targets viral and parasitic double-stranded RNA (dsRNA), and regulates gene expression in eukaryotes. Fire and Mello published a paper in 1998, identifying double-stranded RNAs as gene-silencing agents in the nematode *Caenorhabditis elegans*.¹ Ever since this discovery, there has been interest in utilizing this pathway for therapeutics and biomolecular tools.^{2–4} The most recent FDA-approved siRNA is Onpatro, which is used for the treatment of hereditary transthyretin amyloidosis (hATTR).⁵ Despite this success, siRNAs as therapeutics often come with several known problems, such as poor stability, toxicity, off-target and tissue specific targeting. However, one issue in the field that has largely been overlooked is reversing RNAi activity in the event of adverse siRNA off-target effects. Some recent research shows that short locked nucleic acid-modified oligonucleotides complementary to the seed region of the guide strands can reverse siRNA activity.⁶ However, despite this study, more research and methods to inactivate siRNA function is needed. In this paper, we describe the utility of photoreversibly controlling RNAi using an siRNAzo (azobenzene-containing siRNA).

Several advances over the last decade have led the development of photoresponsive siRNAs, which generally are dsRNAs that are inactive when entered inside of the cell, and then are activated with light. The first example was developed by Friedman and coworkers, in which they used a backbone-modified siRNA labeled with 1-(1-diazoethyl)-4,5-dimethoxy-2-nitrobenzene (DMNPE-N₂). Upon exposure with UV light ($\lambda > 320$ nm), the groups are removed to yield an active siRNA.⁷ Heckel and coworkers have used photoresponsive protecting groups on guanine and thymidine nucleotides of the guide strand of siRNAs, which becomes uncaged to UV light.⁸ Most recently, Mokhir and Meyer developed a 5'-labelled alkoxyanthracenyl siRNA, which becomes uncaged via a singlet oxygen (¹O₂) photogenerated photosensitizer on the 3'-end of the guide strand. Uncaging occurs with green or red light to yield an active siRNA.⁹ Despite these innovative advances, an inactive siRNA complex is *irreversibly* photoactivated to yield an active siRNA. The process cannot be reversed, and it is not entirely clear what effect the by-products of the caged functional groups when released may have on the cell. Having the ability to reversibly control the activity of an siRNA within the cell would offer greater spatial control of the siRNA. This reversibility could bypass and eliminate the undesired off-target side effects.

Azobenzene is an attractive photoresponsive molecule because of its ability to photo-isomerize in the presence of UV and visible light. This causes a large conformational change in the molecule, which can be used to disrupt biomolecular structures.¹⁰ The more stable isomer, *trans* is the normal resting state of the molecule, but through the addition of energy in the form of UV light between 330–365 nm, photo-isomerization occurs and the molecule adopts a *cis* isomeric form. The *cis* form of azobenzene is less stable due to steric hindrance and strain on the N=N bond and thus can be converted back to *trans* with visible light above 450 nm.¹¹ Because of these unique and useful properties, azobenzene has been used in many applications, including its incorporation into oligonucleotides (see Fig. 1) since it is relatively easy to synthesize and has a high quantum yield when photo-switching.¹²

University of Ontario Institute of Technology, Faculty of Science, 2000 Simcoe Street North, Oshawa, Ontario L1G 0C5, Canada.

E-mail: jean-paul.desaulniers@ontariotechu.ca

† Electronic supplementary information (ESI) available. See DOI: 10.1039/c9ob02509j

Communication

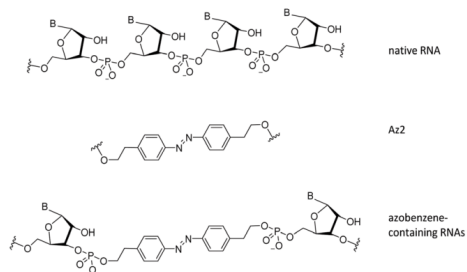


Fig. 1 Structural differences between native RNA, and azobenzene-containing RNAs. Az2 corresponds to the azobenzene unit used in this study.

Previous work in our group utilized azobenzene's photo properties in order to make siRNAzOs, which are siRNA molecules that contain azobenzene.^{13,14} Fig. 2 highlights the photo-switching properties of the siRNAzo. In the native *trans* form, the siRNAzo is active. When the siRNAzo is treated with UV light, the azobenzene unit adopts a *cis* conformation, and thus inactivates the siRNAzo. Restoration of activity can proceed by thermal relaxation and/or visible light.

The siRNAzOs that we generated contained the azobenzene within the central region of the sense strand (see Table 1). siRNAzo 1 replaces positions 8 and 9 from the 5'-end of the sense strand. Moving this azobenzene unit (Az2) one nucleobase at a time, siRNAzOs 2, 3, and 4 replace positions 9 and 10, 10 and 11, and 11 and 12 from the 5'-end of the sense strand, respectively. The siRNAzOs 5–7 designed to target the endogenous *BCL2* gene also contain the azobenzene unit within the central region of the sense strand. Our previous work showed that not only did the siRNAzOs 1–4 have excellent knockdown at picomolar concentrations, but we could also control the siRNAzo's activity through UV inactivation prior to the trans-

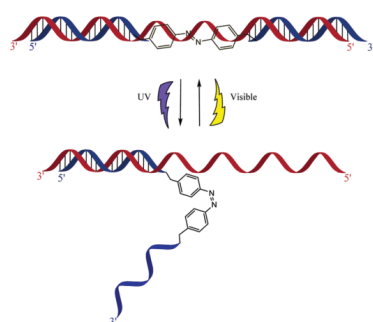


Fig. 2 Photoinduced inactivation and reactivation of siRNAzOs. The blue strand corresponds to the sense strand, and contains the azobenzene moiety. The red strand corresponds to the antisense strand.

Table 1 Table of RNAs used and its target^a

siRNAzo	siRNAzo duplex	Target
wt	5'-CUUACGCUGAGUACUUCGAtt-3' 3'-ttGAAUGCGACUCAUGAAGCU-5'	Luciferase
1	5'-CUUACGC <u>Az2</u> AGUACUUCGAtt-3' 3'-ttGAAUGCGACUCAUGAAGCU-5'	Luciferase
2	5'-CUUACGC <u>Az2</u> GUACUUCGAtt-3' 3'-ttGAAUGCGACUCAUGAAGCU-5'	Luciferase
3	5'-CUUACGC <u>Az2</u> UACUUCGAtt-3' 3'-ttGAAUGCGACUCAUGAAGCU-5'	Luciferase
4	5'-CUUACGC <u>Az2</u> ACUUCGAtt-3' 3'-ttGAAUGCGACUCAUGAAGCU-5'	Luciferase
5	5'-GCCUUC <u>Az2</u> GAGUUCGGUgtt-3' 3'-tCGGAAGAAACUCAAGCCAC-5'	<i>BCL2</i>
6	5'-GCCUUC <u>Az2</u> AGUUCGGUgtt-3' 3'-tCGGAAGAAACUCAAGCCAC-5'	<i>BCL2</i>
7	5'-GCCUUC <u>Az2</u> UUCGGUgtt-3' 3'-tCGGAAGAAACUCAAGCCAC-5'	<i>BCL2</i>

^a **Az2** corresponds to the azobenzene derivative synthesized from 4-nitrophenylethyl alcohol; the top strand corresponds to the sense strand; the bottom strand corresponds to the antisense strand. In all duplexes, the 5'-end of the bottom antisense strand contains a 5'-phosphate group.

fection of the siRNAs.¹³ We also demonstrated the ability to restore siRNA activity through the application of the broad-band visible light greater than 450 nm.

While this work was incredibly promising and useful, we were limited by the azobenzenes propensity to thermally relax back to *trans* when in the *cis* conformation. Azobenzene's half life at 37 °C is approximately 4 hours,¹⁵ and this limited the durations we could do these experiments at, and consequently limiting their usefulness for longer term experiments.

In this current manuscript, and building from our previous work, we demonstrate that our siRNAzOs can be inactivated post-transfection, inside the cells through the controlled application of UV light to the cell culture without damaging the cells. We are also able to reactivate the siRNAzOs with visible light. Furthermore, we are able to complete this deactivation/activation cycle up to two times for an siRNAzo. To the best of our knowledge, this marks the first report of using an active siRNA, and inactivating it within cell culture, and then later reversibly activating it. In order to understand the reversible gene-silencing effect observed in our study, we first must understand the RNAi gene-silencing mechanism.

When a siRNA is incorporated into an active antisense-RISC complex, the sense strand is released. This active antisense strand complex can then target its mRNA for cleavage. However, once this active antisense-RISC complex forms, we are not able to inactivate its function reversibly because the azobenzene modification is contained within the sense strand. Thus, within the cell, there is an equilibrium that exists between unbound siRNAs and its bound active antisense-RISC complex. Yet, out of the total siRNA molecules internalized into the cell, it has been shown that only around 4% or less is actively associated with the RISC complex.¹⁶ By inactivating unbound siRNAs in the cell, we can prevent further loading to

the RISC complex, and prevent the formation of more active antisense-RISC complexes. This in turn would reduce the amount of gene-silencing over time.

In our previous study, we observed UV-mediated inactivation of the siRNAzo to be effective at 8-hour time points, but at 12 hours the siRNAzo resumed some activity. Although the 8-hour time point is optimal for short assays, many gene expression studies go beyond 8 hours, and we wanted to develop a more robust system that was effective beyond this time window. Using the Dual-Luciferase Reporter® Assay (Promega), we modified our procedure (see ESI† for experimental procedures) to transfect active siRNAzos, in which we could inactivate with UV exposure (45 min dose) two hours post transfection. Within the 8-hour assay time-frame, one exposure of UV light was sufficient to keep the unbound siRNAzos inactive, but in order to extend this level of inactivity to a 24 hours window, we exposed the transfected cells to low repeated doses of UV light (a 45 minutes dose of low intensity 365 nm UV light, repeated every four hours, for a total of six UV exposures). Previous literature reported that this amount of UV light for up to 24 hours was not particularly harmful to the cells.¹⁷ We also conducted XTT assays on the cell cultures exposed to UV light, and no loss on cell viability was observed (see ESI S1†). Our gene-silencing results for these two assays are shown in Fig. 3, as a color-coded chart (see Fig. S12–S17 in the ESI† for the corresponding numerical bar graphs).

High luciferase activity is correlated to the intensity of the blue pixel, whereas low luciferase activity correlates to the intensity of the yellow pixel. There is a clear difference shown in luciferase activity between the UV and dark columns for both time points. Initially, at both 8- and 24-hour time points, luciferase activity is low for the dark-treated samples (dark), an

indication of strong RNAi activity. Exposure to UV light causes RNAi activity to diminish and as a result luciferase activity was found to increase as shown by the black and blue pixels in the color-coded chart (UV). More importantly, we were able to keep the unbound siRNAzo inactive for up to 24 hours, without thermal relaxation, which is a significant improvement over our previous study where after 12 hours the siRNAzo was active.¹³ Overall, the siRNAzos in their active form have good activity, however, we are able to inactivate their activity for up to 24 hours post transfection.

In the next experiment, we examined whether we could not only keep the unbound siRNAzo inactive for 24 hours, but also reactivate the unbound siRNAzos at a desired timepoint. The color-coded chart in Fig. 4 shows this data (see Fig. S18–S27 in the ESI† for the corresponding numerical bar graphs). As before, the UV-treated samples (UV) have only moderate to high luciferase activity, the visible-light treated samples (VIS) have moderate to low luciferase activity, and the no light (dark) samples have low luciferase activity. In all cases, we were able to take an inactive siRNAzo (1–4), and restore its RNAi activity as measured by low luciferase activity after visible light exposure.

We also explored whether the siRNAzo would remain intact after multiple on/off cycles. The gene-silencing data for this experiment is shown in Fig. 5 where the UV/VIS/UV/VIS bar (grey) shows that knockdown remains robust after two cycles. The first cycle was performed identically to the 8-hour inactivation assay highlighted in Fig. 3 and 4. After 8 hours, we then observed a 2-hour resting period of darkness to let the cells recover after which the cells were re-exposed to UV light for 45 min. After this exposure, the cells were allowed to rest for 1 h 15 min in the dark and then the visible light was utilized again for 30 min to restore the siRNAzo's activity. This second cycle was an important step to show that after one cycle, siRNAzo activity was maintained. At all three concentrations (160, 400, and 800 pM), activity was restored and this is shown with the grey bar in Fig. 5. There is a clear difference in gene-silencing activity between this grey bar and the blue inactivation bar, even after two doses of UV light. Additionally the UV/VIS/UV corresponds to 1.5 cycles (purple bar), and in Fig. 5 the gene-silencing data illustrates that after one inactivation cycle, we can reactivate and then deactivate the siRNAzo and it remains inactive for the remaining 24 h of the assay at 160 and 400 pM. At the higher concentration 800 pM, full inactivity is not fully restored, but is less active than the two full cycles (UV/VIS/UV/VIS) and the dark control (yellow). In addition, to investigate the effect of metabolism on the siRNAzos, we performed a glutathione reduction assay on the sense strand of an siRNAzo and observed minimal degradation for up to 24 hours as monitored by HPLC (see ESI S38† for details).

In addition, we also examined the inactivation and reactivation of an siRNAzo targeting the endogenous target, *BCL2* (Table 1). This anti-apoptotic endogenous target is of particular interest because it is one of the many oncogenes associated with several cancers that are upregulated.^{18,19} In a previous study of ours, we observed good knockdown of *BCL2* using

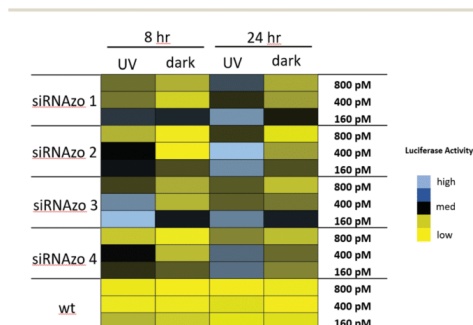


Fig. 3 Normalized firefly luciferase activity for siRNAzos 1–4 and wt at 160, 400 and 800 pM in HeLa cells monitored 8- and 24-hours post-transfection. UV corresponds to the siRNA being exposed under a 365 nm UV lamp for inactivation 2 h post transfection for 45 min (8 h), and for an additional 45 min of UV exposure every 4 hours (24 h). Dark corresponds to siRNAs being transfected in HeLa cells in the absence of UV light. 8-Hour fold changes differences in activity for siRNAzos 1–4 (UV vs. dark) for were between 2–55 fold, and 24-hour fold changes were between 1–7 fold. See ESI S1† for details.

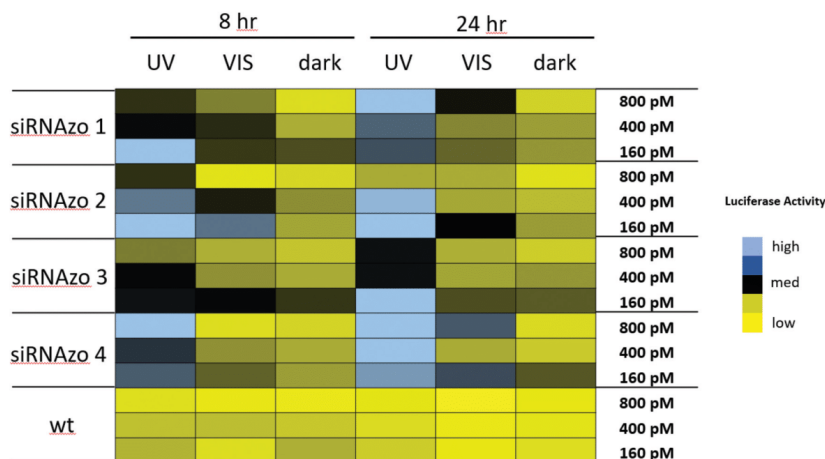


Fig. 4 Normalized firefly luciferase expression for siRNAzOs 1–4 and wt at 160, 400, and 800 pM in HeLa cells monitored 8- and 24-hours post-transfection. UV corresponds to the siRNA being exposed under a 365 nm UV lamp for inactivation 2 h post transfection for 45 min (8 h), and for an additional 45 min of UV exposure every 4 hours (24 h). VIS corresponds to visible light exposure 4 h after transfection. Dark corresponds to siRNAs being transfected in HeLa cells in the absence of UV light. Fold changes for siRNAs 1–4 (UV vs. dark) for 8 h were between 2 and 14 fold, and 24-hour fold change differences were between 3 and 21 fold. See ESI† for details.

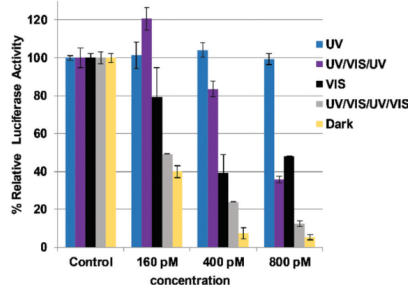


Fig. 5 Normalized firefly luciferase activity for siRNAzo 4 at 160, 400 and 800 pM in HeLa cells monitored 24 hours post-transfection. UV corresponds to the siRNAzo being exposed under a 365 nm UV lamp for inactivation 2 h post transfection for 45 min, and for an additional 45 min of UV exposure every 4 hours (six exposures total). UV/VIS/UV corresponds to one and a half consecutive UV/VIS cycles: UV inactivation, 2 hours post-transfection for 45 min, followed by visible light reactivation at 4 hours after transfection for 30 min. A 2-hour rest period of darkness followed by re-exposure to UV light for 45 min, being re-exposed every 4 hours to UV (45 min) afterwards (5 exposures total). VIS corresponds to visible light exposure 4 h after transfection. UV/VIS/UV/VIS corresponds to two consecutive UV/VIS cycles: UV inactivation, 2 hours post-transfection for 45 min, followed by visible light reactivation at 4 hours after transfection for 30 min. A 2-hour rest period of darkness followed by re-exposure to UV light for 45 min, followed by 1 h 15 min in the dark and then the visible light for 30 min (ESI S1† for details). Dark corresponds to siRNAzo 4 being transfected in HeLa cells in the absence of UV light.

siRNAs bearing a conformationally-constrained biphenyl spacer within the central region of the sense strand.²⁰ Using our photoresponsive protocol highlighted with the luciferase target, we conducted a similar experiment using real-time polymerase chain reaction (RT-PCR) to quantify the gene-silencing results.

The left half of Fig. 6 shows the results of the *BCL2* targeting siRNAzOs 5–7 at the 8-hour time point, with the siRNAzOs being pre-inactivated prior to transfection. Four hours post-transfection, UV light was administered. As demonstrated in Fig. 6, poor RNAi activity of the siRNAzo is observed as indicated by the presence of high *BCL2* expression. In an experiment involving the same transfection setup, visible light was administered four hours post-transfection. As is indicated, excellent gene silencing was observed. The difference between the active and inactive siRNAzo complexes is between two- and five-fold which is to our knowledge the first time an endogenous gene expression silencing profile could be controlled *via* the RNAi pathway in this manner. A dark control experiment involved transfecting an active *BCL2* siRNAzo, and maintaining its active form in the dark. As expected, this experiment showed excellent dose-dependent gene-silencing characteristics.

The right half of Fig. 6 shows the results for the longer 24 hour time point assay, in which we could maintain inactivation of the unbound siRNAzOs over the duration of the assay. As done similarly to the luciferase assays, transfections were carried out with the active form of siRNAzOs 5–7 and 2 hours later was exposed to repeated doses of 365 nm UV light to inactivate it. The changes in gene silencing activity are

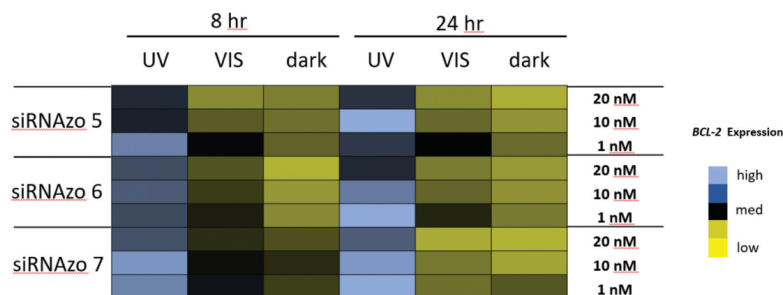


Fig. 6 *BCL2* expression normalized to 18S for siRNAzOs 5–7 at 1, 10 and 20 nM in HeLa cells monitored 8 (left) and 24 (right) hours post-transfection. UV corresponds to the siRNA being exposed under a 365 nm UV lamp for inactivation 2 h post transfection for 45 min (8 h), and for an additional 45 min of UV exposure every 4 hours (24 h). VIS corresponds to visible light exposure 4 h after transfection. Dark corresponds to siRNAzOs being transfected in HeLa cells in the absence of UV light.

between three- and five-fold for the different concentrations. This is consistent with the 8-hour assay. These two experiments show that our siRNAzOs are not only effective against endogenous targets, but we can inactivate their activity with UV light.

To account for the reversible gene-silencing observed by the siRNAzOs, we must consider both the populations of unbound siRNAzOs and siRNAzOs bound to RISC in the cell. The azobenzene modification is located on the sense strand of the siRNAzo. When the RISC-antisense strand is activated, the sense strand is no longer part of the complex. Thus, when UV light enters the cell, it is not capable of reversing the antisense strand from the RISC complex. This system differs in its reversibility mechanism compared to the reported high-affinity short oligonucleotides that reversibly target the siRNA guide strand.⁶ In our system, a population of siRNAzOs will be loaded by the RISC complex to form an active RISC-antisense complex, and another population of siRNAzOs will remain unbound. Thus, by subjecting the cells to UV light, we hypothesize that this would inhibit the loading of remaining free siRNAzOs to the RISC complex. Reactivation of this complex with visible light, would then restore the siRNAzo to its active form, which can then be loaded with more RISC complexes to further gene silence. We believe that this mechanism accounts for the reversible gene-silencing observed.

In conclusion, we are reporting here a significant improvement over prior reports of photoresponsive siRNA technology because we can reversibly control the activity of an exogenous and endogenous target with light. This newfound ability to reversibly control an endogenous target's activity after deployment into the tissue, would be useful for controlling adverse side effects in susceptible individuals. Many prior siRNAs that targeted a variety of diseases resulted in unexpected side effects.²¹ Another potential application for these siRNAzOs is their use as biomolecular tools to examine the effect of gene expression of complex and/or interrelated genes, in real time. Currently, the simultaneous deployment of multiple siRNAs

(siRNA cocktails) is limited because they are concurrently deployed at once post-transfection. Using our siRNAzo technology, we could allow for several different gene-silencing siRNAs to be controlled in real time *via* light. Our future works include red-shifting the azobenzene's isomerization wavelengths out of the UV portion of the spectrum, thereby allowing us to have unique photochemical control of these siRNAs using specific wavelengths.

Conflicts of interest

There are no conflicts to declare.

Acknowledgements

We thank the Natural Sciences and Engineering Research Council (NSERC) for funding.

Notes and references

- 1 A. Fire, S. Q. Xu, M. K. Montgomery, S. A. Kostas, S. E. Driver and C. C. Mello, *Nature*, 1998, **391**, 806.
- 2 L. Aagaard and J. J. Rossi, *Adv. Drug Delivery Rev.*, 2007, **59**, 75.
- 3 A. L. Hopkins and C. R. Groom, *Nat. Rev. Drug Discovery*, 2002, **1**, 727.
- 4 X. Shen and D. R. Corey, *Nucleic Acids Res.*, 2017, **46**, 1584.
- 5 D. Al Shaer, O. Al Musaimi, F. Albericio and B. G. de la Torre, *Pharmaceuticals*, 2019, **12**, 52.
- 6 I. Zlatev, A. Castoreno, C. R. Brown, J. Qin, S. Waldron, M. K. Schlegel, R. Degaonkar, S. Shulga-Morskaya, H. Xu, S. Gupta, S. Matsuda, A. Akinc, K. G. Rajeev, M. Manoharan and V. Jadhav, *Nat. Biotechnol.*, 2018, **36**, 509.

- 7 S. Shah, S. Rangarajan and S. H. Friedman, *Angew. Chem., Int. Ed.*, 2005, **44**, 1328.
- 8 V. Mikat and A. Heckel, *RNA*, 2007, **13**, 2341.
- 9 A. Meyer and A. Mokhir, *Angew. Chem., Int. Ed.*, 2014, **53**, 12840.
- 10 A. S. Lubbe, W. Szymanski and B. L. Feringa, *Chem. Soc. Rev.*, 2017, **46**, 1052.
- 11 C. Brieke, F. Rohrbach, A. Gottschalk, G. Mayer and A. Heckel, *Angew. Chem., Int. Ed.*, 2012, **51**, 8446.
- 12 A. A. Beharry and G. A. Woolley, *Chem. Soc. Rev.*, 2011, **40**, 4422.
- 13 M. L. Hammill, C. Isaacs-Trépanier and J.-P. Desaulniers, *ChemistrySelect*, 2017, **2**, 9810.
- 14 M. L. Hammill, A. Patel, M. A. Alla and J.-P. Desaulniers, *Bioorg. Med. Chem. Lett.*, 2018, **28**, 3613.
- 15 K. Yamana, K. Kan and H. Nakano, *Bioorg. Med. Chem.*, 1999, **7**, 2977.
- 16 Y. I. Pei, P. J. Hancock, H. Zhang, R. Bartz, C. Cherrin, N. Innocent, C. J. Pomerantz, J. Seitzer, M. L. Koser, M. T. Abrams, Y. Xu, N. A. Kuklin, P. A. Burke, A. B. Sachs, L. Sepp-Lorenzino and S. T. Barnett, *RNA*, 2010, **16**, 2553.
- 17 J. D. Stoien and R. J. Wang, *Proc. Natl. Acad. Sci. U. S. A.*, 1974, **71**, 3961.
- 18 M. L. Cleary, S. D. Smith and J. Sklar, *Cell*, 1986, **47**, 19.
- 19 G. Kroemer, *Nat. Med.*, 1997, **3**, 614.
- 20 J.-P. Desaulniers, G. Hagen, J. Anderson, C. McKim and B. Roberts, *RSC Adv.*, 2017, **7**, 3450.
- 21 M. E. Kleinman, K. Yamada, A. Takeda, V. Chandrasekaran, M. Nozaki, J. Z. Baffi, R. J. C. Albuquerque, S. Yamasaki, M. Itaya and Y. Pan, *Nature*, 2008, **452**, 591.

Reversible control of RNA interference by siRNAzOs

Matthew L. Hammill, Golam Islam and Jean-Paul Desaulniers

Supporting Information

Table of Contents

Nucleic Acid and Biological Procedures

Procedure for Oligonucleotide Synthesis and Purification.....	S4
Procedure for performing CD experiments.....	S5
Procedure for absorbance spectra experiments.....	S5
Procedure for Melting Temperature of siRNA Duplexes (T_m).....	S5
Procedure for HPLC Characterization.....	S5
Procedure for Reduced Glutathione (GSH) Degradation Assay.....	S6
Procedure for Maintaining Cell Cultures of HeLa Cells.....	S6
Procedure for siRNA transfections.....	S6
Procedure for <i>in vitro</i> Dual Luciferase Assay.....	S6
Procedure for light inactivation of azobenzene modified siRNA (<i>trans</i> to <i>cis</i>).....	S7
Procedure for light reactivation of azobenzene modified siRNA (<i>cis</i> to <i>trans</i>).....	S7
Procedure for consecutive UV/Vis Light Cycling (1.5x and 2x light cycling).....	S7
Procedures for Real Time PCR.....	S8
Procedure for XTT Assays.....	S10

Figures and Tables

Figure S-1: CD spectra of azobenzene modified spacers replacing two nucleobases targeting firefly luciferase mRNAs.....	S11
Figure S-2: CD spectra of azobenzene modified spacers replacing two nucleobases targeting <i>BCL2</i> mRNAs.....	S11
Figure S-3: Absorbance Profile of siRNA 1 when exposed to UV and Visible light.....	S12
Figure S-4: Absorbance Profile of siRNA 2 when exposed to UV and Visible light.....	S12
Figure S-5: Absorbance Profile of siRNA 3 when exposed to UV and Visible light.....	S13
Figure S-6: Absorbance Profile of siRNA 4 when exposed to UV and Visible light.....	S13
Figure S-7: Absorbance Profile of siRNA 7 when exposed to UV and Visible light.....	S14
Figure S-8: Numerical bar graph showing reduction of normalized firefly luciferase expression for siRNAzo 1 UV/dark 8 h.....	S14
Figure S-9: Numerical bar graph showing reduction of normalized firefly luciferase expression for siRNAzo 2 UV/dark 8 h.....	S15

Figure S-10: Numerical bar graph showing reduction of normalized firefly luciferase expression for siRNAzo 3 UV/dark 8 h.....	S15
Figure S-11: Numerical bar graph showing reduction of normalized firefly luciferase expression for siRNAzo 4 UV/dark 8 h.....	S16
Figure S-12: Numerical bar graph showing reduction of normalized firefly luciferase expression for wt siRNA UV/dark 8 h.....	S16
Figure S-13: Numerical bar graph showing reduction of normalized firefly luciferase expression for siRNAzo 1 UV/dark 24 h.....	S17
Figure S-14: Numerical bar graph showing reduction of normalized firefly luciferase expression for siRNAzo 2 UV/dark 24 h.....	S17
Figure S-15: Numerical bar graph showing reduction of normalized firefly luciferase expression for siRNAzo 3 UV/dark 24 h.....	S18
Figure S-16: Numerical bar graph showing reduction of normalized firefly luciferase expression for siRNAzo 4 UV/dark 24 h.....	S18
Figure S-17: Numerical bar graph showing reduction of normalized firefly luciferase expression for wt siRNA UV/dark 24 h.....	S19
Figure S-18: Numerical bar graph showing reduction of normalized firefly luciferase expression for siRNAzo 1 UV/Vis/dark 8 h.....	S19
Figure S-19: Numerical bar graph showing reduction of normalized firefly luciferase expression for siRNAzo 2 UV/Vis/dark 8 h.....	S20
Figure S-20: Numerical bar graph showing reduction of normalized firefly luciferase expression for siRNAzo 3 UV/Vis/dark 8 h.....	S20
Figure S-21: Numerical bar graph showing reduction of normalized firefly luciferase expression for siRNAzo 4 UV/Vis/dark 8 h.....	S21
Figure S-22: Numerical bar graph showing reduction of normalized firefly luciferase expression for wt siRNA UV/Vis/dark 8 h.....	S21
Figure S-23: Numerical bar graph showing reduction of normalized firefly luciferase expression for siRNAzo 1 UV/Vis/dark 24 h.....	S22
Figure S-24: Numerical bar graph showing reduction of normalized firefly luciferase expression for siRNAzo 2 UV/Vis/dark 24 h.....	S22
Figure S-25: Numerical bar graph showing reduction of normalized firefly luciferase expression for siRNAzo 3 UV/Vis/dark 24 h.....	S23

Figure S-26: Numerical bar graph showing reduction of normalized firefly luciferase expression for siRNAzo 4 UV/Vis/dark 24 h.....	S23
Figure S-27: Numerical bar graph showing reduction of normalized firefly luciferase expression for wt siRNA UV/Vis/dark 24 h.....	S24
Figure S-28: Numerical bar graph showing reduction of normalized <i>BCL2</i> expression for siRNAzo 5 UV/Vis/dark 8 h.....	S24
Figure S-29: Numerical bar graph showing reduction of normalized <i>BCL2</i> expression for siRNAzo 5 UV/Vis/dark 8 h.....	S25
Figure S-30: Numerical bar graph showing reduction of normalized <i>BCL2</i> expression for siRNAzo 5 UV/Vis/dark 8 h.....	S25
Figure S-31: Numerical bar graph showing reduction of normalized <i>BCL2</i> expression for siRNAzo 5 UV/Vis/dark 24 h.....	S26
Figure S-32: Numerical bar graph showing reduction of normalized <i>BCL2</i> expression for siRNAzo 5 UV/Vis/dark 24 h.....	S26
Figure S-33: Numerical bar graph showing reduction of normalized <i>BCL2</i> expression for siRNAzo 5 UV/Vis/dark 24 h.....	S27
Figure S-34: XTT Assay for UV exposed cell viability.....	S27
Figure S-35: Comparative HPLC chromatogram of untreated siRNAzo 5 and UV light exposure.....	S28
Figure S-36: Comparative HPLC chromatogram of untreated siRNAzo 6 and UV light exposure.....	S29
Figure S-37: Comparative HPLC chromatogram of untreated siRNAzo 7 and UV light exposure.....	S29
Figure S-38: GSH assay comparative HPLC chromatograms of untreated siRNAzo 6 and UV light exposure.....	S29
Table S-1: Mass Spectrometry deconvolution results of siRNAzo sense strands 1-7	S30
References.....	S30

Nucleic Acid and Biological Procedures

Procedure for Oligonucleotide Synthesis and Purification

All standard β -cyanoethyl 2'-*O*-TBDMS protected phosphoramidites, reagents and solid supports were purchased from Chemgenes Corporation and Glen Research. Wild-type luciferase strands including the sense and 5'-phosphorylated antisense strand were synthesized. All commercial phosphoramidites were dissolved in anhydrous acetonitrile to a concentration of 0.10 M. The chemically synthesized (azobenzene derivative) phosphoramidites were dissolved in 3:1 (v/v) acetonitrile:THF (anhydrous) to a concentration of 0.10 M. The reagents that were used for the phosphoramidite coupling cycle were: acetic anhydride/pyridine/THF (Cap A), 16% *N*-methylimidazole in THF (Cap B), 0.25 M 5-ethylthio tetrazole in ACN (activator), 0.02 M iodine/pyridine/H₂O/THF (oxidation solution), and 3% trichloroacetic acid/dichloromethane. All sequences were synthesized on 0.20 μ M or 1.00 μ M dT solid supports except for sequences that were 3'-modified, which were synthesized on 1.00 μ M Universal III solid supports. The entire synthesis ran on an Applied Biosystems 394 DNA/RNA synthesizer using 0.20 μ M or 1.00 μ M cycles kept under argon at 55 psi. Standard and synthetic phosphoramidites ran with coupling times of 999 seconds.

Antisense sequences were chemically phosphorylated at the 5'-end by using 2-[2-(4,4'-dimethoxytrityloxy)ethylsulfonyl]ethyl-(2-cyanoethyl)-(N,N-diisopropyl)-phosphoramidite. At the end of every cycle, the columns were removed from the synthesizer, dried with a stream of argon gas, sealed and stored at 4 °C. Cleavage of oligonucleotides from their solid supports was performed through on-column exposure to 1.50 mL of EMAM (methylamine 40% wt. in H₂O and methylamine 33% wt. in ethanol, 1:1 (Sigma-Aldrich)) for 1 hour at room temperature with the solution in full contact with the controlled pore glass. The oligonucleotides were then incubated overnight at room temperature in EMAM to deprotect the bases. On the following day, the samples were concentrated on a Speedvac evaporator overnight, resuspended in a solution of DMSO:3HF/TEA (100 μ L:125 μ L) and incubated at 65 °C for 3 hours in order to remove the 2'-*O*-TDBMS protecting groups. Crude oligonucleotides were precipitated in EtOH and desalted through Millipore Amicon Ultra 3000 MW cellulose. Oligonucleotides were separated on a 20% acrylamide gel and were used without further purification for annealing and transfection. Equimolar amounts of complimentary RNAs were annealed at 95 °C for 2 min in a binding buffer (75.0 mM KCl, 50.0 mM Tris-HCl, 3.00 mM MgCl₂, pH 8.30) and this solution was cooled slowly to room temperature to generate siRNAs used for biological assays. A sodium phosphate buffer (90.0 mM NaCl, 10.0 mM Na₂HPO₄, 1.00 mM EDTA, pH 7.00) was used to anneal strands for biophysical measurements.

Procedure for Performing CD Experiments

Circular Dichroism (CD) spectroscopy was performed on a Jasco J-815 CD equipped with temperature controller. Equimolar amounts of each siRNA (10 μ M) were annealed to their complement in 500 μ L of a sodium phosphate buffer by incubating at 95 $^{\circ}$ C for two minutes and allowing to cool to room temperature. CD measurement of each duplex were recorded in triplicate from 200-500 nm at 25 $^{\circ}$ C with a screening rate of 20.0 nm/min and a 0.20 nm data pitch. The average of the three replicates was calculated using Jasco's Spectra Manager version 2 software and adjusted against the baseline measurement of the sodium phosphate buffer.

Procedure for Absorbance Spectra Experiments

All absorbance spectra measurements were done on a Jasco J-815 CD with temperature controller. Measurement was recorded from 200-500 nm at 10 $^{\circ}$ C at least 3 times. UV treated samples were placed under a UVP UVL-23RW Compact UV lamp 4.00 W 365nm for the indicated time. Visible light treated samples were placed under a 60.0 W daylight bulb from NOMA in standard desk lamp.

Procedure for Melting Temperature of siRNA Duplexes (T_m)

The siRNA duplexes annealed as above were placed in the Jasco J-815 CD spectropolarimeter and then UV absorbance was measured at 260 nm against a temperature gradient of 10 $^{\circ}$ C to 95 $^{\circ}$ C at a rate of 0.5 $^{\circ}$ C per minute with absorbance being measured at each 0.5 $^{\circ}$ C increment. Absorbance was adjusted to baseline by subtracting absorbance of the buffer. The T_m values were calculated using Meltwin v3.5 software. Each siRNA result was the average of 3 independent experiments and the reported values were calculated using Meltwin v3.5 assuming the two-state model.²

Procedure for HPLC Characterization

HPLC chromatograms were obtained on a Waters 1525 binary HPLC pump with a Waters 2489 UV/Vis detector using the Empower 3 software. A C18 4.6 mm x 150 mm reverse phase column was used. Conditions were 5% acetonitrile in 95% 0.1 M TEAA (Triethylamine-Acetic Acid) buffer up to 100% acetonitrile over 40 min.

Procedure for Reduced Glutathione (GSH) Degradation Assay

The GSH assay was performed on the sense strand of siRNA 6 in a 96 well plate at 37 °C. A concentration of 2.7 µM of siRNA was added to 10 mM glutathione and 5 mM TCEP in PBS to a final volume of 100 µL. Dark experiments were performed with no additional treatment at 0, 8, and 24 h time points after which the entire 100 µL was sample was injected into the HPLC and characterized (same conditions as above) to afford the HPLC traces at the different time points. UV treated siRNA was exposed to 5 min of UV light before incubation at 37 °C, and kept in the dark until injection for 0, 8, and 24 h time points. The UV 0 h time point was exposed to UV light and then injected immediately onto the HPLC.

Procedure for Maintaining Cell Cultures of HeLa Cells

For biological analysis of these siRNAs in a live environment, human epithelial cervix carcinoma cells were used (HeLa cells). They were kept in 250 mL vented culture flasks using 25.0 mL of DMEM with 10% fetal bovine serum and 1% penicillin-streptomycin (Sigma) in an incubator set for 37 °C @ 5% CO₂ humidified atmosphere.

Once cell lines became confluent (80-90%) they were passaged by washing 3 times with 20 mL of phosphate buffered saline (NaCl 137 mM, KCl 2.70 mM, PO₄³⁻ 10.0 mM, pH 7.40) and incubated with 5.00 mL of 0.25% trypsin (SAFC bioscience) for 4 min @ 37 °C to detach the cells. The cells were transferred to a 50.0 mL centrifuge tube after the addition of 10.0 mL of DMEM solution and pelleted at 2000 rpm for 5 minutes. The supernatant was discarded and the pellet resuspended in 5.0 mL DMEM with 10% FBS.

A standard haemocytometer was used to obtain cell counts, after which the cells were diluted to a final concentration of 1.00 x 10⁶ cells/mL for subsequent assays. To continue the cell line 1.00 mL of freshly passaged cells was added to 24.0 mL of DMEM/10% FBS and 1% penicillin-streptomycin at 37 °C in a new culture flask while the rest were used for assays.

Procedure for siRNA Transfections

100 µL of cells (total 1.00 x 10⁵) were transfected into 12 well plates (Falcon®) with 1 mL of DMEM (10% FBS, 1% penicillin-streptomycin) and incubated at 37 °C with 5% CO₂. After 24 hours the cells were transfected with various concentrations of siRNAs, along with both pGL3 (Promega) and pRLSV40 luciferase plasmids using Lipofectamine 2000 (Invitrogen) in Gibco's 1X Opti-Mem reduced serum media (Invitrogen) according to the manufacturer's instructions. 1.00 µL of siRNA was added along with 2.00 µL (pGL3 200 ng) and 0.50 µL pRLSV40 (50.0 ng) to 100 µL of 1X Opti-Mem in a microcentrifuge tube and

kept on ice for 5 min. In a different microcentrifuge tube 1.00 μ L of Lipofectamine 2000 (Invitrogen) was mixed with 100 μ L of Gibco's 1X Opti-Mem reduced serum media (Invitrogen) and incubated at room temperature for 5 min. After 5 minutes the tubes were mixed and incubated at room temperature for 20 min and then the entire contents transferred to the wells of the 12 well plate.

Procedure for *in vitro* Dual-Reporter[®] Luciferase Assay

100 μ L of cells (total of 1.00×10^5 cells) were added to 12 well plates (Falcon[®]) with 1 mL of growth media (DMEM 10% FBS, 1% penicillin-streptomycin) and incubated at 37 °C with 5% CO₂. After 24 hours the cells were transfected with 160, 400 and 800 pM concentrations of siRNAs, along with both pGL3 (Promega) and pRLSV40 luciferase plasmids using Lipofectamine 2000 (Invitrogen) in Gibco's 1X Opti-Mem reduced serum media (Invitrogen) according to the manufacturer's instructions. After a set amount of time (8 or 24 h) the cells were incubated at room temperature in 1X passive lysis buffer (Promega) for 20 minutes. The lysates were collected and loaded onto a 96 well, opaque plate (Costar). With a Dual-Luciferase reporter Assay kit (Promega), Lar II and Stop & Glo[®] luciferase substrates were sequentially added to the lysates and enzyme activity was measured through luminescence of both *firefly/Renilla* luciferase on a Synergy HT (Bio-Tek) plate luminometer. The ratio of *firefly/Renilla* luminescence is expressed as a percentage of reduction in *firefly* protein expression to siRNA efficacy when compared to untreated controls. Each value is the average of at least 3 different experiments with standard deviation indicated.

Procedure for Light Inactivation of Azobenzene Modified siRNA (*trans* to *cis*)

The cell culture plates were exposed to a 4.00 W 365 nm UV lamp (UVP) 2 hours after transfection for 8 h assays (1 exposure total) and every 4 h thereafter for 24 h assays (6 exposures total). Luciferase assays were then performed as indicated above at the desired time points.

Procedure for Light Reactivation of Azobenzene Modified siRNA (*cis* to *trans*)

4 hours after the transfection procedure, the plate was exposed to a 60.0 W daylight bulb (NOMA) and left under the visible lamp for the rest of the time before the cells were lysed and the plate read as above.

Procedure for consecutive UV/Vis Light Cycling (1.5x and 2x light cycling)

The first cycle was performed normally: UV inactivation after 2 hours for 45 min, and then visible light reactivation at 4 hours for 30 min. We then observed continued exposure to UV light

every 4 hours for 45 min, as per the normal procedure up to 24 h (1.5x, 5 exposures total) to keep the siRNA inactive. The 2x procedure was identical except after the second UV exposure (45 min), a 1 h 15 min resting period of darkness to let the cells recover was observed after which the cells were re-exposed to visible light for 30 min which restored the siRNA's activity.

Procedures for Real Time PCR

Transfection of HeLa cells with Lipofectamine 2000

Cell transfection procedure was identical to the dual assay procedure, above.

HeLa Cell Reverse Transcription (RT) Preparation

After the expired transfection period the growth medium was removed and the plate was washed twice with PBS. The cells were removed from the plate using 250 μ L of 0.25% trypsin to each well and incubated for 4 minutes at 37 °C with 5% CO₂. The cell suspension was then added to 1 mL of growth medium to inactivate the trypsin and centrifuged at 2000 rpm for 5 min. The supernatant was discarded and the cells were resuspended in 500 μ L of fresh media. The cells in each tube were then counted to ensure a total number of cells between 100-200k per sample. After counting the cells were repelleted as above and washed with 500 μ L of ice-cold PBS and then repelleted and the pellet was placed on ice.

RT-PCR with the Invitrogen cells to cDNA kit II

The following protocol uses reagents found in the Cells-to-cDNA kit purchased from Invitrogen. The pellet on ice was resuspended in 100 μ L of ice cold Cell Lysis II Buffer and each sample was mixed by vortex. The samples were then immediately transferred to a pre-heated 75 °C heat block and left to denature for 10 minutes. The samples were then removed from the water bath and placed on ice. To each centrifuge tube, 2 μ L of DNase I (2 U/ μ L stock) was added and these mixtures were gently vortexed followed by a brief centrifugation to concentrate the sample. A genomic wipeout was accomplished by incubating the DNase I reaction at 37°C for 30 minutes. The samples were then heated to 75 °C for 10 minutes to deactivate the DNase I. To new nuclease-free microfuge tubes, was added 5 μ L of cell lysate (RNA), 4 μ L of dNTP mix (2.5 mM stock for each dNTP), 2 μ L of random decamers (50 μ M stock) and 9 μ L of nuclease-free water. The resulting mixture was then heated to 70 °C for 5 minutes to denature the RNA template, placed on ice for 1 minute, flash centrifuged, and placed on ice. The remaining RT reagents including: 2 μ L of 10X RT Buffer, 1 μ L of M-MLV Reverse Transcriptase (or 1 μ L of nuclease-free H₂O for a no reverse transcription (NRT) Control) and 1 μ L of RNase inhibitor (10 U/ μ L stock) were added, mixed and centrifuged briefly. Reverse transcription was initiated by warming the samples to 42 °C using a

thermal cycler for 60 minutes. Reverse transcriptase was inactivated by incubating the samples at 95°C for 10 minutes. This lysate can be stored for up to 2 weeks at -20 °C.

RNA extraction, cDNA synthesis and RT-qPCR

HeLa cells were transfected with anti-*BCL2* siRNAs as described. RNA extraction, cDNA production and RT-qPCR. Prior to the RNA extraction, each well of the 24-well plate washed twice with 1X PBS. Total RNA was extracted from the HeLa cells using the manufacturer's instructions of the Total RNA Purification Plus Kit (Cat#: 48400. Norgen BioTek Corp, Thorold, ON, Canada). In addition, an on-column DNA digestion was performed using RNase Free DNase I Kit (Cat#:25710. Norgen BioTek Corp, Thorold, ON, Canada). Two microliter of each extracted RNA sample was used to measure the concentration and RNA integrity (A260/280) on the BioDrop Duo Plus (UK), and the presence of the RNA was confirmed by gel electrophoresis on a 1% (w vol-1) agarose gel. Three biological replicates were completed for each Azo-Modified siRNA. The siRNAs were inactivated and reactivated using the exact same procedures as listed above for the firefly/ *Renilla Luciferase* assays.

The RT reaction was performed using the IScript cDNA synthesis kit (Cat #: 1708891. Bio-Rad, Hercules, California) in a total reaction volume of 20µL. The reaction mixture contained 400 ng of total RNA, M-MLV reverse transcriptase, oligo (DT) and random primers. Two negative controls were performed with all reactions. The first control contained the RNA template and all DNase/RT reagents, except for the final addition of the RT enzyme. A second control contained no template (water only) to ensure that all reagents were free from possible contaminants. RT reactions were placed in 200 µL PCR tubes and incubated within a BIORAD T100 Thermal Cycler for 5 min at 25°C followed by 20 min at 46°C, 1 min at 95°C and then held at 4°C. Once cDNA was produced, the products could be amplified (RT-qPCR).

Quantitative RT-PCR

Real-time PCR was performed in a total reaction volume of 20 µL containing 10 µL SsoFast EverGreen Supermix (Bio-Rad, Hercules, California) containing Sso 7-d Fusion Polymerase, 0.5 µM forward primer and reverse primer and 2 µL cDNA template. In the final reaction, cDNA was diluted 40x to produce the best results. Pre-designed primers *BCL2F* 5'-CTG GTG GGA GCT TGC ATC AC-3' and *BCL2R*-5' GCC TGC AGC TTT GTT TC-3' were purchased to target the *BCL2* gene and yielding a 150-bp amplicon and 18S-F 5'-CGG CTA CCA CAT CCA AGG AAG-3' and 18S-R 5'-CGC TCC CAA GAT CCA ACT ACT3' (Integrated DNA Technologies Inc, San Diego, California) were used to target the 18s gene in HeLa cells and yielding a 247-bp amplicon. Reactions were incubated in the Bio-Rad CFX 96 Real-Time Detection System using the

following cycle conditions: 50°C for 10 minutes, 95°C for 10 minutes, followed by 40 cycles at 95°C for 15 seconds and 60°C for 1 minute. Reaction specificity was assessed by melting curve analysis immediately after the qPCR experiment. The efficiency of each primer set for RT-qPCR was determined to be between 95 and 100% using the standard curve method. NRT controls were performed during standard curve analysis to confirm that amplification of the PCR product was cDNA and not genomic DNA. NTC controls were also performed to ensure that amplification of the PCR product was not a result of primer-dimer. Results were analyzed using the Bio-Rad CFX manager 3.1 software where the *BCL2* expression data was normalized against 18s gene as the reference and expression profiles were generated using the comparative Delta-CT method of analysis. The repeatability of the RT-qPCR was assessed by measuring the imprecision of the standard deviations of Cq values compiled from three biological replicates for each treatment and three technical replicates having the same input RNA.

Procedure for XTT Assays

XTT reagents were allowed to thaw in the incubator at 37 °C. Once a consistent liquid with no particles was obtained after thawing, 2.5 mL of XTT Reagent was combined with 0.05 mL of Activation Reagent. 200 µL of this mixture was added to each well and the plates were placed back in the incubator for at least one hour. Plates were read using a BioTek plate reader (Fischer Scientific). All blanks and samples were averaged at both wavelengths. Specific absorbance for UV and non-UV samples were calculated using the following equation:

$$\text{Specific Absorbance at 475 nm} = \text{Test Avg}_{475\text{nm}} - \text{Blank Avg}_{475\text{nm}} - \text{Test Avg}_{660\text{nm}}$$

Cell viability was then assessed and error bars were placed based on standard deviation.

Figures and Tables

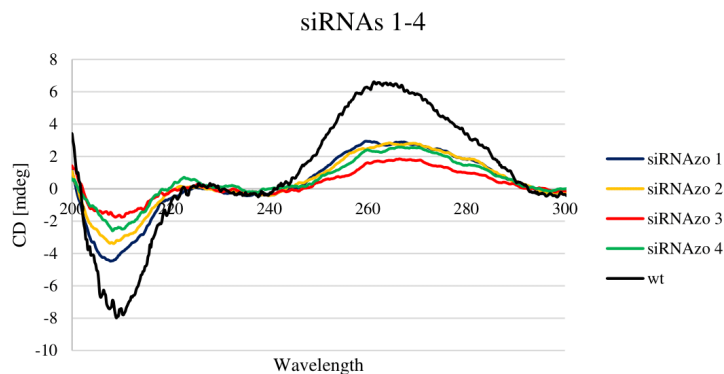


Figure S-1. CD spectra of azobenzene modified spacers replacing two nucleobases targeting firefly luciferase mRNAs. Wildtype and modified anti-*firefly* luciferase siRNAs (10 μ M/duplex) were suspended in 500 μ L of a sodium phosphate buffer (90.0 mM NaCl, 10.0 mM Na₂HPO₄, 1.00 mM EDTA, pH 7.00) and scanned from 200-300 nm at 25 °C with a screening rate of 20.0 nm/min and a 0.20 nm data pitch. All scans were performed in triplicate and averaged using Jasco's Spectra Manager version 2.

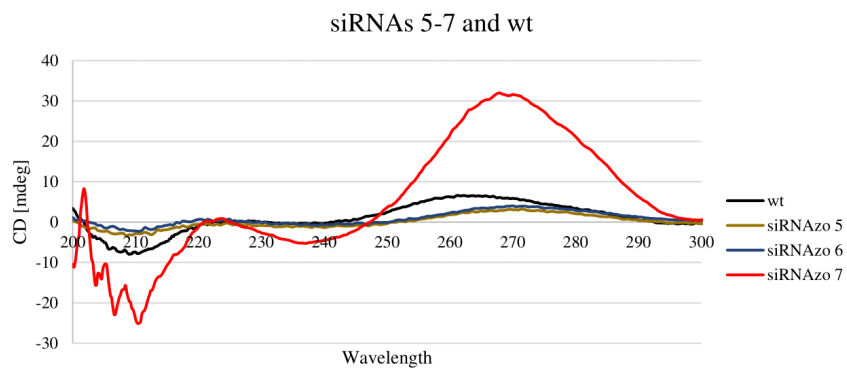


Figure S-2. CD spectra of azobenzene modified spacers replacing two nucleobases targeting *BCL2* mRNAs. Wildtype and modified anti-*BCL2* siRNAs (10 μ M/duplex) were suspended in 500 μ L of a sodium phosphate buffer (90.0 mM NaCl, 10.0 mM Na₂HPO₄, 1.00 mM EDTA, pH 7.00) and scanned from 200-300 nm at 25 °C with a screening rate of 20.0 nm/min and a 0.20 nm data pitch. All scans were performed in triplicate and averaged using Jasco's Spectra Manager version 2. Updated with siRNAs 5 and 6

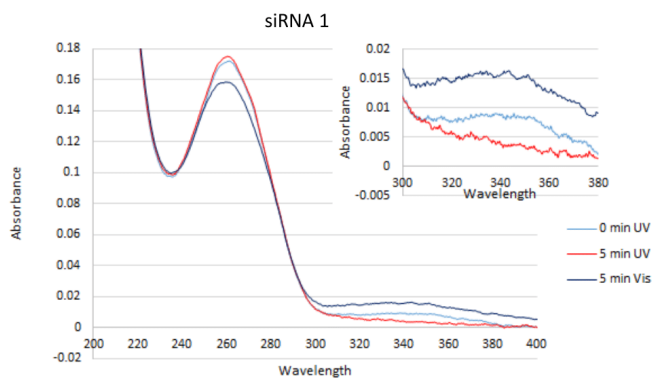


Figure S-3. Absorbance Profile of siRNA 1 when exposed to UV and Visible light in 500 μ L of a sodium phosphate buffer (90.0 mM NaCl, 10.0 mM Na_2HPO_4 , 1.00 mM EDTA, pH 7.00) and scanned from 200-400 nm at 10 $^\circ\text{C}$ with a screening rate of 20.0 nm/min and a 0.20 nm data pitch. Inset: Zoomed in portion of 320-380 nm highlighting azobenzene changes

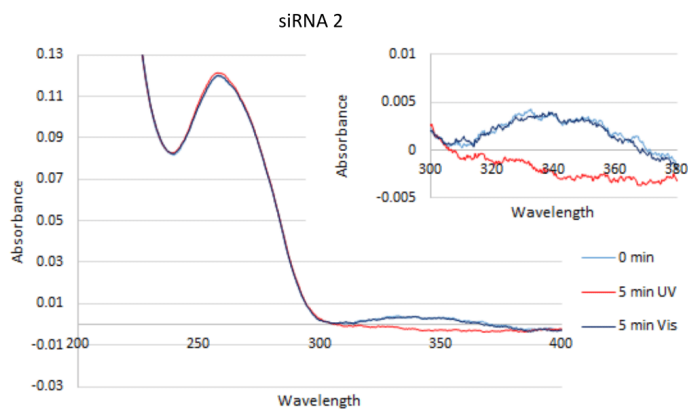


Figure S-4. Absorbance Profile of siRNA 2 when exposed to UV and Visible light in 500 μ L of a sodium phosphate buffer (90.0 mM NaCl, 10.0 mM Na_2HPO_4 , 1.00 mM EDTA, pH 7.00) and scanned from 200-400 nm at 10 $^\circ\text{C}$ with a screening rate of 20.0 nm/min and a 0.20 nm data pitch. Inset: Zoomed in portion of 320-380 nm highlighting azobenzene changes

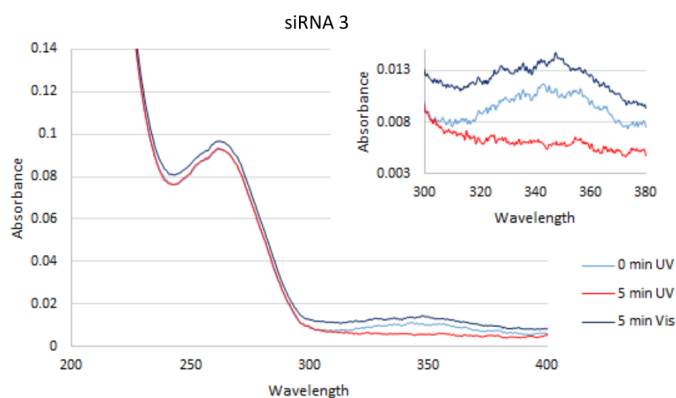


Figure S-5. Absorbance Profile of siRNA 3 when exposed to UV and Visible light in 500 μ L of a sodium phosphate buffer (90.0 mM NaCl, 10.0 mM Na_2HPO_4 , 1.00 mM EDTA, pH 7.00) and scanned from 200-400 nm at 10 $^\circ\text{C}$ with a screening rate of 20.0 nm/min and a 0.20 nm data pitch. Inset: Zoomed in portion of 320-380 nm highlighting azobenzene changes

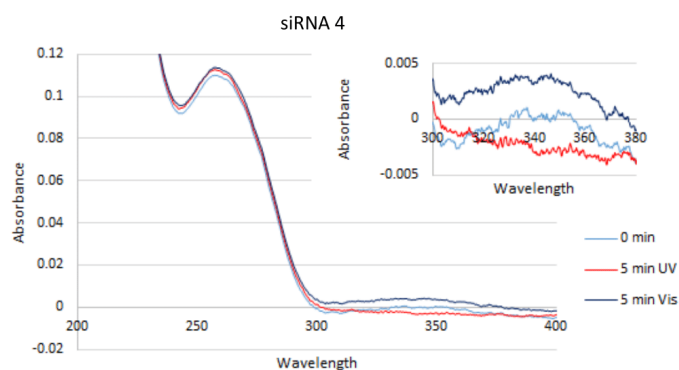


Figure S-6. Absorbance Profile of siRNA 4 when exposed to UV and Visible light in 500 μ L of a sodium phosphate buffer (90.0 mM NaCl, 10.0 mM Na_2HPO_4 , 1.00 mM EDTA, pH 7.00) and scanned from 200-400 nm at 10 $^\circ\text{C}$ with a screening rate of 20.0 nm/min and a 0.20 nm data pitch. Inset: Zoomed in portion of 320-380 nm highlighting azobenzene changes

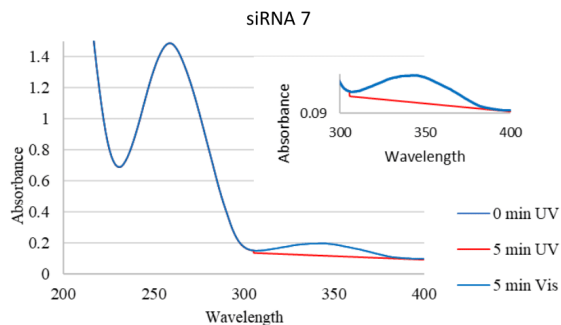


Figure S-7. Absorbance Profile of siRNA 7 when exposed to UV and Visible light in 500 μ L of a sodium phosphate buffer (90.0 mM NaCl, 10.0 mM Na_2HPO_4 , 1.00 mM EDTA, pH 7.00) and scanned from 200-400 nm at 10 $^\circ\text{C}$ with a screening rate of 20.0 nm/min and a 0.20 nm data pitch. Inset: Zoomed in portion of 320-380 nm highlighting azobenzene changes. SiRNAs 5 and 6 have similar profiles (data not shown).

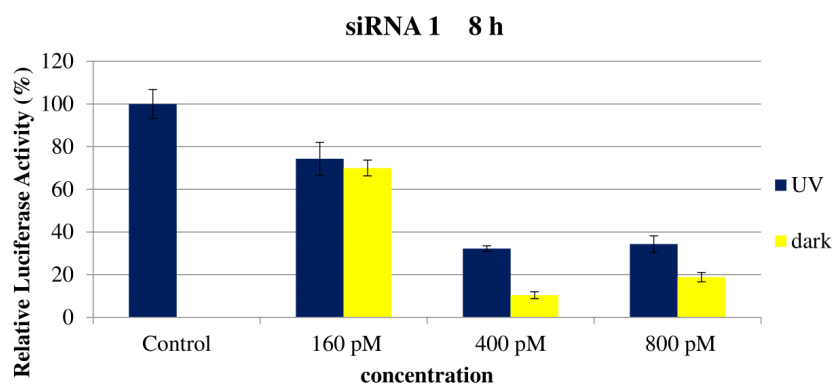


Figure S-8. Numerical bar graph showing reduction of normalized firefly luciferase expression for siRNA 1 at 160, 400 and 800 pM in HeLa cells monitored 8 hours post-transfection. 1) UV corresponds to the siRNA being exposed under a 365nm UV lamp for inactivation 2 h post transfection for 45 min (1 exposure total). 2) Dark corresponds to siRNAs being transfected in HeLa cells in the absence of UV light.

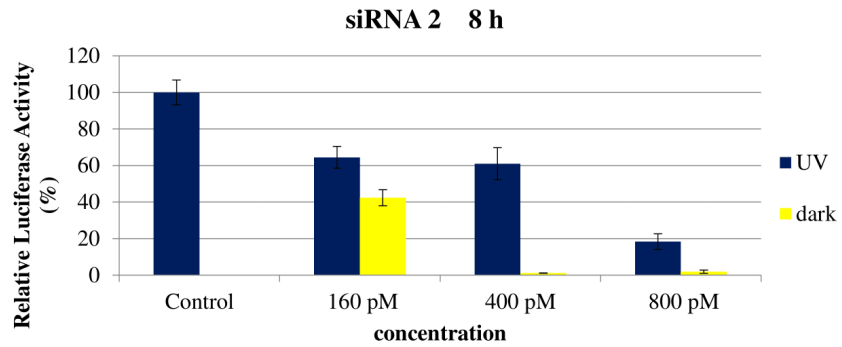


Figure S-9. Numerical bar graph showing reduction of normalized firefly luciferase expression for siRNAzo 2 at 160, 400 and 800 pM in HeLa cells monitored 8 hours post-transfection. 1) UV corresponds to the siRNA being exposed under a 365nm UV lamp for inactivation 2 h post transfection for 45 min (1 exposure total). 2) Dark corresponds to siRNAs being transfected in HeLa cells in the absence of UV light.

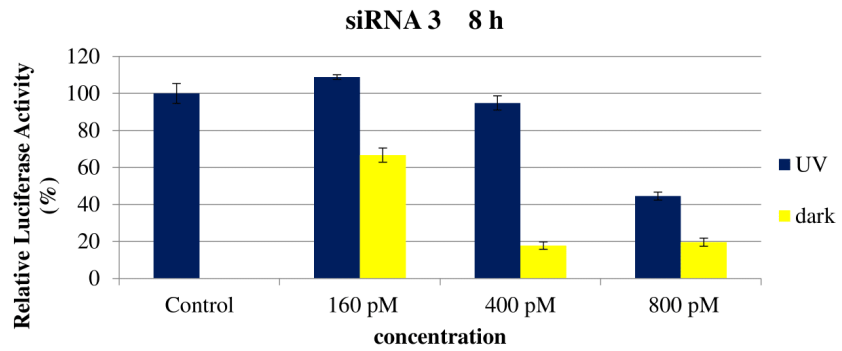


Figure S-10. Numerical bar graph showing reduction of normalized firefly luciferase expression for siRNAzo 3 at 160, 400 and 800 pM in HeLa cells monitored 8 hours post-transfection. 1) UV corresponds to the siRNA being exposed under a 365nm UV lamp for inactivation 2 h post transfection for 45 min (1 exposure total). 2) Dark corresponds to siRNAs being transfected in HeLa cells in the absence of UV light.

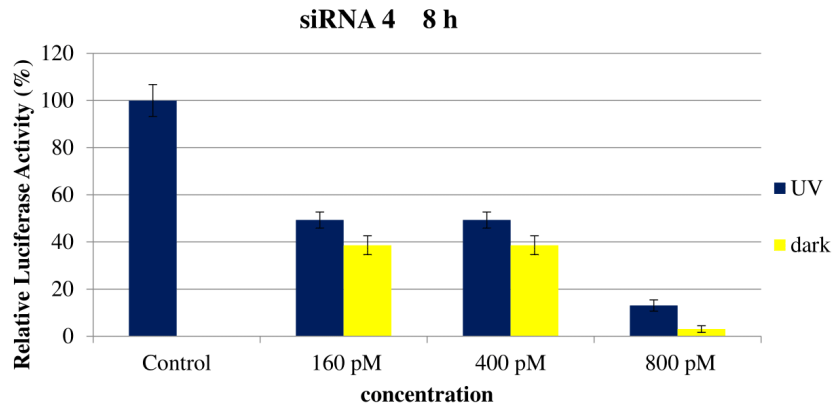


Figure S-11. Numerical bar graph showing reduction of normalized firefly luciferase expression for siRNAzo 4 at 160, 400 and 800 pM in HeLa cells monitored 8 hours post-transfection. 1) UV corresponds to the siRNA being exposed under a 365nm UV lamp for inactivation 2 h post transfection for 45 min (1 exposure total). 2) Dark corresponds to siRNAs being transfected in HeLa cells in the absence of UV light.

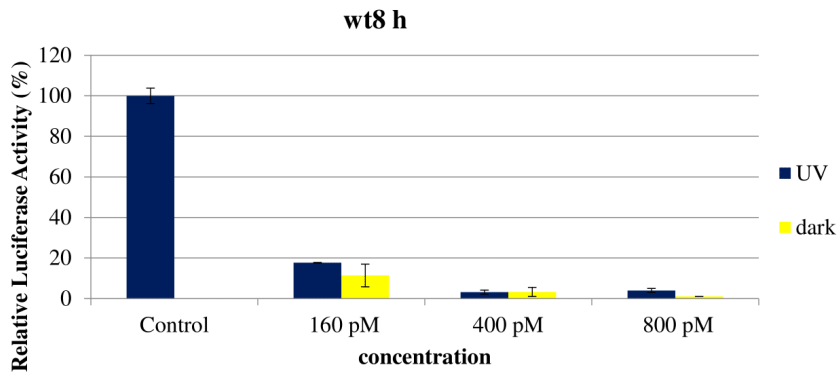


Figure S-12. Numerical bar graph showing reduction of normalized firefly luciferase expression for wt siRNA at 160, 400 and 800 pM in HeLa cells monitored 8 hours post-transfection. 1) UV corresponds to the siRNA being exposed under a 365nm UV lamp for inactivation 2 h post transfection for 45 min (1 exposure total). 2) Dark corresponds to siRNAs being transfected in HeLa cells in the absence of UV light.

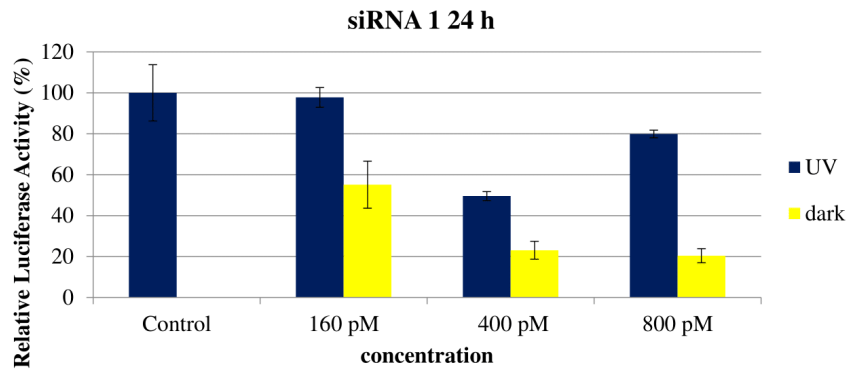


Figure S-13. Numerical bar graph showing reduction of normalized firefly luciferase expression for siRNAzo 1 at 160, 400 and 800 pM in HeLa cells monitored 24 hours post-transfection. 1) UV corresponds to the siRNA being exposed under a 365nm UV lamp for inactivation 2 h post transfection for 45 min and then for every 4 h thereafter (6 exposures total). 2) Dark corresponds to siRNAs being transfected in HeLa cells in the absence of UV light.

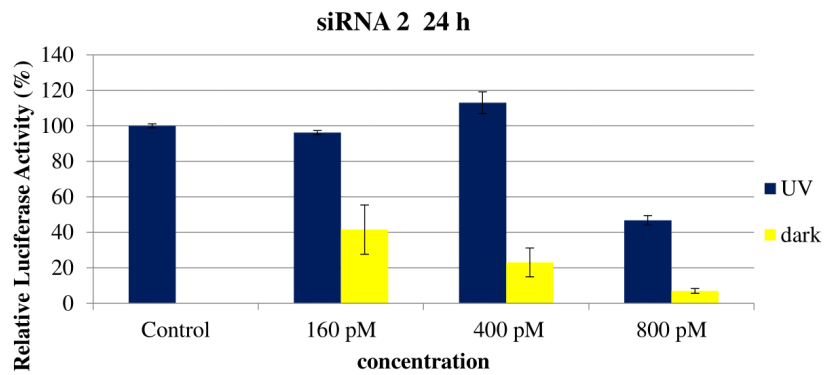


Figure S-14. Numerical bar graph showing reduction of normalized firefly luciferase expression for siRNAzo 2 at 160, 400 and 800 pM in HeLa cells monitored 24 hours post-transfection. 1) UV corresponds to the siRNA being exposed under a 365nm UV lamp for inactivation 2 h post transfection for 45 min and then for every 4 h thereafter (6 exposures total). 2) Dark corresponds to siRNAs being transfected in HeLa cells in the absence of UV light.

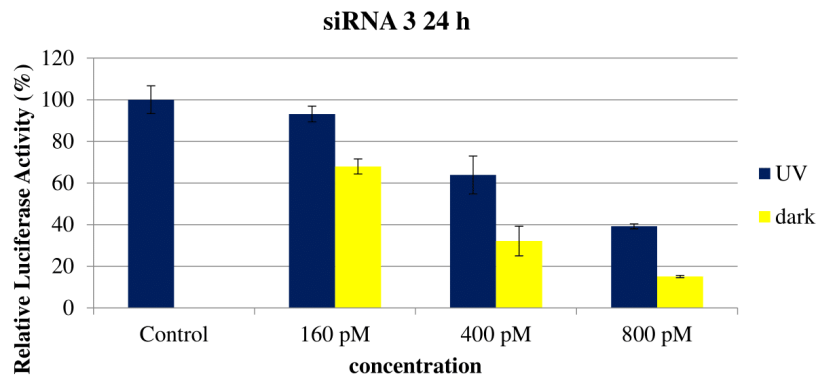


Figure S-15. Numerical bar graph showing reduction of normalized firefly luciferase expression for siRNAzo 3 at 160, 400 and 800 pM in HeLa cells monitored 24 hours post-transfection. 1) UV corresponds to the siRNA being exposed under a 365nm UV lamp for inactivation 2 h post transfection for 45 min and then for every 4 h thereafter (6 exposures total). 2) Dark corresponds to siRNAs being transfected in HeLa cells in the absence of UV light.

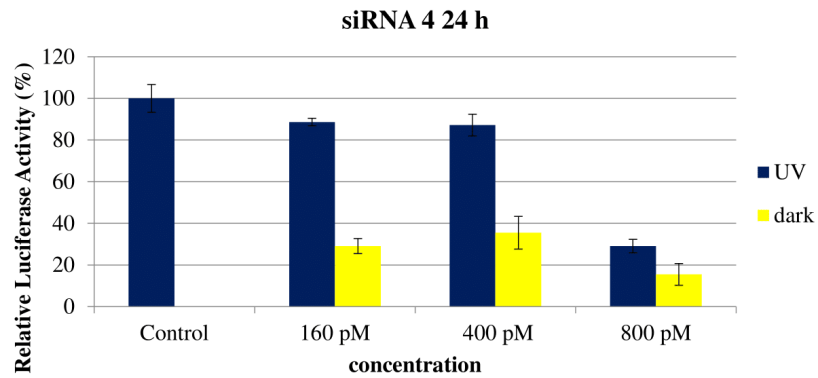


Figure S-16. Numerical bar graph showing reduction of normalized firefly luciferase expression for siRNAzo 4 at 160, 400 and 800 pM in HeLa cells monitored 24 hours post-transfection. 1) UV corresponds to the siRNA being exposed under a 365nm UV lamp for inactivation 2 h post transfection for 45 min and then for every 4 h thereafter (6 exposures total). 2) Dark corresponds to siRNAs being transfected in HeLa cells in the absence of UV light.

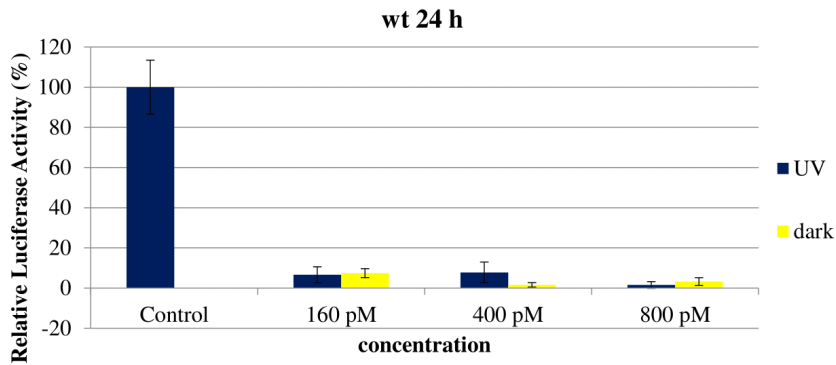


Figure S-17. Numerical bar graph showing reduction of normalized firefly luciferase expression for wt siRNA at 160, 400 and 800 pM in HeLa cells monitored 24 hours post-transfection. 1) UV corresponds to the siRNA being exposed under a 365nm UV lamp for inactivation 2 h post transfection for 45 min and then for every 4 h thereafter (6 exposures total). 2) Dark corresponds to siRNAs being transfected in HeLa cells in the absence of UV light.

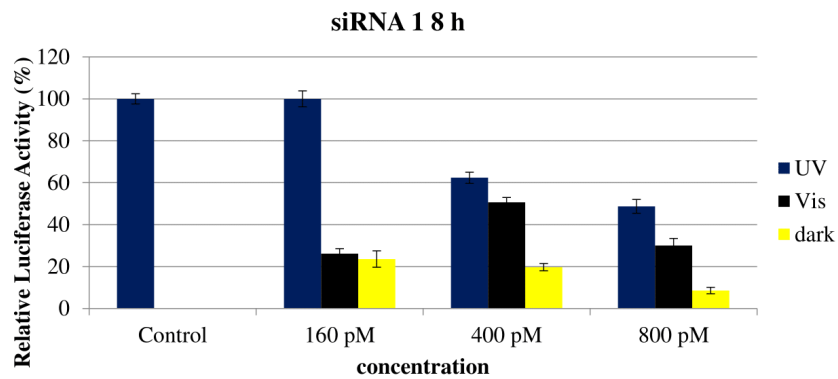


Figure S-18. Numerical bar graph showing reduction of normalized firefly luciferase expression for siRNAzo 1 at 160, 400, and 800 pM in HeLa cells monitored 8 hours post-transfection. 1) UV corresponds to the siRNA being exposed under a 365nm UV lamp for inactivation 2 h post transfection for 45 min. 2) Vis corresponds to visible light exposure 4 h after transfection. 3) Dark corresponds to siRNAs being transfected in HeLa cells in the absence of UV light.

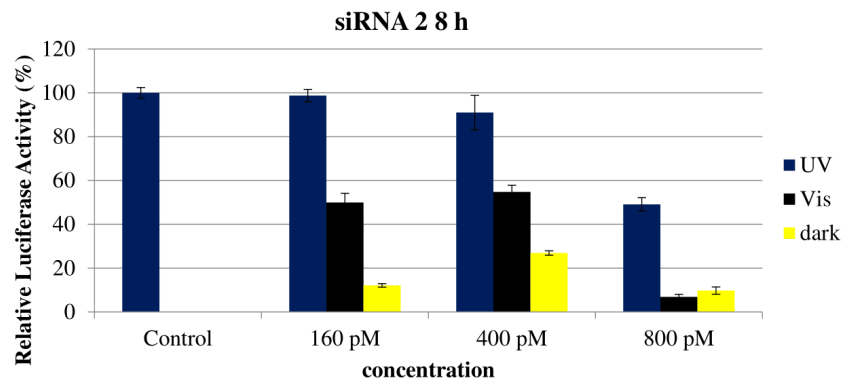


Figure S-19. Numerical bar graph showing reduction of normalized firefly luciferase expression for siRNAzo 2 at 160, 400, and 800 pM in HeLa cells monitored 8 hours post-transfection. 1) UV corresponds to the siRNA being exposed under a 365nm UV lamp for inactivation 2 h post transfection for 45 min. 2) Vis corresponds to visible light exposure 4 h after transfection. 3) Dark corresponds to siRNAs being transfected in HeLa cells in the absence of UV light.

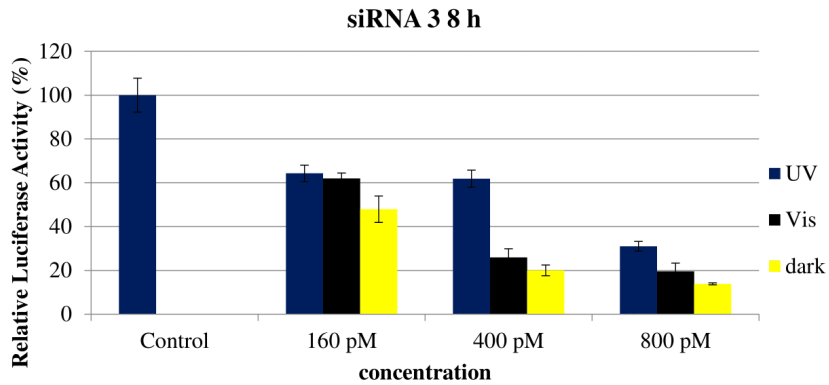


Figure S-20. Numerical bar graph showing reduction of normalized firefly luciferase expression for siRNAzo 3 at 160, 400, and 800 pM in HeLa cells monitored 8 hours post-transfection. 1) UV corresponds to the siRNA being exposed under a 365nm UV lamp for inactivation 2 h post transfection for 45 min. 2) Vis corresponds to visible light exposure 4 h after transfection. 3) Dark corresponds to siRNAs being transfected in HeLa cells in the absence of UV light.

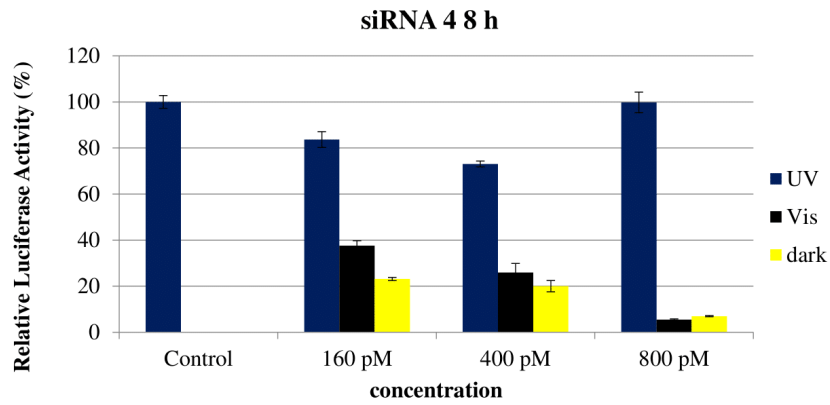


Figure S-21. Numerical bar graph showing reduction of normalized firefly luciferase expression for siRNA 4 at 160, 400, and 800 pM in HeLa cells monitored 8 hours post-transfection. 1) UV corresponds to the siRNA being exposed under a 365nm UV lamp for inactivation 2 h post transfection for 45 min. 2) Vis corresponds to visible light exposure 4 h after transfection. 3) Dark corresponds to siRNAs being transfected in HeLa cells in the absence of UV light.

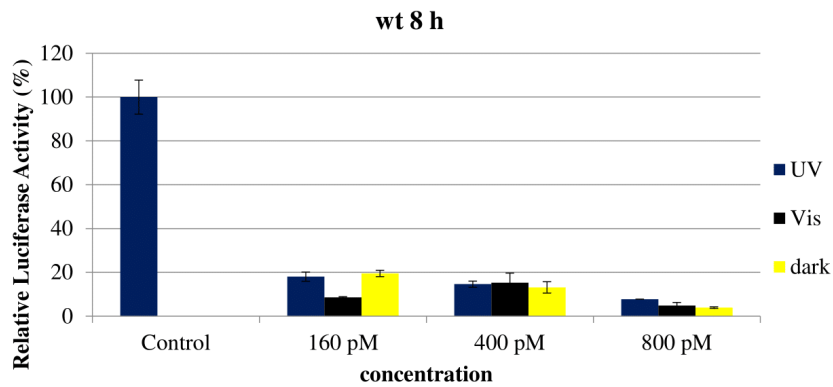


Figure S-22. Numerical bar graph showing reduction of normalized firefly luciferase expression for wt siRNA at 160, 400, and 800 pM in HeLa cells monitored 8 hours post-transfection. 1) UV corresponds to the siRNA being exposed under a 365nm UV lamp for inactivation 2 h post transfection for 45 min. 2) Vis corresponds to visible light exposure 4 h after transfection. 3) Dark corresponds to siRNAs being transfected in HeLa cells in the absence of UV light.

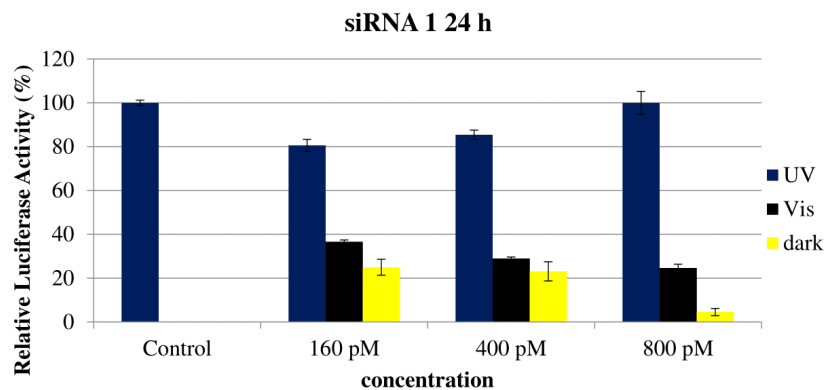


Figure S-23. Numerical bar graph showing reduction of normalized firefly luciferase expression for siRNAzo 1 at 160, 400, and 800 pM in HeLa cells monitored 24 hours post-transfection. 1) UV corresponds to the siRNA being exposed under a 365nm UV lamp for inactivation 2 h post transfection for 45 min, and for an additional 45 min of UV exposure every 4 hours (6 exposures total) 2) Vis corresponds to visible light exposure 4 h after transfection. 3) Dark corresponds to siRNAs being transfected in HeLa cells in the absence of UV light.

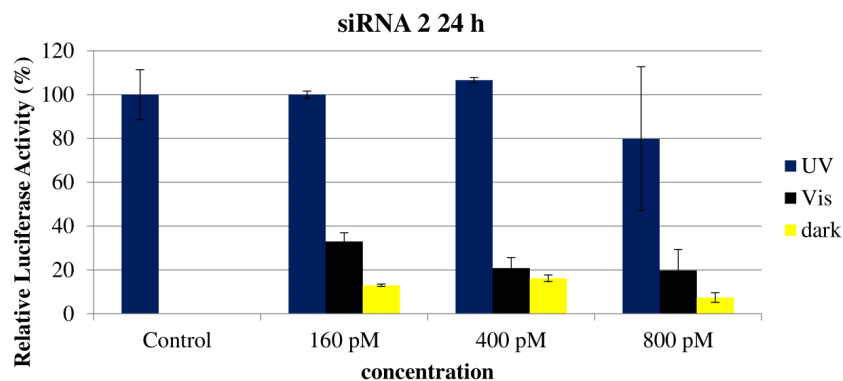


Figure S-24. Numerical bar graph showing reduction of normalized firefly luciferase expression for siRNAzo 2 at 160, 400, and 800 pM in HeLa cells monitored 24 hours post-transfection. 1) UV corresponds to the siRNA being exposed under a 365nm UV lamp for inactivation 2 h post transfection for 45 min, and for an additional 45 min of UV exposure every 4 hours (6 exposures total) 2) Vis corresponds to visible light exposure 4 h after transfection. 3) Dark corresponds to siRNAs being transfected in HeLa cells in the absence of UV light.

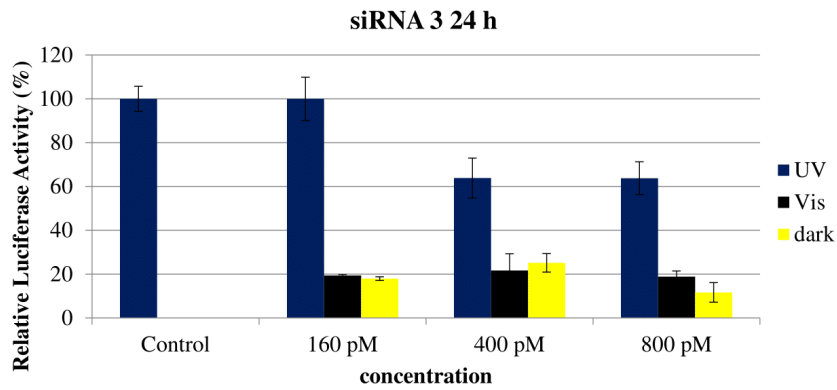


Figure S-25. Numerical bar graph showing reduction of normalized firefly luciferase expression for siRNAzo 3 at 160, 400, and 800 pM in HeLa cells monitored 24 hours post-transfection. 1) UV corresponds to the siRNA being exposed under a 365nm UV lamp for inactivation 2 h post transfection for 45 min, and for an additional 45 min of UV exposure every 4 hours (6 exposures total) 2) Vis corresponds to visible light exposure 4 h after transfection. 3) Dark corresponds to siRNAs being transfected in HeLa cells in the absence of UV light.

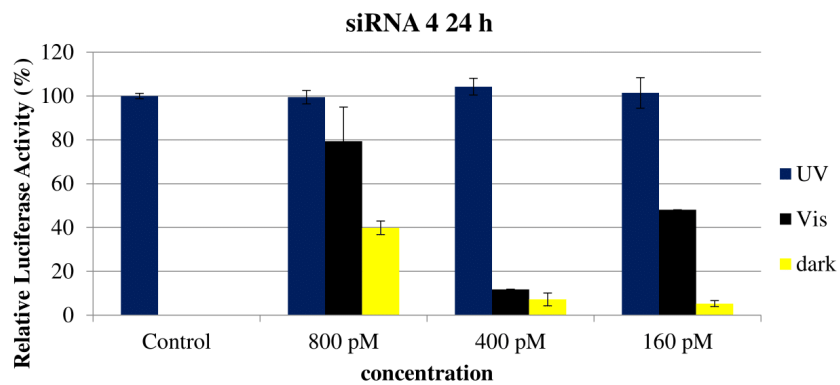


Figure S-26. Numerical bar graph showing reduction of normalized firefly luciferase expression for siRNAzo 4 at 160, 400, and 800 pM in HeLa cells monitored 24 hours post-transfection. 1) UV corresponds to the siRNA being exposed under a 365nm UV lamp for inactivation 2 h post transfection for 45 min, and for an additional 45 min of UV exposure every 4 hours (6 exposures total) 2) Vis corresponds to visible light exposure 4 h after transfection. 3) Dark corresponds to siRNAs being transfected in HeLa cells in the absence of UV light.

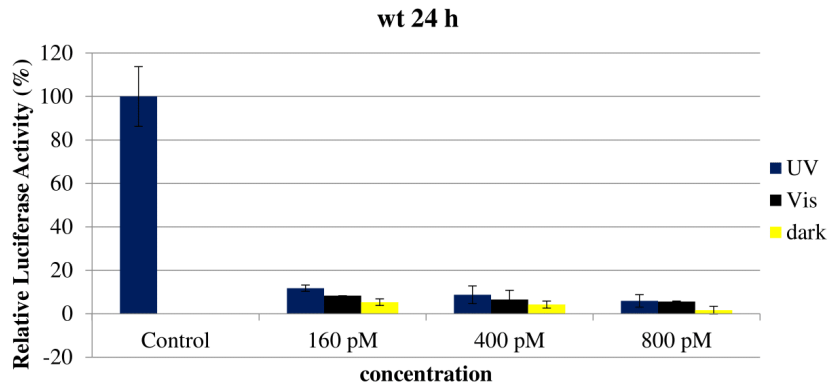


Figure S-27. Numerical bar graph showing reduction of normalized firefly luciferase expression for wt siRNA at 160, 400, and 800 pM in HeLa cells monitored 24 hours post-transfection. 1) UV corresponds to the siRNA being exposed under a 365nm UV lamp for inactivation 2 h post transfection for 45 min, and for an additional 45 min of UV exposure every 4 hours (6 exposures total) 2) Vis corresponds to visible light exposure 4 h after transfection. 3) Dark corresponds to siRNAs being transfected in HeLa cells in the absence of UV light.

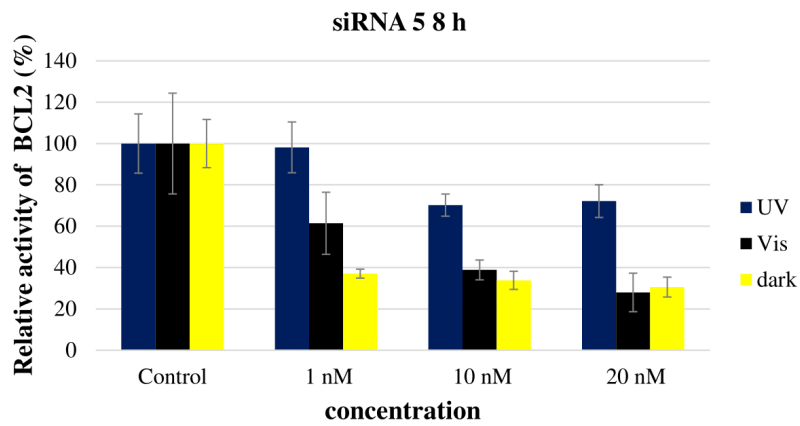


Figure S-28. Numerical bar graph showing reduction of normalized *BCL2* expression for siRNAzo 5 at 1, 10, and 20 nM in HeLa cells monitored 8 hours post-transfection. 1) UV corresponds to the siRNA being exposed under a 365nm UV lamp for inactivation 2 h post transfection for 45 min. 2) Vis corresponds to visible light exposure 4 h after transfection. 3) Dark corresponds to siRNAs being transfected in HeLa cells in the absence of UV light.

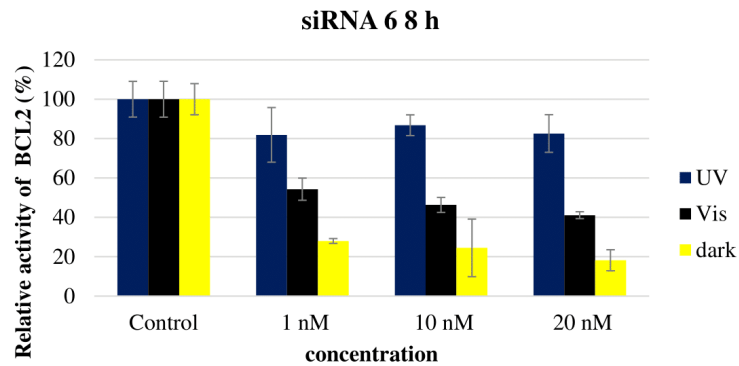


Figure S-29. Numerical bar graph showing reduction of normalized *BCL2* expression for siRNAzo 6 at 1, 10, and 20 nM in HeLa cells monitored 8 hours post-transfection. 1) UV corresponds to the siRNA being exposed under a 365nm UV lamp for inactivation 2 h post transfection for 45 min. 2) Vis corresponds to visible light exposure 4 h after transfection. 3) Dark corresponds to siRNAs being transfected in HeLa cells in the absence of UV light.

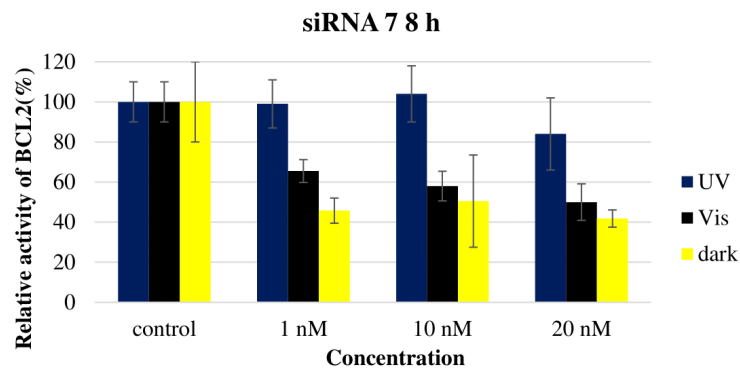


Figure S-30. Numerical bar graph showing reduction of normalized *BCL2* expression for siRNAzo 7 at 1, 10, and 20 nM in HeLa cells monitored 8 hours post-transfection. 1) UV corresponds to the siRNA being exposed under a 365nm UV lamp for inactivation 2 h post transfection for 45 min. 2) Vis corresponds to visible light exposure 4 h after transfection. 3) Dark corresponds to siRNAs being transfected in HeLa cells in the absence of UV light.

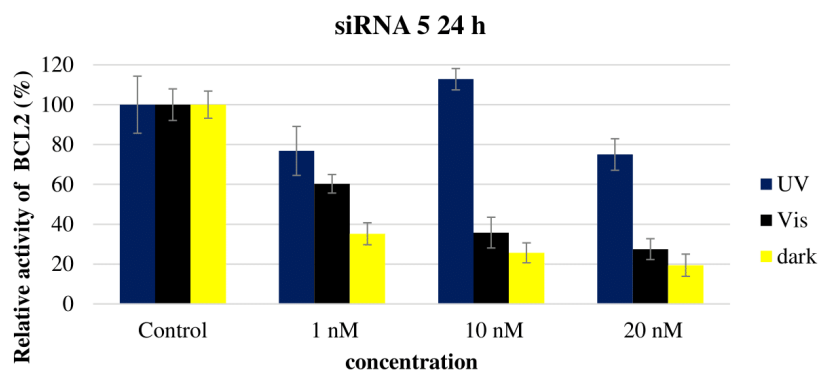


Figure S-31. Numerical bar graph showing reduction of normalized *BCL2* expression for siRNA 5 at 1, 10, and 20 nM in HeLa cells monitored 24 hours post-transfection. 1) UV corresponds to the siRNA being exposed under a 365nm UV lamp for inactivation 2 h post transfection for 45 min, and for an additional 45 min of UV exposure every 4 hours (6 exposures total) 2) Vis corresponds to visible light exposure 4 h after transfection. 3) Dark corresponds to siRNAs being transfected in HeLa cells in the absence of UV light.

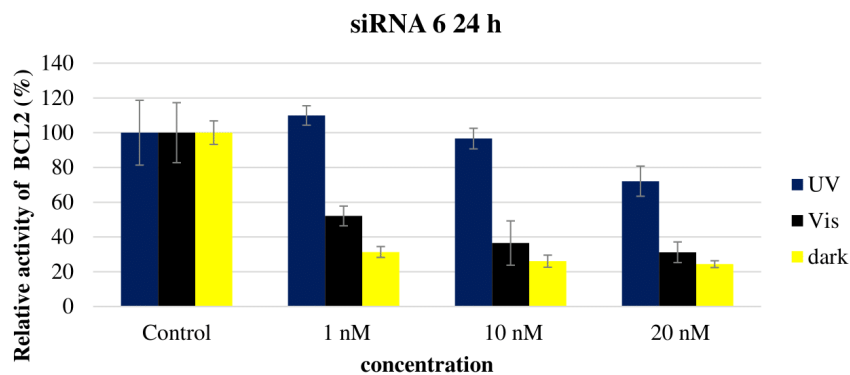


Figure S-32. Numerical bar graph showing reduction of normalized *BCL2* expression for siRNA 6 at 1, 10, and 20 nM in HeLa cells monitored 24 hours post-transfection. 1) UV corresponds to the siRNA being exposed under a 365nm UV lamp for inactivation 2 h post transfection for 45 min, and for an additional 45 min of UV exposure every 4 hours (6 exposures total) 2) Vis corresponds to visible light exposure 4 h after transfection. 3) Dark corresponds to siRNAs being transfected in HeLa cells in the absence of UV light.

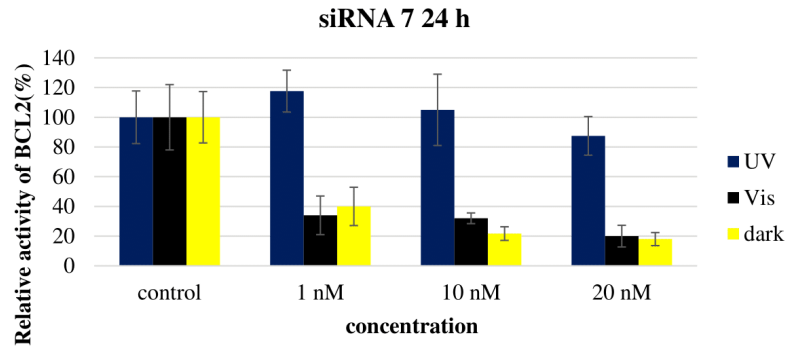


Figure S-33. Numerical bar graph showing reduction of normalized *BCL2* expression for siRNA 7 at 1, 10, and 20 nM in HeLa cells monitored 24 hours post-transfection. 1) UV corresponds to the siRNA being exposed under a 365nm UV lamp for inactivation 2 h post transfection for 45 min, and for an additional 45 min of UV exposure every 4 hours (6 exposures total) 2) Vis corresponds to visible light exposure 4 h after transfection. 3) Dark corresponds to siRNAs being transfected in HeLa cells in the absence of UV light.

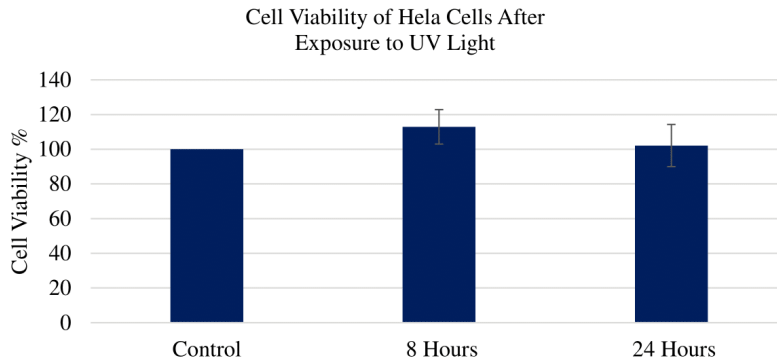


Figure S-34: HeLa cells were exposed to UV Light under a 365nm UV lamp 2 h post transfection for 45 min, (8 h assay) and for an additional 45 min of UV exposure every 4 hours (6 exposures total) (24 h assay). Data showed no significant changes in cell viability when compared to cells not exposed to UV light. The cell viability was determined using an XTT Assay (Promega).

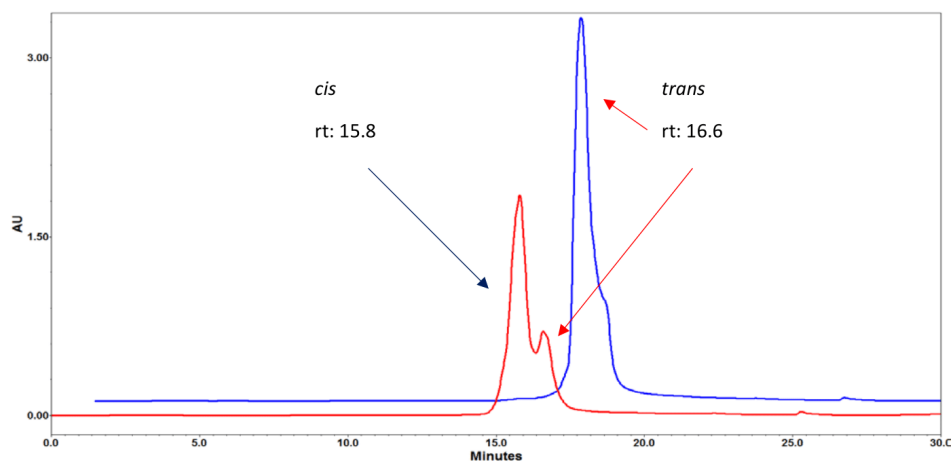


Figure S-35. HPLC chromatogram of sense strand of the sense strand of siRNA 5 showing both *cis* (left) and *trans* (right) peaks. Background (blue): The same sample of siRNA 5 collected and exposed to 60 min UV light. Foreground (red): untreated sense strand of siRNA 5 spectra. Conditions were 5% acetonitrile in 95% 0.1 M TEAA (Triethylamine-Acetic Acid) buffer up to 100% acetonitrile over 30 min. Spectra were processed using the Empower 3 software.

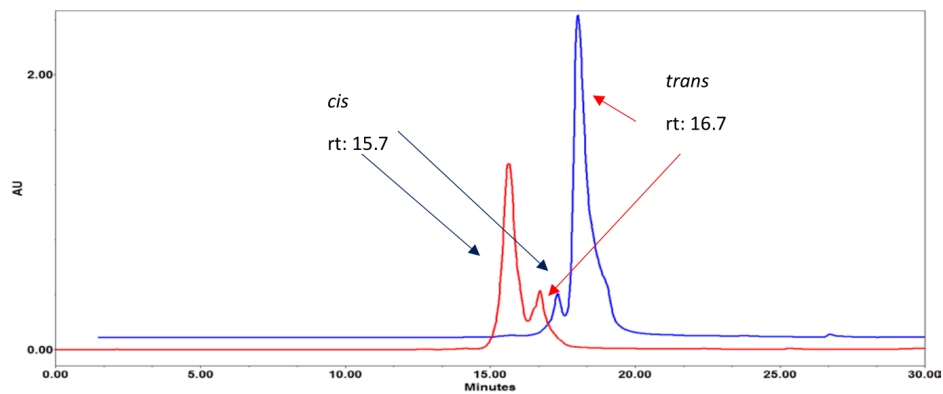


Figure S-36. HPLC chromatogram of the sense strand of siRNA 6 showing both *cis* (left) and *trans* (right) peaks. Background (blue): The same sample of siRNA 5 collected and exposed to 60 min UV light. Foreground (red): untreated sense strand of siRNA 5 spectra. Conditions were 5% acetonitrile in 95% 0.1 M TEAA (Triethylamine-Acetic Acid) buffer up to 100% acetonitrile over 30 min. Spectra were processed using the Empower 3 software.

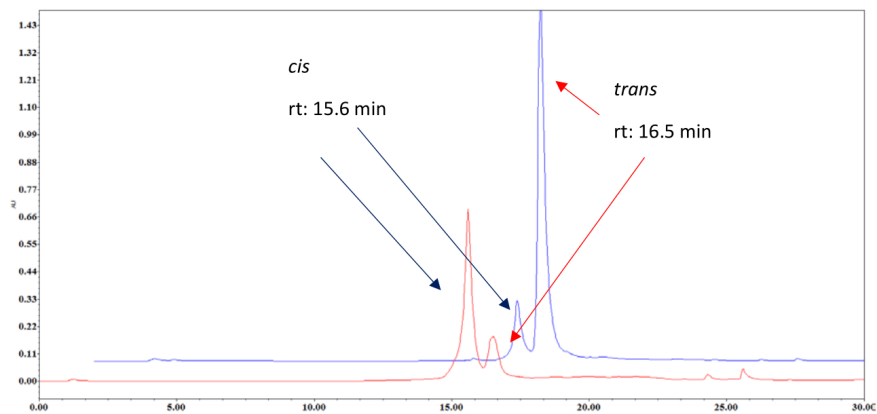


Figure S-37. HPLC chromatogram of the sense strand of siRNA 7 showing both *cis* (left) and *trans* (right) peaks. Background (blue): The same sample of siRNA 5 collected and exposed to 60 min UV light. Foreground (red): untreated sense strand of siRNA 5 spectra. Conditions were 5% acetonitrile in 95% 0.1 M TEAA (Triethylamine-Acetic Acid) buffer up to 100% acetonitrile over 30 min. Spectra were processed using the Empower 3 software.

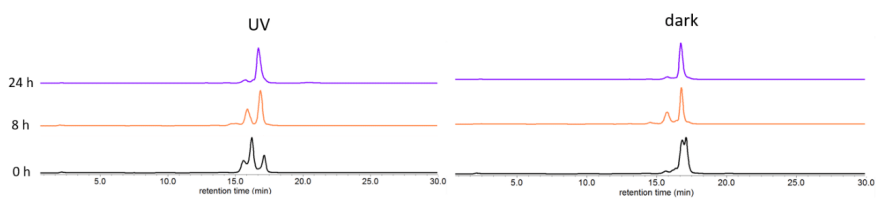


Figure S-38. GSH assay results of the sense strand of the sense strand of siRNAzo 6 showing minimal degradation due to the presence of GSH. UV treated RNA was exposed to 5 min of UV light and then kept at 37 °C until injection. Conditions were 5% acetonitrile in 95% 0.1 M TEAA (Triethylamine-Acetic Acid) buffer up to 100% acetonitrile over 30 min. Spectra were processed using the Empower 3 software.

Table S-1 Sequences of anti-luciferase and anti-*BCL2* siRNAzOs, predicted and recorded mass

siRNAzo	siRNAzo Duplex ^[a]	Predicted Mass of Sense Strand	Actual Mass of Sense Strand ^[b]	Target
1	5'- CUUACGC <u>Az2</u> AGUACUUCGAtt -3' (s) 3'- ttGAAUGCGACUCAUGAAGCU-5'(as)	6367.91	6366.89	luciferase
2	5'- CUUACGCU <u>Az2</u> GUACUUCGAtt -3' (s) 3'- ttGAAUGCGACUCAUGAAGCU-5'(as)	6344.86	6344.91	luciferase
3	5'- CUUACGCUG <u>Az2</u> UACUUCGAtt -3' (s) 3'- ttGAAUGCGACUCAUGAAGCU-5'(as)	6344.86	6344.86	luciferase
4	5'- CUUACGCUGA <u>Az2</u> ACUUCGAtt -3' (s) 3'- ttGAAUGCGACUCAUGAAGCU-5'(as)	6367.91	6366.95	luciferase
5	5'-GCCUUCU <u>Az2</u> GAGUUCGGUtt-3' (s) 3'-ttCGGAAGAAACUCAAGCCAC-5' (as)	6336.91	6336.86	<i>BCL2</i>
6	5'-GCCUUCUU <u>Az2</u> AGUUCGGUtt-3'(s) 3'-ttCGGAAGAAACUCAAGCCAC-5'(as)	6377.82	6377.81	<i>BCL2</i>
7	5'-GCCUUCUUUG <u>Az2</u> UUCGGUtt-3' (s) 3'-ttCGGAAGAAACUCAAGCCAC-5'(as)	6369.76	6369.76	<i>BCL2</i>

References

[a] **Az2** corresponds to the azobenzene derivative synthesized from 4-nitrophenylethyl alcohol; the top strand corresponds to the sense strand; the bottom strand corresponds to the antisense strand. In all duplexes, the 5'-end of the bottom antisense strand contains a 5'-phosphate group.

[b] Deconvolution results for siRNAzOs. ESI-HRMS (ES^+) m/z calculated for siRNAzOs 1-7 $[M+H]^+$

1. M. L. Hammill, C. Isaacs-Trepanier and J. P. Desaulniers, *ChemistrySelect*, **2017**, 2, 9810-9814.
2. McDowell, J.A.; Turner, D. H. *Biochemistry* **1996**, 35, 14077.

Appendix III. Manuscript III and Supplementary Data

Synthesis, Derivatization and Photochemical Control of *ortho*-Functionalized Tetrachlorinated Azobenzene-Modified siRNAs

Matthew L. Hammill,^[a] Golam Islam,^[a] and Jean-Paul Desaulniers^{*[a]}

We report the chemical synthesis and derivatization of an *ortho*-functionalized tetrachlorinated azobenzene diol. A 4',4'-dimethoxytrityl (DMT) phosphoramidite was synthesized for its site-specific incorporation within the sense strand of an siRNA duplex to form *ortho*-functionalized tetrachlorinated azobenzene-containing siRNAs (Cl-siRNAs). Compared to a non-halogenated azobenzene, *ortho*-functionalized tetrachlorinated azobenzenes are capable of red-shifting the $\pi \rightarrow \pi^*$ transition

from the ultraviolet (UV) portion of the electromagnetic spectrum into the visible range. Within this visible range, the azobenzene molecule can be reliably converted from *trans* to *cis* with red light (660 nm), and converted back to *trans* with violet wavelength light (410 nm) and/or thermal relaxation. We also report the gene-silencing ability of these Cl-siRNAs in cell culture as well as their reversible control with visible light for up to 24 hours.

Introduction

Since the report in 1998 by Fire and Mello, the RNA interference (RNAi) pathway has been of great interest for use as an effective therapeutic pathway and as a biomolecular tool for gene silencing.^[1] This endogenous pathway uses double-stranded RNA (dsRNA) as both a defense against unwanted viral infection and as an internal gene expression control. The ability to specifically silence gene targets based on the gene sequence makes this an attractive method to develop valuable therapeutics and biomolecular tools.^[2–4] There are currently two US FDA-approved siRNA therapeutics on the market. The first one, Onpatro, is a treatment for hereditary transthyretin amyloidosis (hATTR)^[5] and the second one, Givlaari treats acute hepatic porphyria.^[6] This recent success of siRNA therapeutics follows a time of hardship for siRNA therapeutics due to many siRNAs failing clinical trials.^[7] Even with this renewed focus on siRNAs, siRNAs are still a challenge to use as therapeutics due to challenges that are well known to the field, such as poor stability, toxicity, off-target effects and tissue specific targeting. Another area that is of interest to siRNA design is the ability to control its activity within a cellular environment. One way to control its activity is to use a photoresponsive functional group. Advancements in the photoresponsive control of siRNAs have shown excellent results. Despite these positive experiments involving photoswitchable siRNAs, improvements are necessary. In this manuscript, we expand on the current knowledge in the field through the synthesis, characterization and biological testing of tetra *ortho*-chlorinated azobenzenes that are incorpo-

rated into the sense (passenger) strand of an siRNA duplex. These tetra *ortho*-chlorinated azobenzene-containing siRNAs are called chlorinated siRNAs (Cl-siRNAs).

The photoresponsive siRNA field has been growing rapidly over the last several years, but most of these chemical modifications involve the inactivation of the payload siRNA, which is then activated at a later time with ultraviolet light inside the cell. A great example of this technology was reported by Freidman and coworkers, in which a nitrobenzene derivative was attached to the siRNA backbone and exposure to 320 nm UV light caused the activation of the siRNA.^[8] The use of similar UV-labile protecting groups have also been used as thymidine and guanine modifications by Mikat and Heckel, which caused a bulge in the duplex, rendering the RNA-induced-silencing-complex (RISC) complex as inoperative until exposure to UV light, which cleaved the groups and activated the siRNA.^[9] Recently, Mokhir and Meyer developed a 5'-labelled alkoxyanthracenyl siRNA, which becomes uncaged via a singlet oxygen (¹O₂) photo-regenerated photosensitizer on the 3'-end of the guide strand. Uncaging occurs with green or red light and yields an active siRNA.^[10] The limitation of these innovations is that siRNA payloads are *irreversibly* photoactivated and cannot be reversed once deployed. These photocages once released are chemical by-products which could have any number of unknown effects on the cells in the tissue. Thus, having greater spatial and temporal control of the siRNA via a *reversible* technology could have far-reaching effects on an siRNA's use as a therapeutic and as a biomolecular tool bypassing and minimizing unwanted off-target effects.

In this regard, azobenzene is a viable photo-responsive molecule because of its ability to photo-isomerize in the presence of UV and visible light. These large conformational changes in the molecule can be used to disrupt biomolecular structures such as duplexes.^[11]

The more stable *trans* isomer is the native state of the molecule, but the addition of high energy UV light in the 330–

[a] M. L. Hammill, G. Islam, Prof. J.-P. Desaulniers
Faculty of Science
University of Ontario Institute of Technology
2000 Simcoe Street North, Oshawa, Ontario L1G 0C5 (Canada)
E-mail: jean-paul.desaulniers@ontariotechu.ca

Supporting information for this article is available on the WWW under
<https://doi.org/10.1002/cbic.202000188>

360 nm range causes the less stable *cis* isomer to become dominant. This sterically hindered *cis* conformer strains the N=N bond, allowing for the use of low energy visible light above 450 nm to be used to convert it back to the more stable *trans* isomer.^[12] These unique and modular properties allow azobenzene to be used in many applications, including its incorporation into oligonucleotides (Figure 1) as it is relatively easy to synthesize and contains a high quantum yield when photoswitching.^[13]

Previous work in our group used this robust ability of azobenzene to photo-isomerize to make siRNAzOs, which are siRNA duplexes that contain azobenzene in the sense strand.^[14,15] Even more recently, we were able to extend the utility of our photoswitchable system by keeping our siRNAs inactive for up to 24 hours.^[16] Our previous system,^[14] in which we inactivated the siRNA before transfection, was limited by the azobenzene's half-life of 4 hours at 37 °C.^[17] This caused the reactivation of the siRNA over time, however the recent advancement we made was to inactivate the siRNA *after* transfection which allowed us to push the inactivation period to 24 hours, whereas previously, after 8 h (reactivation at 12 h) the siRNA would not remain inactive.^[16]

Despite this advancement in our technology, we are still using UV light to cause this change in activity. UV light, while useful, has several issues associated with it such as its toxicity to cells over long exposure times.^[17] High-energy UV light has also been known to cause pyrimidine dimers, and has poor tissue penetration in the body because human skin has evolved to scatter UV light so it could not penetrate the body to damage tissues.^[19] This presents a great hurdle and becomes a major

limitation for photochemically-controlled siRNAs dependent on UV light for therapeutic use.

Recent research on light penetration by Basford and co-workers show that penetration into human tissue is determined not only by wavelength but also light beam intensity and width.^[20] In their study, they reported that higher wavelength light induces deeper penetration. For example, red light penetrates to a depth of 5 mm, with maximum penetration occurring with a beam at least 10 mm wide, while UV gets less than 0.2 mm depth.^[20] This makes red-shifting the wavelength of photo-reactive pharmaceuticals a very high priority since many active therapeutics are not necessarily on the surface of the skin, but embedded within tissues. To accomplish this goal, there has been studies aimed at modifying azobenzene at the *ortho* positions in order to strain the N=N bond so that lower energy visible light can cause the isomerization from *trans* to *cis*. Feringa and co-workers used red-shifted azobenzene derivatives as a control for microbial activity by modifying antibiotics with chlorine and fluorine at the *ortho* positions of the azobenzene moiety and they reported excellent activity and reversibility with red and green light.^[21] Other reports involving photoresponsive control of nucleoside or oligonucleotide derivatives under visible light showed effective control.^[22–25] Other modifications at the *ortho* positions include not only halogens, such as fluorine and chlorine, but thiols, methoxy substituents, and amino containing groups like morpholino and amines.^[26–28] One issue with extending the isomerization point in the longer wavelength area of the spectrum is that these *cis* conformers can become increasingly unstable as they become more red-shifted.^[29] However, this is highly dependent on the modification, as shown with *ortho*-functionalized tetra-substituted chlorines being very unstable in the *cis* conformer.^[30] Trauner and co-workers have developed a novel synthesis system for the late stage functionalization of azobenzenes, by adding chlorinated substituents after the N=N bond has formed, as opposed to modifying the *ortho* position before the dimerization.^[31]

Therefore, in this new manuscript, we report the chemical synthesis of an *ortho*-functionalized tetra-chlorinated azobenzene diol. A DMT-phosphoramidite of the chlorinated azobenzene was synthesized for its incorporation into the siRNAs using solid-phase chemistry to generate red-shifted tetra-chlorinated azobenzene-containing siRNAs (Cl-siRNAzOs). We tested these red-shifted Cl-siRNAzOs in cell culture and were able to control the activity of the Cl-siRNAzO by using red light (660 nm) to convert from *trans* to *cis* and thermal relaxation to revert from *cis* to *trans*.

Results and Discussion

Our hypothesis was that chlorinated azobenzene, in the *cis* form, would distort the siRNA helix, thus rendering it non-functional in a similar manner to our previous research, but without the use of toxic UV light (Figure 2). Being able to control the timing of when an siRNA is active or not active would have enormous benefit for modern medicine.

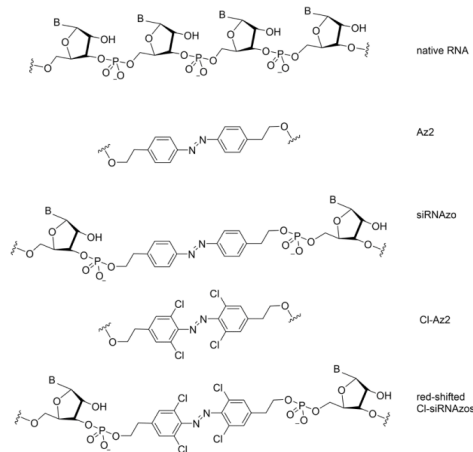


Figure 1. Structural differences between native RNA, and azobenzene-containing RNAs (siRNAzOs). Az2 corresponds to the azobenzene unit synthesized and used by our laboratory in previous studies.^[14–16] Cl-Az2 corresponds to the azobenzene unit used in this study.

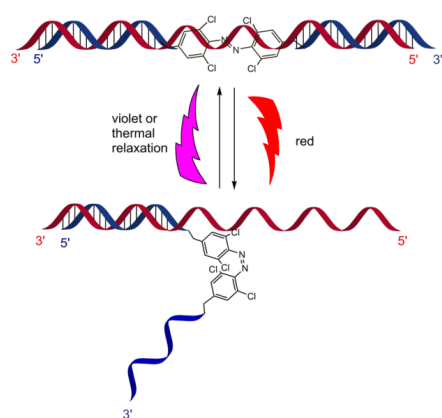
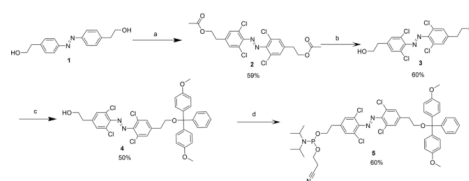


Figure 2. Photoinduced inactivation and reactivation of siRNA duplexes. The blue strand corresponds to the sense strand and contains the azobenzene moiety. The red strand corresponds to the antisense strand.

To start, this involved synthesizing diol **1** from our previously reported procedure.^[14] This diol **1** reacted with *n*-chlorosuccinimide (NCS) and palladium acetate (Pd(OAc)₂) to the *ortho*-functionalized tetrachlorinated azobenzene diacetyl compound **2** in 59% yield. This acetylated compound was deprotected in sodium hydroxide (NaOH) and methanol (MeOH) to afford the diol, compound **3**. This diol was then reacted with 4'-dimethoxytrityl (DMT) chloride to afford the monoalcohol **4**. Finally, the DMT-protected diol was phosphitylated with 2-cyanoethyl diisopropylchlorophosphoramidite in the presence of triethylamine to afford phosphoramidite **5** (Scheme 1). Overall, from compound **1**, phosphoramidite **4** was generated in 11% yield over four steps.

Once the phosphoramidite was synthesized, a small library of Cl-siRNAzOs were synthesized (Table 1). Three different Cl-siRNAzOs were synthesized that target the firefly luciferase mRNA (Table 1). In each Cl-siRNAzo, the azobenzene derivative replaces two nucleosides on the oligonucleotide sense strand. These Cl-siRNAzOs were purified and characterized by mass spectrometry (Table S1 in the Supporting Information). Cl-siRNAzo **1** contains an azobenzene modification (Cl-Az2) that replaces positions 8 and 9, on the sense strand, counting from the 5'-end of the sense strand. This azobenzene insertion partially replaces the Argonaute 2 cleavage site.^[32] siRNAzOs **2** and **3** contain the same azobenzene modification (Cl-Az2) and this modification spans two nucleosides that replace positions 9 and 10, and 10 and 11, of the sense strand, respectively.

These siRNAzOs were then tested for *cis-trans* isomerization, but due to the short half-life of the *cis* isomer, it was difficult to characterize by HPLC (Figures S2 to S4 in the Supporting Information) in any significant amount after exposure to red light. We performed some time-dependent absorbance studies after exposure to red light, and estimate the half-life at 37 °C to



Scheme 1. Synthesis of an *ortho*-functionalized tetrachlorinated azobenzene DMT-phosphoramidite: a) 0.3 equiv. of Pd(OAc)₂ and 8 equiv. of NCS AcOH, 145 °C, 59% (**2**); b) 0.1 equiv. NaOH in MeOH, RT, 0.5 h, 60% (**3**); c) 1 equiv. dimethoxytrityl chloride (DMT-Cl), 3 equiv. TEA, THF, RT, 50% (**4**); d) 3 equiv. 2-cyanoethyl *N,N*-diisopropylchlorophosphoramidite, 10 equiv. TEA, anhydrous CH₂Cl₂/ACN (1:1), RT, 2 h, 60% (**5**).

Table 1. RNAs used and their targets.

siRNA	siRNA duplex	Target
WT	5'-CUUACGCUGAGUACUUCGAtt-3' 3'-ttGAAUGCGACUCAUGAAGCU-5'	luciferase
1	5'-CUUACGC Cl-Az2 AGUACUUCGAtt-3' 3'-ttGAAUGCGACUCAUGAAGCU-5'	luciferase
2	5'-CUUACGC Cl-Az2 GUACUUCGAtt-3' 3'-ttGAAUGCGACUCAUGAAGCU-5'	luciferase
3	5'-CUUACGCUG Cl-Az2 UACUUCGAtt-3' 3'-ttGAAUGCGACUCAUGAAGCU-5'	luciferase

[a] **Cl-Az2** is the azobenzene derivative synthesized from Az2; the top strand corresponds to the sense strand; the bottom strand corresponds to the antisense strand. In all duplexes, the 5'-end of the bottom antisense strand contains a 5'-phosphate group.

be approximately 2 minutes (data not shown). Previous studies of chlorinated azobenzene structures show a half-life from tens of milliseconds^[33] up to 3.5 hours.^[13] Our specific modification turned out to have a very unstable half-life of less than one minute, and so we chose thermal relaxation as the reactivation protocol. Also due to the smaller absorbance profile of the chlorinated azobenzene compared to the original non-chlorinated one, there was no discernible peak representing the Cl-Az2 moiety in the absorbance spectra (data not shown). Despite these challenges, we were still able to characterize the Cl-siRNAzOs via mass spectrophotometry (Table S1). The *ortho*-functionalized tetrachlorinated azobenzene diol **3** itself was characterized via an absorbance graph, and both the *trans* and *cis* isomers and their change in absorbance are visible, with red wavelength light causing the change to *cis*, while violet light or thermal relaxation will restore the *trans* isomer (Figure 3). This finding is in agreement with the literature.^[33]

In addition, these Cl-siRNAzOs also exhibited thermal destabilization because the chlorinated azobenzene moiety replaces two nucleotides within the central region, as measured by UV absorption profiles in melting experiments (Table S1). This is consistent with other studies that place thermally destabilizing units into the central region of the sense strand.^[34–36] Lastly, these siRNAzOs all retained classic A-type helix conformation which is required for the RNAi pathway to function, characterized by circular dichroism (Figure S1).

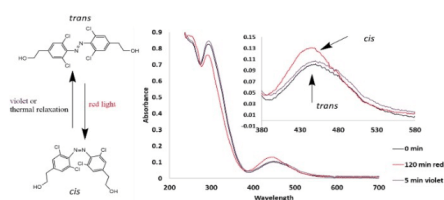


Figure 3. Absorbance profile of Cl-Az2 (compound 3) moiety when exposed to various wavelengths of visible light (red (660 nm) and violet (410 nm)) in methanol. Inset: Zoomed in portion of 400–580 nm highlighting azobenzene changes.

Once the biophysical characterizations were completed, gene silencing was evaluated in the dark with no exposure to light. As the more thermally stable *trans* isomer is dominant at 37 °C, we expected the siRNA to be in the active *trans* form and achieve efficient gene silencing. As expected, and observed in Figure 4, all the Cl-siRNAzOs demonstrated good dose-dependent silencing of the firefly luciferase gene at concentrations between 1 and 4 nM (blue bars). This was observed for both time points, 8 and 24 hours. All three Cl-siRNAzOs show around 90% knockdown at 4 nM, with a decrease to approximately 70–80% knockdown at 1 nM for the various time points and Cl-siRNAzOs. Next, we screened these Cl-siRNAzOs with exposure to red light in order to test for the inactivation, preventing their uptake into the RNAi pathway, and thus preventing gene silencing with the less toxic, low energy and high wavelength light. Previously, it was shown that exposure to higher energy low wavelength UV light could accomplish this effectively, and it could successfully be reversed with broadband visible light.^[16] We hypothesized that instead of disrupting the RISC complex after it had bound the siRNAzo, that we were preventing the uptake of remaining unbound siRNAs in the RNAi pathway with our system. At any one time, it has been reported that only about 4% of the active siRNAs are taken up into the RISC complex immediately upon transfection.^[37] Thus, within our system, the remaining unbound population of siRNAzOs can be inactivated and their uptake into the RNAi pathway prevented.^[17] Our finding demonstrated, that with the new chlorinated azobenzene moiety, we could inactivate the unbound Cl-siRNAzOs with red light and keep them inactive for up to 24 hours as long as the cells were exposed to the red light. In every case, all concentrations and both time points, luciferase activity increased to levels similar to untreated cells, thus indicating poor gene silencing when the cells were exposed to red light (gray bars, Figure 4). There is also a very large difference in gene silencing as compared to the dark exposed Cl-siRNAzOs, demonstrating the functionality of active vs inactive Cl-siRNAzOs. As mentioned previously, due to the poor half-life of the Cl-Az2 moiety, the cell culture had to be exposed to the red light for the entire duration of the assay. The next phase of our experiment involved testing the gene silencing by initially inactivating the siRNA with red light, then allowing the

ambient thermal energy to convert our inactive *cis* form back to its active *trans* isomer. To achieve this, cells were exposed to red light for only the first 2 hours of the assay and the resulting luminescence of the luciferase was determined after 8 or 24 hours. We found that at both the 8- and 24-hour time points, excellent gene silencing was achieved to comparable levels to the control dark treatment (yellow bars). Additionally, we found no degradation of the siRNAzOs via glutathione for up to 24 hours, whether exposed to red light, or kept in the dark (Figure S5). This study demonstrated that we can actively control siRNA activity using chlorinated siRNAzOs (Cl-siRNAzOs) by using only visible wavelength light, which represents a significant advancement over the UV light utilized in our previous system and other reported technologies.^[8–10,14–16] This is an enhancement over our previous generation of siRNAzOs, where higher energy UV light, which is toxic, was required to control the activity of gene-silencing within mammalian cells.

Conclusion

We have synthesized and evaluated red-shifted Cl-siRNAzOs that can be photochemically controlled using visible wavelength light. To our knowledge this is the first time, a system utilizing siRNAs with an azobenzene moiety could be photo-controlled using only visible light, using wavelengths of 660 nm for red, and 410 nm for violet light. We believe this to be an improvement over the previous system, which until now required the use of toxic UV light to induce photochemical control of the siRNA.^[16] Using visible light should not only prove to be less toxic, but there are also no photochemical by-products released, such as in the case of photocages. In addition, this system is also reversible, another improvement over the caging systems available. The short half-life of the *cis* conformer however remains problematic, since constant exposure to red light is inconvenient for use as a bio-molecular tool or a therapeutic. One way to overcome this challenge, is to continue exploring different chemical modifications which not only allow the photocontrol with visible light, but also allow longer half-lives at physiological relevant temperatures, so that inactivation can occur with one short exposure of light, and then be red-activated later at a time of our choice. If overcome, a visible light controllable therapeutic with a long half-life would be very beneficial to the research sector for use as a biomolecular tool, as well as within the pharmaceutical industry where fine-tuned spatiotemporal control of a drug would be desirable. This is an important issue: a paper published from Alnylam® Pharmaceuticals in 2018 disclosed that a short oligonucleotide was capable of reversing the activity of an active siRNA.^[38] Utilization of this system to control off-target effects in a patient undergoing treatment would also be ideal, where red light exposure on sensitive adjacent tissues or surrounding healthy tissue could prevent off-target effects and siRNA-mediated toxicity. Future directions include further exploration of chemical modifications to improve functionality, as well as development of a multi-siRNAzo system, where

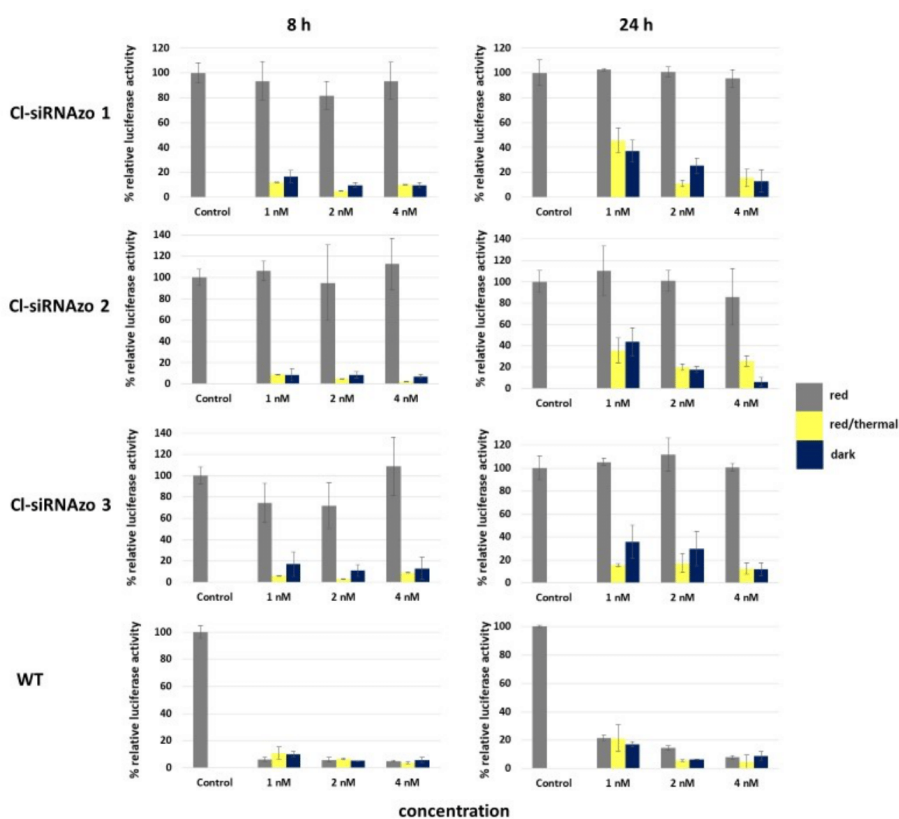


Figure 4. Normalized firefly luciferase expression for Cl-siRNAs 1–3 at 1, 2 and 4 nM in HeLa cells monitored 8 and 24 h post-transfection. Red corresponds to the siRNA being exposed under a multi-wavelength lamp tuned to red light for inactivation immediately after transfection for the entire length of the assay (8 or 24 h). Red/thermal corresponds to red light exposure for the first 2 h after transfection, after which the light was removed and the siRNA was allowed to thermally relax back to the active state for the remaining of the assay (8 or 24 h). Dark corresponds to siRNAs being transfected in HeLa cells in the absence of red light. WT corresponds to wild-type anti-firefly luciferase siRNA.

multiple targets could be activated/inactivated selectively with different wavelengths of light.

Experimental Section

Experimental details are provided in the Supporting Information.

Acknowledgements

We thank the Natural Sciences and Engineering Research Council (NSERC) for funding.

Conflict of Interest

The authors declare no conflict of interest.

Keywords: azobenzene · gene-silencing · photocontrol · siRNA

- [1] A. Fire, S. Q. Xu, M. K. Montgomery, S. A. Kostas, S. E. Driver, C. C. Mello, *Nature* **1998**, *391*, 806.
- [2] L. Aagaard, J. J. Rossi, *Adv. Drug Delivery Rev.* **2007**, *59*, 75.
- [3] A. L. Hopkins, C. R. Groom, *Nat. Rev. Drug Discovery* **2002**, *1*, 727.
- [4] X. Shen, D. R. Corey, *Nucleic Acids Res.* **2017**, *46*, 1584.
- [5] D. Al Shaer, O. Al Musaimi, F. Albericio, B. G. de la Torre, *Pharmaceuticals* **2019**, *12*, 52.

- [6] P. R. D. Brandao, S. S. Títze-de-Almeida, R. Títze-de-Almeida, *Mol. Diagn. Ther.* **2019**, *8*.
- [7] R. L. Setten, J. J. Rossi, S. P. Han, *Nat. Rev. Drug Discovery* **2019**, *18*, 421.
- [8] S. Shah, S. Rangarajan, S. H. Friedman, *Angew. Chem. Int. Ed.* **2005**, *44*, 1328.
- [9] V. Mikat, A. Heckel, *RNA* **2007**, *13*, 2341.
- [10] A. Meyer, A. Mokhir, *Angew. Chem. Int. Ed.* **2014**, *53*, 12840.
- [11] A. S. Lubbe, W. Szymanski, B. L. Feringa, *Chem. Soc. Rev.* **2017**, *46*, 1052.
- [12] C. Briek, F. Rohrbach, A. Gottschalk, G. Mayer, A. Heckel, *Angew. Chem. Int. Ed.* **2012**, *51*, 8446.
- [13] A. A. Beharry, G. A. Woolley, *Chem. Soc. Rev.* **2011**, *40*, 4422.
- [14] M. L. Hammill, C. Isaacs-Trépanier, J.-P. Desaulniers, *ChemistrySelect* **2017**, *2*, 9810.
- [15] M. L. Hammill, A. Patel, M. A. Alla, J.-P. Desaulniers, *Bioorg. Med. Chem. Lett.* **2018**, *28*, 3613.
- [16] M. L. Hammill, G. Islam, J.-P. Desaulniers, *Org. Biomol. Chem.* **2020**, *18*, 41.
- [17] K. Yamana, K. Kan, H. Nakano, *Bioorg. Med. Chem.* **1999**, *7*, 2977.
- [18] Abrams, Y. Xu, N. A. Kuklin, P. A. Burke, A. B. Sachs, L. Sepp-Lorenzino, S. T. Barnett, *RNA* **2010**, *16*, 2553.
- [19] J. D'Orazio, S. Jarrett, A. Amaro-Ortiz, T. Scott, *Int. J. Mol. Sci.* **2013**, *14*, 12222.
- [20] C. Ash, M. Dubec, K. Donne, T. Bashford, *Lasers Med. Sci.* **2017**, *32*, 1909.
- [21] M. Wegener, M. J. Hansen, A. J. M. Driessen, W. Szymanski, B. Feringa, *J. Am. Chem. Soc.* **2017**, *139*, 17979.
- [22] O. Shinzi, I. Syoji, M. Hiroshi, M. Mizuo, *Chem. Lett.* **2010**, *39*, 956.
- [23] H. Nishioka, X. Liang, T. Kato, H. Asanuma, *Angew. Chem. Int. Ed.* **2012**, *51*, 1165.
- [24] Y. Kamiya, T. Takagi, H. Ooi, H. Ito, X. Liang, H. Asanuma, *ACS Synth. Biol.* **2015**, *365*.
- [25] D. Kolarski, W. Szymanski, B. L. Feringa, *Org. Lett.* **2017**, *19*, 5090.
- [26] S. Samanta, T. M. McCormick, S. K. Schmidt, D. S. Seferos, G. A. Woolley, *Chem. Commun.* **2013**, *49*, 10314.
- [27] M. Dong, A. Babalhavaeji, S. Samanta, A. A. Beharry, G. A. Woolley, *Acc. Chem. Res.* **2015**, *48*, 2662.
- [28] O. Sadowski, A. A. Beharry, F. Zhang, G. A. Woolley, *Angew. Chem. Int. Ed. Engl.* **2009**, *48*, 1484.
- [29] J. García-Amorós, D. Velasco, *Beilstein J. Org. Chem.* **2012**, *8*, 1003.
- [30] D. Bleger, J. Schwarz, A. M. Brouwer, S. Hecht, *J. Am. Chem. Soc.* **2012**, *134*, 20597.
- [31] D. B. Konrad, J. A. Frank, D. Trauner, *Chem. Eur. J.* **2016**, *22*, 4364.
- [32] C. Matranga, Y. Tomari, C. Shin, D. P. Bartel, P. D. Zamore, *Cell* **2005**, *123*, 607.
- [33] J. Broichhagen, J. A. Frank, D. Trauner, *Acc. Chem. Res.* **2015**, *48*, 1947.
- [34] T. C. Efthymiou, B. Peel, V. Huynh, J.-P. Desaulniers, *Bioorg. Med. Chem. Lett.* **2012**, *22*, 5590.
- [35] H. Addepalli, Meena, C. G. Peng, G. Wang, Y. Fan, K. Charisse, K. N. Jayaprakash, K. G. Rajeev, R. K. Pandey, G. Lavine, L. Zhang, K. Jahn-Hofmann, P. Hadwiger, M. Manoharan, M. A. Maier, *Nucleic Acids Res.* **2010**, *38*, 7320.
- [36] B. J. Peel, G. Hagen, K. Krishnamurthy, J.-P. Desaulniers, *ACS Med. Chem. Lett.* **2015**, *6*, 117.
- [37] Y. I. Pei, P. J. Hancock, H. Zhang, R. Bartz, C. Cherrin, N. Innocent, C. J. Pomerantz, J. Seitzer, M. L. Koser, M. T. Abrams, Y. Xu, N. A. Kuklin, P. A. Burke, A. B. Sachs, L. Sepp-Lorenzino, S. T. Barnett, *RNA* **2010**, *16*, 2553.
- [38] I. Zlatev, A. Castoreno, C. R. Brown, J. Qin, S. Waldron, M. K. Schlegel, R. Degaonkar, S. Shulga-Morskaya, H. Xu, S. Gupta, S. Matsuda, A. Akinc, K. G. Rajeev, M. Manoharan, V. Jadhav, *Nat. Biotechnol.* **2018**, *36*, 509.

Manuscript received: March 25, 2020
Accepted manuscript online: March 30, 2020
Version of record online: April 22, 2020

ChemBioChem

Supporting Information

Synthesis, Derivatization and Photochemical Control of *ortho*-Functionalized Tetrachlorinated Azobenzene- Modified siRNAs

Matthew L. Hammill, Golam Islam, and Jean-Paul Desaulniers*

Experimental Procedures for the Synthesis of Novel Compounds and Characterizations:

General.....	S3
Synthesis and ¹ H/ ¹³ C NMR Characterizations of Compound 1.....	S3
Synthesis and ¹ H/ ¹³ C NMR Characterizations of Compound 2.....	S3
Synthesis and ¹ H/ ¹³ C NMR Characterizations of Compound 3.....	S4
Synthesis and ¹ H/ ¹³ C NMR Characterizations of Compound 4.....	S4
Synthesis and ¹ H/ ¹³ C/ ³¹ P NMR Characterizations of Compound 5.....	S5
Nucleic Acid and Biological Procedures	
Procedure for Oligonucleotide Synthesis and Purification.....	S5
Procedure for ESI QTOF Measurements.....	S5
Procedure for Performing CD experiments.....	S6
Procedure for Melting Temperature of siRNA Duplexes (<i>T_m</i>).....	S6
Procedure for absorbance spectra experiments.....	S7
Procedure for HPLC Characterization.....	S7
Procedure for Reduced Glutathione (GSH) Degradation Assay.....	S7
Procedure for Maintaining Cell Cultures of HeLa Cells.....	S7
Procedure for siRNA transfections.....	S8
Procedure for <i>in vitro</i> Dual Luciferase Assay.....	S8

Procedure for light inactivation of azobenzene modified siRNA (<i>trans</i> to <i>cis</i>).....	S9
Procedure for Thermal Relaxation and Reactivation of Azobenzene Modified siRNA (<i>cis</i> to <i>trans</i>).....	S9

Figures and Tables

Table S-1: Sequences of anti-luciferase siRNAs, predicted and recorded mass and T_m 's of siRNAs containing the azobenzene spacers.....	S10
Figure S-1: CD spectra of azobenzene modified spacers replacing two nucleobases targeting firefly luciferase mRNAs.....	S10
Figure S-2: HPLC Chromatogram of untreated siRNAzo 1	S11
Figure S-3: HPLC Chromatogram of untreated siRNAzo 2.....	S11
Figure S-4: HPLC Chromatogram of untreated siRNAzo 3.....	S12
Figure S-5: Figure S-38: GSH assay comparative HPLC chromatograms of untreated siRNA 1 and red light exposure.....	S12

$^1\text{H}/^{13}\text{C}/^{31}\text{P}$ NMR Spectra of Compounds

$^1\text{H}/^{13}\text{C}$ NMR Spectra of Compound 1	S13
$^1\text{H}/^{13}\text{C}$ NMR Spectra of Compound 2	S14
$^1\text{H}/^{13}\text{C}$ NMR Spectra of Compound 3	S15
$^1\text{H}/^{13}\text{C}$ NMR Spectra of Compound 4	S16
$^1\text{H}/^{13}\text{C}/^{31}\text{P}$ NMR Spectra of Compound 5	S17
References	S18

Experimental Procedures for the Synthesis of Novel Compounds and Characterizations

General

Unless otherwise indicated all starting reagents used were obtained from commercial sources without additional purification. Anhydrous CH_2Cl_2 and THF were purchased from Sigma-Aldrich and run through a PureSolv 400 solvent purification system to maintain purity. Flash column chromatography was performed with Silicycle Siliacflash 60 (230-400 mesh), using the procedure developed by Still, Kahn and Mitra.¹ NMRs were performed on a Varian 400 MHz spectrophotometer. All ^1H NMRs were recorded for 64 transients at 400 MHz and all ^{13}C NMRs were run for 1500 transients at 101 MHz and all ^{31}P NMRs were recorded for 256 transients at 167 MHz. Spectra were processed and integrated using ACD labs NMR Processor Academic Edition.

Synthesis of 4,4'-bis(hydroxyethyl)-azobenzene – Compound (1)

To a solution of 90.0 mL of 5.70 M $\text{NaOH}_{(\text{aq})}$ 4.00 g of 4-nitrophenethyl alcohol (23.9 mmol, 1.00 equiv.) was added and stirred until fully dissolved. To this solution 6.00 g Zn powder (92.3 mmol, 3.85 equiv.) was slowly added to maintain stirring. After refluxing overnight for 16 h it was then filtered on a Buchner Vacuum filter, and the crystals were suspended in hot methanol. The crystals were collected and filtered again with a gravity filter to remove residual salts and then the methanol solution was removed using a rotary evaporator. Crystals were collected and purified on silica gel column using MeOH (2% to 5%) in CH_2Cl_2 to afford compound **1** as orange crystals (2.34 g, 72%). ^1H NMR (400 MHz, d_6 -DMSO) δ 7.75 - 7.81 (d, J = 8.21 Hz 4H) 7.41 (d, J = 8.21, Hz 4H) 4.71 (t, J = 5.28 Hz, 2H) 3.65 (td, J = 6.84, 5.47 Hz, 4H) 2.80 (t, J = 6.84 Hz, 4H). ^{13}C NMR (101 MHz, d_6 -DMSO) δ ppm 150.84, 144.02, 130.34, 122.79, 62.26, 38.87; ESI-HRMS (ES^+) m/z calculated for $\text{C}_{16}\text{H}_{18}\text{N}_2\text{O}_2$: 271.1441, found 271.1438 [$\text{M}+\text{H}$]⁺

Synthesis of (E)-(diazene-1,2-diylbis(3,5-dichloro-4,1-phenylene))bis(ethane-2,1-diyl) diacetate Compound (2)

To a solution of 6.00 mL of glacial acetic acid 0.5 g of compound **2** (1.85 mmol, 1.00 equiv.) was added to a reactor tube. To that solution 1.9 g NCS (14 mmol, 8 equiv.) and 0.12 g of $\text{Pd}(\text{OAc})_2$ (0.5 mmol, 0.3 equiv.) and stirred at 140 °C overnight (20 h, reflux). After rotary evaporation, the compound was then purified on silica gel using a 1%:99%: acetone/dichloromethane mobile phase. This afforded compound **4** as a dark red crystal (0.54 g, 59%). ^1H NMR (400 MHz, d - CDCl_3) δ ppm 7.35 (s, 4H) 4.34 (t, J =6.72 Hz, 4H) 4.28 (s, 1H) 2.98 (t, J =6.72 Hz, 4H) 2.09 (s, 6H). ^{13}C NMR (101 MHz, d - CDCl_3) δ ppm 170.8, 170.7, 146.0, 140.6,

140.1, 129.8, 129.5, 127.4, 125.9, 63.7, 63.5, 34.2, 34.06, 20.9, 20.8; ESI-HRMS (ES⁺) m/z calculated for C₂₀H₁₈Cl₄N₂O₄: 492.17, found 491.0092 [M+H]⁺

Synthesis of (E)-2,2'-(diazene-1,2-diylbis(3,5-dichloro-4,1-phenylene))bis(ethan-1-ol) – Compound (3)

To a solution of 3.00 mL of 10 mg/mL NaOH in MeOH (0.1 equiv.) 0.2 g of compound **4** (0.4 mmol, 1.00 equiv.) was added to a 20 mL vial. That solution was stirred (1 h, rt.). After rotary evaporation, the compound was then purified on silica gel using a 5%:95%: MeOH/dichloromethane mobile phase. This afforded compound **5** as a dark red crystal (0.12 g, 60%). ¹H NMR (400 MHz, DMSO-*d*₆) δ ppm 7.57 (s, 4 H) 3.69 (t, *J*=6.36 Hz, 4 H) 2.81 (t, *J*=6.36 Hz, 4 H). ¹³C NMR (101 MHz, DMSO-*d*₆) δ ppm 144.7, 144.1 130.7, 130.4, 126.3, 124.7, 61.5, 61.2, 55.3, 40.6, 40.4, 40.2, 40.0, 39.7, 39.5, 39.3, 38.1, 37.8; ESI-HRMS (ES⁺) m/z calculated for C₁₆H₁₄Cl₄N₂O₄: 405.98, found 406.9882 [M+H]⁺

Synthesis of (E)-2-(4-((4-(2-(bis(4-methoxyphenyl)(phenyl)methoxy)ethyl -2,6-dichlorophenyl)diazenyl)-3,5-dichlorophenyl)ethan-1-ol – Compound (4)

To a solution of anhydrous DCM 5.0 mL 0.24 g of compound **5** (0.48 mmol, 1.00 equiv.) was added and stirred until fully dissolved. To the solution 0.2 g of 4,4'-dimethoxytrityl chloride (0.59 mmol, 1.00 equiv.) was added along with 0.41 mL triethylamine (2.93 mmol, 5.00 equiv.) The reaction mixture was stirred vigorously overnight and monitored by TLC. The crude reaction was then concentrated by rotovap and purified on silica gel column using MeOH (2% to 5%) in CH₂Cl₂ to afford compound **6** as a dark red oil (0.21 g, 50%). ¹H NMR (400 MHz, *d*-CDCl₃) δ ppm 7.17 - 7.43 (m, 14 H) 6.77 - 6.88 (m, 4 H) 3.91 (t, 2 H) 3.80 (s, 6 H) 3.37 (t, 2 H) 2.83 - 2.91 (t, 4 H). ¹³C NMR (101 MHz, *d*-CDCl₃) δ ppm 20.8, 20.9, 34.3, 54.5, 55.2, 55.2, 63.8, 76.7, 77.1, 77.4, 86.1, 113.0, 113.1, 113.6, 125.9, 126.5, 127.2, 127.4, 127.8, 127.8, 128.1, 128.3, 128.7, 129.5, 130.0, 130.2, 136.0, 136.1, 138.5, 140.1, 140.5, 142.2, 144.9, 146.9, 158.0, 158.4, 158.5, 170.7; ESI-HRMS (ES⁺) m/z calculated for C₃₇H₃₂Cl₄N₂O₄: 710.47, found 709.1189 [M+H]⁺

2.2.4 Synthesis of (E)-4-((4-(2-(bis(4-methoxyphenyl)(phenyl)methoxy)ethyl)-2,6-dichlorophenyl)diazenyl)-3,5-dichlorophenethyl (2-cyanoethyl) diisopropylphosphoramidite - Compound (5)

To a solution of 4.00 mL of anhydrous DCM/ACN (1:1) 0.14 g of compound **6** (0.2 mmol, 1.00 equiv.) was added to a flame dried flask. To that solution 0.28 mL of anhydrous triethylamine (2.0 mmol, 10.0 equiv.) was added along with 0.13 mL of 2-cyanoethyl *N,N*-diisopropylchlorophosphoramidite with (0.9 mmol, 3.00 equiv.) and stirred at room temperature until TLC showed starting materials were consumed (2 h). After rotary evaporation, the compound was then purified on silica gel using a 68%:30%:2% hexanes/ethyl acetate/triethylamine mobile phase. This afforded compound **7** as a dark red oil (0.1 g, 60%). ¹H NMR (400 MHz, *d*-CDCl₃) δ ppm 7.35 - 7.43 (m, 2 H) 7.16 - 7.35 (m, 12 H) 6.76 - 6.90 (m, 5 H) 3.86 (s, 1 H) 3.81 (s, 6 H) 3.74 - 3.79 (m, 1 H) 3.61 - 3.67 (m, 1 H) 3.37 (s, 1 H) 2.96 (t, *J*=6.24 Hz, 2 H) 2.88 (t, *J*=6.24 Hz, 2 H) 2.79 (t, *J*=6.24 Hz, 2 H) 2.62 - 2.67 (t, *J*=6.24 Hz, 2 H) 1.13 - 1.34 (m, 12 H). ³¹P NMR (162 MHz, *d*-CDCl₃) δ ppm 147.90. ¹³C NMR (101 MHz, *d*-CDCl₃) δ ppm 17.0, 20.3, 20.8, 24.5, 24.6, 24.7, 42.9, 43.0, 50.6, 50.7, 53.2, 54.5, 55.2, 58.2, 58.3, 58.4, 58.5, 59.2, 76.8, 77.1, 77.4, 113.1, 113.6, 117.6, 117.7, 126.5, 127.2, 127.4, 127.8, 128.0, 128.1, 128.3, 128.7, 129.8, 129.9, 130.0, 130.2, 135.9, 136.0, 138.5, 142.6, 144.9, 146.9, 158.0, 158.5, 203.2; ESI-HRMS (ES⁺) *m/z* calculated for C₄₆H₄₉Cl₄N₄O₅P: 910.69, found 910.2711 [M+H]⁺

Experimental Nucleic Acid and Biological Procedures

Procedure for Oligonucleotide Synthesis and Purification

All standard β-cyanoethyl 2'-*O*-TBDMS protected phosphoramidites, reagents and solid supports were purchased from Chemgenes Corporation and Glen Research. Wild-type luciferase strands including the sense and 5'-phosphorylated antisense strand were synthesized. All commercial phosphoramidites were dissolved in anhydrous acetonitrile to a concentration of 0.10 M. The chemically synthesized (azobenzene derivative) phosphoramidites were dissolved in 3:1 (v/v) acetonitrile:THF (anhydrous) to a concentration of 0.10 M. The reagents that were used for the phosphoramidite coupling cycle were: acetic anhydride/pyridine/THF (Cap A), 16% *N*-methylimidazole in THF (Cap B), 0.25 M 5-ethylthio tetrazole in ACN (activator), 0.02 M iodine/pyridine/H₂O/THF (oxidation solution), and 3% trichloroacetic acid/dichloromethane. All sequences were synthesized on 0.20 μM or 1.00 μM dT solid supports except for sequences that were 3'-modified, which were synthesized on 1.00 μM Universal III solid supports. The

entire synthesis ran on an Applied Biosystems 394 DNA/RNA synthesizer using 0.20 μ M or 1.00 μ M cycles kept under argon at 55 psi. Standard and synthetic phosphoramidites ran with coupling times of 999 seconds.

Antisense sequences were chemically phosphorylated at the 5'-end by using 2-[2-(4,4'-dimethoxytrityloxy)ethylsulfonyl]ethyl-(2-cyanoethyl)-(N,N-diisopropyl)-phosphoramidite. At the end of every cycle, the columns were removed from the synthesizer, dried with a stream of argon gas, sealed and stored at 4 °C. Cleavage of oligonucleotides from their solid supports was performed through on-column exposure to 1.50 mL of EMAM (methylamine 40% wt. in H₂O and methylamine 33% wt. in ethanol, 1:1 (Sigma-Aldrich)) for 1 hour at room temperature with the solution in full contact with the controlled pore glass. The oligonucleotides were then incubated overnight at room temperature in EMAM to deprotect the bases. On the following day, the samples were concentrated on a Speedvac evaporator overnight, resuspended in a solution of DMSO:3HF/TEA (100 μ L:125 μ L) and incubated at 65 °C for 3 hours in order to remove the 2'-O-TDBMS protecting groups. Crude oligonucleotides were precipitated in EtOH and desalted through Millipore Amicon Ultra 3000 MW cellulose. Oligonucleotides were separated on a 20% acrylamide gel and were used without further purification for annealing and transfection. Equimolar amounts of complimentary RNAs were annealed at 95 °C for 2 min in a binding buffer (75.0 mM KCl, 50.0 mM Tris-HCl, 3.00 mM MgCl₂, pH 8.30) and this solution was cooled slowly to room temperature to generate siRNAs used for biological assays. A sodium phosphate buffer (90.0 mM NaCl, 10.0 mM Na₂HPO₄, 1.00 mM EDTA, pH 7.00) was used to anneal strands for biophysical measurements.

Procedure for ESI Q-TOF Measurements. All single-stranded RNAs were gradient eluted through a Zorbax Extend C18 HPLC column with a MeOH/H₂O (5:95) solution containing 200 mM hexafluoroisopropyl alcohol and 8.1 mM triethylamine, and finally with 70% MeOH. The eluted RNAs were subjected to ESI-MS (ES⁻), producing raw spectra of multiply-charged anions and through resolved isotope deconvolution, the molecular weights of the resultant neutral oligonucleotides were confirmed for all the RNAs.

Procedure for Performing CD Experiments

Circular Dichroism (CD) spectroscopy was performed on a Jasco J-815 CD equipped with temperature controller. Equimolar amounts of each siRNA (10 μ M) were annealed to their complement in 500 μ L of a sodium phosphate buffer by incubating at 95 °C for two minutes and allowing to cool to room

temperature. CD measurement of each duplex were recorded in triplicate from 200-500 nm at 25 °C with a screening rate of 20.0 nm/min and a 0.20 nm data pitch. The average of the three replicates was calculated using Jasco's Spectra Manager version 2 software and adjusted against the baseline measurement of the sodium phosphate buffer.

Procedure for Melting Temperature of siRNA Duplexes (T_m)

The siRNA duplexes annealed as above were placed in the Jasco J-815 CD spectropolarimeter and then UV absorbance was measured at 260 nm against a temperature gradient of 10 °C to 95 °C at a rate of 0.5 °C per minute with absorbance being measured at each 0.5 °C increment. Absorbance was adjusted to baseline by subtracting absorbance of the buffer. The T_m values were calculated using Meltwin v3.5 software. Each siRNA result was the average of 3 independent experiments and the reported values were calculated using Meltwin v3.5 assuming the two-state model.²

Procedure for Absorbance Spectra Experiments

All absorbance spectra measurements were done on a Jasco J-815 CD with temperature controller. Measurement was recorded from 200 -500 nm at 10 °C at least 3 times. The coloured visible light experiments in Figure 2 were obtained using a 15.0 Watt iLUMI multiple wavelength A19 light bulb to isolate each colour (red centered at 660 nm, blue; 460 nm, green; 540 nm, violet; 410 nm).

Procedure for HPLC Characterization

HPLC chromatograms were obtained on a Waters 1525 binary HPLC pump with a Waters 2489 UV/Vis detector using the Empower 3 software. A C18 4.6 mm x 150 mm reverse phase column was used. Conditions were 5% acetonitrile in 95% 0.1 M TEAA (Triethylamine-Acetic Acid) buffer up to 100% acetonitrile over 30 min.

Procedure for Reduced Glutathione (GSH) Degradation Assay

The GSH assay was performed on siRNA 6 in a 96 well plate at 37 °C. A concentration of 2.7 μM of siRNA was added to 10 mM glutathione and 5 mM TCEP in PBS to a final volume of 100 μL. Dark experiments were performed with no additional treatment at 0, 8, and 24 h time points after which the entire 100 μL was sample was injected into the HPLC and characterized (same conditions as above) to afford the HPLC traces at the different time points. Red treated siRNA was exposed to red light (660 nm) for entire duration

of assay during incubation at 37 °C, and kept in the dark until injection for 0, 8, 24 h time points. The red 0 h time point was exposed to red light for 15 min and then injected immediately onto the HPLC.

Procedure for Maintaining Cell Cultures of HeLa Cells

For biological analysis of these siRNAs in a live environment, human epithelial cervix carcinoma cells were used (HeLa cells). They were kept in 250 mL vented culture flasks using 25.0 mL of DMEM with 10% fetal bovine serum and 1% penicillin-streptomycin (Sigma) in an incubator set for 37 °C @ 5% CO₂ humidified atmosphere.

Once cell lines became confluent (80-90%) they were passaged by washing 3 times with 10 mL of phosphate buffered saline (NaCl 137 mM, KCl 2.70 mM, PO₄³⁻ 10.0 mM, pH 7.40) and incubated with 3.00 mL of 0.25% trypsin (SAFC bioscience) for 4 min @ 37 °C to detach the cells. The cells were transferred to a 50.0 mL centrifuge tube after the addition of 10.0 mL of DMEM solution and pelleted at 2000 rpm for 5 minutes. The supernatant was discarded and the pellet resuspended in 5.0 mL DMEM with 10% FBS.

A standard haemocytometer was used to obtain cell counts, after which the cells were diluted to a final concentration of 1.00 x 10⁶ cells/mL for subsequent assays. To continue the cell line 1.00 mL of freshly passaged cells was added to 24.0 mL of DMEM/10% FBS and 1% penicillin-streptomycin at 37 °C in a new culture flask while the rest were used for assays.

Procedure for siRNA Transfections

100 µL of cells (total 1.00 x 10⁵) were transfected into 12 well plates (Falcon®) with 1 mL of DMEM (10% FBS, 1% penicillin-streptomycin) and incubated at 37 °C with 5% CO₂. After 24 hours the cells were transfected with various concentrations of siRNAs, along with both pGL3 (Promega) and pRLSV40 luciferase plasmids using Lipofectamine 2000 (Invitrogen) in Gibco's 1X Opti-Mem reduced serum media (Invitrogen) according to the manufacturer's instructions. 1.00 µL of siRNA was added along with 2.00 µL (pGL3 200 ng) and 0.50 µL pRLSV40 (50.0 ng) to 100 µL of 1X Opti-Mem in a microcentrifuge tube and kept on ice for 5 min. In a different microcentrifuge tube 1.00 µL of Lipofectamine 2000 (Invitrogen) was mixed with 100 µL of Gibco's 1X Opti-Mem reduced serum media (Invitrogen) and incubated at room temperature for 5 min. After 5 minutes the tubes were mixed and incubated at room temperature for 20 min and then the entire contents transferred to the wells of the 12 well plate.

Procedure for *in vitro* Dual-Reporter Luciferase Assay

100 μ L of cells (total of 1.00×10^5 cells) were added to 12 well plates (Falcon®) with 1 mL of growth media (DMEM 10% FBS, 1% penicillin-streptomycin) and incubated at 37 °C with 5% CO₂. After 24 hours the cells were transfected with 8.00, 20.0, 40.0, 160, 400 and 800 pM concentrations of siRNAs, along with both pGL3 (Promega) and pRLSV40 luciferase plasmids using Lipofectamine 2000 (Invitrogen) in Gibco's 1X Opti-Mem reduced serum media (Invitrogen) according to the manufacturer's instructions. After a set amount of time (8, 12 or 22h) the cells were incubated at room temperature in 1X passive lysis buffer (Promega) for 20 minutes. The lysates were collected and loaded onto a 96 well, opaque plate (Costar). With a Dual-Luciferase reporter Assay kit (Promega), Lar II and Stop & Glo® luciferase substrates were sequentially added to the lysates and enzyme activity was measured through luminescence of both *firefly/Renilla* luciferase on a Synergy HT (Bio-Tek) plate luminometer. The ratio of *firefly/Renilla* luminescence is expressed as a percentage of reduction in *firefly* protein expression to siRNA efficacy when compared to untreated controls. Each value is the average of at least 3 different experiments with standard deviation indicated.

Procedure for Light Inactivation of Azobenzene Modified siRNA (*trans* to *cis*)

Cell culture was exposed to red wavelength light from time 0 h for the entire duration of the assays, either 8 or 24 hours. The lamp used was a 15.0 Watt iLUMI multiple wavelength A19 light bulb switched to red light (660 nm), held directly above the cell culture plates to maximize red light exposure.

Procedure for Thermal Relaxation and Reactivation of Azobenzene Modified siRNA (*cis* to *trans*)

Immediately following transfection cell culture was exposed to red light as above, which was then removed 2 hours post transfection to allow the azobenzene to thermally relax back to the active form of the siRNAzo in the dark. The cells were then lysed and luminescence measured as above in the luciferase assay.

Figures and Tables

Table S-1 Sequences of anti-luciferase siRNAs, predicted and recorded mass and T_m 's of siRNAs containing the azobenzene spacers.^a

siRNAzo	siRNA Duplex	Predicted Mass	Actual Mass ^[b]	^a T_m (°C)	ΔT_m (°C)
wt	5'- CUUACGCU <u>G</u> AGUACUUCGAtt -3' 3'- ttGAAUGCGACUCAUGAAGCU - 5'			74.0	--
1	5'-CUUACGCC <u>Cl-Az2</u> AGUACUUCGAtt-3' 3'-ttGAAUGCGACUCAUGAAGCU-5'	6482.63	6482.66	61.9	- 12.1
2	5'-CUUACGCU <u>Cl-Az2</u> GUACUUCGAtt-3' 3'-ttGAAUGCGACUCAUGAAGCU-5'	6505.67	6504.75	62.5	- 11.5
3	5'-CUUACGCU <u>GCl-Az2</u> UACUUCGAtt-3' 3'-ttGAAUGCGACUCAUGAAGCU-5'	6482.63	6482.67	58.4	- 15.6

[a] **Cl-Az2** corresponds to the azobenzene derivative synthesized from Az2; the top strand corresponds to the sense strand; the bottom strand corresponds to the antisense strand. In all duplexes, the 5'-end of the bottom antisense strand contains a 5'-phosphate group. [b] Deconvolution results for siRNAs. ESI-HRMS (ES^+) m/z calculated for siRNAzos 1-7 $[M+H]^+$

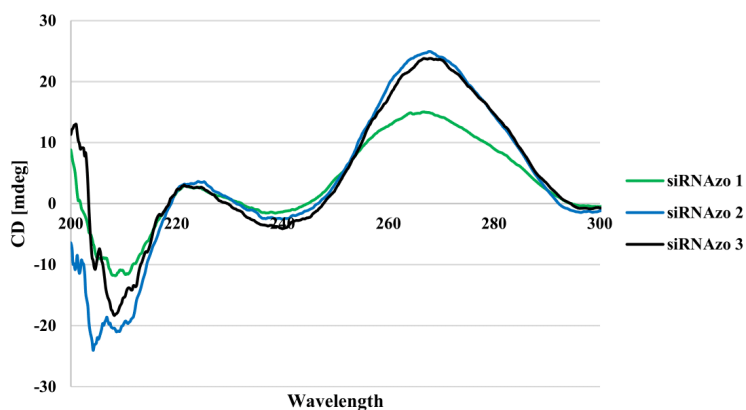


Figure S-1. CD spectra of azobenzene modified spacers replacing two nucleobases targeting firefly luciferase mRNAs. Wildtype and modified anti-*firefly* luciferase siRNAs (10 μ M/duplex) were suspended in 500 μ L of a sodium phosphate buffer (90.0 mM NaCl, 10.0 mM Na_2HPO_4 , 1.00 mM EDTA, pH 7.00) and scanned from 200-300 nm at 25 °C with a screening rate of 20.0 nm/min and a 0.20 nm data pitch. All scans were performed in triplicate and averaged using Jasco's Spectra Manager version 2.

S10

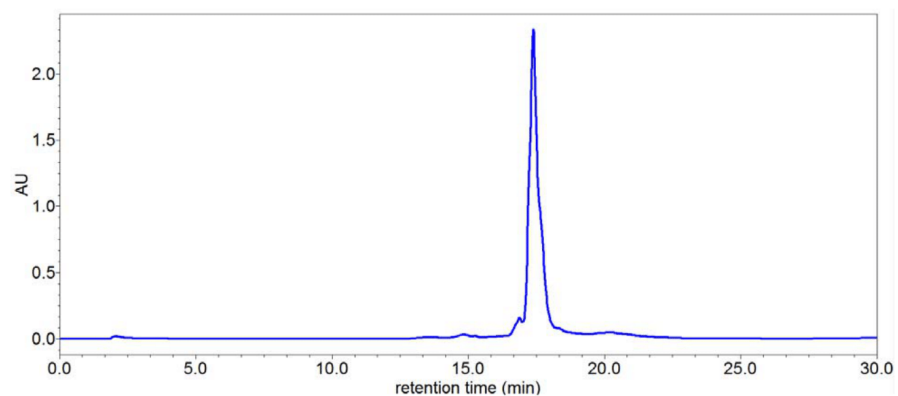


Figure S-2. HPLC chromatogram of siRNA 1. Conditions were 5% acetonitrile in 95% 0.1 M TEAA (Triethylamine-Acetic Acid) buffer up to 100% acetonitrile over 40 min. Spectra were processed using the Empower 3 software.

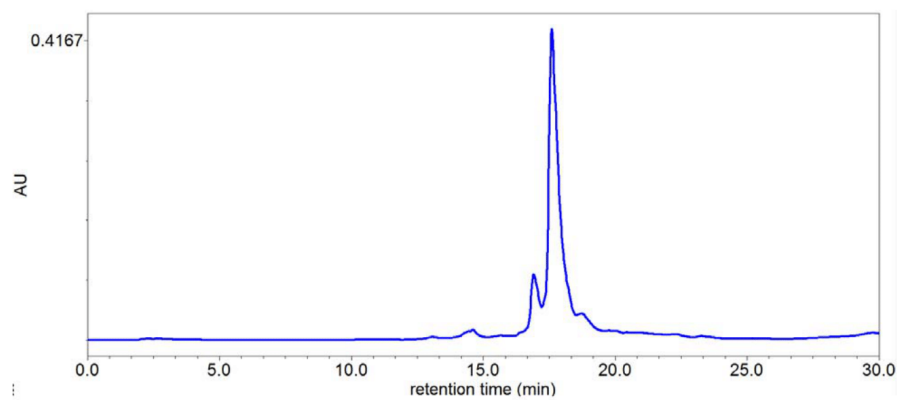


Figure S-3. HPLC chromatogram of siRNA 2. Conditions were 5% acetonitrile in 95% 0.1 M TEAA (Triethylamine-Acetic Acid) buffer up to 100% acetonitrile over 40 min. Spectra were processed using the Empower 3 software.

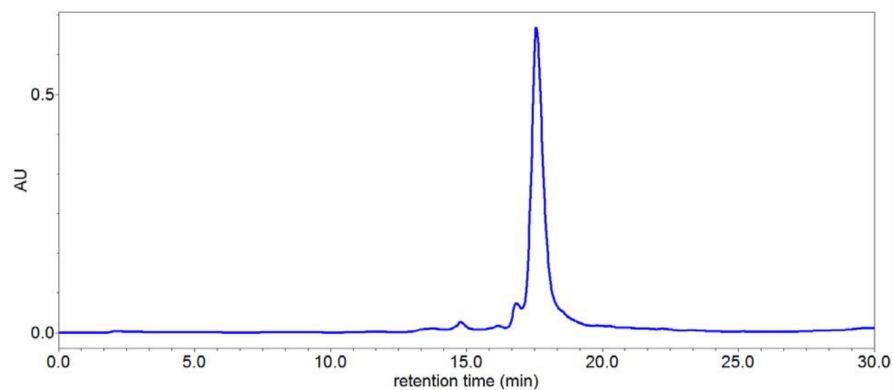


Figure S-4. HPLC chromatogram of siRNA 3. Conditions were 5% acetonitrile in 95% 0.1 M TEAA (Triethylamine-Acetic Acid) buffer up to 100% acetonitrile over 40 min. Spectra were processed using the Empower 3 software.

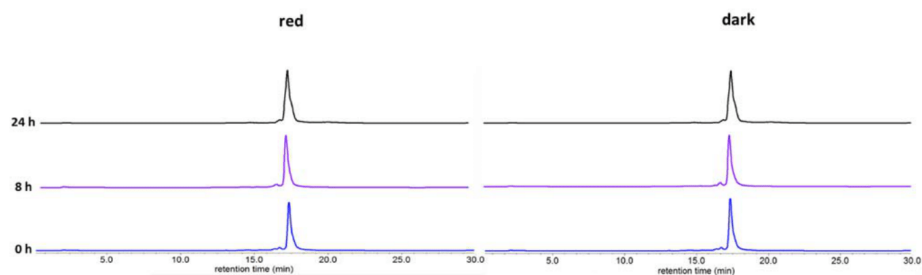
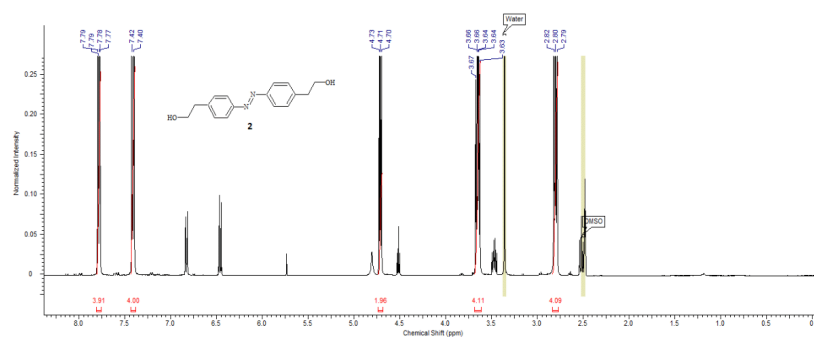


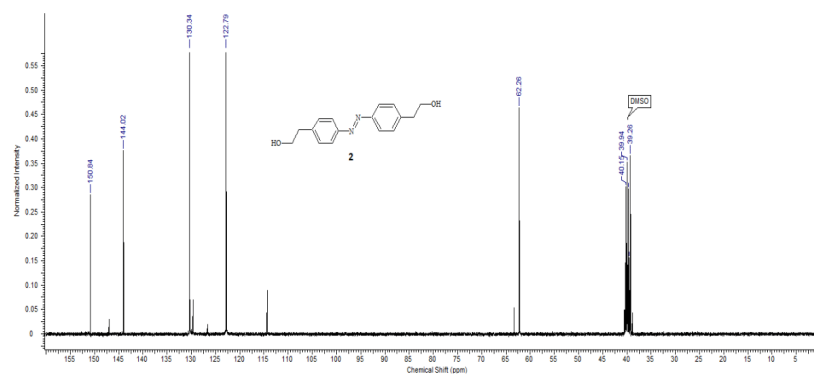
Figure S-5. GSH assay results of the sense strand of siRNA 1 showing minimal degradation due to the presence of GSH. Red treated siRNA was exposed to red light for entire duration of assay during incubation at 37 °C, and kept exposed until injection at 0, 8, 24 h time points. The red 0 h time point was exposed to red light for 15 min and then injected immediately onto the HPLC. Conditions were 5% acetonitrile in 95% 0.1 M TEAA (Triethylamine-Acetic Acid) buffer up to 100% acetonitrile over 30 min. Spectra were processed using the Empower 3 software.

$^1\text{H}/^{13}\text{C}/^{31}\text{P}$ NMR Spectra of Compounds

^1H NMR Spectrum of Compound 1

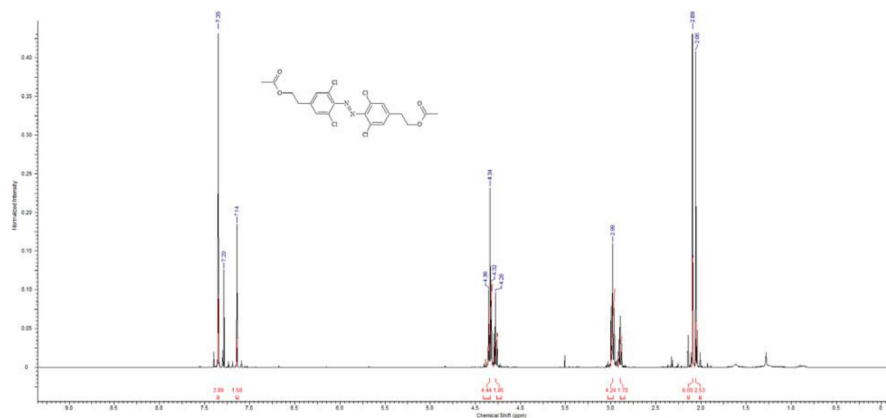


^{13}C NMR Spectrum of Compound 1

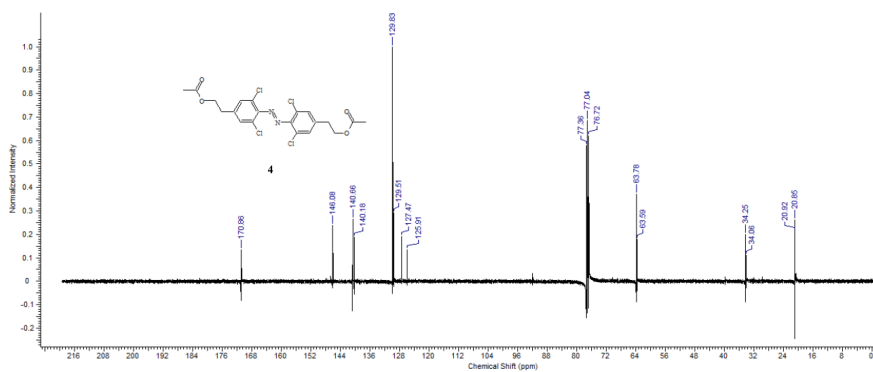


S13

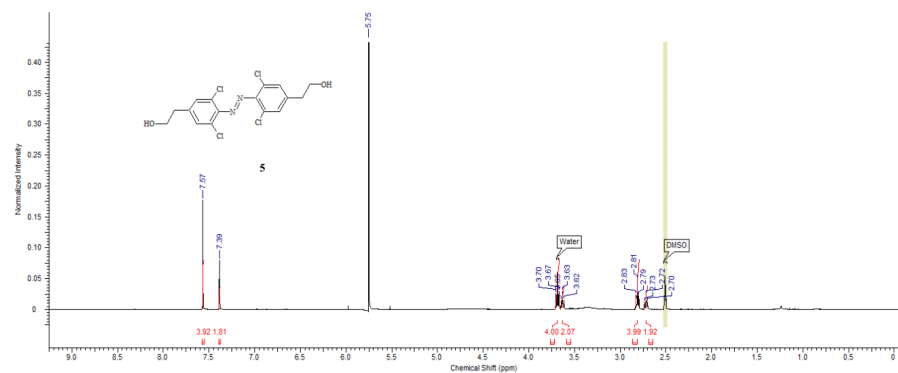
¹H NMR Spectrum of Compound 2



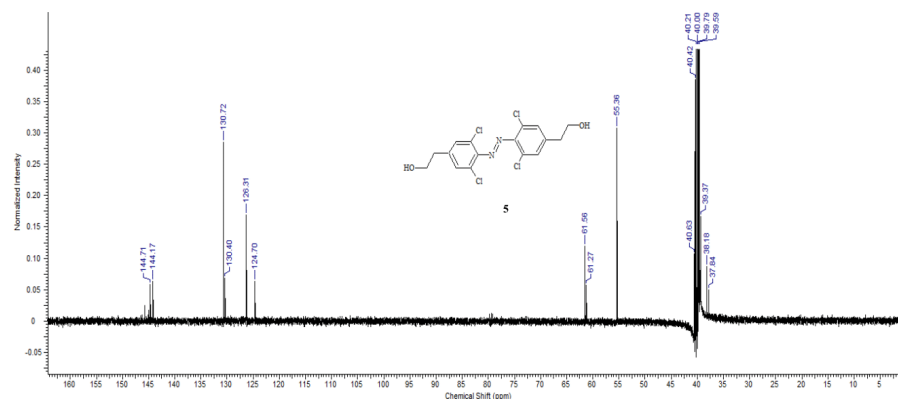
¹³C NMR Spectrum of Compound 2



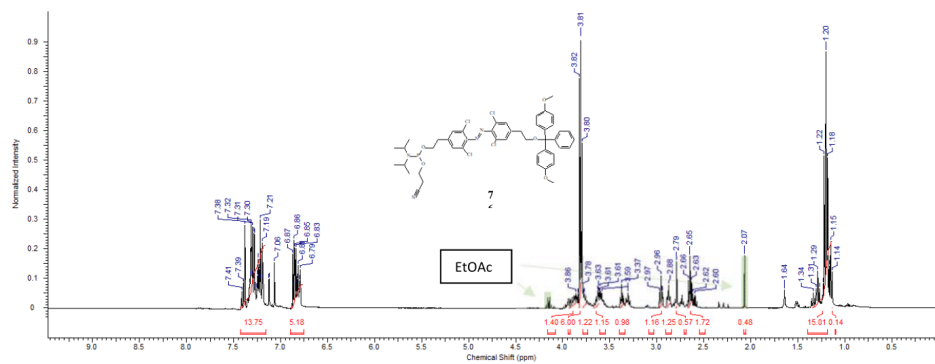
¹H NMR Spectrum of Compound 3



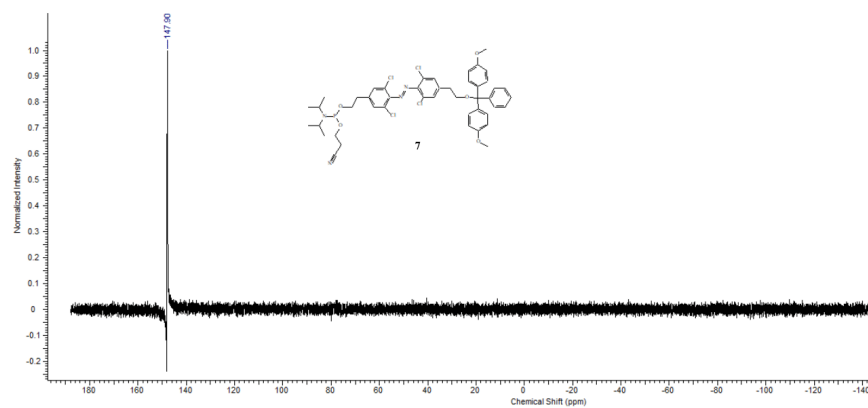
¹³C NMR Spectrum of Compound 3



¹H NMR Spectrum of Compound 5



³¹P NMR Spectrum of Compound 5



References

1. Still, W. C.; Kahn, M.; Mitra, A. J. *Org. Chem.* **1978**, *43*, 2923.
2. McDowell, J.A.; Turner, D. H. *Biochemistry* **1996**, *35*, 14077.

Appendix IV. Preparation Manuscript IV Supplementary Data

Table 5.1. Table of RNAs used and its target.^[a]

siRNAzo	siRNA Duplex	Predicted Mass	Actual Mass ^[b]	^a T _m (°C)	ΔT _m (°C)
wt	5'- CUUACGCUGAGUACUUCGAtt -3' 3'- ttGAAUGCGACUCAUGAAGCU – 5'			74.0	--
F-SiRNAzo-1	5'-CUUACGCUGAGUACUUCGAtt-3' 3'-ttGAAUGCG <u>Az2-4F</u> UCAUGAAGCU-5'	6625.89	6625.25	56	- 17.1

[a] **Az2-4F** corresponds to the azobenzene derivative synthesized from Az2; the top strand corresponds to the sense strand; the bottom strand corresponds to the antisense strand. In all duplexes, the 5'-end of the bottom antisense strand contains a 5'-phosphate group. [b] Deconvolution results for siRNAzos. ESI-qTOF (ES⁺) m/z calculated for F-siRNAzo-1 [M+H]⁺

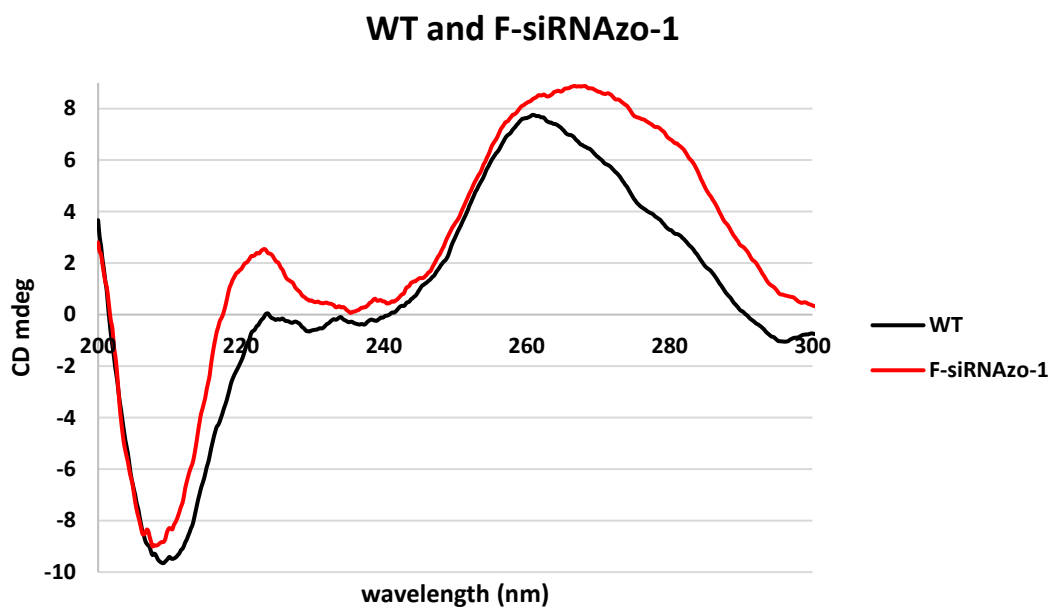


Figure S1. CD spectra of tetra-fluorinated azobenzene modified spacers replacing two nucleobases targeting firefly luciferase mRNAs. Wildtype and modified anti-*firefly* luciferase siRNAs (10 μ M/duplex) were suspended in 500 μ L of a sodium phosphate buffer (90.0 mM NaCl, 10.0 mM Na₂HPO₄, 1.00 mM EDTA, pH 7.00) and scanned from 200-300 nm at 25 °C with a screening rate of 20.0 nm/min and a 0.20 nm data pitch. All scans were performed in triplicate and averaged using Jasco's Spectra Manager version 2.

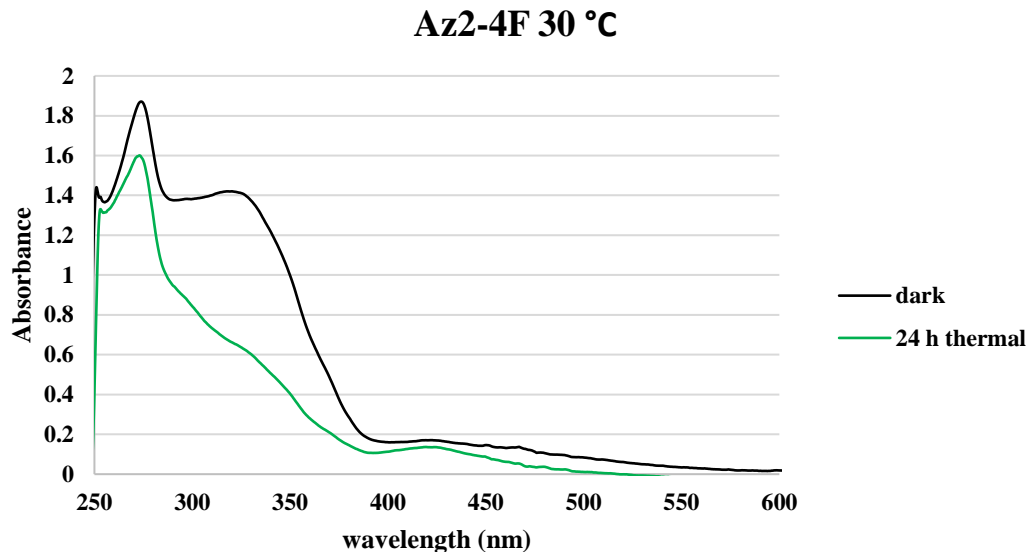


Figure S2. Absorbance Profile of Az2-4F when exposed to 15 min of green 530 nm light using a 4W LED in DMSO, scanned from 250-600 nm at 30 °C with a screening rate of 20.0 nm/min and a 0.20 nm data pitch. 24 h thermal was allowed to sit in the dark at temperature until time elapsed.

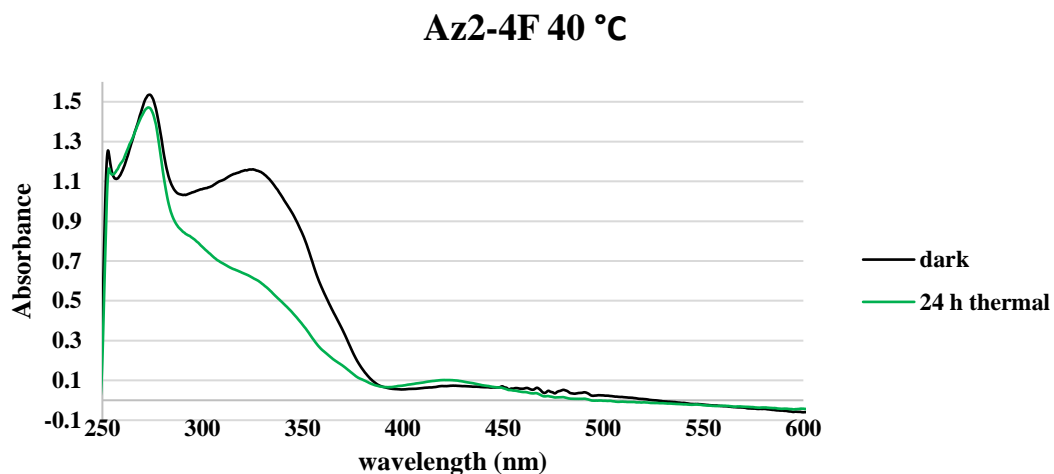


Figure S3. Absorbance Profile of Az2-4F when exposed to 15 min of green 530 nm light using a 4W LED in DMSO, scanned from 250-600 nm at 40 °C with a screening rate of 20.0 nm/min and a 0.20 nm data pitch. 24 h thermal was allowed to sit in the dark at temperature until time elapsed.

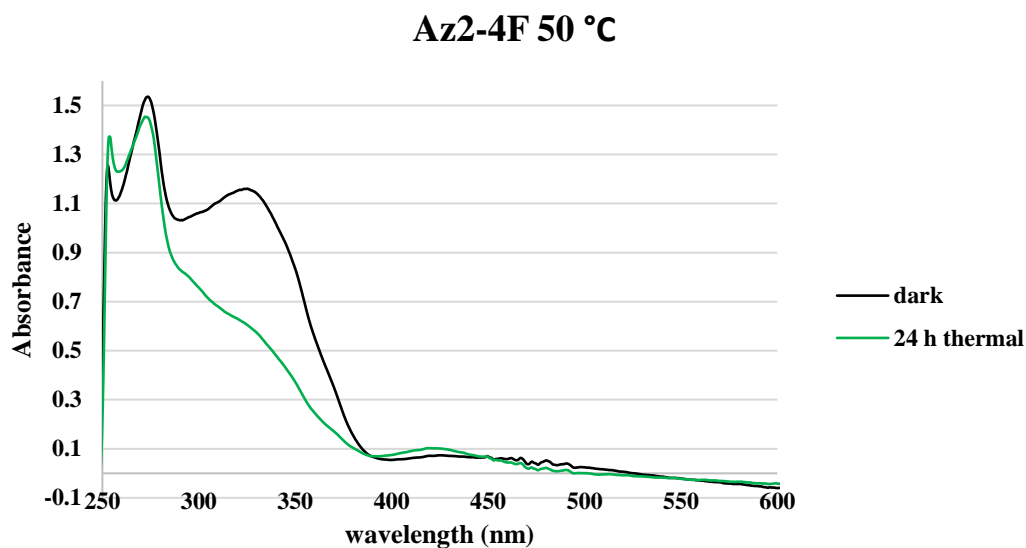


Figure S4. Absorbance Profile of Az2-4F when exposed to 15 min of green 530 nm light using a 4W LED in DMSO, scanned from 250-600 nm at 50 °C with a screening rate of 20.0 nm/min and a 0.20 nm data pitch. 24 h thermal was allowed to sit in the dark at temperature until time elapsed.

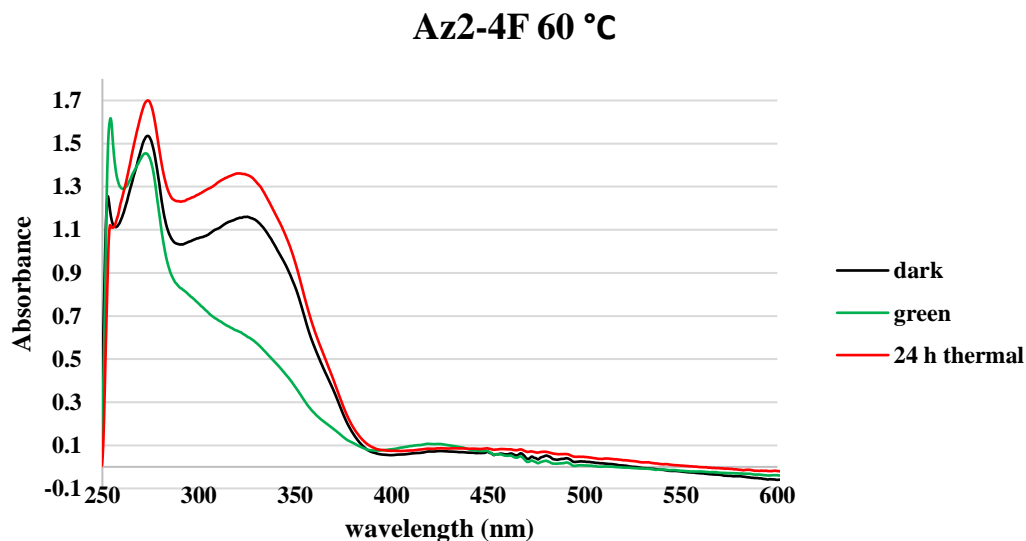


Figure S5. Absorbance Profile of Az2-4F when exposed to 15 min of green 530 nm light using a 4W LED in DMSO, scanned from 250-600 nm at 60 °C with a screening rate of 20.0 nm/min and a 0.20 nm data pitch. 24 h thermal was allowed to sit in the dark at temperature until time elapsed. *Trans* isomer restored after 24 h.

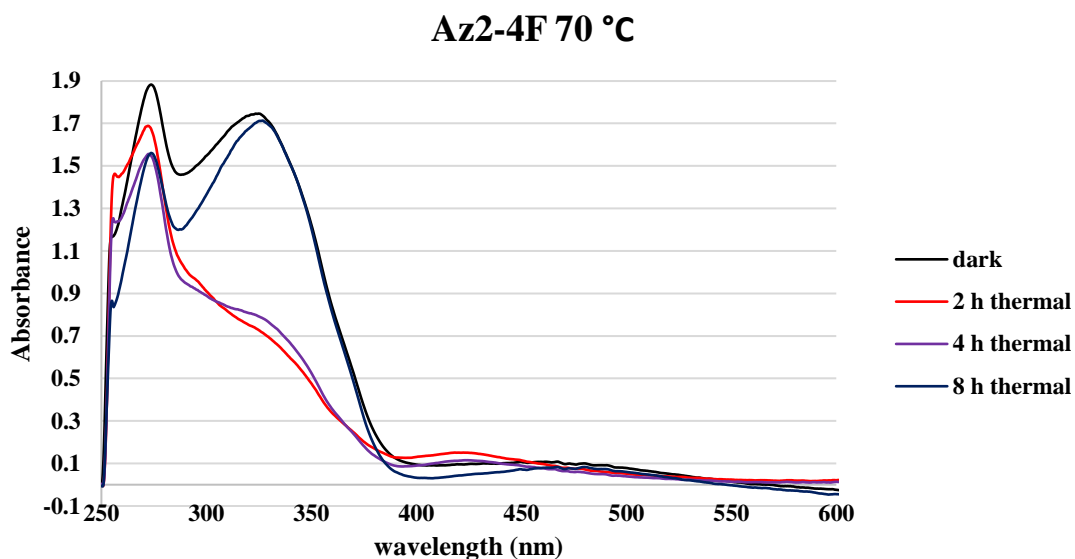


Figure S6. Absorbance Profile of Az2-4F when exposed to 15 min of green 530 nm light using a 4W LED in DMSO, scanned from 250-600 nm at 70 °C with a screening rate of 20.0 nm/min and a 0.20 nm data pitch. 2,4 and 8 h thermal was allowed to sit in the dark at temperature until time elapsed. *Trans* isomer restored after 8 h.

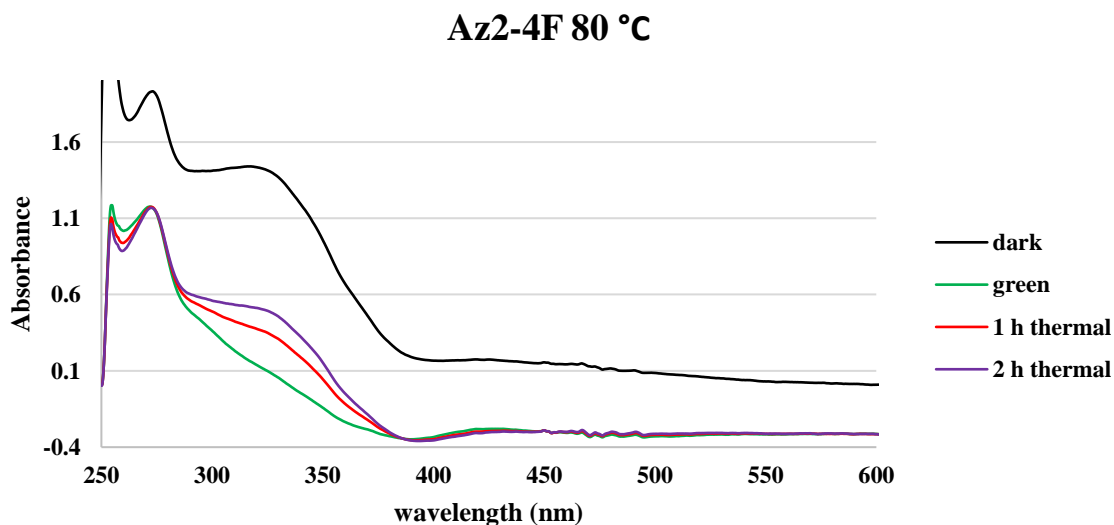


Figure S7. Absorbance Profile of Az2-4F when exposed to 15 min of green 530 nm light using a 4W LED in DMSO, scanned from 250-600 nm at 80 °C with a screening rate of 20.0 nm/min and a 0.20 nm data pitch. 1 and 2 h thermal was allowed to sit in the dark at temperature until time elapsed. *Trans* isomer restored after 2 h.

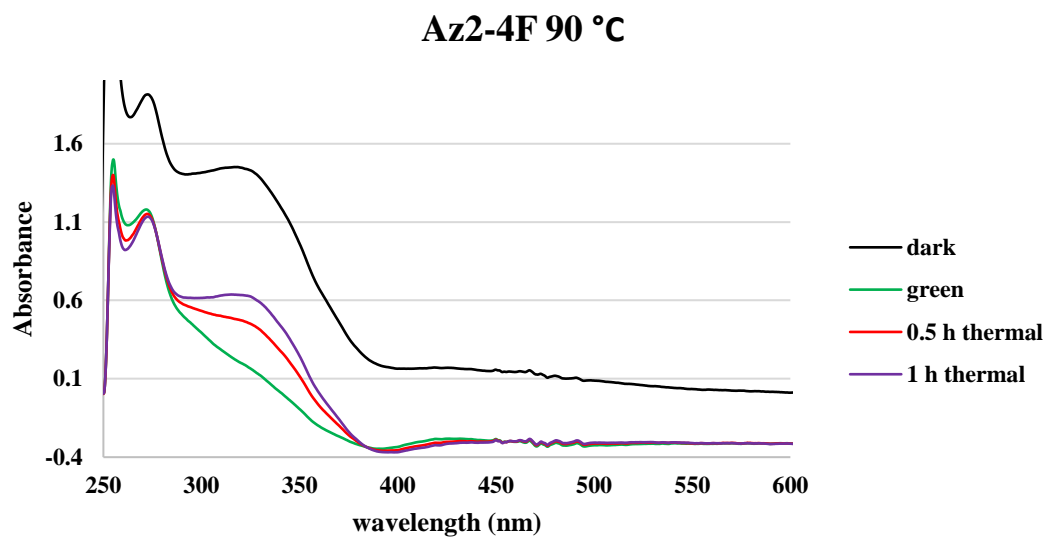
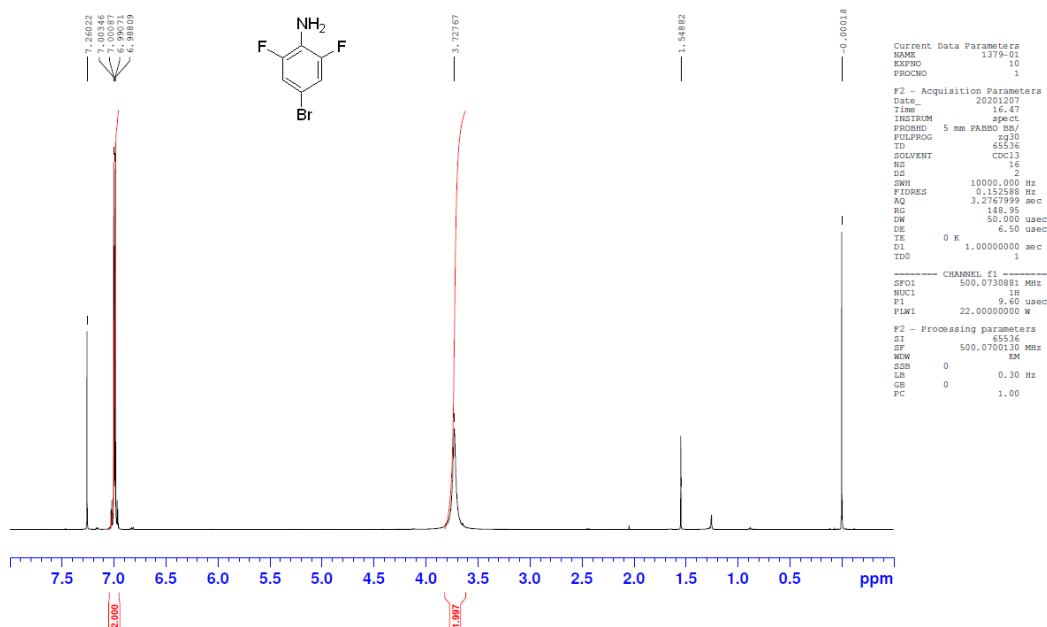


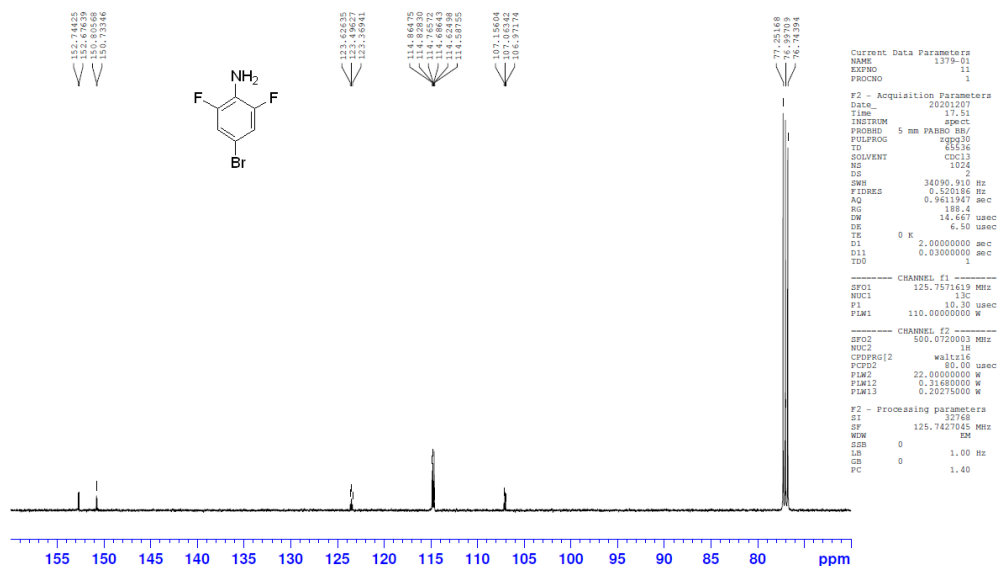
Figure S8. Absorbance Profile of Az2-4F when exposed to 15 min of green 530 nm light using a 4W LED in DMSO, scanned from 250-600 nm at 90 °C with a screening rate of 20.0 nm/min and a 0.20 nm data pitch. 0.5 and 1 h thermal was allowed to sit in the dark at temperature until time elapsed. *Trans* isomer restored after 1 h.

$^1\text{H}/^{13}\text{C}/^{19}\text{F}/^{31}\text{P}$ NMR Spectra of Compounds

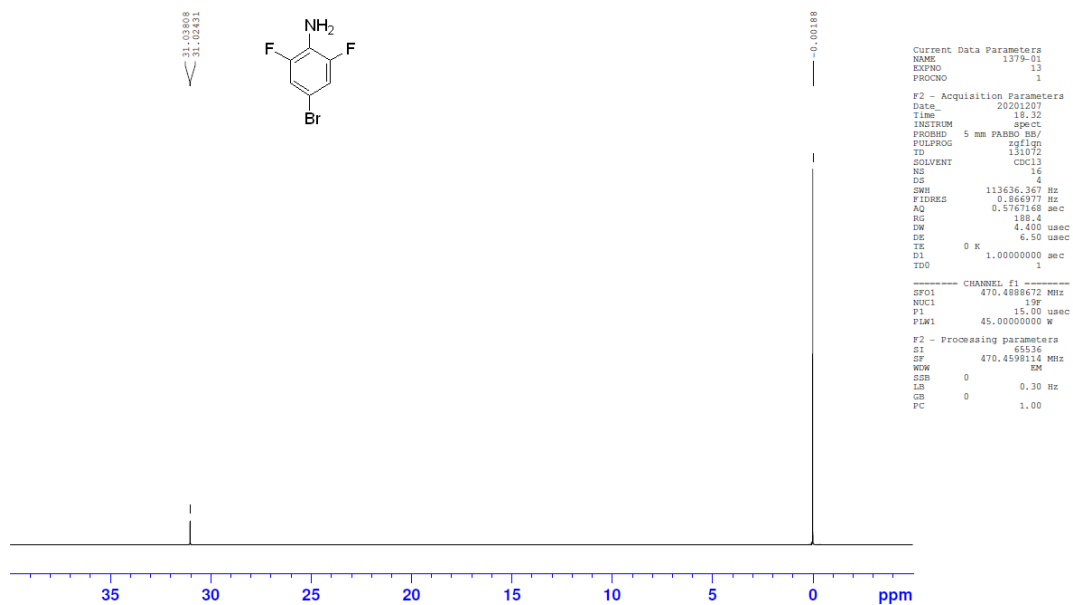
^1H NMR Spectrum of Compound 2



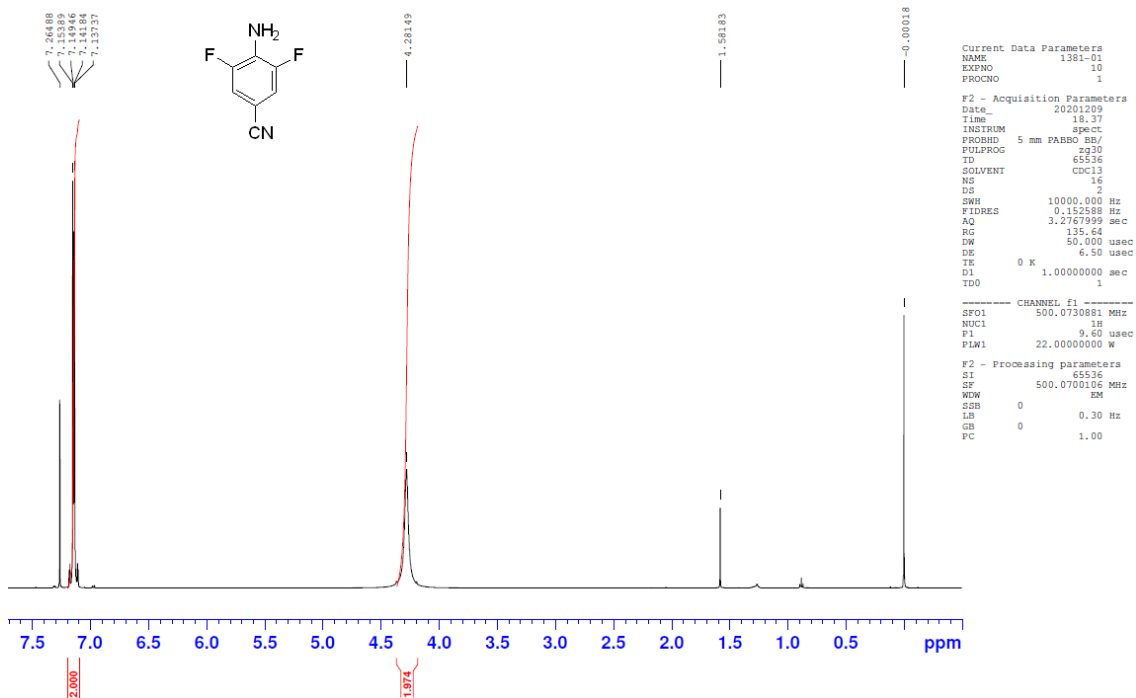
^{13}C NMR Spectrum of Compound 2



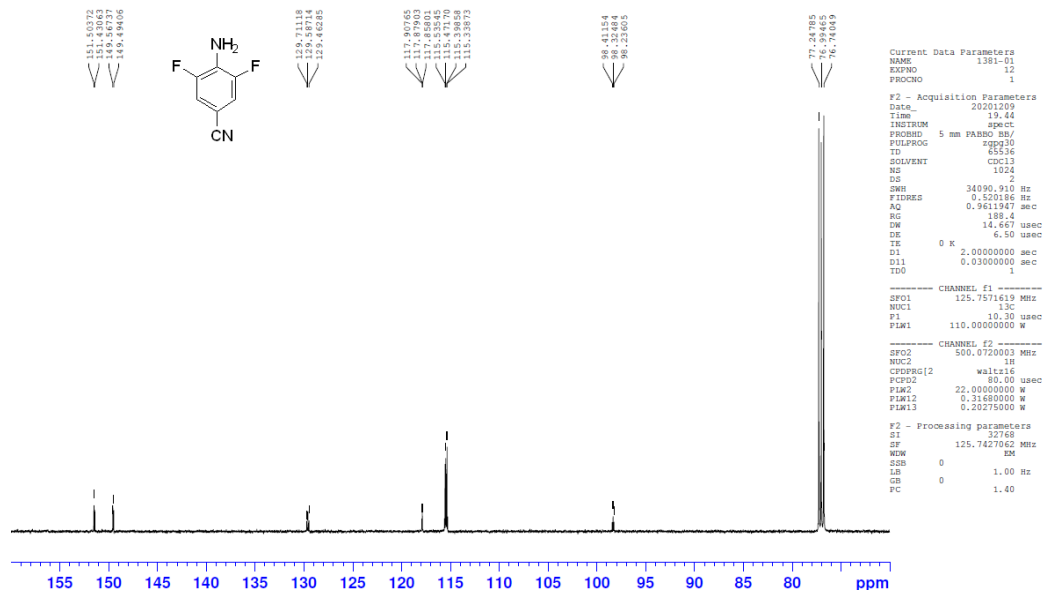
¹⁹F NMR Spectrum of Compound 2



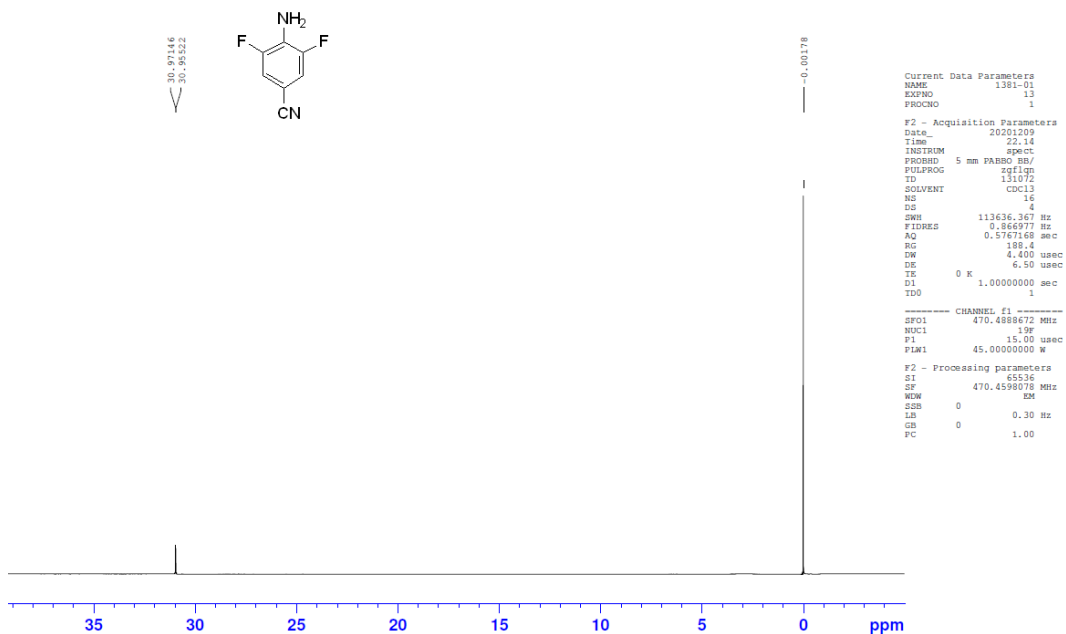
¹H NMR Spectrum of Compound 3



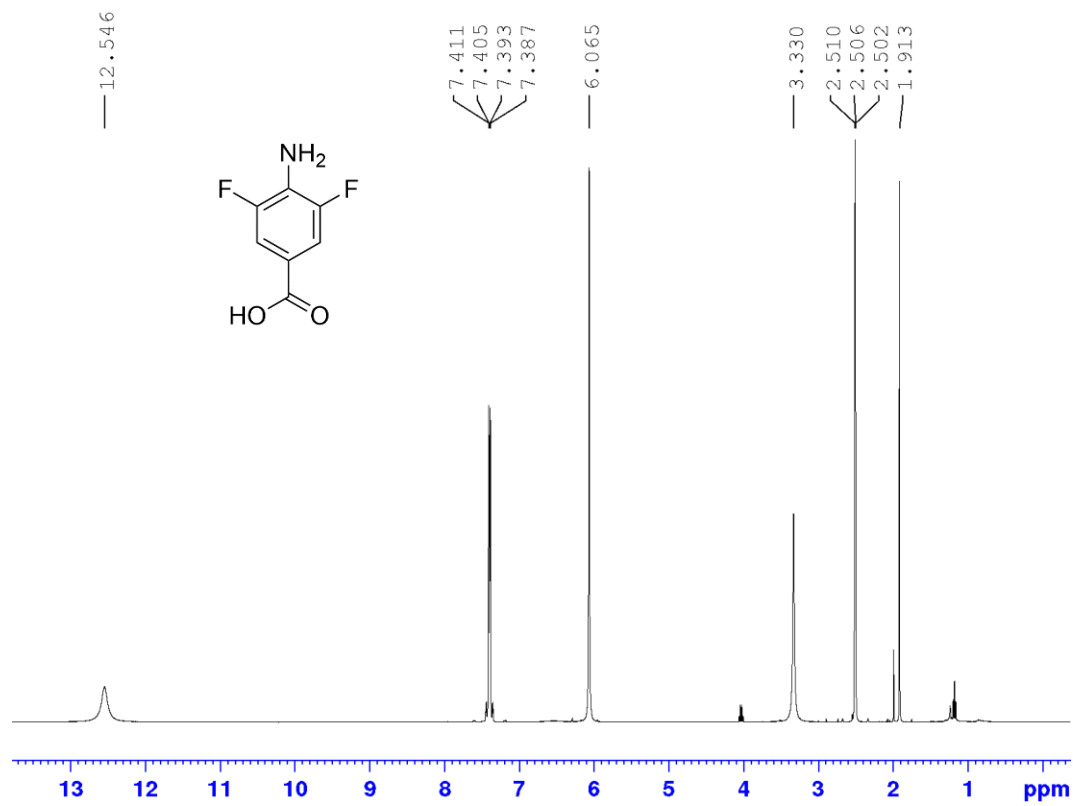
¹³C NMR Spectrum of Compound 3



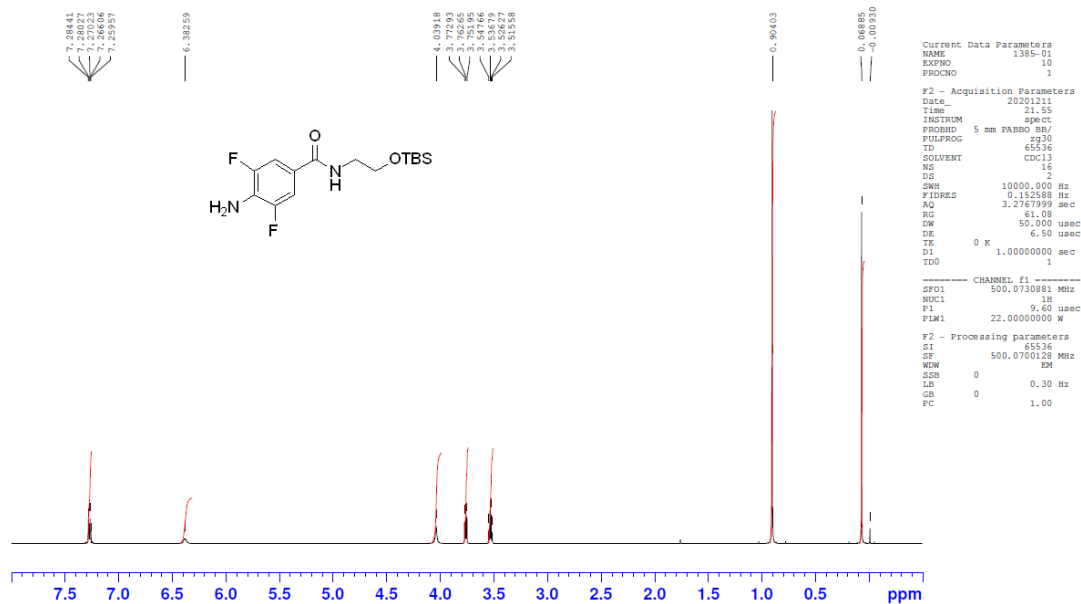
¹⁹F NMR Spectrum of Compound 3



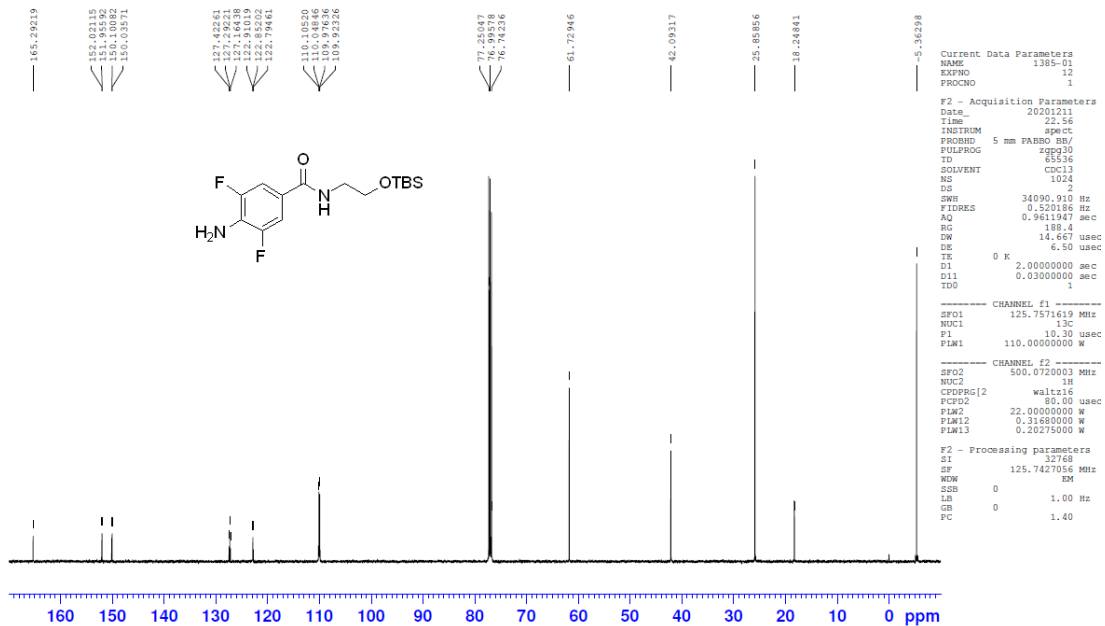
¹H NMR Spectrum of Compound 4



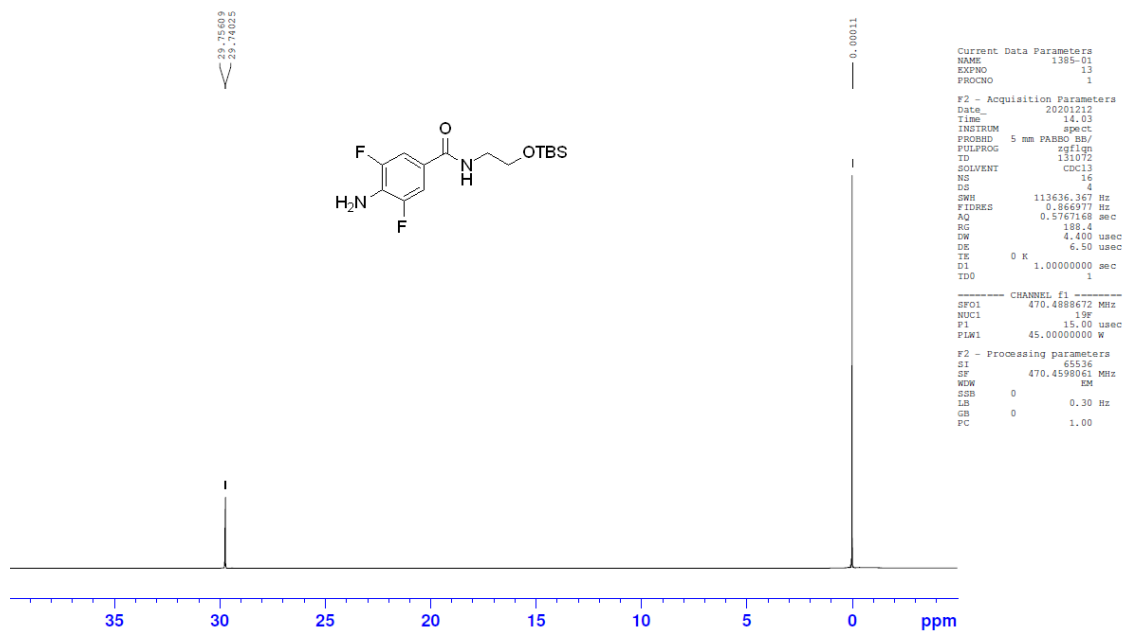
¹H NMR Spectrum of Compound 5



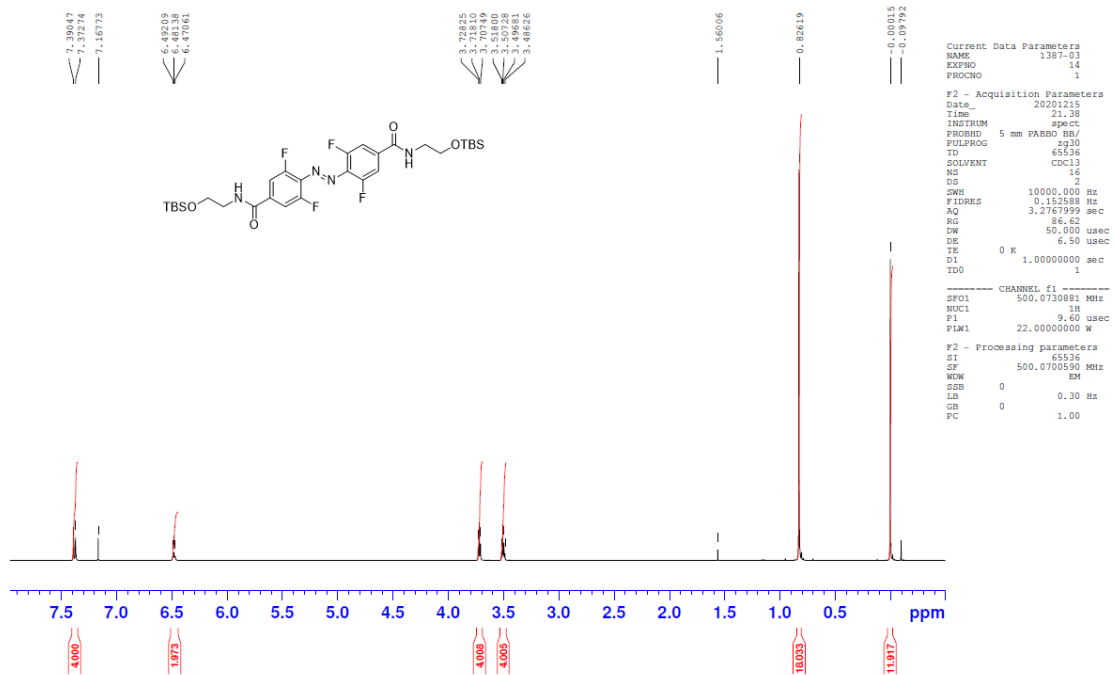
¹³C NMR Spectrum of Compound 5



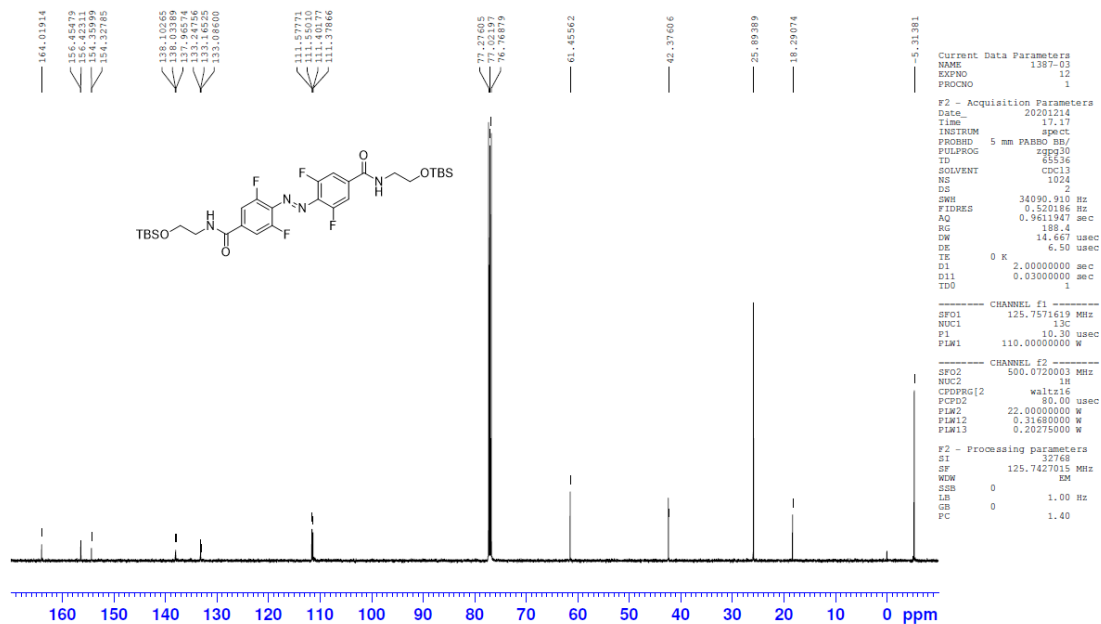
¹⁹F NMR Spectrum of Compound 5



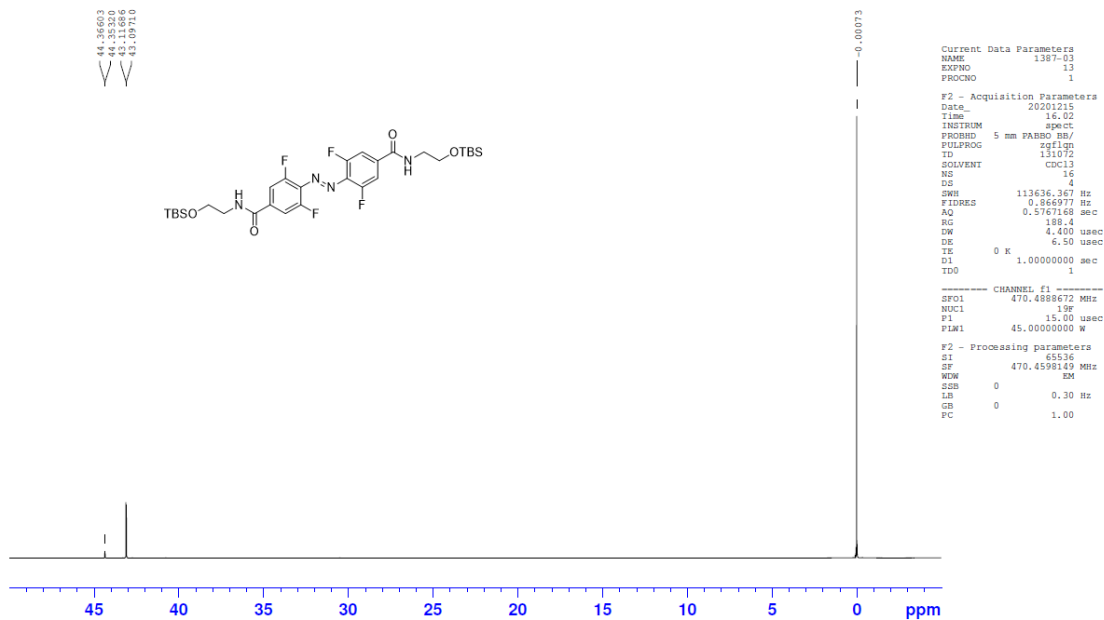
¹H NMR Spectrum of Compound 6



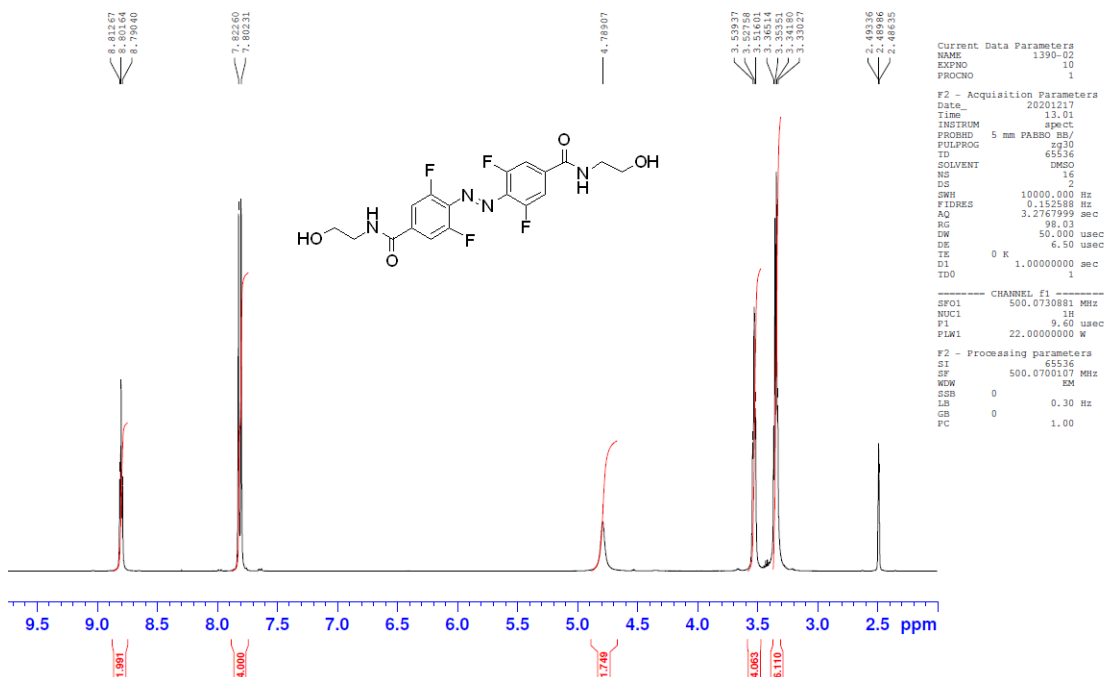
¹³C NMR Spectrum of Compound 6



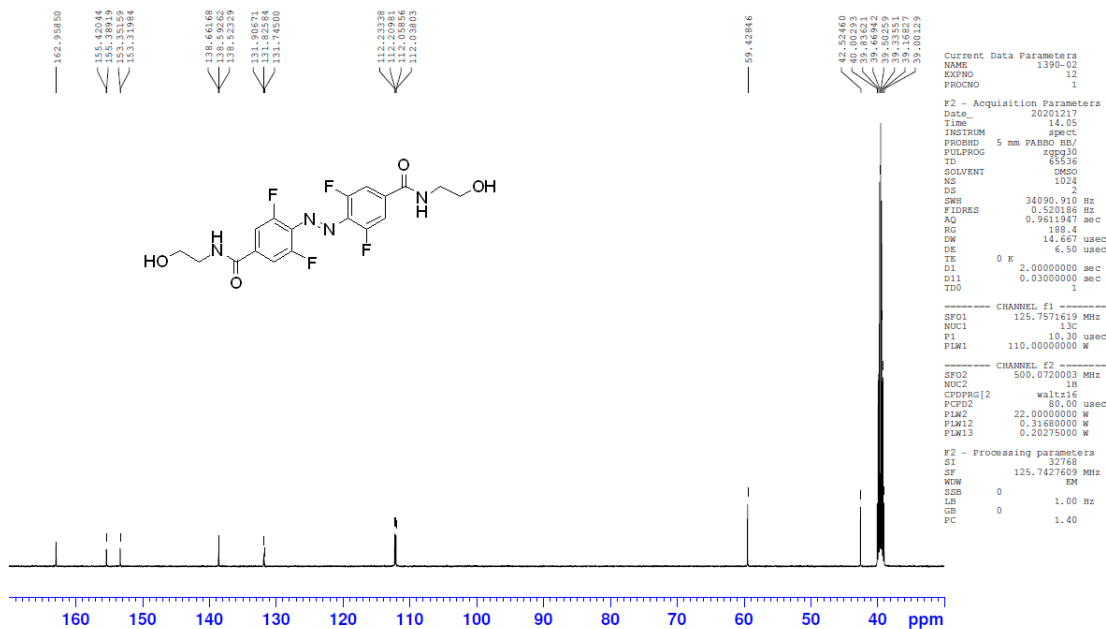
¹⁹F NMR Spectrum of Compound 6



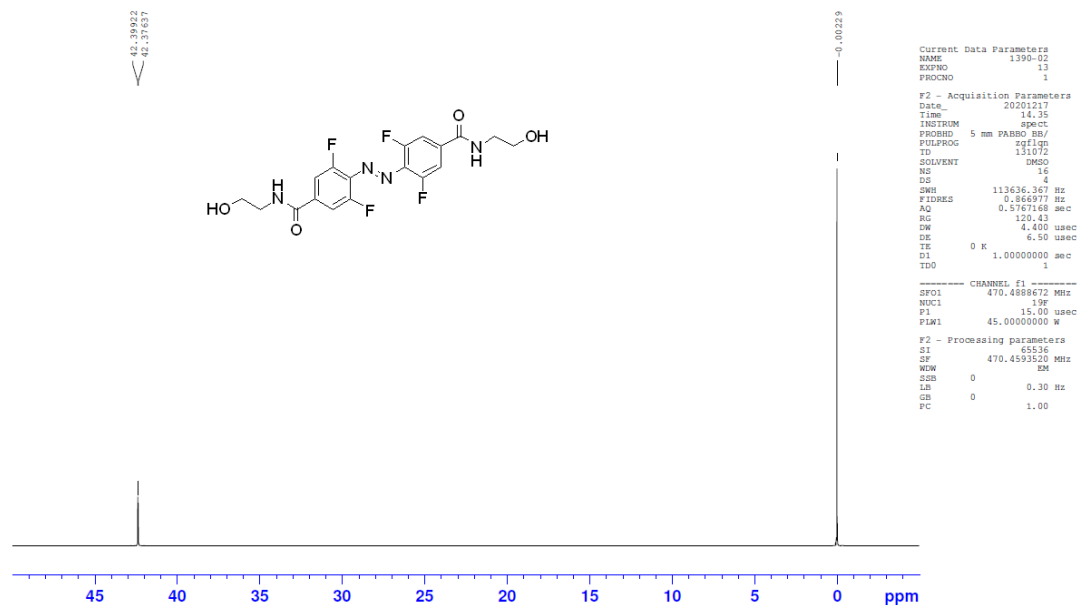
¹H NMR Spectrum of Compound 7



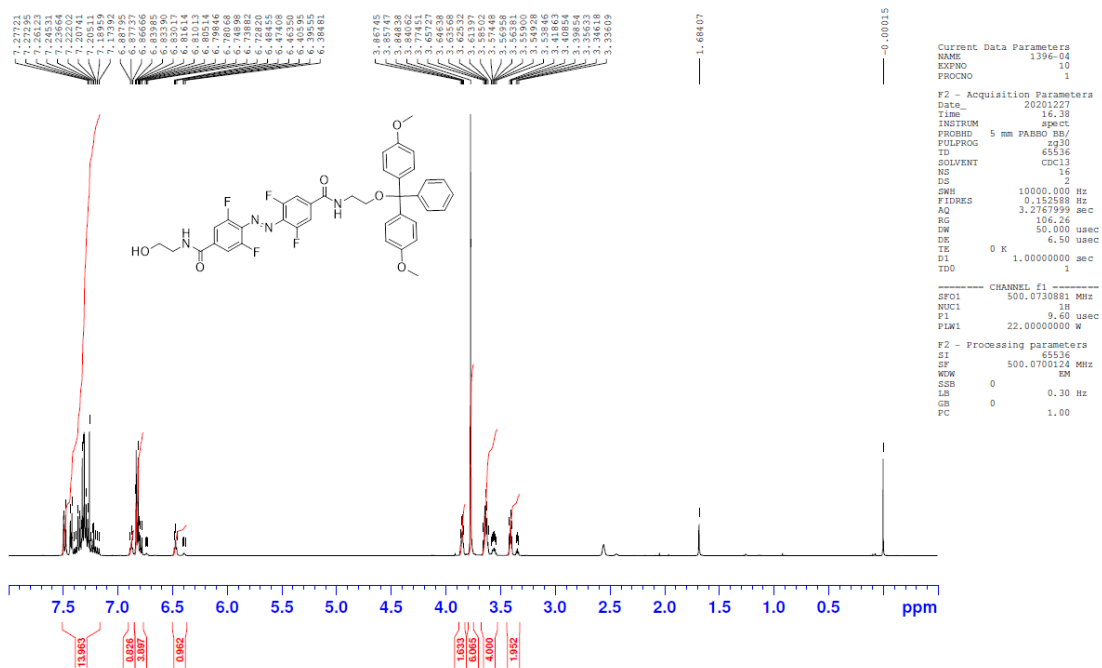
¹³C NMR Spectrum of Compound 7



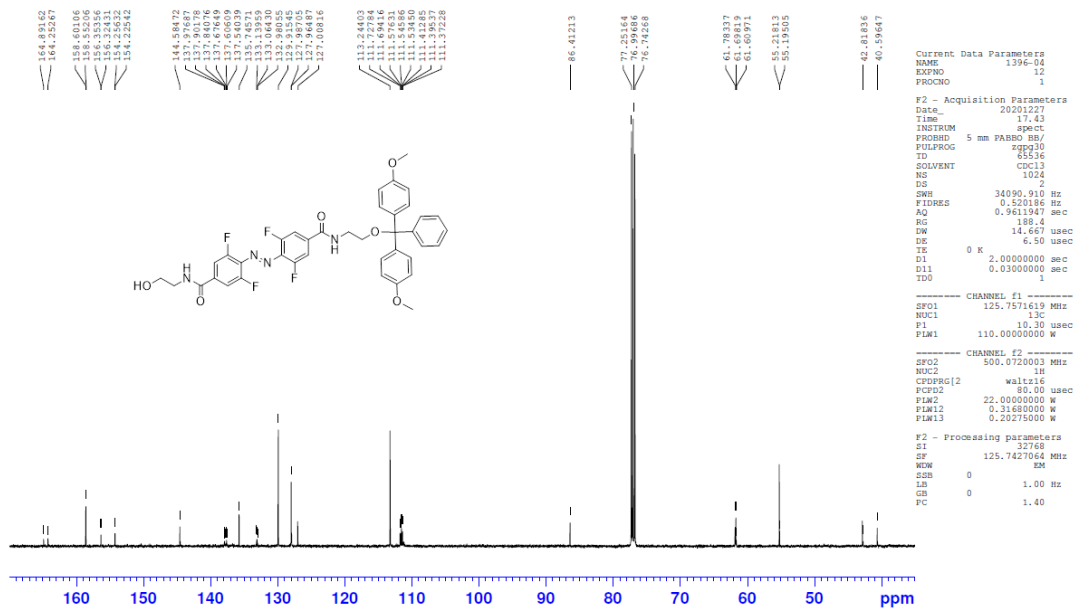
¹⁹F NMR Spectrum of Compound 7



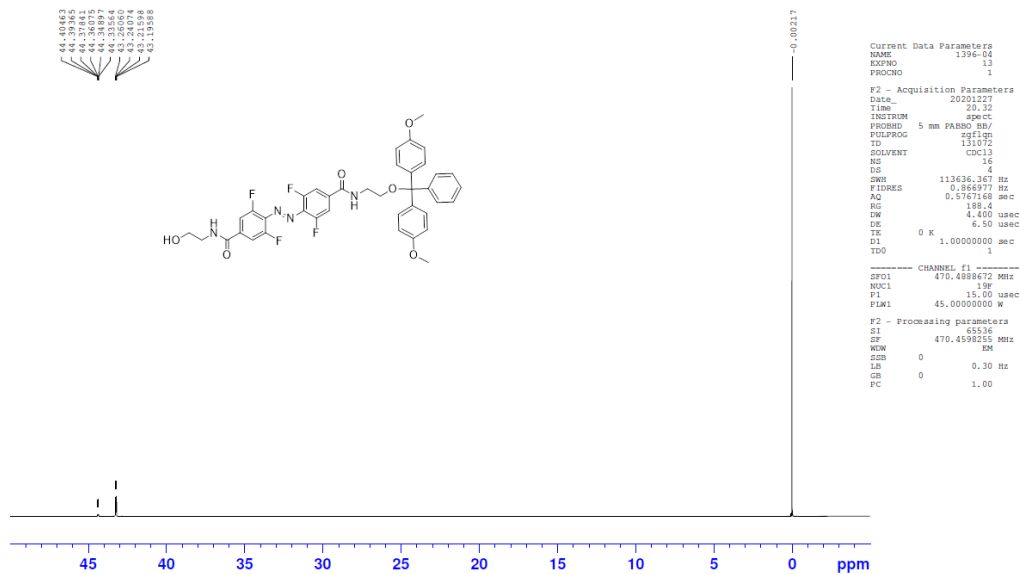
¹H NMR Spectrum of Compound 8



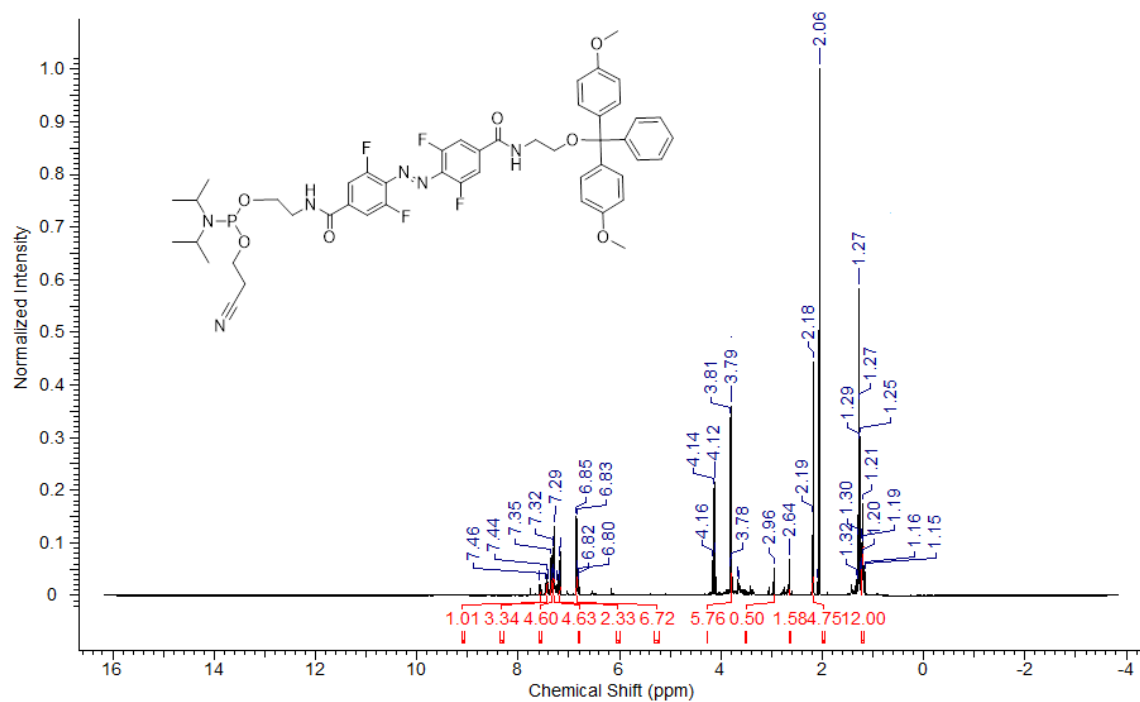
¹³C NMR Spectrum of Compound 8



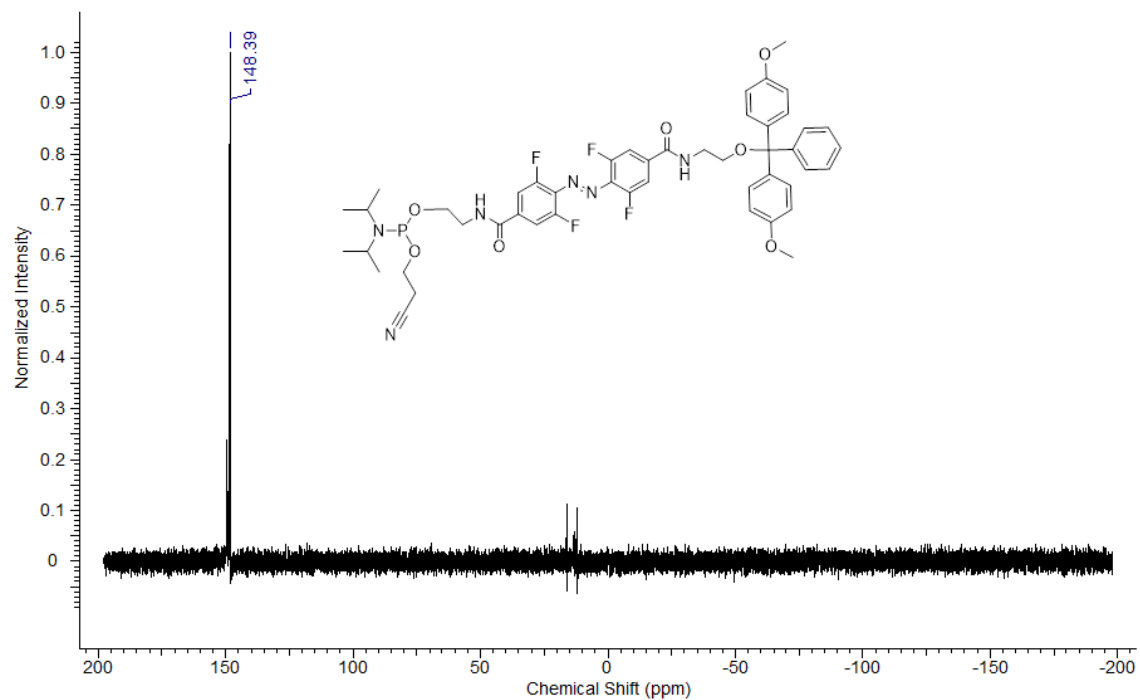
¹⁹F NMR Spectrum of Compound 8



¹H NMR Spectrum of Compound 9



³¹P NMR Spectrum of Compound 9



Appendix V. Copyright Permission Letters

Copyright Permission Letter

DATE: May 14, 2021

- Publication Titles:**
1. Stability and evaluation of siRNAs labeled at the sense strand with a 3'-azobenzene unit
 2. Reversible control of RNA interference by siRNAzOs
 3. Synthesis, Derivatization and Photochemical Control of ortho-Functionalized Tetrachlorinated Azobenzene-Modified siRNAs

I am preparing my Doctor of Philosophy thesis for submission to the School of Graduate and Postdoctoral Studies at the University of Ontario Institute of Technology (Ontario Tech University) in Oshawa, Ontario, Canada. I am seeking your permission to include a manuscript version of the following paper(s) as a chapter in the thesis:

1. Hammill, M. L., Patel, A., Abd Alla, M., and Desaulniers, J. P. (2018) Stability and evaluation of siRNAs labeled at the sense strand with a 3'-azobenzene unit, *Bioorganic & Medicinal Chemistry Letters* 28, 3613-3616. DOI: 10.1016/j.bmcl.2018.10.044
2. Hammill, M. L., Islam, G., and Desaulniers, J. P. (2020) Reversible control of RNA interference by siRNAzOs, *Organic & Biomolecular Chemistry* 18, 41-46. DOI: 10.1039/c9ob02509j
3. Hammill, M. L., Islam, G., and Desaulniers, J. P. (2020) Synthesis, Derivatization and Photochemical Control of ortho-Functionalized Tetrachlorinated Azobenzene-Modified siRNAs, *Chembiochem* 21, 2367-2372. DOI: 10.1002/cbic.202000188

Canadian graduate theses are reproduced by the Library and Archives of Canada (formerly National Library of Canada) through a non-exclusive, world-wide license to reproduce, loan, distribute, or sell theses. I am also seeking your permission for the material described above to be reproduced and distributed by the LAC (NLC). Further details about the LAC (NLC) thesis program are available on the LAC (NLC) website (www.nlc-bnc.ca).

Full publication details and a copy of this permission letter will be included in the thesis.

Yours sincerely,

Matthew Hammill

Permission is granted for:

- a) The inclusion of the material described above in your thesis.
- b) For the material described above to be included in the copy of your thesis that is sent to the Library and Archives of Canada (formerly National Library of Canada) for reproduction and distribution.

Name: Jean-Paul Desaulniers

Title: Professor

Signature: 

Date (dd/mmm/yyyy) 15/05/2021

Copyright Permission Letter

DATE: May 14, 2021

Publication Title: Reversible control of RNA interference by siRNAzOs

Synthesis, Derivatization and Photochemical Control of ortho-Functionalized Tetrachlorinated Azobenzene-Modified siRNAs

I am preparing my Doctor of Philosophy thesis for submission to the School of Graduate and Postdoctoral Studies at the University of Ontario Institute of Technology (Ontario Tech University) in Oshawa, Ontario, Canada. I am seeking your permission to include a manuscript version of the following paper(s) as a chapter in the thesis:

Hammill, M. L., Islam, G., and Desaulniers, J. P. (2020) Reversible control of RNA interference by siRNAzOs, *Organic & Biomolecular Chemistry* 18, 41-46. DOI: 10.1039/c9ob02509j

Hammill, M. L., Islam, G., and Desaulniers, J. P. (2020) Synthesis, Derivatization and Photochemical Control of ortho-Functionalized Tetrachlorinated Azobenzene-Modified siRNAs, *Chembiochem* 21, 2367-2372. DOI: 10.1002/cbic.202000188

Canadian graduate theses are reproduced by the Library and Archives of Canada (formerly National Library of Canada) through a non-exclusive, world-wide license to reproduce, loan, distribute, or sell theses. I am also seeking your permission for the material described above to be reproduced and distributed by the LAC (NLC). Further details about the LAC (NLC) thesis program are available on the LAC (NLC) website (www.nlc-bnc.ca).

Full publication details and a copy of this permission letter will be included in the thesis.

Yours sincerely,

Matthew Hammill

Permission is granted for:

- The inclusion of the material described above in your thesis.
- For the material described above to be included in the copy of your thesis that is sent to the Library and Archives of Canada (formerly National Library of Canada) for reproduction and distribution.

Name: Golam Islam

Title: Dr.

Signature: G.M. Itheshamul Islam

Date (dd/mmm/yyyy) 12/08/2021

Copyright Permission Letter

DATE: May 14, 2021

Publication Title: Stability and evaluation of siRNAs labeled at the sense strand with a 3'-azobenzene unit

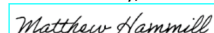
I am preparing my Doctor of Philosophy thesis for submission to the School of Graduate and Postdoctoral Studies at the University of Ontario Institute of Technology (Ontario Tech University) in Oshawa, Ontario, Canada. I am seeking your permission to include a manuscript version of the following paper(s) as a chapter in the thesis:

Hammill, M. L., Patel, A., Abd Alla, M., and Desaulniers, J. P. (2018) Stability and evaluation of siRNAs labeled at the sense strand with a 3'-azobenzene unit, *Bioorganic & Medicinal Chemistry Letters* 28, 3613-3616. DOI: 10.1016/j.bmcl.2018.10.044

Canadian graduate theses are reproduced by the Library and Archives of Canada (formerly National Library of Canada) through a non-exclusive, world-wide license to reproduce, loan, distribute, or sell theses. I am also seeking your permission for the material described above to be reproduced and distributed by the LAC (NLC). Further details about the LAC (NLC) thesis program are available on the LAC (NLC) website (www.nlc-bnc.ca).

Full publication details and a copy of this permission letter will be included in the thesis.

Yours sincerely,



Permission is granted for:

- The inclusion of the material described above in your thesis.
- For the material described above to be included in the copy of your thesis that is sent to the Library and Archives of Canada (formerly National Library of Canada) for reproduction and distribution.

Name: Ayushi Patel

Title: Research student

Signature: 

Date (dd/mmm/yyyy): 14/05/2021

Copyright Permission Letter

DATE: May 14, 2021

Publication Title: Stability and evaluation of siRNAs labeled at the sense strand with a 3'-azobenzene unit

I am preparing my Doctor of Philosophy thesis for submission to the School of Graduate and Postdoctoral Studies at the University of Ontario Institute of Technology (Ontario Tech University) in Oshawa, Ontario, Canada. I am seeking your permission to include a manuscript version of the following paper(s) as a chapter in the thesis:

Hammill, M. L., Patel, A., Abd Alla, M., and Desaulniers, J. P. (2018) Stability and evaluation of siRNAs labeled at the sense strand with a 3'-azobenzene unit, *Bioorganic & Medicinal Chemistry Letters* 28, 3613-3616. DOI: 10.1016/j.bmcl.2018.10.044

Canadian graduate theses are reproduced by the Library and Archives of Canada (formerly National Library of Canada) through a non-exclusive, world-wide license to reproduce, loan, distribute, or sell theses. I am also seeking your permission for the material described above to be reproduced and distributed by the LAC (NLC). Further details about the LAC (NLC) thesis program are available on the LAC (NLC) website (www.nlc-bnc.ca).

Full publication details and a copy of this permission letter will be included in the thesis.

Yours sincerely,

Matthew Hammill

Permission is granted for:

- The inclusion of the material described above in your thesis.
- For the material described above to be included in the copy of your thesis that is sent to the Library and Archives of Canada (formerly National Library of Canada) for reproduction and distribution.

Name: Maria Abd Alla

Title:

Signature: Maria Abd Alla

Date 12/08/2021